Involvement of Histone H1 and H3 Phosphorylation in Oncogene-Mediated Cellular Transformation

By

Deborah Natalie Chadee

A Thesis
Submitted to the Faculty of Graduate Studies
in Partial Fulfillment of the Requirements
for the Degree of
Doctor of Philosophy
Department of Biochemistry and Molecular Biology
University of Manitoba

THE UNIVERSITY OF MANITOBA

FACULTY OF GRADUATE STUDIES

*****

COPYRIGHT PERMISSION PAGE

Involvement of Histone H1 and H3 Phosphorylation in Oncogene-Mediated Cellular Transformation

BY

Deborah Natalie Chadee

A Thesis/Practicum submitted to the Faculty of Graduate Studies of The University of Manitoba in partial fulfillment of the requirements of the degree of

Doctor of Philosophy

This is dedicated to my parents,
Isis and Sylvan

and to my husband,
Arthur

Acknowledgements

As I reflect upon the past 5 years I feel extremely fortunate that my introduction to graduate school was a smooth one. I attribute this to the many people who helped me to overcome the difficulties that arose throughout my program. My supervisor, Dr. Jim Davie, was always available for discussion as well as direct guidance with benchwork. The experiences I had at conferences and in helping with research grants has made my graduate program very fulfilling. His enthusiastic support and guidance has led me through a very rewarding path in graduate studies. An excellent professor and scientist, I am grateful to have had the opportunity to learn from one of the very best in the chromatin field.

I am one of the fortunate students who have benefited from having two excellent supervisors. I am thankful to Dr. J. Wright, also my supervisor, for accepting me as a graduate student and giving me the opportunity to work in his lab. Dr. Wright always offered valuable insight and guidance that helped me maintain different perspectives on my research project. He has incredible enthusiasm and support for all of his lab members and I am very grateful for his input, encouragement and guidance over the past five years.

I began my graduate program working with Bill Taylor who was completing the Ph.D. program with Dr. Wright. Bill helped me to get adjusted when I first arrived in Cell Biology. He was extremely enthusiastic about science and the many discussions (often explanations for me) we had about the project allowed me to get a solid start in this program. I feel fortunate for this experience.

Dr. Jian-min Sun, Dr. Hou Yu Chen and Wei Lee were exceptionally kind and helpful when I joined Dr. Davie's lab. I am truly grateful for their friendship, humour and words of wisdom over the years.

I enjoyed working with all the members of Dr. J. Wright's and Dr. J. Davie's lab and I notably thank Connie Lau, Anne Robbins, Shibani Bal, Dr. Rob Hurta, Helen Zhao and Dr. Aiping Huang for many interesting conversations.

I enjoyed sharing experiences with fellow graduate students Amanda Coutts, Dale Klassen, Denis Bosc, Greg Smith, Mariko Moniwa, Christina Richard, Virginia Spencer, Vern Dolinsky, Zilong Wang, Zhou Xi, Pranati Samadder, Tracey Weiler, Anthony Ashagbley, Lin Ping Choo, Philip Cheng, Doug Lee, Jason Wong, Laura Hart, and Wei Yang Lin. I am especially thankful to Ted Kuschak for leading me in the right direction many years ago.

Many valuable friendships that I have acquired along the way have thoroughly enriched my experience in graduate studies. Mariko Moniwa, Christina Richard, Cheryl Tylipski, Sandra Singhroy, Ileana Silva, Greg Smith, Amanda Coutts, Cristy Villegas, Dr. Huizhou Fan, Dr. Sabine Mai and Shibani Bal made this experience much more interesting and enjoyable both in and out of the lab. I owe a special thanks to Cheryl Tylipski with whom I worked for the last two years. We have struggled through many problems together. Her humor and fun-spirited attitude can cure any dull moment.

Dr. G. Arthur, Dr. R.P. Shiu, Dr. D. Litchfield, Dr. Barbara Triggs-Raine, Dr. P. Choy offered kind words of encouragement and supported my applications for studentships. A special thanks to Dr. G. Arthur for discussions, encouragement and support throughout. I would also like to thank Dr. J. Ausio for the critical evaluation of this thesis. Our collaborator, Dr. David Allis was especially helpful and provided us with reagents that were critical for this work. I am also very grateful for financial support from the Sellers Foundation and the Manitoba Health Research Council.

Arthur Chan was continually challenging my ideas with his sharp logic. This led to many scientific discussions and kept me constantly searching for more answers. The kindest and most generous person I have ever known. With his optimistic outlook, he could always manage to make the impossible seem possible. His technical advice and help throughout the past five years has been invaluable to me. Both my husband and my best friend - I am so lucky.

My husband's family has also been incredibly supportive and encouraging over the past few years, especially through the writing of this thesis.

The long-term friendship and support from Michelle and Corey Moore, Sandra Singhroy, and Hazeline Roche is always remembered.

My family members, Jenny, Karen and Manuel have helped me through the toughest of times and are continuously supportive of all of my endeavors. Finally, I thank my parents who have always stressed the value of a good education. Their constant support and encouragement throughout my years in university has allowed me to enjoy each and every day. They are my inspiration, my role models, and the reason I have progressed to this point.

TABLE OF CONTENTS

LIST OF FIGURES

FIGURE PAGE

LIST OF TABLES

TABLE PAGE

ABBREVIATIONS

A_{260}	absorbance at 260 nm
α-MEM	alpha- minimal essential medium
ATCC	American Type Culture Collection
AUT	acetic acid/urea/triton X-100
bHLH	basic helix-loop-helix
bp	base pair
CAK	cyclin dependent kinase activating kinase
CBP	CREB binding protein
CDI	cyclin dependent protein kinase inhibitor
CDK	cyclin dependent protein kinase
DAPI	diamidinophenolindole
DIG	digoxygenin
DLK	DAP like kinase
DMSO	dimethylsulfoxide
DNase I	deoxyribonuclease I
DRB	5,6-dichloro-1-beta-D-ribofuranosylbenzimidazole
EDTA	(ethylenedinitrilo) tetraacetic acid
EGF-R	epidermal growth factor receptor
EGTA	[ethylenebis (oxyethylenenitrilo)] tetraacetic acid
FACT	facilitates chromatin transcription
FBS	fetal bovine serum

FITC	fluorescein isothiocyanate
G1	gap1
G2	gap2
GAP	GTPase activating protein
GDP	guanine nucleotide diphosphate
GTP	guanine nucleotide triphosphate
h	hour
HAT	histone acetyltransferase
HDAC	histone deacetylase
Hepes	N-(2-hydroxyl)piperazine-N"-(2-ethanesulfonic acid)
HLH	helix-loop-helix
HMG	high mobility group
JNK	Jun N-terminal kinase
kDa	kilodalton
M	mitosis
MAPK	mitogen activated protein kinase
MAR	matrix attachment region
MEK	MAP kinase kinase
MEKK	MAP kinase kinase kinase
min	minute
MNase	micrococcal nuclease
Mo-MSV	Moloney murine sarcoma virus

PAGE	polyacrylamide gel electrophoresis
PBS	phosphate buffered saline
PCA	perchloric acid
PCNA	proliferating cell nuclear antigen
PI(3)K	phosphatidylinositol-3-OH kinase
PIPES	Piperazine-N, N'-bis (2-ethanesulfonic acid)
PKA	c-AMP dependent protein kinase
PKC	protein kinase C
PMSF	phenylmethylsulfonlyfluoride
PP1	protein phosphatase 1
PP2A	protein phosphatase 2A
RasGRP	guanine nucleotide --releasing protein for Ras
Rb	retinoblastoma gene product
RNase A	ribonuclease A
RSF	remodelling and spacing factor
S	synthesis
SAPK	stress activated protein kinase
SAPKK	SAPK kinase
SDS	sodium doedecyl sulfate
SEK	SAPK kinase
SH2	src homology domain 2
SH3	src homology domain 3
SOS	son of sevenless homologue

TAF	TBP associated factor
TBP	TATA binding protein
TCA	trichloriacetic acid
TEMED	N,N,N',N-tetramethylethylenediamine
TF	transcription factor
TPA	12-O-tetradecanoylphorbol-13-acetate
TRIS	tris(hydroxylmethyl)aminomethane
w	weight
v	volume

ABSTRACT

Malignant transformation of a cell is believed to involve the altered expression of specific genes involved in growth regulatory processes. This altered expression could be due to modification at the gene level or at the level of chromatin structure. It has been demonstrated that NIH-3T3 cells transformed with the *ras* oncogene have a more decondensed chromatin structure than the parental cells. Histone H1 and H3 are both required for stabilization of the chromatin fiber and phosphorylation of H1 and/or H3 could lead to chromatin decondensation which may function as a mechanism to regulate gene expression.

We provide evidence that the level of phosphorylated H1b (pH1b) is elevated in cells that are transformed with *ras*, *raf*, *fes*, *mos*, or *myc* oncogenes. We demonstrate that pH1b is localized near nuclear sites of transcription and splicing and phosphorylation of H1b is dependent upon ongoing transcription and replication.

It has been reported that stimulation of serum starved mouse fibroblasts with growth factors or phorbol esters results in a rapid phosphorylation of histone H3 that is concurrent with the transcriptional activation of c-*fos* and c-*jun*. We provide evidence that Ser-10 of H3 is the site phosphorylated in response to EGF (epidermal growth factor) or phorbol ester and TPA (12-O-tetradecanoylphorbol 13-acetate) stimulation. In addition, we demonstrated that pH3 is associated with TPA induced c-*fos* and c-*myc* genes.

We observed an increased level of pH3 in oncogene-transformed cells that was not due to differences in cell cycle distributions. Furthermore, in an inducible-*ras* cell line we observed that induction of *ras* oncogene expression resulted in increased levels of both pH1b and pH3. The H1b and H3 phosphatase activities of *ras*-transformed (C3) and parental (10T½) cells was similar, however, the activity of CDK2 (a candidate H1 kinase) appears to be elevated in the C3 cells. We found that the major H1b and H3 phosphatase in 10T½ cells is PP1 (protein phosphatase 1).

We propose that the increased levels of the phosphorylated forms of H1b and H3 in the oncogene-transformed cells is a result of increased H1b and H3 kinase activities in these cells. Increased levels of pH1b and pH3 could lead to decondensation of chromatin and aberrant expression of genes (for example c-*fos* and c-*myc*) thereby facilitating the process of malignant transformation.

INTRODUCTION

Cancer refers to many different diseases, all of which arise from deregulation of cellular growth processes. Understanding the process by which tumor cells become malignant is critical for the development of treatment and for prevention of spread of the cancer. The key to our understanding of the process of cellular transformation and metastasis lies in our knowledge of the growth regulatory mechanisms of normal cells. A normal cell possesses central growth regulatory systems that prevent abnormal proliferation. In cancer, however, there is a break down of these regulatory mechanisms which results in continuous and uncontrolled cellular proliferation. Therefore, cancer cells can proliferate autonomously into "new growths" or neoplasms. There are two types of neoplasms, benign and malignant. A benign tumor is a growth that remains in its original location and does not invade the surrounding tissue. A malignant tumor is one that can invade the surrounding tissue and spreads (metastasizes) to distant organs through the circulatory system. Only a malignant tumor is referred to as cancer and two thirds of all cancer patients die as a result of metastasis of the disease (reviewed in (Cooper, 1995)).

Almost all tumors arise from a single cell of origin. A tumor is developed from a single cell that sustained multiple transforming events that triggered its abnormal proliferation. Malignant transformation is believed to be a complex multi-step process and a number of successive genetic alterations occur before a fully malignant phenotype is developed. Ultimately, cancer cells can

metastasize, invade normal tissues and disrupt their function. The process of metastasis involves a number of stages. For example, in the stages of carcinoma development the first step is the formation of a preneoplastic lesion termed epithelial dysplasia. Dysplasia is the result of the alteration of a single cell that causes abnormal proliferation and establishment of a preneoplastic cell population. The next stage is the development of carcinoma *in situ* which involves the formation of localized tumors that have not invaded the adjacent tissue. The progression of carcinoma *in situ* to malignant, invasive carcinoma occurs when cancer cells at the primary tumor site invade the neighbouring tissue. This process also likely involves the acquisition of additional mutations in the tumor cells that increases their growth potential (Fig. 1). In the first step of metastasis cancer cells must detach from their tissue of origin and cross two basement membranes. The first membrane separates the epithelium from the mesenchyme and the second surrounds the surface of the endothelial cells that line the blood vessels (reviewed in (Aznavoorian et al., 1993)). The basement membrane contains Type IV collagen and laminin and many cancer cells secrete type IV collagenase which breaks down the collagen and helps the cells pass through the basement membrane. After crossing the basement membrane, the cancer cell must breach the tissue-blood barrier. This occurs when the cell comes in contact with a nearby blood vessel and through a process called intravasation, the cell breaks through the subendothelial basement membrane by retracting endothelial cells that line the blood vessel and enters the bloodstream. After transport in the bloodstream, the cell enters a new tissue by the process of

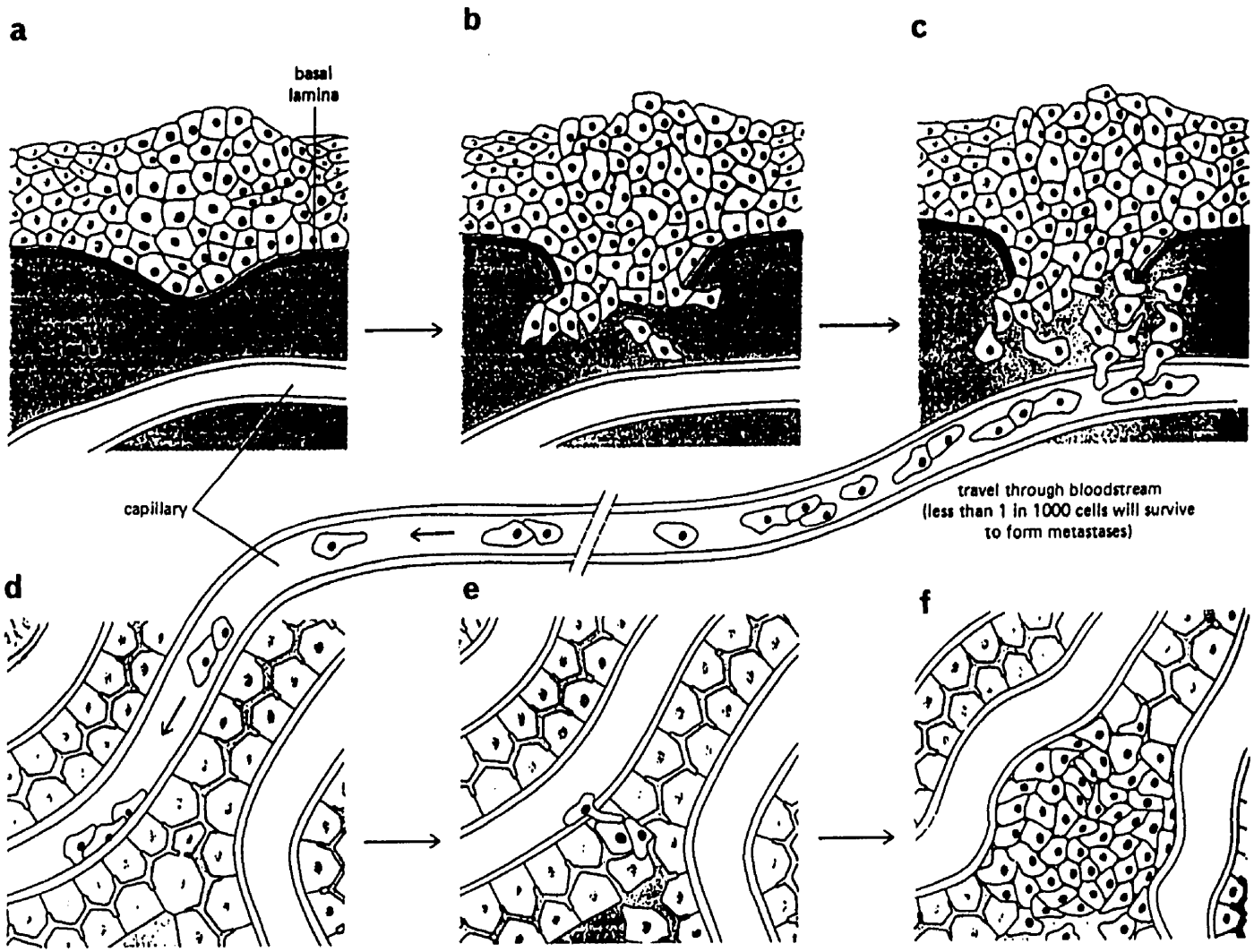

Figure 1. **Overview of stages of metastic progression.** (a) benign tumour present in bronchial epithelium (b) cancer cell detaches from tissue of origin and crosses the basement membranes (c) intravasation and breaching of tissue-blood barrier (d) cancer cells adhere to capillary wall in liver (e) extravasation and breaching of the blood-tissue barrier (f) establishment of secondary site and formation of secondary colony.

extravasation that also involves retraction of subendothelial cells and dissolution of the basement membrane. In this process the blood tissue barrier is breached and the cancer cell establishes at a secondary site and forms a secondary colony (Aznavoorian et al., 1993).

Researchers have studied cancer development and progression using whole animals; however, there are often variables that cannot be controlled for in the intact organism. The establishment of *in vitro* cell culture systems enabled cancer researchers to study and compare various characteristics of normal cells and cancer cells under controlled conditions. There are a number of distinct characteristics that distinguish normal cells from cancer cells. Normal cells exhibit, anchorage dependent growth, requirement for growth factors, contact inhibition of movement, flat morphology, and high adhesiveness (Cooper, 1995). Cancer cells, however, exhibit a lack of requirement for growth factors, anchorage independent growth, no contact inhibition of movement, a rounded morphology and low adhesiveness. The work presented in this thesis deals with experiments performed using cultured mouse fibroblast cell lines.

There are number of factors that can predispose an individual to cancer. They include, exposure to chemical carcinogens, exposure to radiation, hormonal stimulation, viral infection, genetic predisposition, chromosomal instability, and altered DNA repair mechanisms. All of these factors have one element in common, they all affect the cellular DNA (Cooper, 1995).

Oncogenes

In 1969 Huebner and Todaro proposed that genes responsible for regulating normal growth development could go awry and result in deregulated growth as observed in cancer (Huebner and Todaro, 1969). These genes were referred to as "oncogenes" and this idea became known as the oncogene hypothesis. Oncogenes act in a dominant positive regulatory manner and often increase gene expression or increase the activity of the oncoprotein. In contrast, there are genes that can function as negative regulators of cellular transformation called tumor suppressor genes. The loss of function of a number of these genes can significantly contribute to the development of the malignant phenotype.

Ras

The first human oncogene identified from the EJ bladder carcinoma was a cellular homolog of the *rasH* oncogene of Harvey sarcoma transforming viruses (Coffin et al., 1981). The *ras* oncogene sequences found in the virus were from rat DNA sequences that had become integrated into the viral genome. These rat DNA sequences gave the virus the transforming capability. Gene transfer techniques using DNA from the T24 EJ bladder carcinoma cell line was shown to induce transformation of NIH-3T3 cells. This was the first example of a biologically active human tumor oncogene (Shih and Weinberg, 1982). Later, another oncogene identified in human lung carcinoma was determined to be the human proto-oncogene corresponding to the Kirsten sarcoma virus oncogene, *rasK*. *RasH* and *rasK* are members of a *ras* family of genes and in 1983 an

additional related tumor oncogene was isolated from a neuroblastoma and thus designated *rasN*. The *ras* oncogenes identified in human tumors and viruses are activated and can induce cell transformation. Their normal cellular counterparts or proto-oncogenes, however, cannot induce cellular transformation. The distinct difference between the *ras* oncogene and the *ras* proto-oncogene was a point mutation that resulted in a single amino acid substitution at position 12 in the Ras protein. Normal Ras protein has a glycine at position 12, however, in the activated Ras protein, the glycine has been substituted to a valine. This single amino acid change is responsible for the conversion of the normal Ras protein into the actively transforming oncoprotein. Amino acid substitutions at other positions in the Ras protein such as codons 13 and 61 have also been found to be activating and mutations in Ras have been found in a wide variety of human tumors. The Ras protein is a 21 kDa plasma-membrane associated guanine nucleotide binding protein that is involved in intracellular signal transduction. The Ras protein can exist in two states: an active state that contains a bound GTP (guanine nucleotide triphosphate) molecule and an inactive state that contains a bound GDP (guanine nucleotide diphosphate) molecule. Ras is activated by the replacement of bound GDP for GTP. Regulatory proteins called guanine nucleotide releasing factors, or GRFs, interact with Ras and promote the formation of the GTP bound protein. The Drosophila Sos (Son of Sevenless) protein is homologous to exchange proteins that activate Ras by inducing the loading of GTP. Other regulatory proteins, GTPase activating proteins (GAPs) enhance the intrinsic GTPase activity of Ras resulting in hydrolysis of GTP to

GDP. Therefore, the relative activity of Ras is determined by the activities of the GRFs and GAPs. The substitution at residue 12 is believed to disrupt the hydrolytic activity of Ras and therefore it remains in a GTP bound state and is constitutively active. Although these regulatory proteins are important in determining Ras activity, it is clear that Ras activity is also regulated by other factors. Another important factor in Ras protein activation is its subcellular localization to the plasma membrane. A 15-carbon isoprenyl (farnesyl) group that is covalently linked to Ras by a farnesyltransferase, mediates the association of Ras with the cell membrane. It has been demonstrated that this posttranslational modification is necessary for Ras transforming ability (Shih and Weinberg, 1982; Hancock et al., 1989; Cox et al., 1992; Schafer and Rine, 1992). The identification of inhibitors of the Ras farnesyltransferase has been of great interest for anti-cancer drug development (reviewed in (Tamanoi, 1993)).

Ras is now known to be a member of a superfamily of low molecular weight GTP binding proteins that function in a diverse array of intracellular signaling pathways. These functions include cellular proliferation (Ras and Rap), intracellular vesicular trafficking (Rab and Arf), oxidase generation (Rac and Rap), and cytoskeletal control (Rho and Rac).

Normal cellular Ras is believed to function in the integration of extracellular signals acting on cell surface receptors. The inhibition of Ras function by micro-injection of anti-Ras antibodies inhibits the growth of Src tyrosine kinase transformed fibroblasts (Smith et al., 1986). This finding indicated that Ras functions downstream of activated tryrosine kinases (Smith *et*

al., 1986). A collection of discoveries made in the early 1990's made a major contribution to the understanding of the function of Ras in the transmission of extracellular signals from a receptor tyrosine kinase (Fig. 2). Ras activity in mammalian cells is stimulated by tyrosine kinase receptors such as the insulin receptor and the epidermal growth factor receptor (EGF-R). Sem5/Grb2 is an adaptor protein, which consists of two src-homology-3 (SH3) domains and a src-homology-2 (SH2) domain. SH2 domains are binding sites for specific tyrosine phosphoproteins and SH3 domains are binding sites for specific proline rich motifs (reviewed in (Feller et al., 1994)). Sem5/Grb2 can interact with mammalian tyrosine kinases through its SH2 domain and it can also interact with the mammalian SOS proteins (mSOS1 and mSOS2) through its SH3 domain (Egan et al., 1993). The activation of a tyrosine kinase receptor on the cell surface can induce the formation of a SOS-Sem5/Grb2-tyrosine kinase receptor multiprotein complex. Upon activation of a tyrosine kinase receptor, SOS is recruited to the plasma membrane by the adaptor protein Sem5/Grb2 where it is now in the vicinity of its target, Ras. As previously mentioned, SOS promotes the formation of the GTP bound Ras thereby resulting in its activation. Ras activation triggers the phosphoryation of a cascade of downstream kinases, eventually affecting nuclear transcription factors such as c-Fos and c-Myc which stimulate cellular proliferation (Egan and Weinberg, 1993). Activated Ras binds the serine/threonine kinase Raf, and promotes its translocation to the plasma membrane. The translocation of Raf to the membrane as well as its interaction

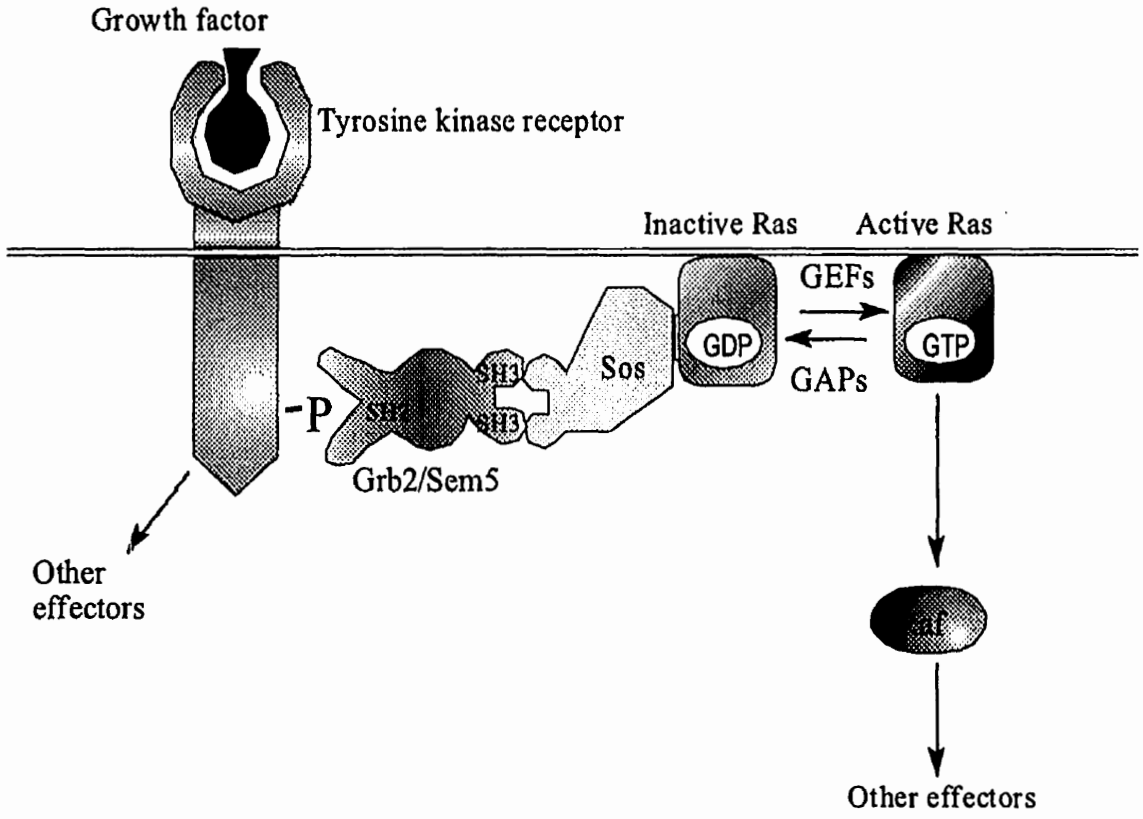

Figure 2. **Transmission of extracellular signals from a receptor tyrosine kinase.** Sem5/Grb2, an adaptor protein, can interact with mammalian tyrosine kinases through its SH2 domain and it can also interact with the mammalian SOS proteins through its SH3 domain. Upon activation of the receptor, the adaptor protein Sem5/Grb2 recruits SOS to the plasma membrane where it interacts with its target, Ras. SOS promotes the formation of the GTP-bound, active form of Ras. Activated Ras associates with the serine/threonine kinase Raf, localizing it to the plasma membrane and contributing to its activation.

with Ras, are key factors which contribute to its activation (Leevers et al., 1994; Zhang et al., 1993).

Another protein which is regulated by Ras is phosphatidylinositol-3-OH kinase (PI(3)K). Ras has been shown to interact directly with the catalytic subunit of PI3K in a GTP-dependent manner through the Ras effector site. Therefore, Ras may also be involved in regulating lipid mediated signalling (Rodriguez-Viciana *et al.*, 1994). There is also evidence that Ras is activated upon TPA (an analog of diacylglcerol) treatment of cells (Ebinu et al., 1998). A guanyl nucleotide–releasing protein for Ras called RasGRP has been shown to have calcium and diacylglycerol binding domains. Activation of Ras, by RasGRP, can cause transformation in fibroblasts. Treatment of cells with TPA (12-O-tetradecanoylphorbol 13-acetate) resulted in changes in cell morphology and in sustained activation of Ras/MAPK signaling (Ebinu et al., 1998) that was dependent upon the association of RasGRP with the membrane. The membrane partitioning and Ras/MAPK signalling was not observed when the DAG-binding domain was deleted. RasGRP is expressed in cells of the nervous system and it was suggested that it may couple changes in DAG and calcium concentrations to Ras activation (Ebinu et al., 1998).

Raf

The *raf* oncogenes were first encountered in chicken and mouse retroviruses (Jansen et al., 1984). The three members of the *raf* oncogene family are c-*raf*-1, A-*raf*, and B-*raf*. The Raf oncoproteins are Ser/Thr protein kinases

and c-Raf-1, A-Raf, and B-Raf are 75% identical in their C-terminal kinase domains. Two other conserved domains are found in the N-terminal half of the Raf proteins that are involved in regulation of Raf kinase activity. The deletion of negative regulatory sequences in the amino terminal domain is the major event that transforms a *raf* proto-oncogene into a *raf* oncogene. This deletion results in the increased activity of the carboxyl terminal kinase domain. The activated Raf kinase can phosphorylate the protein phosphatase Cdc25 and the proapototic protein BAD (Wang et al., 1996; Wang and Reed, 1998). In addition, Raf can phosphorylate MEK, also referred to as MAP (mitogen-activated protein) kinase kinase (Kyriakis et al., 1992). MEK it is a dual specificity kinase which can phosphorylate its substrate, MAP kinase, on both threonine and tyrosine residues (Cowley et al., 1994; Kyriakis et al., 1992).

MAP kinase

The MAP kinase signal transduction pathways have been highly conserved throughout eukaryotic evolution. Mammalian cells have parallel MAP kinase pathways that can respond to different types of extracellular stimuli (reviewed in (Denhardt, 1996)). Using these pathways, the cell is able to simultaneously integrate and respond to multiple external stimuli (Fig. 3). Each of the three known MAP kinase pathways have a central three-tiered core of protein kinases starting upstream with MAP3Ks (MAP kinase kinase kinase, for example Raf). MAP3K's phosphorylate and activate MEKs (MAP kinase kinases) and in turn, MEK's phosphorylate and activate the MAPK's (p44 and

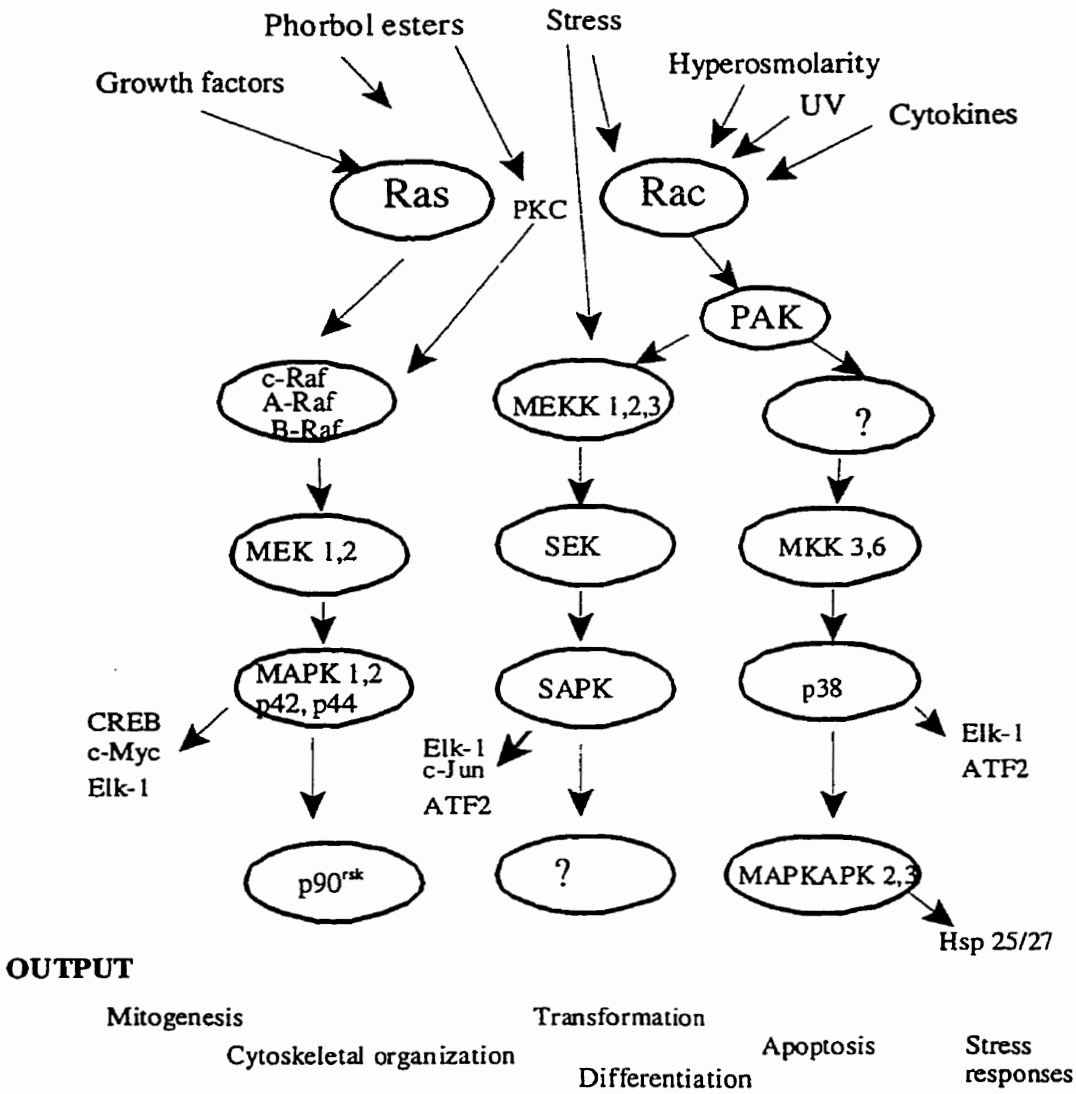

Figure 3. **Mammalian MAP kinase signaling pathways.** Mammalian cells have parallel MAP kinase signaling pathways that can integrate and respond to different types of extracellular stimuli such as growth factors and stress. Each of the three known MAP kinase pathways have a central three-tiered core of protein kinases starting upstream with MAP3Ks (Raf, for example). MAP3K's phosphorylate and activate MEKs (MAP kinase kinases) and in turn, MEK's phosphorylate and activate the MAPK's (p42 and p44). Activation of each pathway results in the stimulation of phosphorylation of a cascade of downstream kinases eventually affecting nuclear transcription factors such as c-Fos, c-Jun and c-Myc. The activation of these different pathways results in output responses such as mitogenesis, cytoskeletal organization, apoptosis, transformation, stress responses and differentiation. Adapted from Denhardt (1996).

p42) (Denhardt, 1996; Madhani and Fink, 1998). Proteins which have been implicated in the activation of the MAP3K's include the GTPases of the Rasfamily, members of the Ste20 and Sps1 families, and adaptor proteins that couple to cytokine receptors (Denhardt, 1996; Madhani and Fink, 1998). Two other parallel MAP kinase subfamilies are the stress activated protein kinases, or SAPK's and p38's. These pathways are activated by a broad spectrum of environmental stresses such as ionizing radiation, DNA damage, protein synthesis inhibitors, osmotic stress, and heat shock (Kyriakis and Avruch, 1996b). Also, inflammatory cytokines of the tumor necrosis factor family and ischemic and reperfusion injury can activate these pathways (Kyriakis and Avruch, 1996a). Unlike the MAPK's, the SAPK's and the p38s are poorly activated by mitogens such as EGF and insulin (Kyriakis et al., 1995). In response to the stress stimuli, the SAPKKs (SEKs) are phosphorylated and acitvated by MEKKs. The activated SAPKs phosphorylate and activate the SAPKs. The SAPKs can regulate gene expression through directly phosphorylating and activating transcription factors such as c-Jun and Elk-1 (Kyriakis et al., 1994).

In mammalian systems, the Ras/MAP kinase pathway has been most extensively studied (Fig. 4). The activation of this pathway occurs mainly through the stimulation of receptor tyrosine kinases by mitogenic agonists (Blumer and Johnson, 1994). For example, epidermal growth factor can stimulate the epidermal growth factor receptor on the cell surface. This stimulation results in autophosphorylation of the receptor, recruitment of adaptor

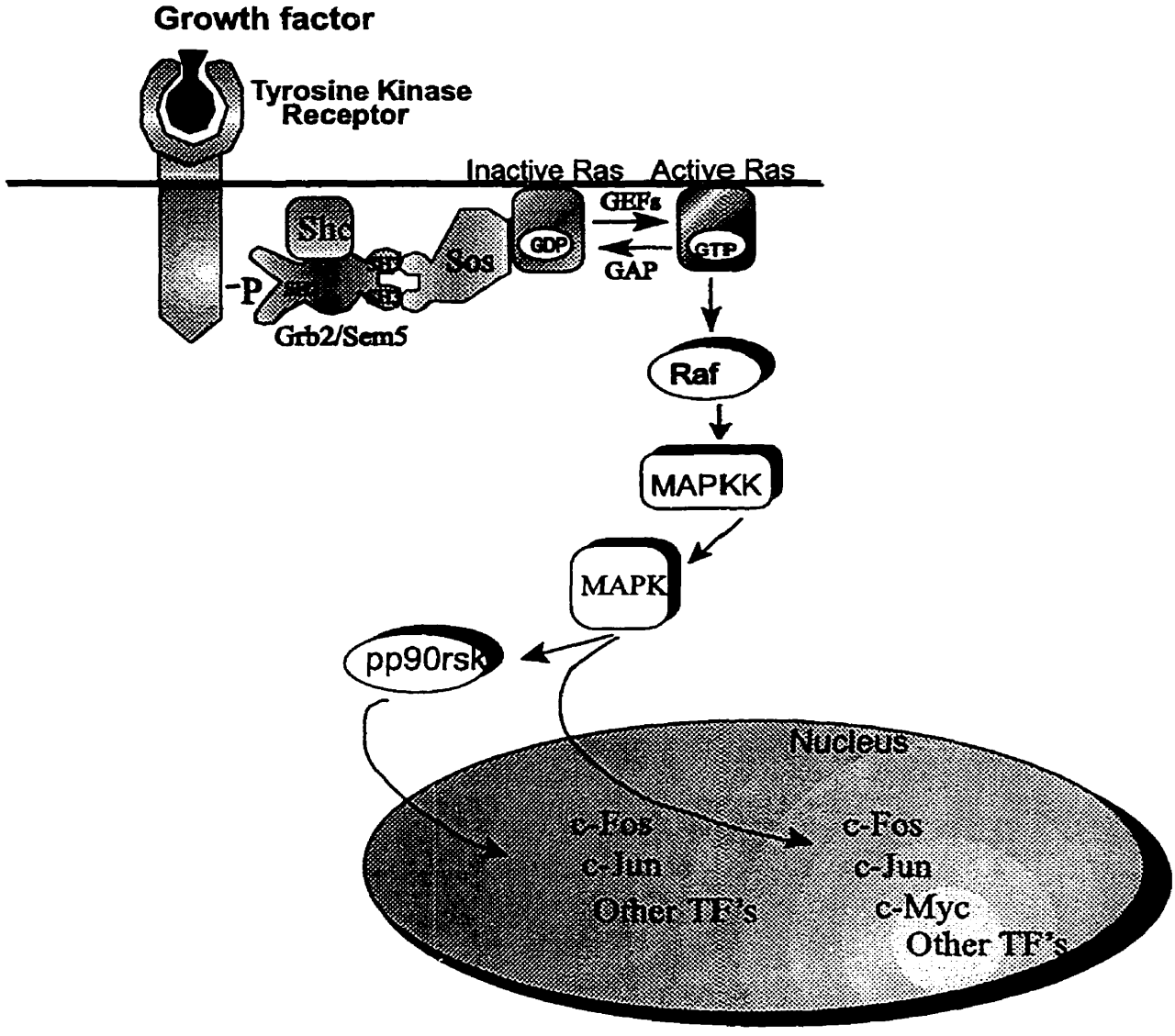

Figure 4. **The Ras/MAP kinase pathway.** Activation of this pathway occurs mainly through the stimulation of receptor tyrosine kinases by mitogenic agonists. This stimulation results in autophosphorylation of the receptor, recruitment of adaptor proteins, and eventual activation of Ras. Activated Ras triggers the phosphoryation of a cascade of downstream kinases eventually affecting nuclear transcription factors (TF's) such as c-Fos and c-Myc which stimulate cellular proliferation.

proteins, and eventual activation of the Ras/MAP kinase pathway. Treatment of cells with the phorbol ester, TPA, results in the activation of specific PKC (protein kinase C) isoforms that can phosphorylate the Raf serine/threonine kinase and activate the MAP kinase pathway (Frawley et al., 1994; Schonwasser et al., 1998; Kolch et al., 1993). Also, TPA has been shown to activate this pathway by inducing Ser phosphorylation of Shc, another adaptor molecule that can interact with GRB2 through its SH2 domain (El-Shemerly et al., 1997; Ravichandran et al., 1995). Generally, phosphorylation of Shc on tyrosine 317 can be induced by tyrosine kinases and cytoplasmic receptors and this results in the recruitment of Grb2-SOS complex to the membrane allowing SOS to activate Ras (Ravichandran et al., 1995).

Activation of the MAP kinases also provides a direct link of this signal transduction pathway from the cytoplasm to the nucleus. Upon activation by phosphorylation, MAP kinase is translocated from the cytoplasm to the nucleus (Sanghera et al., 1992). In the nucleus, active MAP kinase can phosphorylate and activate transcription factors such as c-Fos, c-Myc and c-Jun which are known to stimulate cellular proliferation (Davis, 1995). MAP kinases can also phosphorylate and activate other cytoplasmic kinases such as $p90^{rsk}$ (RSK) (Zhao et al., 1996). RSK can translocate to the nucleus where it phosphorylates a number of nuclear proteins such as c-Fos, c-Jun, serum response factor, and Nur77 (Fig. 4) (Chen et al., 1992). The constitutive expression of MAP kinase kinase has been shown to transform mouse fibroblasts (Mansour et al., 1994; Cowley et al., 1994). Gradually scientists have found many other proteins that

can impact upon the MAP kinase pathway. Among these are the oncoproteins Fes and Mos.

Fes

The human c-*fes* gene encodes a 93 kDa non-receptor protein tyrosine kinase. *Fes* was first recognized as a cellular homolog of a transforming retroviral oncoprotein. Later, *c-fes* was found to be expressed mostly in myeloid cells of granulocytic and monocytic lineages (Feldman et al., 1985) (MacDonald et al., 1985; Smithgall et al., 1988) and Fes has a direct role in myeloid differentiation. The mechanisms involved in this process and the identity of the substrates of the Fes tyrosine kinase are of great interest. One interesting, *in vitro* substrate of Fes is the Ras GTPase-activating protein GAP. It has been demonstrated that transformation of Rat-2 fibroblasts with an avian homolog of *fes*, v-*fps*, results in increased phosphorylation of GAP. Hjermstad *et al.* (1993) identified GAP as a substrate for human c-Fes. They showed that GAP could form stable complexes with autophosphorylated Fes protein. It was suggested that GAP-Fes association might produce unique effects on GAP biological activity and modifiy its interactions with other proteins (Hjermstad *et al.* 1993). Another substrate of Fes is the human BCR serine / threonine protein kinase (Maru et al., 1995). BCR has a GAP domain and an SH2 domain and co-expression of BCR in Sf-9 cells with Fes resulted in tyrosine phopshorylation of BCR and formation of a stable BCR-Fes protein complex (Maru et al., 1995). Deletion of the homologous N-terminal BCR binding domain of v-*fps* abolished the transforming activity and the tyrosine

phosphorylation of BCR *in vivo*. The tyrosine phosphorylation of BCR in v-*fps* transformed cells results in its association with the GRB-2/SOS complex (Ras guanine nucleotide exchange factor complex). The authors suggested that BCR may couple the Fes protein tyrosine kinase and Ras signaling pathways (Maru et al., 1995). Further evidence that demonstrates a role for Ras in Fes transformation comes from a study by Li and Smithgall (1998). They showed that Rat-2 fibroblast transformation by Fps/Fes tyrosine kinase requires Ras and Rac. Expression of a dominant-egative Ras, Rac, or Cdc42 inhibited v-Fps- and c-Fes- induced growth of Rat-2 cells in soft agar. Also, dominant negative mutants of Ras specifically inhibited MAP kinase activation by Fes. Therefore, Ras and other small G proteins appear to be required for fibroblast transformation by Fps/Fes tyrosine kinases (Li and Smithgall, 1998). All of these results suggest that Fes may act at the level of Ras- GAPs and GEFs to modulate Ras activation of the MAP kinase pathway.

Mos

Another oncoprotein that can strongly activate the MAP kinase pathway is Mos. The v-*mos* oncogene of the Moloney murine sarcoma virus (Mo-MSV) encodes a serine/threonine protein kinase. v-*mos* expression has been found to cause fibrosarcomas in mice and v-Mos can transform fibroblasts in culture (Canaani et al., 1979; Maxwell and Arlinghaus, 1985). The cellular homolog, c-*mos*, when placed under the control of long terminal repeat sequences of Mo-MSV can also transform fibroblasts (Blair et al., 1981). C-*mos* normally is

expressed in germ line cells and is undetectable in somatic cells. Studies on Xenopus and mouse oocytes have implicated Mos as an important regulator of meiosis and Mos has been found to be necessary for metaphase arrest of oocytes at meiosis stage II (reviewed in (Yew et al., 1993)). A *c-mos* knockout mouse has been made and the male mice are fully viable and fertile. The female mice, however, are viable but have a reduced fertility due to the inability of mature eggs to arrest during meiosis (Colledge et al., 1994; Hashimoto et al., 1994). When *mos* is expressed in mammalian somatic cells the result is uncontrolled cell proliferation. Mos can potently activate the MAP kinase pathway in oocytes and also when inappropriately expressed in somatic cells (Nebreda and Hunt, 1993; Posada and Cooper, 1992). Mos can activate the MAP kinase pathway by directly phosphorylating MAP kinase kinase on critical serine residues within its catalytic domain resulting in its activation (Resing et al., 1995).

Myc

The Myc protein plays a critical role in the regulation of cellular proliferation (Luscher and Eisenman, 1990) and deregulated *myc* expression often results in loss of cell cycle control. The *myc* family includes v-*myc*, c-*myc*, N-*myc*, L-*myc*, B-*myc* and s-*myc* (for review see (Luscher and Eisenman, 1990))(Kato and Dang, 1992). The *myc* oncogene was first identified as the cellular homolog of a transforming sequence from the MC29 avian retrovirus (Sheiness and Bishop, 1979; Duesberg et al., 1977). Later, chromosomal

translocations of the c-*myc* gene were found in patients with Burkitts lymphoma, a B-cell malignancy (Dalla-Favera et al., 1982; Taub et al., 1982). This translocation placed c-*myc*-coding sequences adjacent to the regulatory elements of the immunoglobulin (Ig) heavy chain gene which is highly expressed in B-cells. The result of this translocation was elevated levels of c-*myc* gene expression and similar mechanisms of c-*myc* activation have been found in murine plasmacytomas (Taub et al., 1982) and rat immunocytomas (Pear et al., 1988).

In gene transfer experiments, transfection of an activated c-*myc* gene alone can lead to immortalization of rat fibroblasts (Mougneau et al., 1984). However, under many conditions, *myc* overexpression alone in primary rat embryo fibroblasts fails to induce transformation. Co-expression of activated c-*myc* with the *ras* oncogene resulted in malignant transformation (Land et al., 1983; Lee et al., 1985). C-*myc* can therefore co-operate with other oncogenes to induce malignant transformation (Land et al., 1983; Taylor et al., 1994). It has been demonstrated that mammary tumors that were derived from c-*myc* overexpressing transgenic mice have high levels of MAP kinase activity. The anchorage independent growth of these cells was strongly inhibited by a specific inhibitor of Map kinase kinase. These results demonstrate that c-Myc requires the MAP kinase pathway to maintain the transformed phenotype. It was suggested that the transforming ability of c-Myc may require cooperating signals such as growth factor receptors that emanate from the cell membrane (Amundadottir and Leder, 1998).

C-*myc* expression is highly correlated with cellular proliferation. In normal cells, *c-myc* expression is higher in actively proliferating cells and lower in cells which are terminally differentiated (Lachman and Skoultchi, 1984). In 1983, the laboratories of Dr. Charles Stiles and Dr. Philip Leder demonstrated that the c-*myc* gene is rapidly and transiently induced following growth factor stimulation (Kelly et al., 1983). These findings lead to the suggestion that c-Myc and c-Fos may function to modulate gene expression in response to proliferative stimuli. The *c-myc* gene encodes a nuclear phosphoprotein of approximately 62-64 kDa. C-Myc is a DNA binding protein that binds specifically to the core sequence "E-box" motif CACGTG. The N-terminal portion of the molecule contains an activation domain and the carboxyl terminal domain of the protein contains functionally important DNA sequences that are homologous to DNA sequences from leucine zipper and helix–loop-helix (HLH) classes of proteins. The helix-loop-helix domain is comprised of two amphipathic α-helical regions separated by a loop and the leucine zipper domain consists of a long α-helix with intermittent leucine residues (Landschulz et al., 1988). C-Myc and other transcription factors contain both the leucine zipper and the HLH domains and often a region of basic amino acids precedes the HLH domain, hence called bHLH. These domains function in mediating protein dimerization. C-Myc protein dimerizes poorly with itself, however, a protein termed Max has been found to heterodimerize with c-Myc (Blackwood and Eisenman, 1991). This heterodimerization occurs through the bHLH domain of Max and the Myc-Max heterodimer can bind CACGTG sequences and activate transcription of target

genes. The Myc-Max heterodimer therefore seems to be the functional form of Myc in cells. A Max-Max homodimer can also form and bind DNA; however, this dimer lacks an activation domain and its binding to the Myc DNA element results in repression of transcription. Another protein, Mad can also dimerize with Max and act as a transcriptional repressor (Zervos et al., 1993). As mentioned previously, Myc is a nuclear phosphoprotein and one of the kinases that can phosphorylate c-Myc and c-Fos is MAP kinase. Phosphorylation of c-Myc by MAP kinase resulted in increased c-Myc activity. Many studies have demonstrated that overexpression of c-Myc resulted in increased mRNA levels of the cell cycle regulatory molecules cyclins A, D1 and E (Daksis et al., 1994; Jansen-Durr et al., 1993). These results provided a link between mitogen-stimulated signal transduction and cell cycle regulation.

c-Fos

In 1987, a human cellular transcription factor was identified, called AP-1, that interacted with sequences in the regulatory elements of genes that were induced by growth factors or phorbol esters. In 1984, c-*fos* expression had been shown to be rapidly and transiently induced by growth factor stimulation of different cell types. It was suggested that Fos might modulate transcription of genes when stimulated by growth factors (Kelly et al., 1983). Later it was demonstrated that AP-1 was actually a heterodimer of c-Fos and c-Jun proteins and that Fos and Jun cooperate to activate transcription of AP-1 target genes (Halazonetis et al., 1988; Chiu et al., 1988). The constitutive expression of c-Fos

protein has been shown to be oncogenic (Miller et al., 1984). Overexpression of c-*fos* requires both the increased transcription of the c-*fos* message and the stabilization of the *c-fos* mRNA (Miller et al., 1984). The phosphorylation of c-Fos on its C-terminus has also been shown to enhance its transforming activity (Chen et al., 1996).

Cell cycle regulation

Deregulation of cell cycle events can lead to abnormal cell proliferation and tumor development. The cell cycle can be divided into four different phases. The phases that involve DNA synthesis (S phase) and mitosis (M phase) are separated by gaps of time that vary in length called G1 and G2 phases. G1 (gap 1) is a stage where the cell is diploid or 2N, is metabolically active but not undergoing DNA synthesis. The cell advances into S (synthesis) phase where DNA replication occurs and the DNA content of the cell increases from 2N to 4N. The cell then progresses through G2 (gap 2) phase and then into M (mitosis) where the cell divides into two diploid daughter cells. The average time required to complete one cell cycle is about 20 hours, however, this can vary significantly in different cells. Based on the current understanding of cell cycle control, these cell cycle phases are regulated by checkpoints. One of the most crucial checkpoints is the START checkpoint that occurs late in G1 phase. At this point, cells decide whether or not to commit themselves to another round of DNA replication. The cell has to integrate a variety of internal and external signals at this point before determining if to proceed to the next phase. Other cell cycle

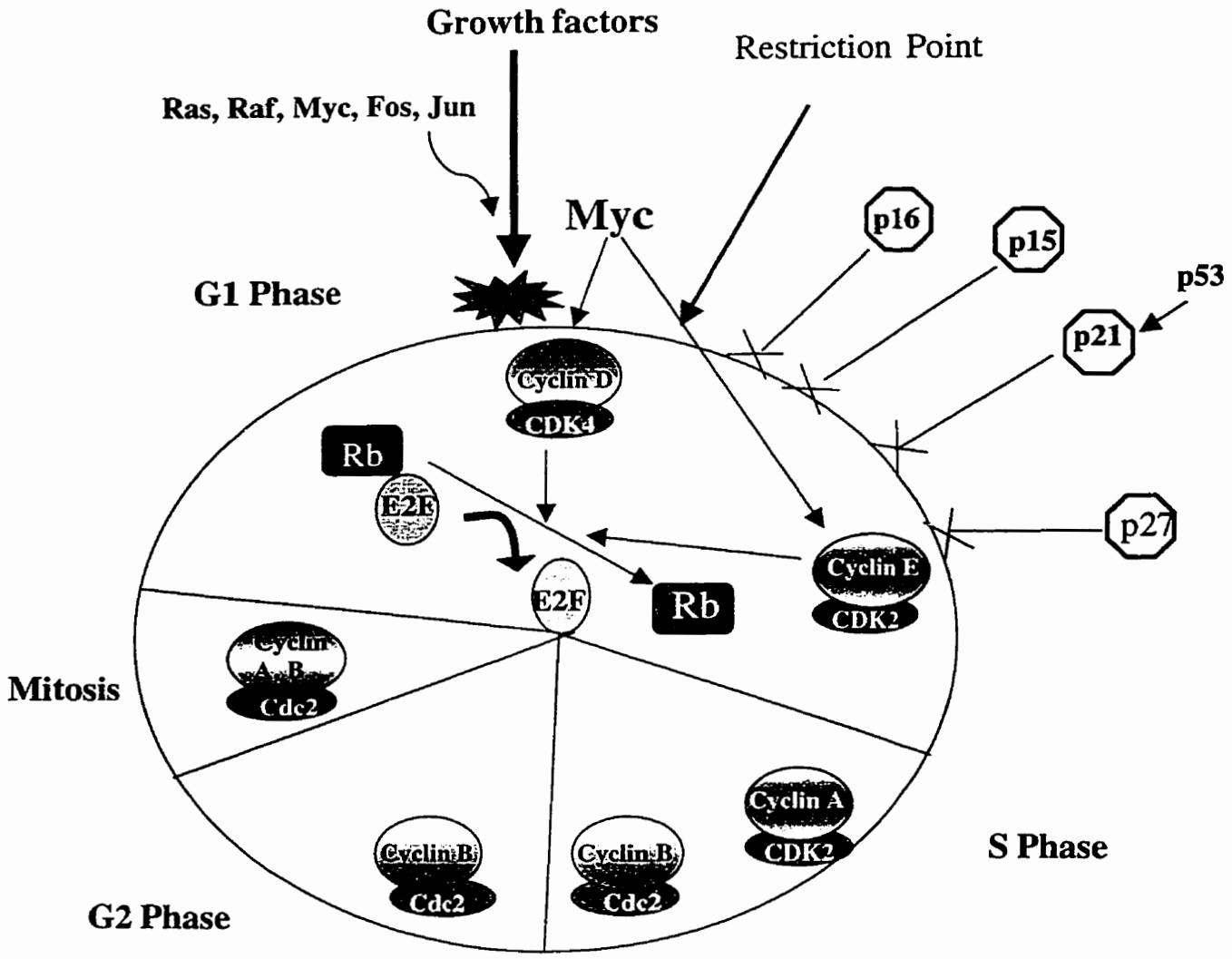

Figure 5. **Regulation of the mammalian cell cycle**. The major cell cycle transitions of the eukaryotic cell are controlled by the cyclin-dependent protein kinases (CDK's). Activation of CDKs requires the association with a partner cyclin. CDK activity can be inhibited by phosphorylation or by binding to inhibitory cyclin dependent kinase inhibitors (CDIs). The regulation of the START restriction checkpoint is closely linked to the cyclin D–CDK complexes. The D-cyclins are inducible by growth factors and can activate CDK4 and CDK6 to drive the cells through the restriction point. The phosphorylation of Rb by CDK4-cyclin D or CDK2-cyclin E complexes results in the release of E2F which can then activate transcription of immediate early genes and advance the cells through G1. Some CDIs include $p16^{ink}$, p15, p27 and p21. P15 and p16 both bind and inhibit only CDK4 and CDK6. P21 binds to and inhibits a number of CDKs including cyclin D-CDK4, cyclin E-CDK2 and cyclin A-CDK2. Also, p21 is activated by wild type p53 in response to DNA damage.

checkpoints occur at S phase and M phase. In general, the major cell cycle transitions of the eukaryotic cell are controlled by the cyclin-dependent protein kinases (Fig. 5) (CDK's, reviewed in (Morgan, 1995)). The protein levels of the various CDK's remain relatively constant throughout the cell cycle and CDK activity is regulated by a number of factors. One of the important steps in the activation of CDKs is the association with a partner cyclin. Cyclins are a group of regulatory proteins whose levels oscillate during the cell cycle. A second key step in CDK activation is the phosphorylation of the CDK on a conserved threonine 160 by the CDK-activating kinase (CAK). In turn, CDK activity can be inhibited by phosphorylation of a conserved threonine tyrosine pair or by binding to inhibitory cyclin dependent kinase inhibitors (CDIs) reviewed in (Harper and Elledge, 1996).

In mammalian cells, the regulation of the START checkpoint is closely linked to the cyclin–CDK complexes consisting of cyclins D1, D2, and D3 and CDK4 and 6. The D-cyclins activate CDK4 and in some cells CDK6 (Bates et al., 1994; Meyerson and Harlow, 1994) to drive the cells through the START restriction point. The expression of the D cyclins in early G1 phase is very short and is inducible by growth factors (Won et al., 1992). The alteration of D type cyclin levels could cause deregulation of START and contribute to oncogenesis.

In G1, it has been determined that D-type cyclins are directly involved in the regulation of the tumor suppressor Rb (retinoblastoma gene product). Rb is normally hypophosphorylated in G1 and bound to the transcriptional activator E2F. In this form, Rb prevents E2F from binding to and activating its target

genes and cells remain arrested in G1 phase. Recently, another mechanism by which Rb represses transcription from E2F promoters has been elucidated. It has been determined that Rb recruits a histone deacetylase (HDAC1) that deacetylates the tail domains of core histones producing a chromatin structure that inhibits transcription. Deacetylation of core histones has long been associated with repression of gene transcription. Histone deacetylases have consequently emerged as a key element in cell cycle control. For gene promoters that are resistant to histone deacetylase activity, repression is mediated by direct inhibition of transcription factors. The phosphorylation of Rb by CDK4-cyclin D complexes relieves this inhibition by promoting the release of E2F (reviewed by (Hinds and Weinberg, 1994)). E2F is then available to activate transcription of immediate early genes which allows the cells to advance through G1 (Brehm et al., 1998; Luo et al., 1998; Magnaghi-Jaulin et al., 1998).

Overexpression of CDK4 and CDK6 has been demonstrated in different tumor cell lines, however, no mutations in CDK4 have been detected in any human tumors (Hinds and Weinberg, 1994; Tam et al., 1994). The CDIs $p16^{ink}$, p15, p27 and p21 bind and inhibit CDK-cyclin complexes and thus are negative regulators of cell cycle progression. P15 and p16 both bind and inhibit only CDK4 and CDK6 (Hannon and Beach, 1994). The p16 gene is rearranged, deleted or mutated in a large number of tumor cells lines (Kamb et al., 1994; Nobori et al., 1994) and these findings lead to the suggestion that p16 could be a tumor suppressor gene. There is also very strong evidence that the CDI, p21, has a role in cellular transformation. P21 binds to and inhibits a number of CDK-

cyclin complexes which include cyclin D-CDK4, cyclin E-CDK2 and cyclin A-CDK2 (involved at the G1/S phase boundary) (Gu et al., 1993; Xiong et al., 1993; el-Deiry et al., 1994). P21 also binds and inhibits PCNA (proliferating cell nuclear antigen), a component of the DNA replication machinery (Waga et al., 1994). P21 therefore plays an important role in the inhibition of progression of cells into S phase. Interestingly, while normal cells have most of their cyclin-CDK complexes bound to p21/PCNA in G1, transformed cells lack this association (Xiong et al., 1993). P21 is thought to be activated by wild type p53 in response to DNA damage. When DNA damage occurs, activation of p53 (Lu and Lane, 1993) is believed to cause an increase in p21 levels and inhibition of CDK4-cyclin D and CDK2-cyclin E complexes. Cells would therefore be arrested in G1 phase of the cell cycle. In cells which have a mutant p53, p21 induction in response to DNA damage does not occur and cells proceed to replicate damaged DNA which contributes to genetic instability and cellular transformation (Hartwell, 1992)

As previously mentioned, cyclin E-CDK2 is involved late in G1 and is thought to act after the D-cyclins. Cyclin E levels increase late in G1 and remain elevated until early S phase when it is degraded. Overexpression of cyclin E does accelerate entry into S phase (Resnitzky et al., 1994) and deregulation of cyclin E-CDK2 may be involved in cellular transformation. It has been demonstrated that transformed mammalian cells are deficient in kinase-mediated control of progression through G1 phase of the cell cycle (Crissman et al., 1991). Overexpression of cyclin E has been found in human mammary tumors (Keyomarsi and Pardee, 1993) (Keyomarsi et al., 1994; Leach et al.,

1993) and several isoforms of cyclin E have been detected in only tumor tissues (Said and Medina, 1995). In addition, increased CDK2-cyclin E activity has been detected in highly tumorigenic hyperplasias and neoplasias in comparison to low tumorigenic hyperplasias (Said and Medina, 1995) and premature activation of cyclin E-CDK2 has been observed in cells lacking functional Rb (Herrara et al., 1996). Cyclin E has been implicated as a potential prognostic marker for breast cancer because alterations in cyclin E expression become progressively worse with increasing stage and grade of the tumor (Keyomarsi et al., 1994). Interestingly, inhibition of cell cycle progression in breast cancer cells by antiestrogens is associated with inhibition of CDK2 activity (Watts et al., 1995). Collectively, these results support a role for altered cyclin E-CDK2 activity in the process of cellular transformation.

After the cell has committed to progress into S phase and replicate its DNA, a number additional checkpoints are in place to ensure the ordered progression of events. In a normal cell, S phase is preceded by M phase and this order must be strictly maintained to prevent cells from undergoing an extra round of S phase. An important regulator of this process is the Cdc2-cyclin B complex. Many elegant experiments using temperature sensitive mutants of Cdc2 have shown that Cdc2-cyclin B complex identifies a cell as being in G2 (which follows S phase) and inhibits S phase from occurring again (reviewed in (Nurse, 1994)). A sequence of events occur that lead to the activation of Cdc2. First, the accumulation of cyclin B during late G2 occurs and cyclin B associates with Cdc2. Next, Cdc2 is phosphorylated on Thr161 (by CAK) and on Tyr 15 (by

Wee 1). The final activation step is the dephosphorylation of Cdc2 (by Cdc25) on Tyr 15 and this leads to full activation of the kinase and progression into M phase (reviewed in (King et al., 1994)). Active Cdc2 can phosphorylate a wide range of cellular substrates such as HMG1(Y), p70S6 kinase, myosin II light chain and histone H1 (Komatsu et al., 1997; Papst et al., 1998; Reeves and Nissen, 1995; Arion et al., 1988). At the end of mitosis, dephosphorylation of Thr 161 and degradation of cyclin B inactivate Cdc2. Generally, the presence of a particular CDK-cyclin complex will define the cell's position in the cell cycle. Alteration in the levels or activity of the CDK-cyclin complexes may result in deregulation of cell cycle control and contribute to cellular transformation. One of the interesting substrates for the CDK-cyclin complexes is histone H1 and H1 is often used as a substrate for CDK-cyclin kinase assays. The only exception to this is CDK4 (Matsushime et al., 1992).

The nucleus

The nucleus is the largest organelle in the cell and it occupies approximately 10% of the cell's total volume. It is composed of a nuclear envelope that is formed from two membranes, an inner membrane and an outer membrane (Fig. 6). The outer membrane is continuous with the endoplasmic reticulum. These two membranes are phospholipid bilayers and they contain pores that allow selected molecules to be actively transported into and out of the cytoplasm. Networks of intermediate filaments provide mechanical support for the nuclear envelope. A network of nuclear lamins that exists just inside the

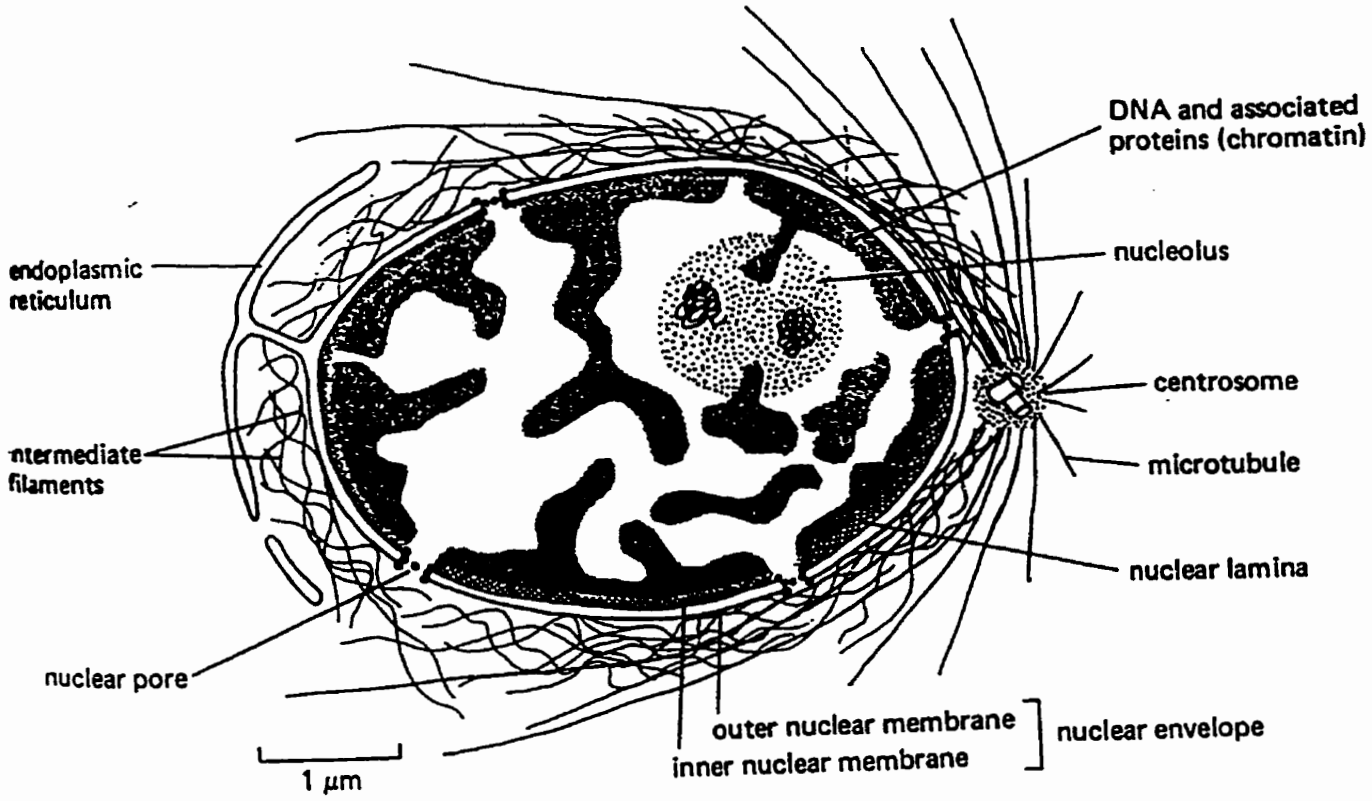

Figure 6. **The structure of the nucleus**. The nucleus is composed of a nuclear envelope that is formed from an inner and outer membrane. The outer membrane is continuous with the endoplasmic reticulum. These two membranes are phospholipid bilayers and they contain pores that allow selected molecules to be actively transported into and out of the cytoplasm. A layer of intermediate filaments that exists inside the nucleus (nuclear lamina) and a layer of intermediate filaments that surrounds the outer nuclear membrane both provide support to the nuclear envelope. Taken from Molecular Biology of the Cell, second edition.

nucleus (called the nuclear lamina) and a layer of intermediate filaments that surrounds the outer nuclear membrane provide support to the nuclear envelope. Within the nucleus exists a filamentous nuclear matrix and associated with the matrix are nuclear processes such as transcription, replication and dynamic histone acetylation (reviewed in (Davie, 1997)). Cellular transformation is accompanied by alterations in both nuclear and cytoplasmic organizations and pathologists have long observed aberrations in nuclear structure in cancer cells. Nuclei from different stages of disease progression exhibit changes in shape and chromatin structure that correlates with malignancy (Holth et al., 1998). As a result, aberrant nuclear and cellular structure can serve as markers for malignant transformation.

The cytoskeleton and nuclear matrix in cancer

The process of cellular transformation is accompanied by changes in nuclear and cytoplasmic organizations. The shape of a cell is attributable to a three-dimensional tissue matrix that links the nuclear matrix, cytoskeleton and extracellular matrix (reviewed in (Holth et al., 1998)). The cytoskeleton consists of microfilaments, microtubules and intermediate filaments. Chemical signaling events directly impact upon molecules that can influence the cytoskeleton. Contacts between the cytoskeleton and the nuclear matrix are also present. Furthermore, evidence suggests that intermediate filaments are also present in the nucleus (Spencer et al., 1998). Possibly changes in intermediate filament structure may influence gene expression through altering chromatin organization

(Holth et al., 1998). Cancer cells have a drastic alteration in their intermediate filament composition and this alteration may be a significant event in the establishment of the malignant phenotype (Holth et al., 1998).

The nuclear matrix is defined as the nuclear structure present following the salt extraction of nuclease-digested nuclei (reviewed by (Davie, 1995)). The protein composition of the nuclear matrix is tissue and cell type specific. Many transcription factors are associated with the nuclear matrix and it has been proposed that the nuclear matrix recruits transcription factors and facilitates their interaction with regulatory DNA elements. The nuclear matrix is directly associated with transcribed DNA sequences through matrix attachment regions (MARs) (Holth et al., 1998). Typically MARs refer to anchorage points at the base of DNA loops. Our laboratory has demonstrated that various nuclear matrix bound transcription factors are also bound to nuclear DNA sequences *in situ* (Samuel et al., 1998). Therefore, the nuclear matrix is not simply a storage site for inactive transcription factors; rather they are functional in terms of their association with nuclear DNA sequences. Our laboratory has also shown that the profile of nuclear matrix proteins is altered in oncogene-transformed cells and in tumor tissues (Samuel et al., 1998; Samuel et al., 1997). Using two-dimensional gel electrophoresis, nuclear matrix proteins were examined from a variety of human breast epithelial cancer cell lines. Several proteins were identified that were present only in the breast epithelial cancer cell lines and not in the spontaneously immortalized, control cell line (Samuel et al., 1997). In the

future, detection of changes in specific nuclear matrix proteins in cancer cells may be very useful as prognostic and diagnostic markers in cancer.

Functional organization of the nucleus

The investigation of nuclear processes such as transcription and replication has been mainly through biochemical and molecular biological approaches. Advances in electron microscopy and confocal microscopy have allowed researchers to adopt another method of studying gene expression that can complement already existing biochemical data. Methods of staining nuclei with fluorescent probes have allowed visualization of the spatial organization of different nuclear structures. Specific probes that recognize splicing factors, RNA Pol II and pre-mRNA have been very useful in studying the subnuclear organization of RNA Pol II transcription.

Indirect immunofluorescence studies have revealed that splicing factors are localized to 20-50 discrete speckle domains in the nucleus (reviewed in (Spector, 1993). A less concentrated and more diffuse localization of splicing factors is observed in the surrounding nucleoplasm. At the level of the light microscope, the speckled domains are the same as interchromatin granule clusters that can be seen at the electron microscope level (Spector et al., 1991). The speckled domains (interchromatin granule clusters) are located at the core of the larger nuclear compartment called the "transcript domain" and are surrounded by perichromatin fibrils (Carter et al., 1993). Poly (A) RNA has been shown to accumulate in the transcript domain. There are conflicting views as to

the fuction of the interchromatin granule clusters. One view is that they are sites of storage, assembly and recycling and that splicing takes place on the perichromatin fibrils where pre-mRNA is synthesized (Spector, 1993; Spector et al., 1991; Carter et al., 1993). Another view is that the interchromatin granule clusters are the sites of pre-mRNA processing (Xing et al., 1993). Data presented by Hendzel and Bazett-Jones somewhat resolved this discrepancy (Hendzel and Bazett-Jones, 1995). They have observed, by high-resolution electron microscopy, individual RNA polymerase II transcription units that originate outside of the transcript domain and terminate within the transcript domain on the outer surface of the interchromatin granule cluster (Hendzel and Bazett-Jones, 1995). It was suggested that individual transcript units may feed into single transcript domains where transcriptional processing may occur. Based on this data, they have suggested that the interface of the interchromatin granule cluster is the area that is functional in pre-mRNA processing (Hendzel and Bazett-Jones, 1995). There is also evidence that a dynamic and coordinated relationship between RNA Pol II transcription and transcript processing exists. When RNA Pol II transcription is inhibited, the interchromatin granule clusters increase in diameter and the perichromatin fibrils disappear. The splicing machinery basically relocalizes to enlarged interchromatin granule clusters (O'Keefe et al., 1994). In addition, when transcription inhibition is reversed, the numerous small speckled domains reappear; further indicating the dynamic nature of these processes (Bregman et al., 1995). In the future, similar

microscopy-based studies will allow researchers to have a more thorough and complete look at the nucleus and its functions.

Regulation of gene expression

The expression of a gene can be controlled at different levels. These include transcriptional control, RNA processing control, RNA transport control, translational control, mRNA degradation control and protein activity control. The control of gene expression at the level of transcription will be discussed in further detail. Eukaryotic cells contain three types of RNA polymerases, RNA polymerase I, II and II. The major difference between eukaryotic and prokaryotic RNA polymerases is that prokaryotic RNA polymerases bind directly to the promoter whereas eukaryotic polymerases bind to promoters only in the presence of other specific proteins that are already bound to the DNA. The three eukaryotic RNA polymerases are responsible for transcribing different types of genes. RNA polymerase II transcribes genes that encode proteins. RNA polymerase I transcribes the large ribosomal RNAs. RNA polymerase III transcribes small RNAs such as the small 5S ribosomal RNA and the transfer RNAs. In eukaryotic cells, sequence specific DNA binding proteins function to activate or repress expression of particular gene sequences. In eukaryotes, a set of transcription factors assembles in a specified order on a promoter. The minimal set of factors required for accurate transcription is TFIIB, TFIID, TFIIE, TFIIF, TFIIH, pol II and TFIIA. TFIID is composed of the TATA-binding protein

(TBP) and approximately ten TBP-associated factors called TAFs (Fig. 7) (reviewed in (Struhl, 1996)). In the first step, TFIID binds to the TATA element. The TAFs are believed to function in responding to transcriptional activators (Tjian and Maniatis, 1994). TFIID and TBP support the basal level of transcription. Different activator proteins bound to enhancer elements can participate in stimulating transcription. The activation domains of the activator proteins can interact with specific TAFs and these contacts can increase the binding of TFIID to the TATA and thereby stimulate transcription (Struhl, 1996). The TATA element is present in most but not all eukaryotic genes. Generally, the overall effect on gene activity depends upon the activating and repressing influences present. Differences in the transcription of a specific gene in different tissues may reflect the presence of tissue-specific positive or negative regulatory proteins bound to enhancer elements of the gene. In addition to specific regulatory proteins, the modulation of chromatin structure can also significantly influence gene expression. A chromatin remodelling multiprotein complex called SWI/SNF that functions in disrupting nucleosomes is present in stoichiometric amounts associated with the RNA pol II holoenzyme (Wilson et al., 1996). The presence of SWI/SNF in the pol II holoenzyme may cause changes in chromatin structure that stabilizes the transcriptional complex. The SWi/SNF-dependent effects on chromatin structure, however, are not sufficient in mediating the response to transcriptional activator proteins since they are also observed in promoters that are transcriptionally inactive (Wilson et al., 1996). An RNA Pol II

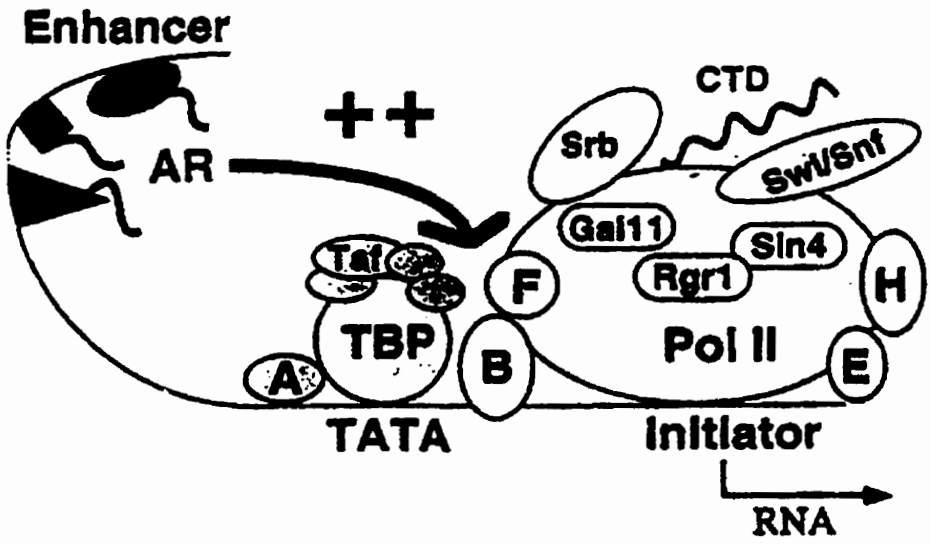

Figure 7. **Schematic illustration of pol II and other proteins present at a eukaryotic promoter.** Activator proteins bind to enhancer elements stimulate transcription by interacting with components of the TFIID and pol II holoenzyme. TFIIA is considered to be part of the TFIID group and TFIIB, TFIIE, TFIIF, TFIIH are considered part of the pol II holoenzyme. Taken from Struhl (1996). See text for details.

complex containing SWI-SNF and the histone acetyltransferases CBP (CREB binding protein) and PCAF has also been isolated (Cho et al., 1998).

Structural alterations of chromatin that occur during transcription can be observed as changes in the distribution of proteins bound to specific DNA sequences within the gene. The binding of sequence specific DNA binding proteins to their target sequences results in the development of Dnase I hypersensitive sites in the DNA. These sites arise from the formation of altered nucleosomes or altered histone-DNA complexes that make the DNA accessible to DNaseI digestion. When the β-globin gene expression is induced, there is an increase in the DNase I sensitivity over a large domain of the locus. For a gene that is transcriptionally repressed, DNAase 1 sensitive regions are no longer observed (Weintraub and Groudine, 1976; Larsen and Weintraub, 1982). Other studies demonstrate that the upstream nontranscribed region of the transcriptionally active somatic 5S ribosomal RNA gene is packaged with acetylated histone H4 and is sensitive to MNase (micrococcal nuclease) digestion. The same region of the oocyte, transcriptionally silent, 5S ribosomal RNA gene is packaged with hypoacetylated histone H4 and is less sensitive to MNase digestion (Howe et al., 1998). Generally, the DNA of transcriptionally active genes is more sensitive to nuclease digestion than the DNA of transcriptionally inactive genes.

Chromatin compaction in the nucleus

Eukaryotic DNA must be extensively packaged in order for it to reside in the nuclear space. The eukaryotic genome is of tremendous length and therefore requires a level of packaging that will place 2 m of DNA into a nucleus with a diameter of 5 to 10 μM. This level of packaging is achieved by the association of the DNA with histones to form chromatin. The chromatin is folded into higher order structures (Fig. 8) which range from the 30 nm structure to the condensed chromosomes present in mitosis (reviewed in (Getzenberg et al., 1991)). The presence of histones in all eukaryotic organisms reflects the requirement for cells to condense and package their DNA.

Chromatin Structure

Nucleosome structure

The basic repeating unit of chromatin is the nucleosome. It consists of 146 bp of DNA wrapped around a histone octamer that contains two dimers of core histones H2A and H2B and a tetramer of core histones H3 and H4. Histone H1 interacts with the nucleosome and the linker DNA that bridges adjacent nucleosomes. The X-ray crystal structure of the nucleosome has been solved to a resolution of 2.8 Angstroms (Luger et al., 1997) (Fig. 9). The individual histone polypeptides have a common structural helix-loop-helix that has been previously named the "histone fold" (Arents et al., 1991). The histone fold structural motif is composed of three α-helices connected by two loops. In the H2A-H2B and H3-H4 histone pairs these motifs form crescent shaped heterodimers that bind 2.5

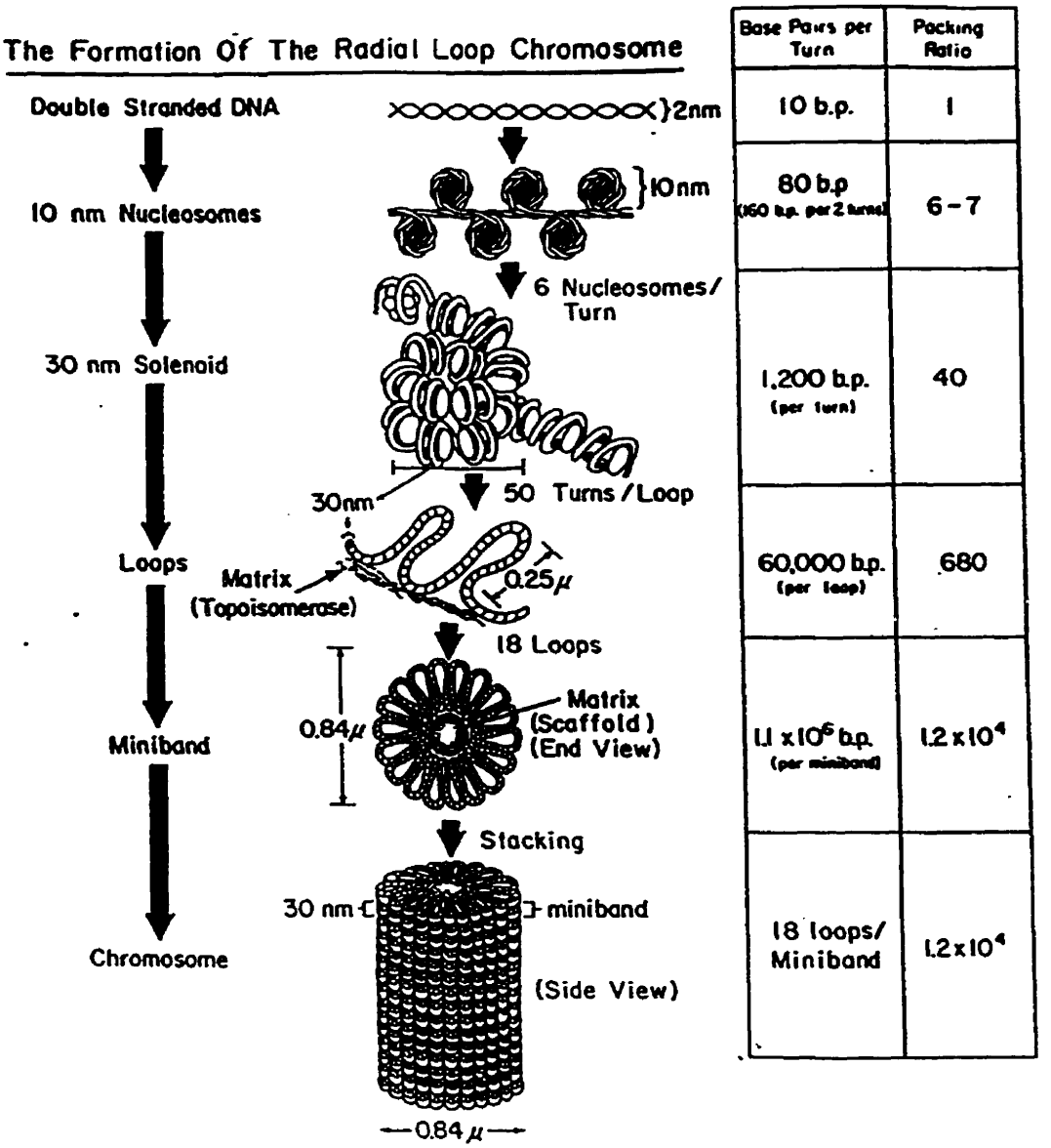

Figure 8. **Diagramatic representation of different orders of chromatin condensation.** The 10 nm fibre is composed of 160 bp of DNA wrapped twice around histone octamers. The 10 nm fibre is further wound at 6 nucleosomes per turn to form a 30 nm chromatin filament. The 30 nm filament forms loops that are attached approximately every 60,000 b.p. to the nuclear matrix at nuclear matrix attachment regions (MARs). Eighteen radial loops are wound to form a miniband unit and the minibands stack along a central axis to form the chromatid. Topoisomerase II is found in the center of the metaphase chromosome. Taken from Getzenberg et al. (1991).

Richmond Lab Crystal Structure of the Nucleosome at 2.8 Angstrom Resolution

Luger et al, 1997. Nature 389: 251-260

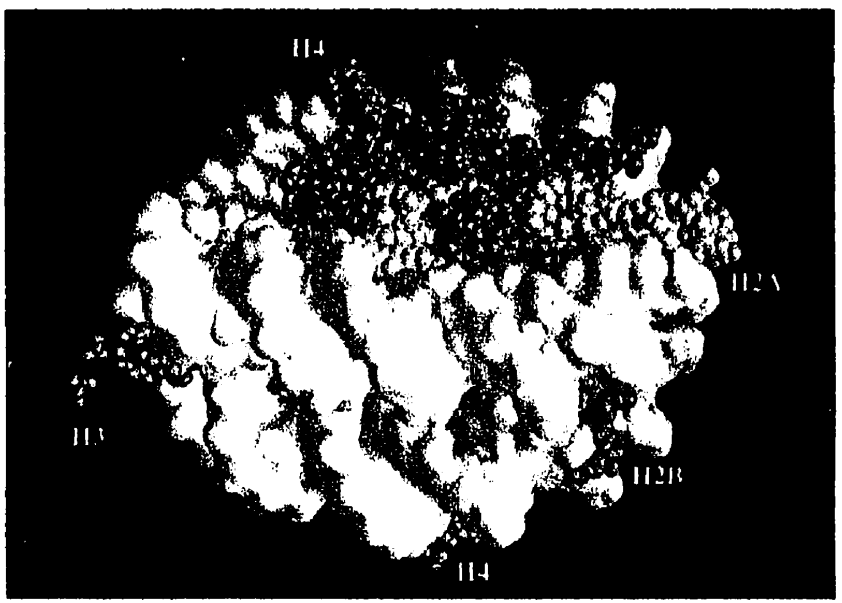

Figure 9. **X-ray crystal structure of the nucleosome.** The relative position of the four core histones in the nucleosome is indicated. Taken from Luger et al., (1997).

turns of DNA double helix (Luger et al., 1997). The octamer consists of four histone-fold dimers of H3-H4 and H2A-H2B pairs. The interaction between H3-H4 pairs occurs through a 4-helix bundle that is formed from the H3-H3 histone folds. The H2A-H2B pairs interact with the tetramer through a 4-helix bundle formed between the H2B and H4 histone folds. The crystal structure reveals that the DNA contacts with the histone octamer do not follow a regular path around the protein. Instead, the DNA is more curved at particular points along the nucleosome surface than others (Luger et al., 1997). It was suggested that this curvature may function to distort the DNA and encourage binding of particular transcription factors (Luger et al., 1997). The projection of the histone tails beyond the DNA is also observed in this model. At physiological ionic strength, chromatin exists as a highly condensed fiber of approximately 30 nm in diameter. The extensive packaging of DNA as chromatin provides an obstacle for cellular processes such as transcription and replication that require access to the DNA.

An interesting and long-standing question has been how does the transcriptional machinery process DNA that is assembled as chromatin? A number of models have been proposed which attempt to address this question. One model suggests that there is a direct transfer of octamers out of the path of the transcription complex (Clark and Felsenfeld, 1991). They provide evidence that a histone octamer can step around a transcribing polymerase without leaving the template. In this model, the DNA ahead of the polymerase uncoils from the octamer as the DNA behind coils around it (Studisky et al., 1994). A second model suggests that there is a disruption of the histone octamer with a change in

the histone domains that interact with the DNA (Nacheva et al., 1989). A third model proposes that the histone octamer ahead of the polymerase is released, and after the transcriptional complex passes, the histones may rebind (Widmer et al., 1984). The "progressive displacement" model proposed by Van Holde *et al.* (1992) suggests the approach of the RNA polymerase triggers the release of one H2A-H2B dimer from the nucleosome. This destabilization of the nucleosome will then promote release of DNA from an H3-H4 pair of the tetramer, allowing transcription to proceed through the dyad axis. Transcription proceeds through H3-H4 contacts eventually causing the release of the second H2A-H2B dimer, while the first H2A-H2B dimer rebinds. Transcription proceeds through remaining DNA and the second H2A-H2B dimer is recaptured. This model encompasses ideas from all of the previous models emphasizing the dynamic nature of chromatin (Van Holde et al., 1992)

The involvement of proteins that participate in remodelling chromatin is an important factor in this complex issue. Nucleosomes inhibit transcription at both the initiation and elongation steps. Recently, LeRoy *et al.*, (1998) described a chromatin-remodelling protein complex comprised of RSF (remodelling and spacing factor) and FACT (facilitates chromatin transcription) that can overcome both nucleosome inhibited steps of transcription (LeRoy et al., 1998). RSF disruption of nucleosomes facilitates the binding of activator proteins to upstream elements. The remodelled template then promotes the access of transcription factors and RNA Pol II, thus establishing chromatin that is competent to initiate transcription. The elongation through nucleosomes is then facilitated by

complexes like FACT that are able to overcome nucleosome-mediated inhibition of transcription (LeRoy et al., 1998).

Histone structure

The histones are present in the somatic cells of all eukaryotic organisms. The core histone structure consists of a long amino terminal domain, a histone fold, and a short carboxyl terminal domain. Core histones exhibit a number of common features. As previously mentioned, they possess a characteristic histone fold motif. They have high amounts of lysine and arginine residues and this enrichment of basic residues gives the histones a net positive charge at physiological pH. Some of the core histones are highly conserved in evolution; for example, the sequence of H4 from bovine and pea differs by only two amino acids. Many organisms have multiple copies of the histone genes and there exists different primary sequence variants of each histone.

Histone H1

The H1 histones are a heterogeneous group of several subtypes that differ in amino acid sequence (Cole, 1987; Lennox and Cohen, 1988; Parseghian et al., 1994). Histone H1 is a 21 kDa protein which binds the nucleosome core particle and fixes the points of DNA entry and/or exit (Van Holde, 1988). Recent evidence suggests that the H1 globular domain bridges one terminus of the DNA and the center DNA gyre (Zhou et al., 1998). H1 has three distinct structural domains, a short basic N-terminal domain, a central globular core, and a long C-

terminal domain. The H1 globular core interacts with the nucleosome core particle through contacts with H2A and H4. The N- and C-terminal domains are lysine rich and bind to linker DNA (Van Holde, 1988). It has been demonstrated that in order for the chromatin fiber to properly fold, the globular core and tail domains of H1 as well as the N-terminal tail domain of H3 must be present (Marion et al., 1983a; Marion et al., 1983b). Histone H1 is generally considered as a repressor of transcription, however, more recently it has been demonstrated that H1 can function as a positive or negative regulator of gene expression *in vivo* (Shen and Gorovsky, 1996).

H1 subtypes

The realization that many histone variants existed prompted studies to determine if different histone variants had different functions. Studies examining various murine and human H1 subtypes have lead to the suggestion that the subtypes do differ functionally. The H1 subtypes of the mouse have been extensively studied. The murine H1 subtypes consist of $H1^0$, H1a, H1b, H1c, H1d, and H1e. Many very interesting observations have been made about the mouse H1 subtypes. First, there are differences in the proportions of the H1 subtypes in dividing and non-dividing tissues of the mouse (Lennox and Cohen, 1983b). In murine liver, kidney and lung H1a and H1b and H1d are present at 1 week after birth; however, they decline to nearly undetectable levels by 8-16 weeks (Lennox and Cohen, 1983b). H1a is no longer present between 4-16 weeks when cells are no longer dividing. The levels of the other subtypes, H1e

and $H1^0$ and H1c increase markedly. There are no tissue specific H1 subtypes observed in the somatic tissues (Lennox and Cohen, 1983b). Generally, H1a and H1b seem to be synthesized in substantial amounts only in dividing cells whereas H1c, H1d, H1e and $H1^0$ are synthesized in dividing and non-dividing cells. The alteration of the composition of the subtypes is a process that accompanies the formation of nondividing cells (Lennox and Cohen, 1983b). The combination of changes in the pattern of synthesis and a differential loss of subtypes gives rise to the complement of subtypes present after the formation of nondividing cells.

Histone H3

Histone H3 is a 15 kilodalton protein that has a long N-terminal domain, a central globular domain, and a short carboxyl terminal domain. The N-terminal domain of H3 is exposed in chromatin and it has been shown to interact with the linker region and associate with H1 (Belyavsky et al., 1980). It has been proposed that H1 and the N-terminal domain of H3 are both required for proper chromatin folding (Marion et al., 1983a; Marion et al., 1983b; van Holde and Zlatanova, 1996; Leuba et al., 1998). In addition, H1 interacts with the N-terminal domain of H3 and may have a suppressive effect on H3 phosphorylation at mitosis (Shibata and Ajiro, 1993). It has been suggested that phosphorylation of H1 at mitosis releases this suppressive effect allowing access of the N-terminal domain of H3 for phosphorylation (Shibata and Ajiro, 1993). The H3 N-terminal domain can also undergo phosphorylation, methylation and acetylation.

Histone Modifications

The N-terminal domains of the core histones can be post-translationally modified by acetylation, methylation, phosphorylation and ADP- ribosylation and the C-terminal domains of histones H2A and H2B can be ubiquitinated (Fig. 10) (reviewed in (Van Holde, 1988)).

Histone Acetylation

All of the four core histones can undergo acetylation. Histone acetyltransferases catalyze the addition of acetyl groups to the ε-amino groups of specific lysine residues on the N-terminal tails of the core histones. Core histone acetylation is a dynamic process and histone deacetylases catalyze the reverse reaction by removing acetyl groups from the N-terminal domains. Generally, transcribed DNA sequences are associated with acetylated histones (Hebbes et al., 1988; Hebbes et al., 1992; Ip et al., 1988; Boffa et al., 1990; Hendzel et al., 1991b; Davie and Candido, 1978). A role for core histone acetylation was first proposed in 1964 by Dr. Vincent Allfrey (Allfrey et al., 1964). He noted that acetylation seemed to reduce how tightly the histones associated with the nucleosomal DNA and he suggested a role for core histone acetylation in facilitating transcription. Acetylated core histones are closely associated with transcriptionally poised or active genes (reviewed in (Davie, 1997). The acetylation of the N-terminal tails disrupts folding of the chromatin fibre and interactions with non-histone chromosomal proteins (Garcia-Ramirez et al., 1995; Edmondson et al., 1996). Experiments using antibodies that recognize

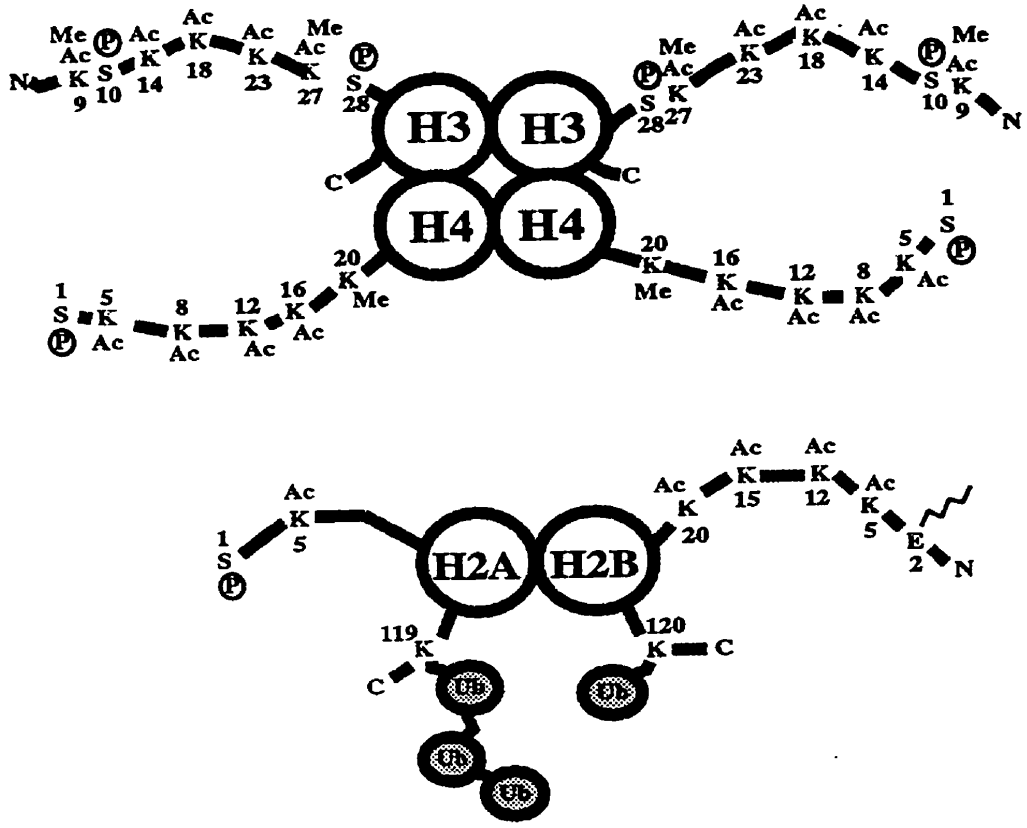

Figure 10. **Post translational modifications of core histones by acetylation, methylation, ubiquitination, and phosphorylation.** Sites of acetylation (Ac), methylation (Me), ubiquitination (Ub), and phosphorylation (P) are indicated. N indicates the amino terminus. The step ladder structure is poly ADP ribosylation.

acetylated sites of core histones have been a powerful tool in examining the association of acetylated histones with transcriptionally active gene sequences. Hebbes *et al.,* (1992) generated an antibody that specifically recognizes acetylated lysine residues of core histones. They demonstrated in immunoprecipitation experiments that chromatin containing acetylated histone was enriched in transcribed sequences (from 15 day chicken embryo erythrocytes) (Hebbes et al., 1992). An extremely exciting discovery in 1997, by Dr. David Allis' group, provided a fundamental link between histone acetylation and gene transcription. They found that the *Tetrahymena* histone acetyltransferase was homologous to the yeast transcriptional coactivator, GCN5 (Brownell et al., 1996). This finding suggested that the transcriptional coactivator may itself possess histone acetyltransferase activity and this started a wave of activity in the chromatin field. When tested, they found that GCN5 did possess histone acetyltransferase activity. Other transcriptional regulators such as $TAF_{II}250$ and CBP have now also been found to possess histone acetyltransferase activity (Mizzen et al., 1996; Bannister and Kouzarides, 1996; Ogryzko et al., 1996). There is now a substantial amount of data that supports the hypothesis that histone acetylation plays an integral role in the regulation of gene transcription. Histone acetylation also has a role in DNA replication, DNA repair and spermatogenesis.

Histone Ubiquitination

The ubiquitination of cytoplasmic proteins is a widely known process where ubiquitin is covalently attached to proteins that are to be targeted for proteolysis (reviewed in (Ciechanover et al., 1984)). The ubiquitination of histones has also been observed. Histones H2A and H2B are modified by the addition of ubiquitin to the ε-amino group of the C-terminal tail through formation of an isopeptide bond. Generally H2A is ubiquitinated to a greater extent than H2B. Ubiquitination is a dynamic process and there are enzymes that cleave the isopeptide bond between the ε-amino groups and ubiquitin. The function of histone ubiquitination remains elusive. Studies have indicated that uH2A is formed continuously during interphase, and there is a rapid turnover of bound ubiquitin in dividing and non dividing cells (Goldknopf et al., 1980a; Wu et al., 1981). It has been suggested that ubiquitination may open chromatin structure and correlative evidence exists that supports this hypothesis. For example, it has been demonstrated that ubiquitinated H2A (uH2A) is converted to H2A when transcription is ceased during erythropoiesis in the chicken (Goldknopf et al., 1980b). Interesting results from our laboratory revealed that the inhibition of transcription in T47D-5 cells (human breast cancer cell line) using the transcriptional inhibitors DRB, and actinomycin D caused a drastic decrease in the level of uH2B (Davie and Murphy, 1990). Removing the DRB from the cell medium reverses the effect of transcription inhibition by DRB. Upon removal of transcription inhibition by DRB, the levels of uH2B were restored to normal levels. As a result, the ubiquitination of H2B was coupled to ongoing

transcription. Treatment of the cells with aphidicolin, an inhibitor of replication, did not have any affect on the levels of uH2B. Also, treatment of the cells with heat shock, a process that represses the expression of most genes and induces the expression of a few genes, resulted in the loss of all monoubiquitinated histone species. This was the first demonstration of a histone modification being dependent upon transcription and it was proposed that the transcriptional process disrupts the chromatin structure such that the site of ubiquitination is available to be modified. The ubiquitination of H2B would then prevent the refolding of the nucleosome and thereby facilitate further rounds of transcription (Davie and Murphy, 1990).

Histone Poly ADP-ribosylation

Poly ADP ribosylation of various proteins has been observed in eukaryotes. ADP-ribosylation occurs by the transfer of an ADP ribose from nicotinamide adenine dinucleotide (NAD^+) to an acceptor molecule. Each ADP-ribose can in turn act as an acceptor for another ADP-ribose group and therefore a chain of ADP-ribose groups can be formed on an acceptor protein. Significant amounts of ADP-ribose have been found associated with H2B and H3 and much smaller amounts are associated with H2A and H4 (reviewed in (Van Holde, 1988). Histone H1 has been shown to be the most extensively modified by ADP-ribosylation. When cellular DNA is damaged, the level of ADP-ribose associated with the histone rises (Van Holde, 1988). A role for ADP-ribosylation in DNA repair has therefore been suggested. The ADP-ribosylation of histones is

maximal during G2 phase of the cell cycle when the levels of the ADP-ribose polymerase is maximal. The process of ADP-ribosylation is a dynamic one since there are nuclear enzymes that degrade the ADP-ribose.

Histone Methylation

Histones H3 and H4 can undergo methylation of the ε-amino groups of lysine side chains on the amino terminal domains. Murray (1963) first demonstrated the presence of methylated histones in the cell. The specificity of methylation has been conserved throughout evolution for example, in almost all eukaryotes examined, residue 20 of H4 is methylated and residues 9 and 27 of H3 are methylated. It has been suggested that unlike acetylation and phosphorylation, histone methylation occurred throughout the bulk of the genome (Thomas et al., 1975). Experiments performed by other groups suggest, however, that non-random methylation of histones in specific regions of chromatin may exist (Reneker and Brotherton, 1991). In addition, newly methylated histones may be associated with acetylated histone species (Reneker and Brotherton, 1991; Hendzel and Davie, 1991a)

Histone phosphorylation

Ord and Stocken first demonstrated phosphorylation of histones, in 1966 (Ord and Stocken, 1966). All core histones and histone H1 can undergo phosphorylation. There are two different types of histone phosphorylation. One type occurs on hydroxyl groups of Ser and Thr residues and the other type

occurs on lysine, histidine and arginine residues through P-N linkages (Van Holde, 1988). The latter type is less studied since the P-N linkages are labile and lost in acid extraction of histones. Phosphorylation of histones on specific serine and threonine residues will be examined in this thesis. *In vivo* phosphorylation of histone H4 has been demonstrated on the N-terminal serine residue. H3 is phosphorylated *in vivo* on Ser 10 (Paulson and Taylor, 1982; Ajiro and Nishimoto, 1985) and *in vitro* by c-AMP dependent kinase on Ser 28. H2B is phosphorylated on serine 32 and 36 *in vitro* by c-AMP dependent and c-GMP dependent kinases (Hashimoto et al., 1976; Glass and Krebs, 1982). H2A is phosphorylated *in vivo* on the N-terminal serine in trout testes (Sung and Dixon, 1970) and *in vitro* by c-AMP-dependent kinase at serine 19. In Tetrahymena, the C-terminal serines 122, 124, 129, of H2A.1 and Ser 122 and Ser 128 of H2A.2 are *in vivo* phosphorylation sites (Fusauchi and Iwai, 1984). H1 phosphorylation will be discussed next.

H1 phosphorylation

H1 phosphorylation has been extensively studied in a variety of different cell types. H1 can be phosphorylated on the N-terminal and C-terminal domains of the molecule on Ser/Thr residues that are part of –Ser/Thr-Pro-X-Lys/Arg consensus sequence motifs (Fig. 11) (Hill et al., 1991). The phosphorylation of H1 is cell cycle dependent with the highest level of phosphorylation occurring in M-phase. In G1 phase of the ceil cycle, the lowest number of sites is phosphorylated and there is a gradual increase in the number of sites that are

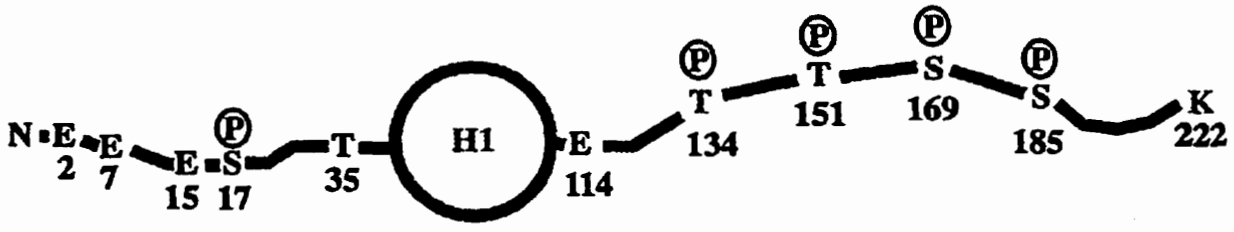

Figure 11. **Sites of histone H1b phosphorylation.** The sites of phosphorylation of H1b are indicated (P). These sites are also contained within Cdc2/Cdk2 kinase consensus sequence motifs. N refers to the amino terminus.

phosphorylated throughout S and G2 phases. In M phase, when chromatin is highly condensed, the maximum number of sites is phosphorylated (Fig. 12) (Van Holde, 1988). Cell cycle controlled phosphorylation of H1 is interesting and this process may be controlled by the cell cycle regulated kinases CDC2/CDK2 (Roth et al., 1991). Different H1 subtypes are phosphorylated to varying extents. Lennox *et al.* (1982) analyzed the phosphorylation states of the different murine H1 subtypes and they observed striking differences among the degree of phosphorylation of the different subtypes during interphase. These differences were evident in both the proportion of molecules present as phosphorylated forms and in the number of phosphate groups per molecule (Lennox et al., 1982). In addition, they observed that actually two types of phosphorylations occurred. Most phosphorylations did not significantly alter the mobility of the protein in an SDS polyacrylamide gel; however, there was one type of phosphorylation that did result in the protein having a slower mobility in SDS polyacrylamide gels. This type of phosphorylation was designated as "c" phosphorylation (for example c-phosphorylated H1b or c-pH1b) since they believed it might reflect an alteration in the protein conformation upon phosphorylation (Lennox et al., 1982). Lennox *et al.* (1982) and Talasz *et al.* (1996) have analyzed the phosphorylated forms of H1 at different phases of the cell cycle. In both of these studies acid/urea/triton (AUT) gel electrophoresis was used to separate the phosphorylated H1 subtypes. AUT gels are commonly used to separate highly basic proteins like histones and the separation is based on the size, charge, and hydrophobicity of

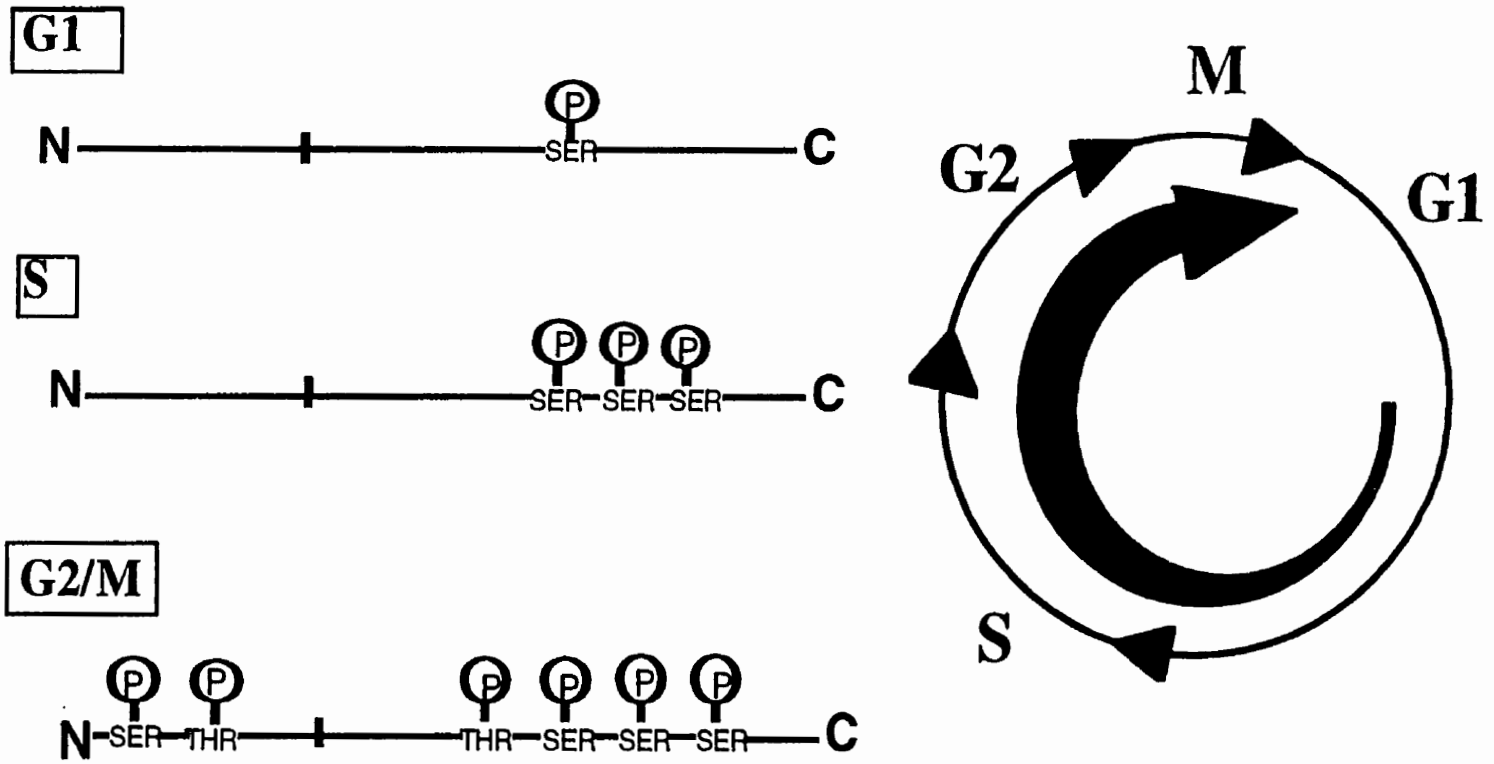

Figure 12. **Cell cycle regulation of histone H1 phosphorylation in CHO cells.** In G1, the lowest number of H1 sites are phosphorylated and an increasing number of sites are phosphorylated as cells progress through the cell cycle. Adapted from Hohmann (1983).

the protein (Delcuve and Davie, 1992). The results from both of these studies indicate that mouse H1b has the highest number of phosphate groups per molecule in interphase (Lennox et al., 1982; Talasz et al., 1996). Talasz *et al.* (1996) grouped the subtypes into two categories, those with low phosphorylation levels (H1a, H1c, $H1^{0}$) and those with high phosphorylation levels (H1b, H1d, and H1e). They also point out that the number of "SPKK" motifs corresponded with the maximal number of phosphorylation sites found. The data is summarized in Fig. 13. The observations that the H1 subtypes are present at distinctly different levels in dividing and nondividing tissues and that different subtypes are phosphorylated to varying degrees during interphase implies that they may be functionally distinct. Ajiro *et al.* (1981) have analyzed the phosphorylated subtypes of HeLa cells and they also have discovered distinct differences between the two human subtypes H1A and H1B. Upon analysis of the phosphorylation sites of human histones H1A and H1B during the HeLa S-3 cell cycle, they observed that H1B had more phosphorylated forms than H1A. They also observed two different S-phase phosphorylations, one that precedes and one that follows the onset of replication. This led to the suggestion that the phosphorylation of H1 at a particular site on the C-terminal may produce a chromatin conformation that permits DNA replication (Ajiro et al., 1981a). The authors suggested that the differences of H1A and H1B with respect to the number of phosphorylated forms may have different effects on the chromatin conformation and that subtype selective phosphorylations may represent a means of modulating chromatin organization (Ajiro et al., 1981a).

Table 1: Maximal Number of Phosphate Groups per Histone Molecule during the G1 and S Phases and Mitosis[a]

	late G1	late S	mitosis
H1a	1	1	4
H1b	2 (2)	3 (3)	5 (5)
H1c	1 (1)	1 (1)	4 (4)
H1d	1 (1)	2 (2)	5 (5/6)
H1e	1 (1)	2/3 (3)	4 (5)
$H1^0$	1	1	3 (3)

[a] Values are numbers of phosphate groups per molecule of histone variants from mouse fibroblasts and from rat glioma cells (in parentheses). The phosphate groups of $H1^0$ from the G1 and the S phase and of H1a are determined only from mouse fibroblasts.

Figure 13. **In vivo phosphorylation of H1 subtypes.** Phosphorylated H1 subtypes present at different cell cycle phases. The H1 subtypes can be grouped into two categories, those with low phosphorylation levels (H1a, H1c, $H1^0$) and those with high phosphorylation levels (H1b, H1d, and H1e). Taken from Talasz et al. (1996).

As previously mentioned, there is a strong correlation between the presence of highly phosphorylated H1 and chromatin condensation in mitosis. This correlation lead to the assumption that H1 phosphorylation drives mitotic chromatin condensation, however, there remains no evidence for a direct role of H1 phosphorylation in inducing chromatin condensation. Instead, it has been observed that H1 phosphorylation destabilizes chromatin structure and weakens its binding to DNA (Hill et al., 1991). Evidence that supports the involvement of H1 phosphorylation in the regulation of chromatin structure during replication comes from studies done with salt-treated SV40 minichromosomes reconstituted with differentially phosphorylated forms of H1. The minichromosomes reconstituted with S-phase H1 had higher replication efficiency than those reconstituted with G0- or M-phase H1 (Halmer and Gruss, 1995). It was suggested that the chromatin structure induced by the phosphorylation of H1 affects the efficiency of replication. Also, in a number of different eukaryotic systems H1 phosphorylation appears to be correlated with decondensation of chromatin rather than condensation (Fig. 14) (Roth and Allis, 1992). For example, the ciliated protozoa Tetrahymena contain two nuclei, a micronucleus and a macronucleus. The micronuclei are transcriptionally inactive and divide mitotically whereas, the macronuclei are transcriptionally active and divide amitotically. During conjugation, the old macronuclei become transcriptionally inactive, the chromatin becomes condensed and histone H1 is dephosphorylated (Roth and Allis, 1992). In avian erythropoeisis, the immature erythrocyte that

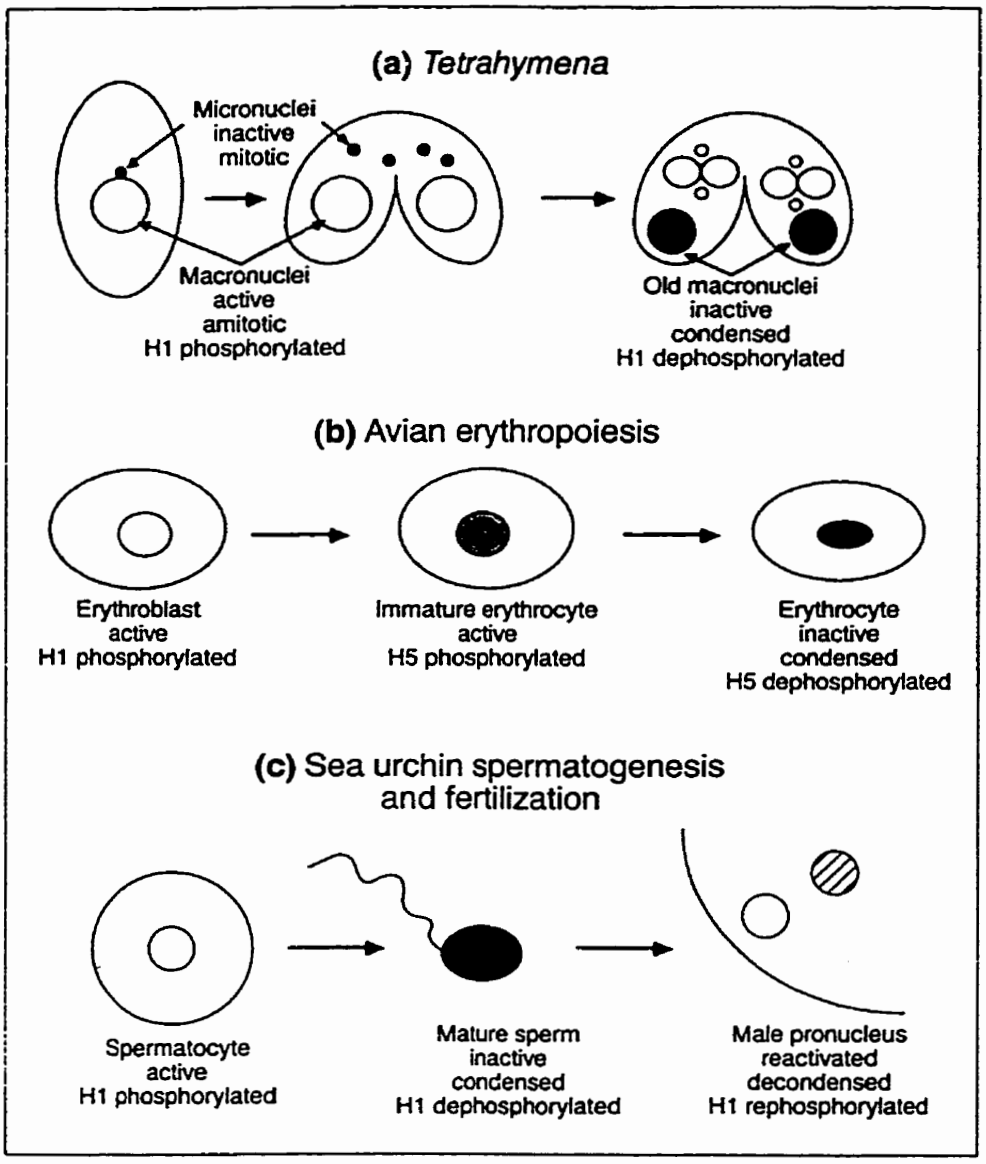

Figure 14. **Correlation between H1 phosphorylation and decondensation of chromatin.** In Tetrahymena (a) during conjugation, the old macronuclei become transcriptionally inactive and this process involves the condensation of the chromatin and the dephosphorylation of H1. In avian erythropoeisis (b), the immature erythrocyte that is transcriptionally active contains highly phosphorylated histone H5 (avian H1 variant). In the mature erythrocyte H5 is dephosphorylated and this is accompanied by the compaction of chromatin into a transcriptionally inactive state. In sea urchin spermatogenesis (c), the transcriptionally active spermatocyte H1 is phosphorylated, however, in the mature sperm where the chromatin becomes highly condensed, H1 is dephosphorylated. Upon fertilization, the male pronucleus is reactivated, the chromatin decondensed and H1 is rephoshorylated. Taken from Roth and Allis (1992)

is transcriptionally active contains highly phosphorylated histone H5 (avian H1 variant). In the mature erythrocyte H5 is dephosphorylated and this is accompanied by the compaction of chromatin into a transcriptionally inactive state. A third example of the association of dephosphorylated H1 with condensed chromatin is found in sea urchin spermatogenesis. In the transcriptionally active spermatocyte H1 is phosphorylated, however, in the mature sperm where the chromatin becomes highly condensed, H1 is dephosphorylated. Upon fertilization, the male pronucleus is reactivated, the chromatin decondensed and H1 is rephoshorylated. In all three of these systems, H1 phosphorylation is correlated with decondensation of chromatin and dephosphorylated H1 is associated with highly condensed chromatin (Roth and Allis, 1992). In the mammalian cell cycle, H1 phosphorylation is highest in M phase when the chromatin is highly condensed into mitotic chromosomes. This presents a clear contradiction to the three systems described above. Roth and Allis (1992) have presented a revised model for the role of histone phosphorylation in chromatin condensation that addresses the function of H1 phosphorylation both in interphase and in mitosis. They proposed that when H1 is unphosphorylated, the positively charged H1 tails shield the negative charge of the linker DNA phosphates. Phosphorylation of H1 would weaken the H1-DNA interactions and the exposed negative charge of the DNA phosphate backbone would cause repulsion of the adjacent DNA fibres and allow access of the DNA to factors involved in transcription or replication (Roth and Allis, 1992). During mitosis, they propose that H1 phosphorylation would result in transient

decondensation of chromatin which would allow access of the DNA to specific chromatin condensing factors such as topoisomerase II. Varying levels of phosphorylated H1 are achieved during different stages of the cell cycle by the presence and activity of particular H1 kinases (such as CDK2/CDC2). The outcome of decondensation of the chromatin by phosphorylation of H1 at different cell cycle phases would depend on the specific factors that access the DNA during each cell cycle phase. In support of this model, data from a number of research groups have suggested a role for H1 phosphorylation in gene transcription and these studies will be discussed next (Lu. et al., 1995; Sweet et al., 1996; Lee and Archer, 1998).

H1 phosphorylation and transcription

Many studies have focussed on elucidating the functional role of histone H1 phosphorylation. Recent studies suggest that H1 phosphorylation may have a role in gene transcription. Lu *et al.* (1995) demonstrated that phosphorylated and dephosphorylated histone H1 reside in distinct chromatin domains in Tetrahymena macronuclei. They observed that dephosphorylated H1 is found in condensed chromatin bodies; however, phosphorylated H1 is enriched at the periphery of the chromatin bodies and in the surrounding decondensed euchromatin which is undergoing active transcription. It was suggested that phosphorylation of linker histone plays an important role in establishing transcriptional competence in macronuclei. In addition, in Tetrahymena macronuclear development the dephosphorylation of H1 is clearly associated

with the formation of condensed chromatin and transcriptional silencing (Sweet et al., 1996). More recently, Lee and Archer (1998) demonstrated that inactivation of the MMTV promoter is associated with dephosphorylation of H1 and reactivation of the promoter is associated with rephosphorylation of histone H1. Collectively these studies provide evidence for a close relationship between phosphorylation of H1 and gene transcription.

Histone H3 phosphorylation

The N-terminal domain of H3 can be phosphorylated on Ser 10 and Ser 28 (Taylor, 1982; Shibata et al., 1990) (Fig. 15). Though most of the studies on H3 phosphorylation have focussed on the mitosis-associated phosphorylation, H3 phosphorylation also occurs in G1. Phosphorylation of histone H3 has been implicated in the establishment of transcriptional competence of early response genes. Mahadevan *et al.* (1991) observed that a 15 kDa protein is rapidly phosphorylated when serum starved cells are treated with growth factors and phorbol esters. This phosphorylation occurs concurrently with the transcriptional activation of the early response genes c-*fos* and c-*jun*. Microsequence analysis was performed on the protein and it was identifed as histone H3. Induction of H3 phosphorylation by mitogens occured even in the presence of transcription inhibitors and therefore this phosphorylation event is not a secondary effect arising from transcriptional activation of the early response genes. The speed of the intracellular signaling was very rapid and phosphorylation of H3 was observed within 5 minutes. The phosphorylation of H3 was maximal at 1h and

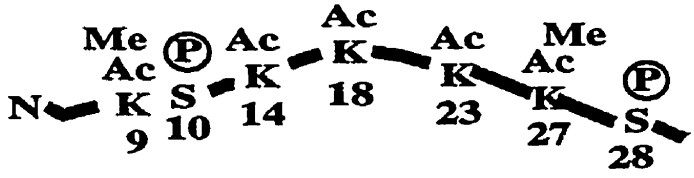

Figure 15. **H3 phosphorylation sites.** Histone H3 can be phosphorylated on the N-terminus at Ser 10 and Ser 28. Ser 10 is a mitosis specific phosphorylation.

no longer detectable after 3h. As previously mentioned, H3 can be phosphorylated on Ser 10 or Ser 28. The target site(s) for mitogen-induced phosphorylation, however, was not determined in these experiments. It was suggested that these different agents all elicit a common nuclear signaling event that may modulate nucleosomal structure and function thereby contributing to reguation of proto-oncogene induction. Further studies on mitogen-induced phosphorylation revealed that the phosphorylation does not occur on all H3 molecules. Instead, it is restricted to a small fraction of H3 histones that are extremely sensitive to sodium butyrate-induced hyperacetylation (Barratt et al., 1994a). The acetylation of H3 itself does not predispose H3 to phosphorylation and similarily the phosphorylation does not predispose H3 to enhanced acetylation (Barratt et al., 1994a). These results implied that the mitogen-regulated H3 kinase and butyrate-sensitive deacetylases act on a common, extremely small population of nucleosomes. Furthermore, this population is not selected by the utilization of particular H3 variants. Therefore, it was suggested that the mitogen-regulated kinase and the acetyltransferase are restricted to a small fraction of nucleosomes and that chromatin modulation by these processes at specific areas of the genome may be involved in early gene activation (Barratt et al., 1994a). The induction of H3 phosphorylation occurs when cells are treated with a wide range of agents such as growth factors, phorbol esters, and protein synthesis inhibitors. In addition, the phosphorylation of chromatin-associated protein, HMG-14, also occurs under these conditions (Barratt et al., 1994b). The ERK pathway is strongly activated in response to EGF and TPA, and the

JNK/SAPK pathway is strongly activated in response to anisomysin (protein synthesis inhibitor) and okadaic acid. H3 and HMG-14 phosphorylation is triggered by activation of either the ERK or the SAPK/JNK pathways and therefore neither pathway is absolutely essential for this response (Cano et al., 1995). Anisomycin and growth factor treatment of cells also results in activation of p70/p85^{S6k} and phsophorylation of S6 ribosomal protein (Franco and Rosenfeld, 1990). This kinase can be completely inhibited by rapamycin, an immunosuppresant. Studies by Kardalinou *et al.* (1994) demonstrate that ablation of EGF-, TPA- or anisomycin- stimulated S6 phosphorylation while rapamycin has no affect on H3 phosphorylation or on c-*fos* and c-*jun* induction. Therefore, it has been proposed that a rapamycin-defined area upstream of p70^{S6K} exists that contains a bifurcation to histone H3 and HMG-14 phosphorylation, and c-*fos* and c-*jun* induction in the nucleus (Kardalinou et al., 1994). A model proposed by Cano *et al.* (1995) suggests that the induction of early response genes, c-*fos* and c-*jun*, requires H3 and HMG-14 phosphorylation as an essential prerequisite (Franco and Rosenfeld, 1990). The identity of the H3 kinase remains unknown, but it is clear that the kinase would have to be inducible by both the growth factor- and stress- activated MAP kinase pathways.

Studies focussed on H3 phosphorylation during mitosis include a recent study by Wei *et al.* (1998) which reveals that Ser-10 phosphorylation of H3 is correlated with both mitotic and meiotic divisions in Tetrahymena micronuclei and this phosphorylation closely coincides with chromosome condensation. Hendzel *et al.* (1997) describe a precise spatial and temporal correlation between H3

phosphorylation and the initial stages of chromatin condensation. They observed that mitosis-specific phosphorylation of H3 on Ser-10 initiates primarily within percentromeric heterochromatin during late G2, spreads in an ordered fashion throughout the condensing chromatin, and is complete just prior to the formation of the prophase chromosomes (Hendzel et al., 1997). They suggested that phosphorylation of H3 at Ser-10 may regulate protein-protein interactions to promote binding of factors that drive chromatin condensation or H3 phosphorylation may co-ordinate chromatin decondensation associated with M-phase (Hendzel et al., 1997).

H1 and H3 (kinases and phosphatases)

The different kinases which have been shown to phosphorylate H1 *in vitro* are c-AMP and c-GMP dependent kinases and the growth associated H1 kinases (CDK's) (Van Holde, 1988). The CDK's are believed to be involved in the cell cycle dependent phosphorylation of H1. Swank *et al.*, 1997 demonstrate that four distinct cyclin-dependent kinases can phosphorylate H1 at all of the growth related phosphorylation sites *in vitro* (Swank et al., 1997). Since there appears to be no site selectivity among these kinases the authors suggest that the *in vivo* cell cycle dependent H1 phosphorylations must involve differential accessibility of H1 sites at different stages of the cell cycle (Swank et al., 1997). In Tetrahymena, the kinase which phosphorylates H1 in macronuclei (which divide amitotically) is distinct from the H1 kinase active in the micronuclei (which divide mitotically). Sweet *et al.* (1993) demonstrated that PKA (c-AMP dependent

protein kinase) or a PKA-like kinase is responsible for the phosphorylation of H1 in micronuclei. In macronuclei, however, a Cdc2-like kinase is involved. The identity of the H3 kinase remains unknown; although phosphorylation of H3 has been correlated with PKA activity (Waring et al., 1997). Waring *et al.* (1997) have demonstrated that treatment of thymocytes with gliotoxin, which induces apoptosis, is accompanied by phosphorylation of histone H3 and DNA fragmentation. When apoptosis is inhibited by genistein (which also inhibits PKA), histone H3 phosphorylation is also inhibited (Waring et al., 1997). Su *et al.* (1998) have shown that during mitosis, H3 phosphorylation correlates well with CDK1 activity in syncytial divisions of Drosophila embryos. *In vitro* studies identify H3 as a substrate for a number of other different kinases such as $pp90^{rsk}$, DLK (DAP like kinase), and a new 180 kDa kinase that phosphorylates prothymosin and H2B (Perez-Estevez et al., 1997; Kogel et al., 1998; Chen et al., 1992). Further studies are needed to identify the *in vivo* kinase(s) that phosphorylate H3, in G1 phase and in mitosis.

The state of phosphorylation of a protein is dependent upon a balance of phosphatase and kinase activities in the cell. Paulson *et al.* (1996) have suggested that protein phosphatase 1 is the H1 phosphatase. They found that inhibition of H1 phosphatase activity in metaphase arrested HeLa cells was achieved with okadaic acid and microcystin LR at concentrations which strongly suggest that PP1 (protein phosphatase 1) is the H1 phosphatase (Paulson et al., 1996). Interestingly, PP1 is also subject to phosphorylation by CDK2, which results in a decrease in its activity (Dohadwala et al., 1994). Changes in PP1

activity occur during the cell cycle with a high level of activity in G0, a progressive decrease in the activity in G1 and S phases, and in M phase there is a sharp increase in the activity again (Dohadwala et al., 1994). Possibly, the phosphorylation of both PP1 and H1 by CDKs may control the level of H1 phosphorylation throughout the cell cycle.

Histone modifications and cellular transformation

Phosphorylation of H1 is cell cycle regulated and when there is deregulation of cell cycle control such as in cancer, an accompanying change in histone phosphorylation and possibly chromatin structure may also occur. There is evidence that oncogene-transformed cells have an altered chromatin structure (Laitinen et al., 1990; Mello and Chambers, 1994; Chadee et al., 1995). Such a change in chromatin structure could be a result of alterations of levels of histone subtypes or in the post-translational modification of the histones. The analysis of the involvement of histone modification in cellular transformation has been limited. The main exception being histone H1 phosphorylation which has been the focus of a number of studies involving oncogene-transformed cell lines and tumor tissues of mouse. Lennox *et al.* (1982) analyzed the phosphorylated forms of H1 in cell lines derived from murine teratocarcinomas. They identify H1b as the subtype, which is the most highly phosphorylated species. Increased phosphorylation of H1b has also been observed in tumor tissues of mouse (Lewis lung carcinoma) in comparison to normal lung tissues (Giancotti et al., 1987). It has been reported that some transformed cells have alterations in the

amounts of H1 variants and it was suggested that they might be significant in cell transformation (Tan et al., 1982). In addition, NIH-3T3 cells transformed by the c-Ha-*ras* oncogene have been shown to have a decrease in the histone $H1^{\circ}$ subtype and an increase in nucleosome repeat length (Laitinen et al., 1994). The authors suggest that the decrease in $H1^{\circ}$ may play a role in chromatin changes in transformed cells by weakening internucleosomal interactions and destabilizing the chromatin structure. Interestingly, fibroblasts lacking the tumor suppressor Rb also exhibit an increased level of phosphorylated H1 and relaxed chromatin structure and it was suggested that deregulation of CDK2 may be directly involved (Herrara et al., 1996). The retinoblastoma protein has been found to exist in a complex with histone deacetylase and the transcriptional activator E2F and transcriptional repression mediated by the tumor suppressor Rb may occur through recruitment of a histone deacetylase (Magnaghi-Jaulin et al., 1998; Brehm et al., 1998; Luo et al., 1998). When Rb is phosphorylated, E2F is released allowing transcription of E2F regulated genes, one of which is cyclin E. As previously mentioned, cyclin E complexed with CDK2 is thought to be involved in phosphorylation of H1 in transformed cells (Fig. 16). Possibly, an altered chromatin structure acquired by deregulation of processes that control histone modifications such as phosphorylation of H1 and H3 may facilitate aberrant gene expression in the process of cellular transformation.

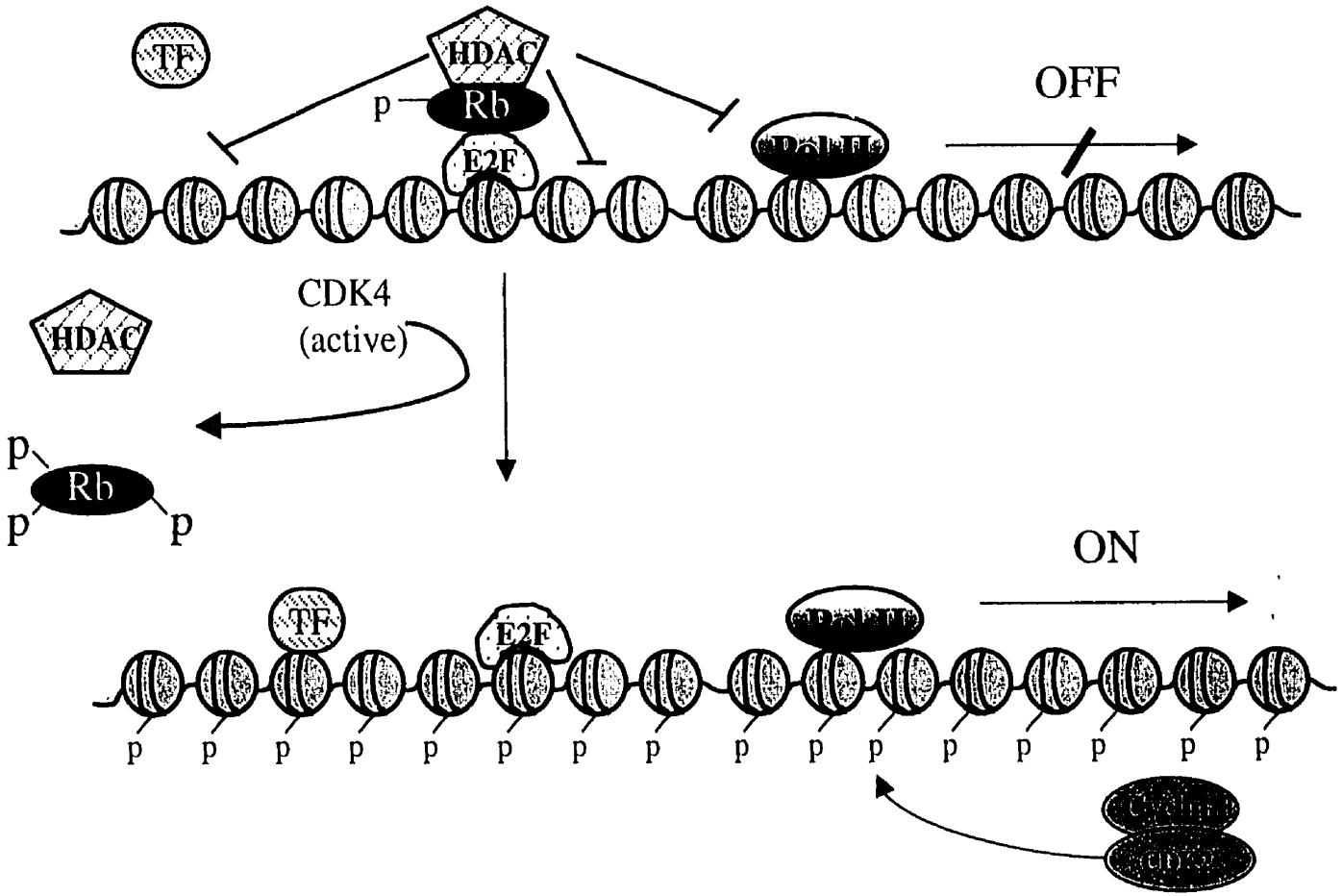

Figure 16. **The cancer chromatin connection: Regulation of gene expression by Rb and histone deacetylase**. The retinoblastoma protein has been found to exist in a complex with histone deacetylase and the transcriptional activator E2F. This complex prevents expression from E2F-bound promoters. HDAC1 may cause removal of acetyl groups from the core histones causing tighter binding between the DNA and the histones. When Rb is phosphorylated, E2F is released allowing transcription of E2F regulated genes, one of which is cyclin E. Cyclin E /CDK2 kinase is believed to be involved in phosphorylation of H1 in transformed cells and this phosphorylation may influence gene expression by modulating chromatin structure. Adapted from Depinho (1998).

Objectives

It has been reported that *ras*-transformed NIH-3T3 cells have a more open chromatin structure than parental cells. Upon confirming these observations in our own laboratory, we proceeded to analyze the H1 subtype composition of parental and *ras*-transformed cells and found no significant differences between the cell lines. With the knowledge that H1 and H3 are critical in stabilization of the chromatin fiber, our main objective was to analyze the phosphorylation of H1 and H3 in parental and oncogene-transformed cells to determine if oncogene-transformed cells had higher levels of phosphorylated H1 and/or H3 than the parental cells. We hypothesized that persistent activation of the Ras/MAPK pathway in oncogene-transformed cells may lead to increased H1 and/or H3 kinase activities and increased levels of phosphorylated H1 and/or H3. An increased level of phosphorylated H1 and/or H3 may lead to chromatin decondensation and aberrant gene expression, thus facilitating the process of malignant transformation. To address this hypothesis, we compared the H1 subtype composition, phosphorylated H1b and H3 levels, and H1 and H3 kinase and phosphatase activities in parental and oncogene-transformed cells. In addition, we studied the association of phosphorylated H1b and/or H3 with transcriptional processes by transcriptional inhibition studies, chromatin immunoprecipitations, and indirect immunofluorescence analysis.

MATERIALS AND METHODS

Cell lines and culture conditions

Cell lines

The parental 10T½ and NIH-3T3 cell lines were obtained from the American Type Culture Collection (ATCC) (Rockville, MD). The cell lines Ciras-2 and Ciras-3 were derived from 10T½ mouse fibroblast cells by transfection with the T24 H-*ras* oncogene (Egan et al., 1987). These cells contain a constitutively overexpressed T24 H-*ras* oncogene (Egan et al., 1987). The 10T½ cell line was also used to isolate cell lines expressing combinations of *ras*, *myc* and mutant p53. The derivation of these cell lines by transfection of 10T½ cells with plasmids expressing *ras*, *myc* and mutant p53 has been previously described (Taylor et al., 1994). The transfectants are R-2 (T24-Ha-*ras*), RM-5 (T-24-Ha-*ras* plus c-*myc*), RP-4 and RP-6 (T24-Ha-*ras*, c-*myc* plus the proline-193 mutant form of murine p53), and RMP6 (T24-Ha-*ras*, c-*myc* plus the proline-193 p53 mutant). The NIH-3T3 mouse fibroblast cell lines transformed with human c-*myc*, v-*mos*, v-*fes*, or A-*raf* were NIH/hmyc1, Mos 1, Fes 1, and NIH/9IV#5, respectively (Egan et al., 1987). NIH-3T3 mouse fibroblasts cell lines transfected with inactive MAP kinase kinase or transfected and transformed with constitutively active MAP kinase kinase were K97M and ΔN3S222D, respectively (Mansour *et al.*, 1994; a gift from Dr. Natalie Ahn) (Mansour et al., 1994). The 2H1 cell line was derived from 10T½ cells by transfection with the T-24 Ha-*ras*

oncogene which is under the control of a metallothionein promoter (Haliotis et al., 1990).

Culture conditions

Cell lines were grown in plastic tissue culture plates (Nunc, Denmark) in a humidified atmosphere containing 7% CO_2 in media supplemented with penicillin G (100 units/ml) and streptomycin sulfate (100 µg/ml). The *ras*-transformed cell lines Ciras-2 and Ciras-3, and NIH-3T3 derived cell lines were grown in α-MEM (plus 10% fetal bovine serum (Intergen, Purchase, N.Y.)). When cells reached 80% confluence they were trypsinized and an aliquot containing one tenth the number of cells was added to a new plate containing fresh medium. For 150 mm plates, cells were seeded at approximately 4×10^5 cells per plate and for 100 mm plates, cells were seeded at approximately 1×10^5 cells per plate.

Long term storage of cells

Cells from a 100 mm plate at approximately 80% confluence were removed by trypsinization, centrifuged for 5 min, and resuspended in α-MEM (Gibco, Grand Island New York) plus 10% FBS and 10% (v/v) dimethylsulfoxide (DMSO)(Sigma, St. Louis, MO). Cells were resuspended at approximately 5×10^6 cells/ml in this freezing medium and the solution was added to a cryotube (Nunc, Denmark) which was stored at –80°C. When cells were removed from storage for culturing, the vial was thawed out rapidly by placing the cryotube in a 37°C incubator for 2-3 min. The contents of the tube were added to a culture plate

containing growth medium. When the cells attached to the culture plate (3-5 hours later) the medium containing DMSO was removed and replaced with fresh medium.

Cell counting

Cells were counted with a hemocytometer (American Optic) and at least 150 cells were counted for each determination.

Cell removal by trypsin

The monolayer was washed twice with phosphate buffered saline, pH 7.3 (PBS) which contains 140 mM NaCl, 2.7 mM KCl, 1.6 mM KH_2PO_4 and 8.1 mM Na_2HPO_4. Two ml of trypsin solution (Sigma, St. Louis, MO; Difco Laboratories) and 2 mM ethylenediaminetetraacetate (EDTA) in phosphate buffered saline (PBS) was added to culture plates. The cells were incubated in this solution for 2 to 5 min. The trypsin was inactivated by the addition of two volumes of 10% FBS in α-MEM. The cells were then collected into a 10 ml plastic tube and pelleted by centrifugation at 1000 x g for five min. The pellet was washed twice with PBS, pH 7.3 and stored at -80°C.

Preparation of cells for flow cytometric analysis

The proportion of cells in the different cell cycle phases was determined by fluorescent-activated cell sorting (Blosmanis *et al.*, 1987). 3 x 10^6 were harvested by trypsinization and washed twice in 5 ml of PBS, pH 7.3. The cells

were centrifuged at 1000 x g and the cell pellet was resuspended in 2 ml of PBS, pH 7.3. This cell suspension was added dropwise while vortexing to 4 ml of prechilled 95% ethanol. At this step the suspension can be stored at 4 °C for further use. The ethanol-fixed cells were pelleted at 1000 x g for 5 min and the supernatant was discarded. The cells were resuspended in 2 ml of PBS, pH 7.3 containing 5 µg/ml RNAase A (Sigma, St. Louis MO) and incubated at 37 °C for 30 min. After incubation, 1 µl of ethidium bromide (10 µg/µl stock) was added to the tube and the cells were vortexed. The tubes were then wrapped in aluminum foil (to keep the suspension in the dark) and taken to Dr. E. Rector for flow cytometric analysis.

Manipulation of cell lines

Arrest of cells in G1 or G2/M phases of the cell cycle

Four x 10^5 cells were plated per 150 mm plate, and grown for 72 h. Fresh medium (10% FBS in αMEM) containing 2 mM hydroxyurea (Sigma, St. Louis, MO) was then added to the plates and were grown for an additional 24 h (Ashihara and Baserga, 1979). This treatment arrested cells at the G1/S boundary of the cell cycle. To arrest cells in mitosis, after 72 h of growth in, fresh medium containing 0.06 µg/ml colcemid (Sigma, St. Louis, MO) was added to the plates and the cells were incubated for an additional 16 h. After treatment, cells were harvested by trypsinization and used for histone isolation as well as for flow cytometric analysis.

Induction of *ras* oncogene expression in 2H1 cells

2H1 cells were grown as described above and then the medium was changed to fresh medium for the control cells, or medium containing 100 μM $ZnSO_4$ (to induce the *ras* oncogene) for 24 h. The cells were trypsinized, pelleted and stored at –80 °C for further use.

Manipulation of cell lines with transcription and replication inhibitors

For some experiments, cells were treated with inhibitors of transcription or replication. The transcription inhibitor actinomycin D (Sigma, St. Louis, MO) was reconstituted in 95% ethanol at a concentration of 10 mg/ml. Actinomycin D was added to 10T½ or Ciras-2 cell medium (α-MEM plus 10% FBS) at a final concentration of 10 μg/ml for 30 and 70 minutes. For control cells, no inhibitor was added to the medium. The transcription inhibitor DRB (5,6-dichloro-1-beta-D- ribofuranosylbenzimidazole) (Sigma, St. Louis, MO) was reconstituted with 95% ethanol at a concentration of 150 mM. DRB was then added to 10T½ or Ciras-2 cell medium (α-MEM plus 10% FBS) at a final concetration of 150 μM. 10T½ cells were incubated with DRB for 30, 70 min and 2h and the Ciras-2 cells were incubated with DRB for 2h and 3h time periods. For reversal of transcription inhibition by DRB, the DRB containing medium was removed after 70 min and replaced with fresh medium without DRB and the cells were allowed to recover for 2 h. The replication inhibitor aphidicolin (Sigma, St. Louis, MO) was reconstituted in 95% ethanol at a concentration of 10 mM. Aphidicolin was then added to the 10T½ or Ciras-2 cell medium (α-MEM plus 10% FBS) at a final

concentration of 10 μM and the cells were incubated for 30 min. In some experiments the 10T½ cells were treated with 10 μg/ml actinomycin D plus 10 μM aphidicolin or 150 μM DRB plus 10 μM aphidicolin for 30 min. Ciras-2 cells were treated with 10 μg/ml actinomycin D plus 10 μM aphidicolin or 150 μM DRB plus 10 μM aphidicolin for 70 min. After all treatments, the medium was removed and the cells were washed twice with PBS, pH 7.3, pelleted and stored at –80 °C for further use.

Serum starvation and mitogen stimulation of cells

10T½ cells were grown as described above and then serum starved in medium containing 0.5% FBS for 24 h. The cells were then either untreated, or treated with 50 ng/ml EGF (epidermal growth factor) (Sigma, St. Louis, MO) or 100 nM TPA (12-O-tetradecanoylphorbol 13-acetate) (Sigma, St. Louis, MO) for 5 or 30 minutes. After treatment, the medium was removed and the monolayer was washed twice with PBS, pH 7.3 and trypsinized. The cells were collected by centrifugation stored at -80 °C.

Isolation of Nuclei and Micrococcal Nuclease Digestion

All steps were performed on ice unless otherwise stated. The cell pellets of approximately 3 x 10^6 cells were resuspended in 5 ml TMN lysis buffer (10 mM Tris-HCl, pH 8.0, 100 mM NaCl, 300 mM sucrose, 2 mM $MgCl_2$, 1% (v/v) thiodiglycol, 1 mM PMSF) using a glass Dounce homogenizer and glass pestle B. The suspension was made 0.5% (v/v) Triton X-100 and passed through a 22

gauge needle three times. The nuclei were collected by centrifugation at 1500 x g in a SS-34 rotor for 6 min. The pellet was resuspended in 5 ml TMN lysis buffer and then the nuclei were collected by centrifugation. The nuclei were resuspended in digestion buffer (10 mM Tris-HCl, pH 8.0, 50 mM NaCl, 300 mM sucrose, 3 mM $MgCl_2$, 1% (v/v) thiodiglycol, and 1 mM PMSF) to 9.5 A_{260} units/ml. The DNA concentration of the nuclear suspension was determined by mixing 10 µl of nuclear suspension with 990 µl of a 2M NaCl / 5M Urea solution and the absorbance was measured at 260 nm in a spectrophotometer. The suspension of nuclei was incubated at 37^0C. $CaCl_2$ was added to 1 mM followed by the addition of micrococcal nuclease to 15 A_{260} units/ml. At various times of incubation, an aliquot was removed, and the digestion terminated by placing the sample on ice and adding EDTA (pH 7.5) to 20 mM. To check for possible endogenous nuclease activity, nuclei were incubated in digestion buffer with $CaCl_2$ for the entire length of the experimental incubation period (mock digestion). Further, nuclei resuspended in digestion buffer were also stored on ice in the presence of EDTA, but in the absence of $CaCl_2$ and micrococcal nuclease. DNA extractions were carried out as described previously (Delcuve and Davie, 1989), except that the samples were incubated with SDS instead of sodium N-dodecylsarcosine and proteinase K instead of pronase. The nucleosomal organization of the nuclear DNA was analyzed by electrophoresis in 1% agarose gels (procedure performed by Dr. R. Hurta).

Isolation of Histones

For the isolation of histones, $5x10^5$ cells were plated per 150 mm plate, grown in 8% calf serum in α-MEM and harvested 72 h later by trypsinization. Approximately $4x10^7$ to $1x10^8$ cells were used for histone preparation. Harvested cells were washed twice with PBS, pH 7.3 and homogenized in a glass homogenizer in 5 ml Nuclear Preparation buffer (10 mM Tris-HCl, pH 7.6, 150 mM NaCl, 1.5 mM $MgCl_2$, 0.65% Nonidet-P40, and 1 mM PMSF). Nuclei were recovered by centrifugation at 1500 x g for 10 min. All centrifugations were carried out at 4°C. Nuclei were resuspended in 3 ml RSB buffer (10 mM Tris-HCl pH 7.5, 3 mM $MgCl_2$, 10 mM NaCl, and 1 mM PMSF). To isolate H1, nuclei were extracted with 5% perchloric acid (PCA) (Davie and Delcuve, 1991). For some experiments, cells were extracted directly with 5% PCA, or nuclei were extracted with 0.4 N H_2SO_4 and then extracted with 5% PCA. The supernatant contained predominantly histone H1 and HMG (high mobility group) proteins. The PCA precipitate contained the nucleosomal histones. The supernatant was dialyzed using 6-8000 molecular weight exclusion dialysis tubing (Spectra-Por) with 0.1 N acetic acid and then with distilled H_2O at 4°C. The samples were lyophilized and resuspended in distilled H_2O. For the isolation of total histone, nuclei were extracted with 0.4 N H_2SO_4. The samples were precipitated with 18% trichloroacetic acid (TCA), and then washed with acetone-HCl solution (99.5% acetone (v/v), 0.5% HCl (v/v)) and once with 100% acetone. The samples were then resuspended in distilled H_2O. Protein concentrations were determined as described below.

Metabolic Labelling of H1

Metabolic labelling was carried out as previously described (Yasuda et al., 1981). Briefly, 2.5 x 10^6 cells (per 150 mm plate) were grown for 24 h. The monolayers were washed twice with PBS, and then 5 ml of phosphate free α-MEM containing 100 µCi/ml orthophosphate ^{32}P (ICN, St. Laurent, Que). Cells were incubated for 2 h, trypsinized and then washed twice with PBS, pH 7.3. H1 was isolated as described above. ^{32}P-labelled H1 was separated by SDS 15% polyacrylamide gel electrophoresis as described below and dried gels exposed to film.

Treatment of histone H1 with alkaline phosphatase

Two µl of histone H1 protein (1µg/µl) was mixed with 7 µl of 1 x phosphatase buffer (dilute from 10 x stock : 33 µl 1.5 M Tris, pH 8.8, 10 µl 100 mM $MgCl_2$, 10 µl 10 mM $ZnCl_2$), and 1 µl bacterial alkaline phosphatase (0.01 units) (Sigma). The mixture was incubated for 16h at 37 °C. After the incubation SDS loading buffer was added to the sample and the histone was analyzed on an SDS gel.

Quantitation of protein

For quantitation of histones a TCA turbidity assay was used. Ten µl or 100 µl of sample were diluted to 0.8 ml with distilled H_2O. To this sample, 0.4 ml o

light scattered by the precipitate formed in the sample. The spectrophotometer was adjusted to zero with a solution of 16.6% (w/v) TCA. The protein concentration was calculated using the following formula:

10 µl sample: A400 reading x 12900= x µg/ml protein

100 µl sample: A400 reading x 1290= x µg/ml protein

Quantitation of total cellular proteins from a whole cell extract was performed using the Bio-Rad protein assay. The manufacturer's instructions were followed. The sample was diluted to 0.8 ml using H_2O. 200 µl of dye reagent was then added to the diluted sample and the sample was mixed. The absorbance of the sample at 595 nm was then measured and the protein was quantitated using a standard curve generated by a known range of bovine serum albumin standards.

Quantitation of DNA

A 1/100 dilution of DNA in a solution of 5M urea/ 2M NaCl was prepared. DNA samples were quantitated by measuring the absorbance at 260 nm in a spectrophotometer. The spectrophotometer was adjusted to zero against a solution of 5 M urea/2M NaCl. One A_{260} unit is equal to 50 µg of pure DNA.

Polyacrylamide gel electrophoresis

SDS polyacrylamide gel electrophoresis (SDS-PAGE)

Proteins were separated in SDS polyacrylamide slab gels (Laemmli, 1970). The running gel was comprised of 12.5% or 15% acrylamide which was added from a 30% (w/v) stock, 0.1% (w/v) SDS, and 375 mM Tris, pH 8.8. To this solution 0.15% (w/v) ammounium persulfate and 0.03% (v/v) TEMED was added and the gel was poured and allowed to polmerize for approximately 1h. The stacking gel was comprised of 3% (w/v) acrylamide, 0.1% (w/v) SDS and 125 mM Tris, pH 6.8, 0.15 % (w/v) ammonioum persulfate and 0.08% (v/v) of TEMED. The stacking gel was poured on top of the running gel and allowed to polymerize. The appropriate amount of gel solution was made according to the size of gel that was needed. Gels were run in either a minislab apparatus (Idea Scientific) or in a Protean II apparatus (Biorad, Mississauga, ON). For gels run with the Idea Scientific apparatus the dimensions were 8 cm high with approximately 6 cm of separating gel. For gels run with the Protean II apparatus the dimensions were approximately 15 cm high with 11 cm of separating gel. For better separation of H1 subtypes, gels of 20 cm height with approximately 16 cm of separating gel were run using the Protean II apparatus. The gels run in the minislab Idea Scientific apparatus were run towards the anode at 170 volts for 1.5 h. For the Protean II apparatus, gels were run towards the anode at 42 milliamps for approximately 2 h. The running buffer was comprised of 193 mM glycine, 1% (w/v) SDS, 25 mM Tris-HCl, pH 8.3. Sample loading buffer for SDS-PAGE (4 x stock: 277 mM SDS, 396 mM Tris, 402 mM dithiothreitol, 40% (v/v)

glycerol, 0.4% (w/v) bromophenol blue, pH 6.8) was added to the sample prior to electrophoresis. Samples were boiled for 5 min, centrifuged at 10, 000 x g for 10 min, and loaded on the gel. A standard of prestained proteins (Rainbow Marker, Amersham, Oakville, ON) was also run to track migration of proteins of different molecular weights.

Acetic acid-urea-triton X-100 polyacrylamide gel electrophoresis (AUT PAGE)

Histone proteins were analyzed by AUT (acetic acid/6.7 M urea/0.375% (v/v) Triton X-100) 15% polyacrylamide gels. The running and stacking gel solutions were made in the following proportions:

Stock solution	Separating gel (15%)	Stacking gel (6%)
29.2 % acrylamide/ 0.8 % bisacrylamide	80.0 ml	25.0 ml
4% TEMED/ 43% acetic acid	20.0 ml	-
Urea	64.0 g	40.0 g
Temed	-	1 ml
Riboflavin (0.004%)	16.0 ml	10 ml
3 M potassium acetate, pH 4.0	-	12.5 ml
0.3 M Triton X-100	3.2 ml	2.0 ml
thiodiglycol	1.6 ml	1.0 ml

The gels were poured and polymerized by placing them in front of a white light source. Reducing mix prepared as a 1:1:1 ratio of Tris-Acetate, pH 8.8 / H_2O / β-mercaptoethanol was added to the histone samples at approximately one fifth the volume of the sample and incubated for 15 min. AUT sample loading buffer (2 x stock: 8 M urea, 0.75 M potassium acetate, 30% (w/v) sucrose, 0.1% (w/v) pyronin y) was then added to 1 x. The histone samples were then loaded on to the gel without boiling or centrifugation. The running buffer used was 0.9 N acetic acid and the proteins were run toward the cathode. When the Idea Scientific apparatus was used the gels were run at 200 volts for 3.5 hours at 4 °C. For better separation of phosphorylated H1 isoforms, the Protean II (Biorad, Mississauga, ON) apparatus was used. These gels were run for 18-22 h at 200 volts at 4 °C.

Staining of proteins with Coomassie Brilliant Blue

Gels were stained in a solution containing 0.40% (w/v) Serva Blue (Coomassie Brilliant Blue G250 equivalent), 45% (v/v) methanol, 9% (v/v) acetic acid. Gels were stained for 2 h to overnight. After staining, the gels were placed in a destaining solution composed of 25% (v/v) methanol, 12.5% (v/v) acetic acid for 1-2 h. The gels were then placed in a solution of 5% (v/v) methanol and 7.5% (v/v) acetic acid for storage.

Detection of proteins by immunoblotting

Immunodetection of phosphorylated H1b protein

H1 histone was separated by SDS- or AUT- polyacrylamide gel electrophoresis and transferred to nitrocellulose membrane as described (Delcuve and Davie, 1992). Anti-phosphorylated H1 IgG (a gift from Dr. C.D. Allis) was isolated as described by Lu *et al.* (1994). The antibody specifically recognizes highly phosphorylated histone H1 and in mouse fibroblasts, the antibody only detects the phosphorylated H1b subtype. The membrane containing H1 was stained with india ink for 1h and then blocked with 7.5% (w/v) non-fat dry milk in TBS (0.1 M Tris-HCl, pH 8.0, 0.3 M NaCl). The membrane was then incubated with anti-phosphorylated H1 IgG (1:1000 dilution) in TTBS (0.1 M Tris-HCl, pH 8.0 , 0.3 M NaCl, 0.4% (v/v) Tween-20) for 1 h and washed in TTBS for 0.5 h. The membrane was then incubated in goat anti-rabbit antibody linked to horseradish peroxidase (Sigma, St Louis, MO) in TTBS for 20 min.

Immunodetection of phosphorylated H3 protein

Total histone was isolated and separated by SDS polyacrylamide gel electrophoresis. The histones were transferred to nitrocellulose membrane as described previously (Delcuve and Davie, 1992). The anti-phosphorylated H3 IgG was a gift from Dr. C.D. Allis. A description of the method that was used to isolate the antibody can be found in Hendzel *et al.* (1998). This antibody specifically recognizes phosphorylated Ser-10 of histone H3. The procedures

used for immunochemical staining of phosphorylated H3 were identical to those used for immunochemical staining of phosphorylated H1 except the primary antibody dilution was 1:5000 instead of 1:1000 and the Tween concentration in the TTBS buffer was 0.2% (v/v) instead of 0.4% (v/v). The ECL system (Amersham, Oakville, ON) was used to detect pH1b protein.

Immunodetection of B1C8 protein

For detection of the B1C8 antigen in total cellular protein from 10T½ cells, whole cell extracts were prepared as described above and cellular proteins were separated by SDS PAGE. The electroblotting and india ink staining conditions are identical to those described above for anti-phosphorylated H1. The membrane was stained with B1C8 monoclonal antibody and goat anti-mouse antibody linked to horseradish peroxidase as described in (Wan et al., 1994).

Immunodetection of Ras protein

For detection of Ras protein in cellular extracts, cellular proteins from whole cell extracts were separated by SDS gel electrophoresis and transferred to nitrocellulose as described previously (Delcuve and Davie, 1992). The membrane was stained with india ink and incubated with anti-Ras monoclonal antibody (Santa Cruz Inc., Santa Cruz, CA). The procedures used for immunochemical staining of Ras were identical to those used for immunochemical staining of phosphorylated H1 except the primary antibody dilution was 1:500 instead of 1:1000, the secondary antibody was goat anti-

mouse antibody linked to horseradish peroxidase (Sigma, St Louis MO), and the Tween-20 concentration in the TTBS buffer was 0.05% (v/v) instead of 0.4% (v/v).

Quantitation and analysis of proteins from immunoblots

To quantitate the relative amount of phosphorylated H1b in each sample, we first prepared a Western blot that contained increasing amounts of Ciras-2 H1. The resulting autoradiogram was scanned, and the values obtained were linear up to 5 µg of Ciras-2 H1 histones. For each film this procedure was repeated to ensure that the value (ie. level of phosphorylated H1b) obtained with each preparation of H1 was in the linear range. Identical amounts of protein were loaded onto a SDS 15% polyacrylamide gel. The Coomassie Blue-stained gel pattern was scanned to obtain the relative amount of the H1 subtypes in each H1 sample. A standard curve was also generated by loading various amounts of Ciras-2 H1. The loading of each H1 sample was then corrected by dividing the amount of phosphorylated H1b (the value from the scanned autoradiogram) by the amount of total H1b (sum of H1b and c-phosphorylated histone H1b on Coomassie Blue-stained SDS gel pattern). The relative increase in phosphorylated H1b in each of the H1 preparations isolated from the oncogene- or MAP kinase kinase-transformed cell lines was divided by the value obtained for the parental cell line (10T½ or NIH-3T3). For phosphorylated H3, the loading of each H3 sample was corrected by dividing the value obtained for H3 by the value obtained for the amount of H3 (from the Coomassie blue stained gel). The

relative increase in phosphorylated H3 in each of the preparations isolated from the oncogene-transformed cell lines was divided by the value obtained for the parental cell line.

Indirect immunofluorescence analysis

Indirect immunofluorescence was carried out as previously described (Lu et al., 1994). 1 x 10^5 cells were plated onto glass coverslips that were placed onto the bottom of each 9.4 cm^2 well of a six-well plate. The cells were incubated for 24 h and then washed twice with of PBS, pH 7.3 (1 ml per well). Cells were extracted with cytoskeletal buffer (10 mM PIPES, pH 6.8, 100 mM NaCl, 300 mM sucrose, 3 mM $MgCl_2$, 1 mM EGTA, 1.2 mM PMSF) containing 0.5% (v/v) Triton X-100 for 7 min at 4 °C to remove soluble proteins (Wan *et al.*, 1994; Durfee *et al.*, 1994). Cells were then fixed in formaldehyde fixative (2% formaldehyde in PBS) for 20 min. The formaldehyde fixative was removed and the cells were incubated with anhydrous methanol (1 ml per well) for 20 min. The cells were then washed three times in PBS containing 10% FBS. One ml of primary antibody solution (anti pH1b or anti pH3 antibody diluted 1:100 in PBS containing 10% FBS) was added to each well and the cells were incubated for 1h at 37°C. The antibody solution was removed and the cells were washed three times with PBS. The secondary antibody (FITC [fluorescein isothiocyanate]- labelled goat anti-rabbit antibody) (Sigma, St. Louis, MO) was diluted 1:200 in PBS plus 10% FBS and one ml of this solution was added to each well. Each experiment was

done in triplicate and the values obtained for pH1b levels represent the average of three separate experiments.

Colocalization of phosphorylated H1b with the B1C8 nuclear matrix antigen was done by mixing both primary antibodies, anti-phosphorylated H1b and B1C8 monoclonal antibodies, followed by goat anti-rabbit IgG FITC (Sigma, St. Louis, MO) and goat anti-mouse IgM (Texas red; Jackson ImmunoResearch Laboratories, Inc.) Cells were stained with anti-pH3 followed by goat anti-rabbit IgG Cye 3 (Sigma, St. Louis, MO) (performed by Dr. M. Hendzel). In addition, cells were co-stained with DAPI (diamidinophenolindole) (Sigma, St. Louis, MO). Digital optical sectioning of nuclei was performed as previously described by (Rattner et al., 1996) with the exception that the z-axis optical offsets between fluorescence channels was calculated and compensation was made at the data collection stage. Images were then imported into Adobe Photoshop v.2.51 and the contrast was enhanced.

CHIP Assays

10T½ cells were serum starved and either not treated or stimulated with TPA for 30 min. The cells were then treated with 1% formaldehyde for 8 min (final concentration in the medium) to cross-link histones to DNA. The cells were collected, washed twice in PBS, pH 7.4 and then washed for 10 min in solution 1 (0.25% (v/v) Triton X-100, 10 mM EDTA, 0.5 mM EGTA, 10 mM HEPES, pH 7.5) and 10 min in solution 2 (0.2 M NaCl, 1 mM EDTA, 0.5 mM EGTA, 10 mM HEPES, pH 7.5). The pellet was resuspended in lysis buffer (150 mM NaCl, 25

mM Tris-Cl, pH 7.5, 5 mM EDTA, 1% (v/v) Triton X-100, 0.1% (w/v) SDS, 0.5% sodium deoxycholate) and sonicated for 4 min in 15 second bursts at 4°C. The lysate was diluted 10-fold in lysis buffer and anti-pH3 antibody was added and incubated at 4 °C overnight. Immunoprecipitated complexes were collected by adding protein A agarose beads (Pierce, Rockville, IL) for 1h at 4°C. Immunoprecipitates were washed once with RIPA (150 mM NaCl, 50 mM Tris-HCl, pH 8.0, 0.1% SDS, 0.5% sodium deoxycholate, 1.0% NP-40), once in high salt wash (500 mM NaCl, 1.0% NP-40, 0.1% SDS, 50 mM Tris-HCl, pH 8.0), once in LiCl wash (250 mM LiCl, 1.0% NP-40, 0.5% sodium deoxycholate, 1 mM EDTA, 50 mM Tris-HCl, pH 8.0) and twice in TE buffer (10 mM Tris-HCl, pH 8.0, 1 mM EDTA). The beads were then treated with RNAase (50 µg/ml) for 30 min at 37 °C and then proteinase K overnight. The crosslinks were reversed by heating the sample at 65 °C for 6 h and the DNA was extracted with phenol/chloroform and ethanol precipitated. The DNA was then labelled using the DIG DNA non-radioactive labelling system (Boehringher Mannheim, Lavalle, Que). The various genes of interest were slotted onto a nylon membrane and probed with the immunoprecipitated, labelled DNA. Hybridizations were done at 68 °C overnight.

The four cloned DNA sequences used were IGκ, c-*fos*, c-*myc* and prolactin. All are mouse genomic sequences except for prolactin, which is a mouse cDNA. For IGκ, a 2.85 kb Bam H1 - Hind III fragment containing the entire coding region of the gene was isolated from the recombinant plasmid pG19/45 (Cockerill and Garrard, 1986). A 2.6 kb Bgl 1 fragment from the

recombinant pSVfos plasmid carrying the entire mouse genomic c-fos gene was isolated (Schonthal et al., 1988). A 2.1 kb Pvu II fragment from the mouse genomic *c-myc* DNA sequence containing a segments of exon 2 and extending into exon 3 was isolated (Bernard et al., 1983). A 0.8 kb mouse prolactin cDNA insert that contains the entire coding region of the gene was isolated from the Gem 2 plasmid (Colosi et al., 1987).

Plasmid preparation and isolation of DNA fragments

Large scale plasmid preparations were performed as described in (Sambrook et al., 1989). A colony of JM109 E.coli that was transformed with the appropriate plasmid was inoculated into 5 ml of LB medium containing 50 µg/ml ampicillin. The suspension was incubated overnight in a shaking incubator at 37°C. After the incubation, the suspension was transferred to one litre of LB medium and incubated at 37 °C with shaking overnight. The cells were collected by centrifugation at 4000 x g for 10 min and then washed once in 25 ml of ice cold STE buffer (0.1 M NaCl, 10 mM Tris-HCl, pH 7.8, 0.1 mM EDTA. The cell pellet was resuspended in 10 ml of solution I (50 mM glucose, 25 mM Tris-HCl, pH 8.0, 10 mM EDTA) containing 5 mg/ml lysozyme. The suspension was transferred to a Beckman SW27 polyallomer tube and 20 ml of solution II (0.2N NaOH, 1% SDS) was added. The suspension was placed on ice for 10 min. Fifteen ml of an ice-cold solution of 5M potassium acetate (pH 4.8) was then added and the tube was covered with parafilm and mixed by inverting. The tube was placed on ice for another 10 min and then centrifuged at 12,000 x g for 30

min at 4 °C. The supernatant was transferred into two Corex tubes and extracted twice with a 1:1 phenol/chloroform solution. 0.6 volumes of isopropanol was added and the tube was inverted several times to mix the solution well. The DNA was recovered by centrifugation in a Sorvall rotor at 12,000 g for 30 min at room temperature. The pellet was washed with 70% ethanol and then dried in a vacuum desiccator. The pellet was finally dissolved in a total volume of 4 ml of TE buffer, pH 8.0 and incubated with 10ug/ml RNase A for 2h. The plasmids were analyzed by restriction enzyme digestion.

The various plasmids were incubated with the appropriate restriction enzyme at 37°C for 1h. The digested DNA fragments were separated on a 0.8% agarose gel containing 2.5 µg/ml ethidium bromide. The DNA fragments were visualized by ultraviolet light and the fragment of interest was excised from the gel with a scalpel. The DNA fragment was isolated from the gel using a Gene Clean kit (Bio101, Vista, CA). The recovered DNA was then checked again on an agarose gel for purity. DNA samples were stored at –20 °C.

Determination of kinase an phosphatase activies

Determination of phosphatase activity

A cell pellet containing 4 x 10^5 10T½ or Ciras-3 cells was lysed in buffer (10 mM Tris-HCl, pH 7.6, 150 mM NaCl, 1.5 mM $MgCl_2$, 0.65% Nonidet-P40, and 1 mM PMSF). The lysate was centrifuged at 10,000 x g for 10 min. The pellet was discarded and the supernatant was stored at –20 °C for further use. 20 µg of cell extract was incubated with either 2 µg of H1 histone (isolated by perchloric

acid extraction of 10T½ cells arrested with colcemid as described above) or 5 µg of total histone (isolated by sulfuric acid extraction of 10T½ cells arrested with colcemid as described above). Okadaic acid (Sigma, St. Louis, MO) was added to the reaction at a concentration of either 2 nM or 100 nM and the reaction was incubated at 37 °C for 15, 30, 45 or 60 minutes and then stopped by the addition of SDS loading buffer. For the 0 min time point the reaction was immediately stopped by the addition of SDS loading buffer after all components of the reaction were mixed. The samples were then subjected to SDS PAGE and Western blotting with either the anti-pH1b antibody or the anti-pH3 antibody was performed to detect the amount of phosphorylated H1b or phosphorylated H3 in each sample. Densitometric analysis of the Western blots was performed and the relative amount of phosphorylated H1b or phosphorylated H3 in each sample was calculated as described above.

Determination of CDK2 kinase activity

One 150 mm plate containing 3 x 10^6 cells was lysed with SB250 buffer (250 mM NaCl, 25 mM Tris-Cl, pH 7.5, 5 mM EDTA, 1% v/v Triton X-100, 0.5 % w/v Na deoxycholate). The cells were scraped with a rubber policeman and collected into a microfuge tube. The sample was centrifuged at 10 000 x g for 10 min. The pellet was discarded and the protein concentration of the supernatant was determined by the Bio-Rad method. Five µl of CDK2 antibody (Santa Cruz) was added to three mg of protein extract and the sample was rotated for 1 h at 4°C. Forty µl of protein A agarose beads (Pierce, Rockville, IL) resuspended as

a 1:1 slurry in SB250 was added and the sample was rotated at 4 °C for a further 30 min. The immune complexes were collected by centrifugation at 1000 x g for 5 min at 4 °C. The beads were washed twice with 10 volumes of SB250 and twice with 10 volumes of TE buffer, pH 8.0. The beads were resuspended in 17 µl of 1 x kinase buffer (50 mM TRIS, pH 7.5, 5 mM $MgCl_2$, 1.25 mM EGTA, 1 mM NaF, 1 mM Na orthovanadate, 25 mM β-glycerophosphate, 0.5 mM DTT) and 50 µM ATP, 1 µg histone H1 and 2.5 µCi [γ^{32}P]ATP was added and the final reaction volume was made up to 20 µl with distilled H_2O. The mixture was incubated at 30 °C for 30 min and then SDS loading buffer was added to stop the reaction. The samples were boiled and separated by SDS-PAGE. The gels were dried and exposed to film.

Determination of pp90^{rsk} kinase activity

pp90^{RSK} kinase assays were carried out exactly as described for the CDK2 kinase assays except anti-pp90^{rsk} antibody (Santa Cruz) was used for the immunoprecipitation, 10 µg of total histone instead of histone H1 was used as substrate and the kinase buffer used consisted of 20 mM Hepes pH 7.2, 10 mM $MgCl_2$, 3 mM β-mercaptoethanol, 50 µM ATP and 0.1 mg BSA/ml. Also the final washes of the beads were: twice in Buffer A (1% (v/v) NP-40, 0.5% Na deoxycholate, 100 mM NaCl, 10 mM Tris-Cl, pH 7.2, 1 mM EDTA, 1 mM Na orthovanadate, 2 mM DTT, and 1 mM PMSF), twice in Buffer B (1 M NaCl, 0.1% NP-40, 10 mM Tris-Cl, pH 7.2, 1 mM Na orthovanadate, 1 mM PMSF, and 2 mM

DTT), once in ST buffer (150 mM NaCl, 50 mM Tris-Cl, pH 7.2) and three times with TE buffer, pH 8.0 (Chen and Blenis, 1990).

Determination of MAP kinase activity

Cell extracts were prepared as described for CDK2 kinase assays. The MAP kinase activity from the cell extracts was measured using a MAP kinase assay kit (Upstate Biotech. Inc., Lake Placid, NY). The assay was performed exactly as described in the manufacturers instructions. Briefly, 3 mg of protein was incubated with anti-MAP kinase (Erk 1, 2) antibody that was conjugated to protein A agarose beads. The immune complexes were precipitated as described above for CDK2 kinase assays. The immunoprecipitated kinase was incubated with myelin basic protein substrate and [γ^{32}P]ATP (3000 Ci/mmol)(Amersham, Oakville, ON) for 30 min at 30 °C. The sample was spotted onto p81 phosphocellulose paper and then the paper was washed thoroughly with 0.8% phosphoric acid. The radioactive signal on phosphocellulose paper was detected by liquid scintillation counting.

Part 1: Increased Phosphorylation of Histone H1 in Mouse Fibroblasts Transformed with Oncogenes or Constitutively Active MAP Kinase Kinase

Introduction

Cell lines

Mouse fibroblasts cell lines were used for all of the studies described throughout this thesis. Phosphorylated histone H1 and/ or phosphorylated histone H3 was analyzed from three different panels of cell lines. The cell lines of the three panels are described in Table I with respect to the transforming gene, tumor latency and metastatic potential. The first panel consisted of a 10T½ control parental cell line and cell lines derived by transfection of 10T½ cells with a T-24 Ha-*ras* oncogene (NR4, Ciras-2, Ciras-3, R-2, see Table 1). The parental 10T½ cells are not tumorigenic and not metastatic whereas the *ras*-transformed R-2 and NR-4 cells are tumorigenic but poorly metastatic. The *ras*-transformed Ciras-2 and Ciras-3 cells are highly metastatic and tumorigenic (Table I)(Egan et al., 1987). Additional cell lines were derived by transfection of 10T½ cells with combinations of T-24 Ha-*ras*, c-*myc* and mutant p53 (RM-5, RP-4, RP-6, RMP-6; Table I)(Taylor et al., 1994). All of these cell lines, except for the parental 10T½ cells, were tumorigenic and only RP-4 and RMP-6 were metastatic (Table I). The second panel consisted of an NIH-3T3 (clone 7) control parental cell line and cell lines derived by transfection of the NIH-3T3 cells with v-*fes*, v-*mos*, c-*myc*, or A-*raf* oncogenes (Fes 1, Mos 1, NIH/hmyc 1, NIH/91V#5;

Table I

Tumorigenic and malignant properties of 10T½ mouse fibroblasts transformed by oncogenes or constitutively active MAP kinase kinase.

Cell line	Gene	Tumor Latency (days)*	Metastatic Potential (# of lung tumors)
10T½	-	NA	0
NR4	Ha-*ras*	0.7	2
Ciras-2	Ha-*ras*	6.5	118
Ciras-3	Ha-*ras*	6.5	121
R-2	Ha-*ras*	15	0
RM-5	Ha-*ras*, c-*myc*	11	0
RP-4	Ha-*ras*, p53	12.8	11
RP-6	Ha-*ras*, p53	10.2	0
RMP-6	Ha-*ras*, c-*myc*, p53	7.4	85.1
NIH 3T3 (clone 7)	-	NT	0
Fes 1	v-*fes*	6.4	178
Mos 1	v-*mos*	NT	29
NIH/hmyc1	c-*myc*	13.7	1
NIH/91V#5	A-*raf*	6.2	38
NIH 3T3	NT	NT	NT
K97	NT	NT	NT
ΔN3S222D	NT	NT	NT

The properties of these cell lines have been described previously (Taylor et al., 1994; Egan et al., 1987b; Egan et al., 1987a).
*Tumor latency was determined after subcutaneous injection of $3x10^5$ cells into immunocompetent C3H/HeN syngenic mice for ceil lines 10T½, Ciras-2, Ciras-3, NR-4, R-2, RM-5, RP-4, RP-6, and RMP-6 (Egan et al., 1987a; Taylor et al., 1994).
For cell lines Fes 1, Mos 1, NIH/hmyc, and NIH/91V#5, $3X10^5$ cells were injected into BALB/c nu/nu mice (Egan et al., 1987b).
NT- Not tested

see Table 1)(Egan et al., 1987). All of the oncogene-transformed cells were tumorigenic and metastatic with the exception of the *c-myc* cell line that was tumorigenic but poorly metastatic. The parental NIH-3T3 cell line is not tumorigenic and not metastatic. A third panel consisted of NIH-3T3 parental cells transfected with a wild type MAP kinase kinase, a catalytically inactive MAP kinase kinase, or a constitutively active MAP kinase kinase (NIH-3T3, K97, ΔN3S222D) (Mansour et al., 1994). In this panel, only the ΔN3S222D cell line transfected with a constitutively active MAP kinase kinase was tumorigenic (Mansour et al., 1994). The MAP kinase activity of each of the 10T½, Ciras-2, Ciras-3, NIH-3T3 (clone 7), Fes1, Mos 1, NIH/hmyc 1, and NIH/91V#5 cell lines was compared (Fig. 17). We observed that all of the oncogene-transformed cells had a higher level of MAP kinase activity in comparison to the parental cells.

Histone H1 phosphorylation

H1 histones are phosphorylated at serine and threonine residues located in the N- and C-terminal domains of the protein (Van Holde, 1988). H1 phosphorylation increases dramatically as cells progress through the cell cycle (Lu et al., 1994; Hohmann, 1983). Phosphorylation of H1 begins in G1, continues at an increasing rate and extent throughout S and G2 and reaches a maximum in mitosis. The H1 subtypes, however, differ in their extent of phosphorylation and the scheduling of some of their phosphorylation during the cell cycle (Hohmann, 1983). Phosphorylation of the H1 subtypes is likely to influence their interaction with DNA and, in turn, modulate chromatin structure

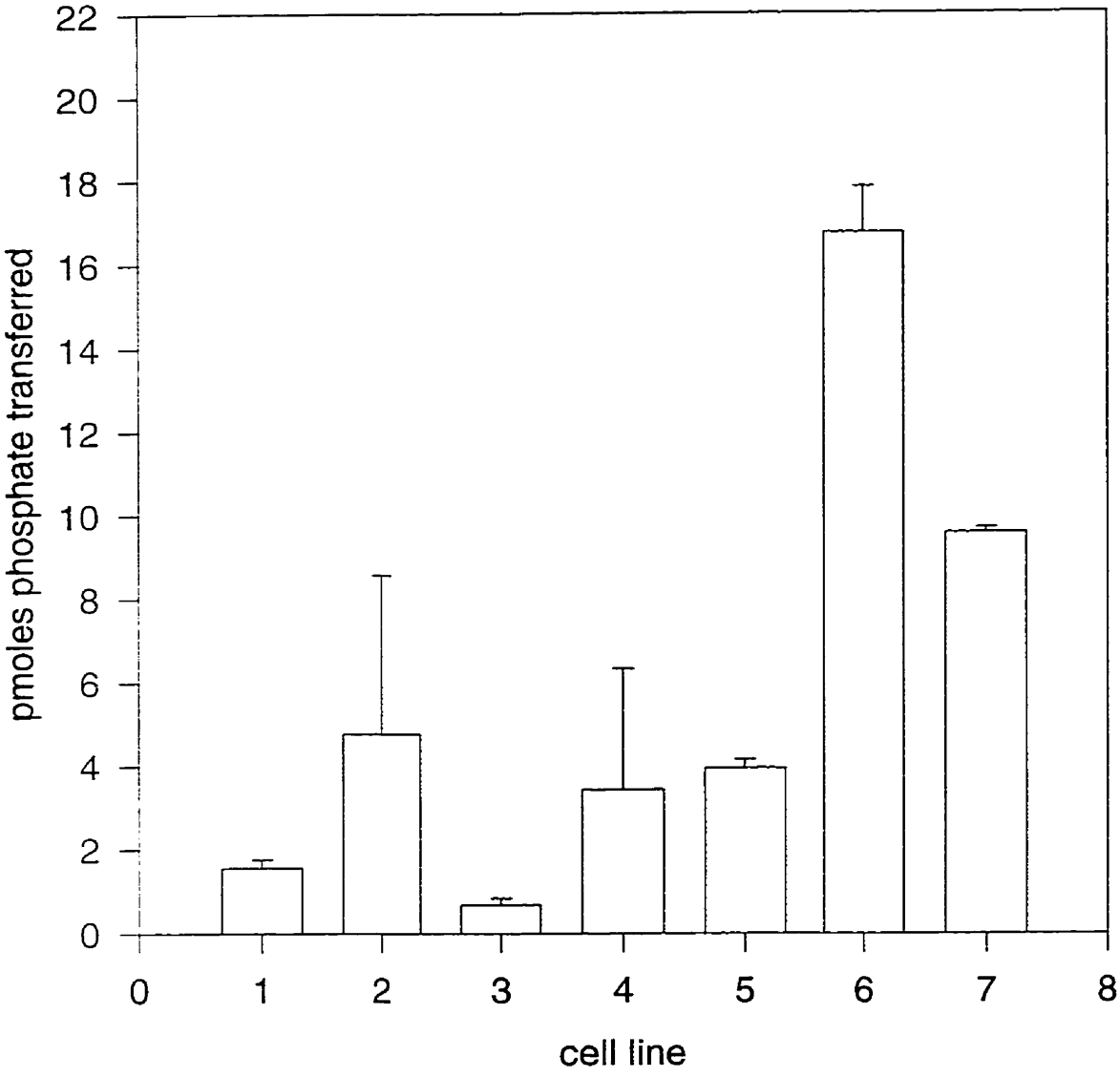

Figure 17. **MAP kinase activity in oncogene-transformed cells**. MAP kinase was immunoprecipitated from cellular protein extracts of (1) 10T½, (2) Ciras-3, (3) NIH-3T3, or NIH-3T3 cells transformed with (4) *fes*, (5) *mos*, (6) *myc*, or (7) *raf* oncogenes. Kinase assays were performed in triplicate and myelin basic protein was used as a substrate.

(Hill et al., 1991; Roth and Allis, 1992; Lu. et al., 1995; Sweet et al., 1996; Halmer and Gruss, 1996b). Laitinen *et al.* (1990) observed that *ras*-transformed mouse (NIH-3T3) fibroblasts had a more decondensed nucleosomal structure than normal fibroblasts. Such an alteration in chromatin structure may result from alterations in H1 subtype levels or amounts of phosphorylated H1. Expression of oncogenic *ras* leads to persistent activation of the MAP kinase pathway through its interaction with the oncoprotein Raf (a serine/threonine kinase). Activated Raf phosphorylates MAP kinase kinase which, in turn, phosphorylates and activates MAP kinase. Phosphorylated MAP kinase translocates to the nucleus where it acts upon a number of nuclear targets such as the transcription factor c-Myc. Increased expression of c-Myc has been shown to lead to upregulation of cyclin E mRNA(Jansen-Durr et al., 1993). Cyclin E, when complexed with its partner CDK2, can phosphorylate a number of different proteins one of which is histone H1. The expression of oncogenic *ras* may lead to increased activity of an H1 kinase through persistent activation of the MAP kinase pathway. We proposed that decondensation of chromatin in *ras*-transformed mouse fibroblasts may arise from altered levels of phosphorylated histone H1 in these cells.

Expression of oncogenic *ras* and persistent activation of the MAP kinase pathway may lead to increased expression of a histone H1 kinase resulting in elevated levels of phosphorylated H1. To test this hypothesis we compared the nucleosomal organization, histone H1 subtypes, and histone H1 phosphorylated isoforms of *ras*-transformed and parental 10T½ mouse fibroblasts. For this

study, we used a panel of mouse fibroblast cell lines which consists of a parental cell line, 10T½, and two *ras*-transformed cell lines, Ciras-2 and Ciras-3. *Ras*-transformed 10T½ cell lines Ciras-3 and Ciras-2 are tumorigenic and highly metastatic (Table I) (Egan et al., 1987).

Results

Ras-transformed cells have a more decondensed nucleosomal structure than parental cells

We first compared the nucleosomal organization of Ciras-3 cells to that of the parental 10T½ cells (performed by Dr. Robert Hurta). To address the concern that the sensitivity of DNA to micrococcal nuclease digestion may be due to differences in cell cycle distributions of the two cell lines, flow cytometric analysis was performed for both cell lines (Fig. 18, legend). We observed that cell cycle distributions for 10T½ and Ciras-3 were very similar. Nuclei isolated from Ciras-3 and 10T½ mouse fibroblasts were incubated with micrococcal nuclease, and the DNA fragments resolved on agarose gels. Fig. 18 shows that the nuclear DNA of Ciras-3 cells was processed to smaller DNA fragments at a rate greater than that observed for the chromatin of parental cells. Nuclear DNA of Ciras-2 cells was digested at a rate similar to the chromatin of Ciras-3 cells (not shown). Ciras-3 and 10T½ nuclei had very low levels of endogenous nuclease activity (see Fig. 18, lane M). Micrococcal nuclease digested DNA was also analyzed from NIH-3T3 cells and c-*myc* transformed NIH-3T3 cells (cell line

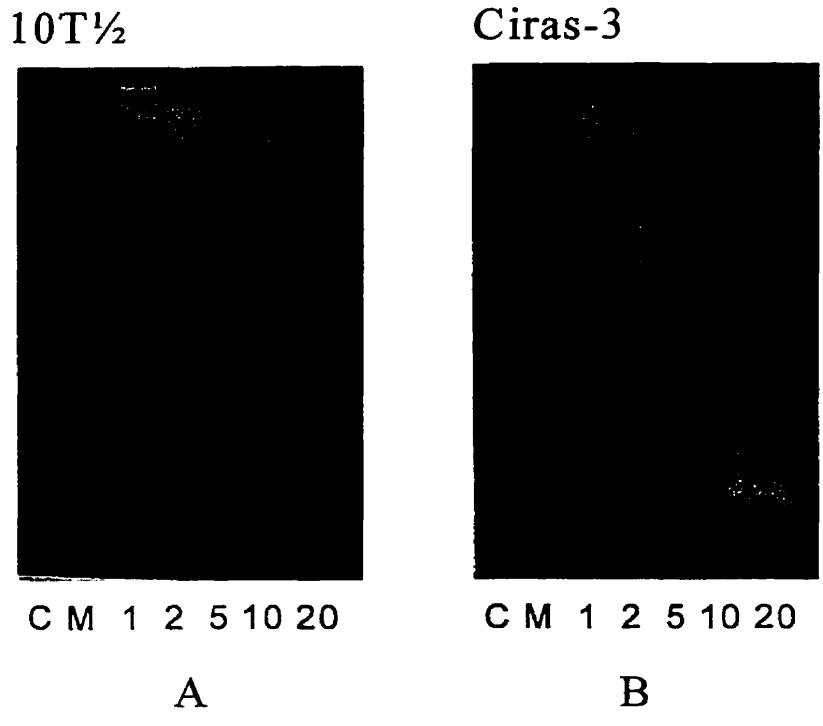

Figure 18. **Nucleosomal organization of chromatin from *ras*-transformed and parental mouse fibroblasts**. Mouse fibroblast 10T½ (panel A) or Ciras-3 (panel B) nuclei at 0.27 or 0.34 mg DNA/ml, respectively, were digested with micrococcal nuclease for various times (min, indicated at bottom of figure). DNA fragments (10T½, 15 µg; Ciras-3, 20 µg) were resolved on 1% agarose gels which were stained with ethidium bromide. The cell cycle distribution of the cells used in this analysis was as follows: G1, 48.2 (47.1); S, 22.8 (23.6); G2/M, 29.0 (29.3) for 10T½ (Ciras-3). C is the control, undigested DNA. M is the mock DNA digestion which was incubated for 20 min in the absence of enzyme.

NIH/hmyc1). The nuclear DNA of c-*myc* transformed cells was digested at a faster rate than that of the parental NIH-3T3 cells (data not shown, performed by Dr. Robert Hurta). Thus, in agreement with Laitinen *et al.* (1990, 1995), these results provided evidence consistent with the observation that *ras*- and *myc*-transformed mouse fibroblasts have a less condensed chromatin structure than the parental cells.

Ras-transformed cells have elevated levels of phosphorylated H1

H1 is responsible for stablilizing higher order structure of chromatin. A significant reduction in the content of H1 in *ras*-transformed cells might result in a less condensed chromatin than that of the parental cell chromatin. Fig. 19A and B show, however, that the chromatin of parental and *ras*-transformed mouse fibroblasts (Ciras-2) had similar amounts of H1 relative to the core histones (histones H2A, H2B, H3, H4). Thus, these data suggest that differences in the chromatin structure of oncogene-transformed and parental mouse fibroblasts are not due to a change in the level of H1.

Changes in the content of H1 subtypes and/or modified histone H1 isoforms could account for the observed alterations in chromatin (Laitinen et al., 1994). Therefore, we next investigated the level of H1 subtypes and H1 modified forms in nuclei from cells. H1 was isolated by perchloric acid extraction from the nuclei of 10T½ fibroblasts and transformed derivatives of these cells (Ciras-2, Ciras-3) and resolved by SDS PAGE, AUT PAGE or two-dimensional

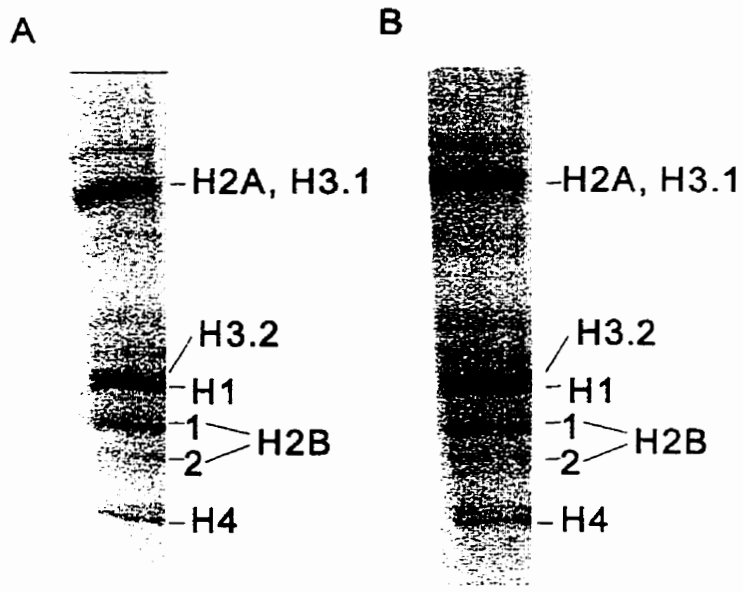

Figure 19. **Histone composition of *ras*-transformed and parental mouse fibroblasts**. Total histone (10 µg) isolated from mouse fibroblast 10T½ (A) or Ciras-2 (B) cells was electrophoretically resolved on an AUT-15% polyacrylamide gel and the gel was stained with Coomassie blue.

polyacrylamide gel electrophoresis (SDS by AUT), which separates H1 subtypes and their phosphorylated isoforms.

Lennox and Cohen (1988b) have shown that some of the mouse H1 subtypes (H1b and H1c) undergo two types of phosphorylation. One phosphorylated isoform has an altered mobility in SDS gels. This type of phosphorylation is called c-phosphorylation because of its effect on protein conformation. The other phosphorylated isoform retains the same mobility as the parent band. The c-phosphorylated isoforms of H1 subtypes H1b and H1c migrate slower than the unmodified H1 subtype on SDS gels. Using the nomenclature of Lennox *et al.* (1982), Fig. 20 shows that H1 subtypes H1b, d, e, c, and $H1^0$ were present in both *ras*-transformed (lanes 2 and 3) and parental (lane 1) 10T½ mouse fibroblast nuclei. Subtype H1a was absent in these cell lines and previously, other rodent cell lines have also been found to lack H1a (Talasz et al., 1993). Fig. 20 shows that H1 from *ras*-transformed cell nuclei had greater amounts of an H1 isoform (c-pb) running slower than H1b and an isoform (c-pc) migrating between H1c and H1d, e on SDS gels. Fig. 21 shows H1 subtypes resolved on an AUT gel. In a two-dimensional gel (AUT into SDS) (Fig. 22) greater amounts of the c-pb and c-pc subtypes are observed in the *ras*-transformed cells (panel B) in comparison to the parental cells (panel A).

To gain further evidence that H1 of *ras*-transformed and parental mouse fibroblasts were differentially phosphorylated, cells were metabolically labelled with ^{32}P orthophosphate, and H1 electrophoretically resolved on SDS polyacrylamide gels (Fig. 23). H1 of parental 10T½ cells was labelled to lower

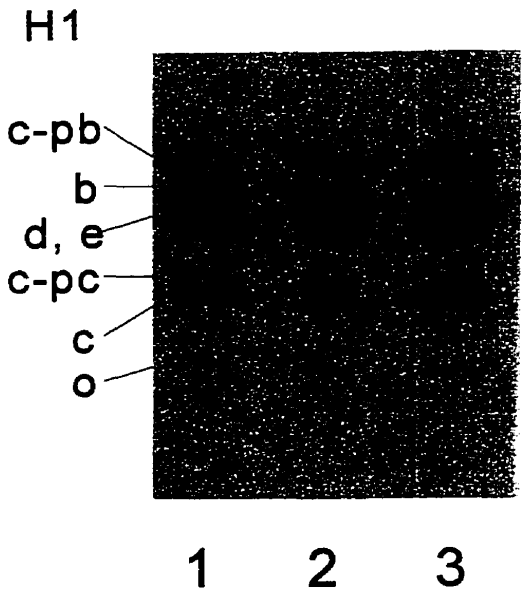

Figure 20. **Analysis of H1 from *ras*-transformed and parental mouse fibroblasts by SDS PAGE.** H1 was isolated from 10T½ (lane 1), Ciras-2 (lane 2), and Ciras-3 (lane 3) mouse fibroblasts. H1 (2 µg) was electrophoretically resolved on an SDS 15% polyacrylamide gel and stained with Coomassie Blue. pb is the phosphorylated isoform of H1b. c-pb and c-pc are the c-phosphorylated isoforms of H1b and H1c, respectively.

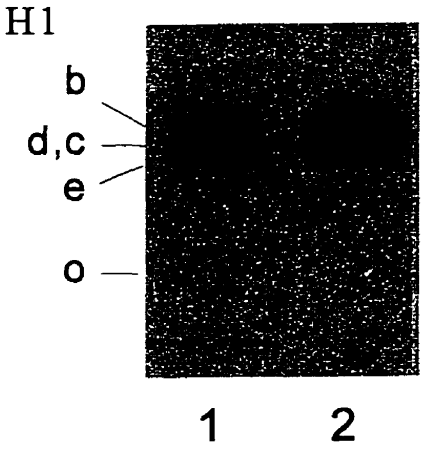

Figure 21. **Analysis of H1 from *ras*-transformed and parental mouse fibroblasts by AUT-PAGE.** H1 was isolated from 10T½ (lane 1) and Ciras-2 (lane 2) mouse fibroblasts. H1 (2 µg) was electorphoretically resolved on an AUT 15% polyacrylamide gel and stained with Coomassie Blue.

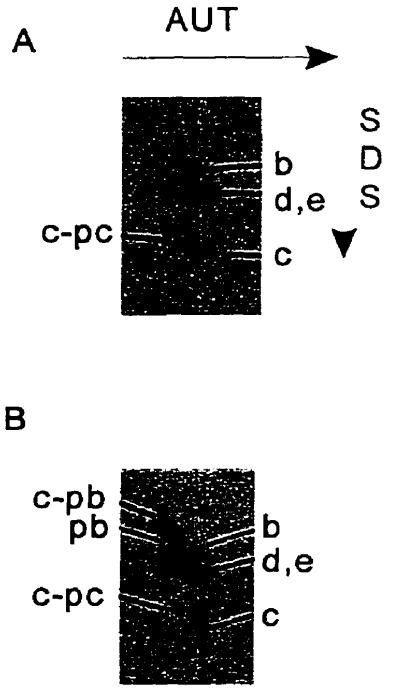

Figure 22. **Two-dimensional PAGE analysis of H1 isolated from parental and *ras*-transformed mouse fibroblasts**. H1 was isolated from 10T½ (panel A) and Ciras-2 (panel B) mouse fibroblasts. H1 subtypes were separated by AUT PAGE in the first dimension and by SDS PAGE in the second dimension. c-pc and c-pb are the phosphorylated forms of pc and pb respectively.

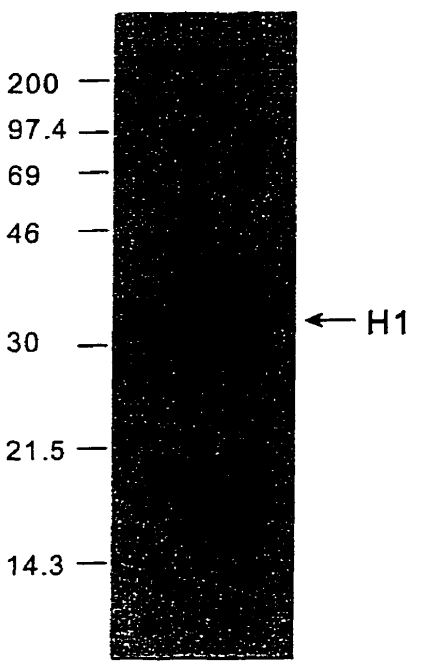

Figure 23. **Incorporation of ^{32}P into histone H1 from normal and *ras*-transformed mouse fibroblasts.** H1 histones were extracted from cells metabolically labelled with ^{32}P orthophosphate, separated by SDS PAGE, and dried gels were exposed to film. Two µg of histone from 10T½ (lane 1), NR4 (lane 2) and Ciras-3 (lane 3) were loaded per lane.

levels than the H1 isolated from *ras*-transformed cells (Ciras-2, lane 3) or (NR4, lane 2). Densitometric analysis of autoradiograms of labelled H1, resolved on SDS gels, indicated that labelling of H1 from the highly metastatic Ciras-2 cell line was approximately 5-fold higher than in the parental 10T½ cell line. Another smaller, labelled protein is also present and it is also labelled to a higher extent in the Ciras-2 and NR4 cells in comparison to the 10T½ cells. Contaminating, acid soluble proteins that could be present in the H1 preparation are HMGs (high mobility group proteins). One possibility is that this phosphoprotein belongs to the HMG-I protein family, which migrate at a similar position on an SDS gel.

Previous studies have shown that the level of H1 phosphorylation varies considerably during the cell cycle. Possibly, a greater percentage of the *ras*-transformed mouse fibroblasts were in S and G2/M phases of the cell cycle than that of the parental cells. The proportion of cells in the different phases of the cell cycle was determined by flow cytometry of cells stained with ethidium bromide (Table II). The *ras*-transformed cells had fewer cells in G2/M phase of the cell cycle, where H1 phosphorylation is at its peak, than did the parental cells. Further, the Ciras-3 cells had a greater percentage of the cell population in G1 than did the 10T½ cells. Therefore, it is clear that the increased level of H1 phosphorylation in the *ras*-transformed cells was not due to differences in the proportion of these cells in G2 and M phases of the cell cycle.

Table II. Distribution of the *ras*-transformed and parental 10T½ cells in the various phases of the cell cycle and relative content of phosphorylated H1 subtypes.

Cell Line	Cell Cycle Phase (% distribution)			Relative level of phosphorylated H1 subtype		
	G1	S	G2/M	c-pH1b	pH1b	c-pH1c
10T½	59	16	25	1.0	1.0	1.0
Ciras-2	44	34	22	2.8	3.8	1.9
Ciras-3	65	22	13	2.8	4.2	2.0

The percentage of cells in each cell cycle phase is shown. These cells were used to isolate H1 analyzed by SDS-PAGE and by Western blot analysis with an anti-phosphorylated H1 antibody (Fig. 26). The level of the phosphorylated H1 subtype in the *ras*-transformed cells compared to that in the parent 10T½ cells was determined as described in "Materials and methods".

Elevated level of pH1b in *ras*-transformed cells

An antibody was generated against a hyperphosphorylated isoform of Tetrahymena macronuclear H1 (Lu et al., 1994). This antibody is highly selective for the phosphorylated isoforms of human and *Tetrahymena* H1. The antibody detects only one band in mouse 10T½ total cellular protein extracts (Fig. 24). For H1 isolated from the *ras*-transformed and parental 10T½ mouse fibroblast cell lines, the anti-phosphorylated H1 antibody detected only one of the phosphorylated H1 subtypes (pH1b) resolved by SDS polyacrylamide gel electrophoresis (Fig. 25). When the levels of phosphorylated H1 were analyzed, interestingly, the pH1b species recognized by this antibody comigrated with the unmodified parental band on SDS gels, while c-phosphorylated isoform of histone H1b (c-pb) was not detected by the antibody. However, incubation of H1 with alkaline phosphatase prior to gel electrophoresis and blotting negated the ability of the antibody to detect any of the H1 subtypes (Fig. 26, panel B). Treatment of H1 with alkaline phosphatase also resulted in reduction or disappearance of c-phosphorylated isoforms (Fig. 26, panel A). The amounts of the c-pb and c-pc were approximately 2- to 3-fold greater in the *ras*-transformed cells (Fig. 26 and Table II). These observations provided evidence that the level of the phosphorylated H1 was elevated in *ras*-transformed cells. The level of the pH1b isoform in *ras*-transformed and parental cell lines was determined in Western blot experiments with the anti-phosphorylated H1 antibody. Fig. 25 shows that the amount of pH1b was greater in the *ras*-transformed cells (Ciras-2 and Ciras-3) than in the parental 10T½ cells. The *ras*-transformed cells had an

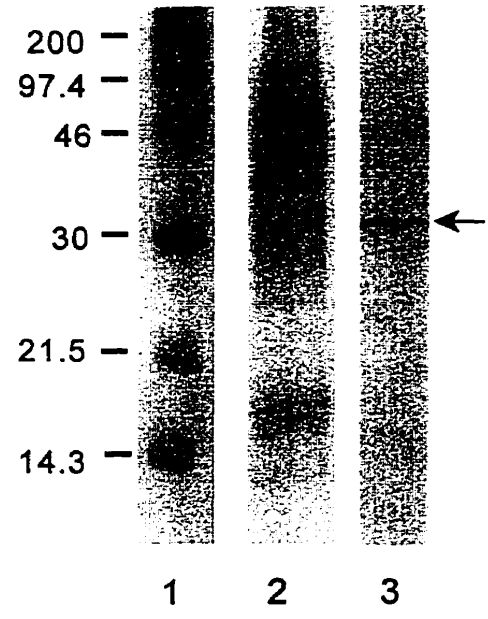

Figure 24. **Detection of phosphorylated H1 in 10T½ whole cell extracts.** 50 µg of protein from 10T½ whole cell extracts was separated on an SDS 15% polyacrylamide gel. The proteins were transferred to nitrocellulose membrane and immunochemically stained with anti-phosphorylated H1 antiserum. A Coomassie blue stained gel of molecular weight markers (lane 1) and protein from cell extract (lane 2) is shown. The immunochemically stained membrane is shown in lane 3 and the arrow indicates the single band detected by the antibody.

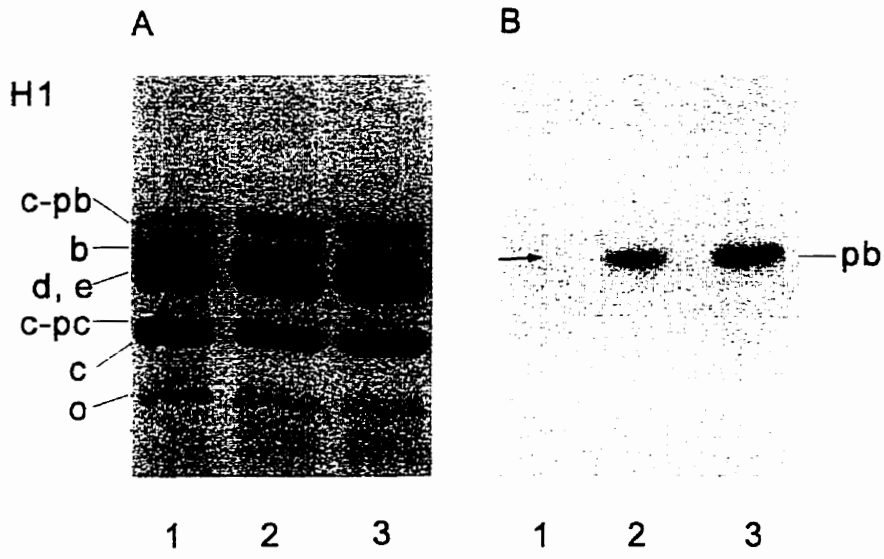

Figure 25. **Phosphorylated H1 subtypes of *ras*-transformed and parental mouse fibroblasts.** H1 (2 µg) isolated from 10T½ (lane 1), Ciras-2 (lane 2), or Ciras-3 (lane 3) was resolved on SDS 15% polyacrylamide gels. Panel A shows the India ink stained pattern of H1 transferred to the membranes. The membrane shown in panel B was immunochemically stained with the anti-phosphorylated H1 antibody. pb, c-pb, and c-pc are the phosphorylated isoforms of H1b and c-phosphorylated isoforms of H1b and H1c, respectively.

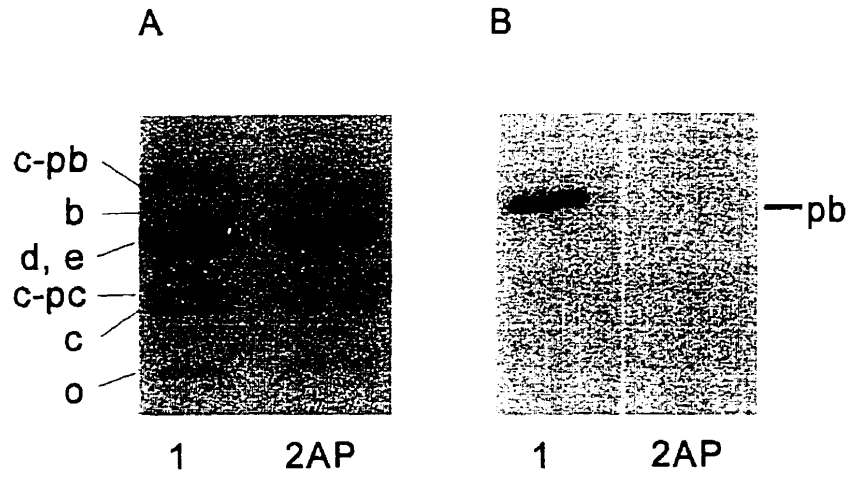

Figure 26. **Immunodetection of phosphorylated H1b.** H1 (2 µg) isolated from Ciras-2 was untreated (lane 1) or treated with alkaline phosphatase (lane 2AP). H1 was resolved on an SDS 15% polyacrylamide gel and transferred to nitrocellulose membrane. Panel A shows the India ink stained patterns of H1 transferred to the membrane. The membrane shown in panel B was immunochemically stained with the anti-phosphorylated H1 antibody. pb, c-pb, and c-pc are the phosphorylated isoforms of H1b and c-phosphorylated isoforms of H1b and H1c, respectively.

approximate 4-fold increase in the level of pH1b (Table II). Similar results were obtained when H1 was acid extracted directly from the cells.

Ras-transformed cells in the G1/S phase of the cell cycle have elevated amounts of pH1b

Analysis of the proportion of cells in the different phases of the cell cycle showed that the cell cycle distributions of the *ras*-transformed and parental cells were similar (Table II). Thus, the elevated levels of the pH1b in *ras*-transformed cells could not be accounted for by a greater percentage of the *ras*-transformed cells being in the S or G2/M phases of the cell cycle. These observations suggested that G1/S phase *ras*-transformed cells had a higher amount of phosphorylated H1 than parental 10T½ cells. To determine the level of phosphorylated H1 in G1/S phase, 10T½, Ciras-2 and R-2 (*ras*-transformed mouse 10T½ fibroblasts that are tumorigenic but not metastatic) cells were treated with hydroxyurea which arrests cells in G1/S phase of the cell cycle. Hydroxyurea is a DNA synthesis inhibitor that specifically inhibits ribonucleotide reductase (McClarty *et al.*, 1990). The distribution of the hydroxyurea-treated cells in different phases of the cell cycle was determined. Fig. 27 shows that hydroxyurea-treated cells had few cells in G2/M, with the majority of the cells being in G1 (73% for 10T½, 68% for Ciras-2). H1 was isolated from hydroxyurea-treated 10T½, R-2, and Ciras-2 cells and immunoblotting was performed with the anti-pH1b antibody. The results showed that the *ras*-transformed cell lines had higher levels (3-4-fold) of pH1b compared to

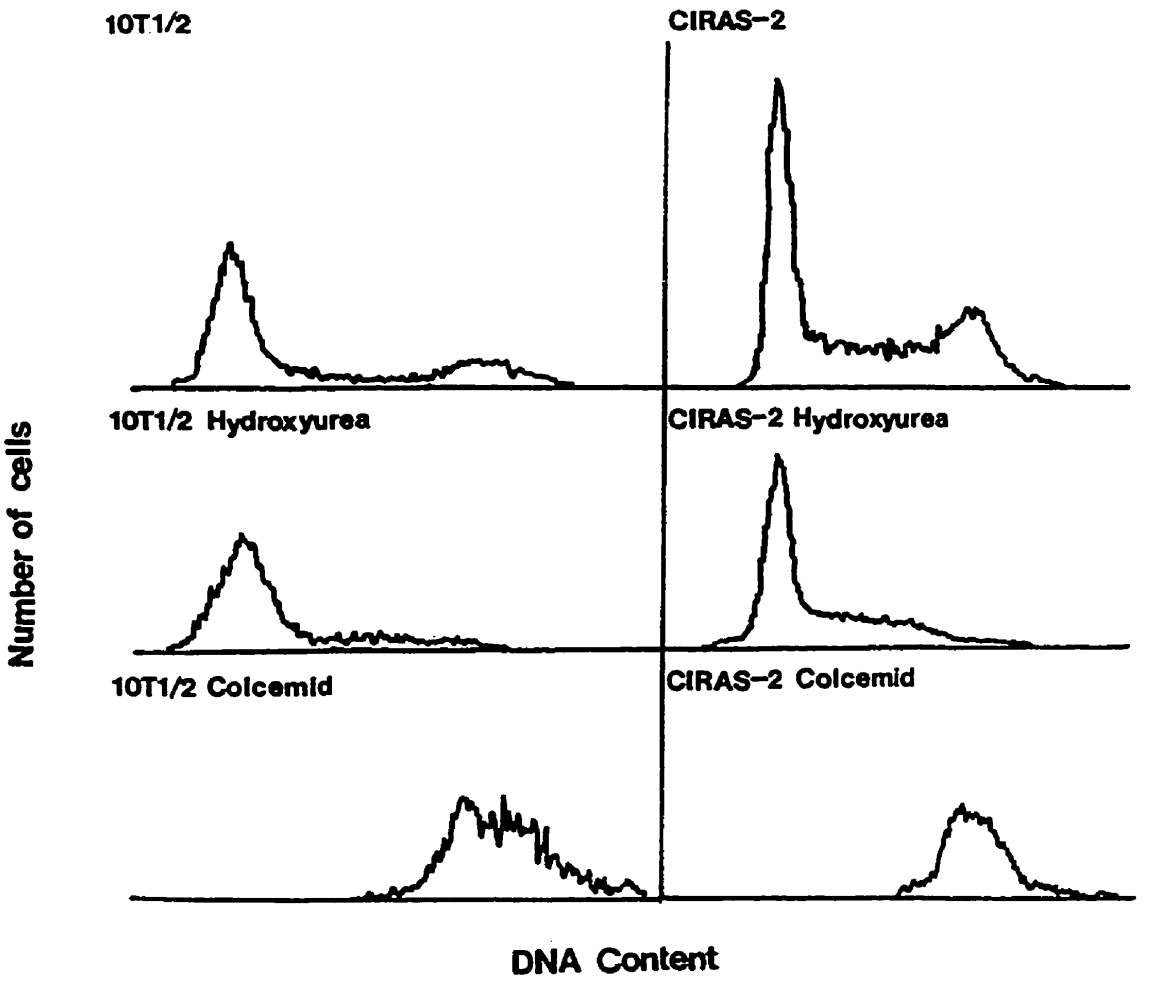

Figure 27. **Effect of hydroxyurea or colcemid on cell cycle progression of *ras*-transformed and parental mouse fibroblasts.** Parental 10T½ cells and *ras*-transformed Ciras-2 cells were either untreated (top panels) or treated with 2 mM hydroxyurea for 24 h (middle panels) or with 0.06 μg/ml colcemid for 16 h (bottom panels). DNA content in the ethidium bromide-stained cells was determined by flow cytometry. The number of cells is represented on the y axis, and the amount of DNA (fluorescence intensity) is shown on the x axis.

the parental cells (Fig. 28, Table III). The levels oc-pH1b and H1c were also greater in the *ras*-transformed cells than in the parental cells (Table III). *Ras*-transformed Ciras-2 cells treated with colcemid, which arrests cells at mitosis (Fig. 29), had high levels of hyperphosphorylated histones. Although phosphorylation of H1 subtypes should be maximal in mitotically arrested Ciras-2 cells, the anti-phosphorylated H1 antibody still detected only the pH1b isoform (Fig. 29). Thus, it appears that the anti-phosphorylated H1 antibodies are remarkably specific for the H1b isoform. The levels of phosphorylated histone H1 attained by treatment of cells with colcemid was much higher than expected based on the signal that we determined to be attributable to the M phase population. We suspected that the treatment of cells with drugs such as colcemid might increase the H1 kinase activity, consequently generating artificially high levels of phosphorylated H1 in comparison to the naturally occurring levels of mitotic phosphorylated H1.

Phosphorylation of histone H1 in cell lines transformed with oncogenes encoding protein kinases

Oncogenic *ras* can lead to the persistent activation of the MAP kinase pathway. In this pathway activated *Ras* activates Raf, a protein-serine kinase, which in turn activates MAP kinase kinase and then MAP kinase (Avruch et al., 1994; Lange-Carter and Johnson, 1994). MAP kinases stimulate the activity of transcription factors (e.g., c-Myc), leading to the induction of cyclins and

Table III. Relative level of phosphorylated H1 subtypes in hydroxyurea-arrested 10T½ and *ras*-transformed mouse fibroblasts

Cell Line	Relative level of phosphorylated H1 subtype		
	c-pH1b	pH1b	c-pH1b
10T½	1.0	1.0	1.0
Ciras-2	1.7	4.0	1.3
R-2	1.9	3.1	1.3

The cell lines 10T½, Ciras-2, and R-2 cells were treated with hydroxyurea. The H1 isoforms were resolved on SDS gels, and the level of phosphorylated H1 on Coomassie Blue-stained gel patterns or Western blots (shown in Fig. 28) was determined as described in "Materials and methods".

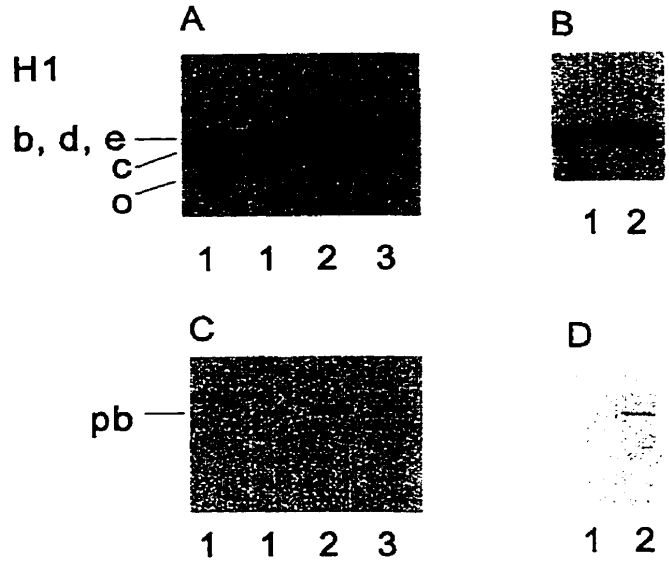

Figure 28. **Immunoblot analysis of phosphorylated H1 isoforms of normal and *ras*-transformed mouse fibroblasts treated with hydroxyurea.** Cells (10T½, lane 1; Ciras-2, lane 2; R2, lane 3) were treated with 2 mM hydroxyurea for 24 h. H1 was resolved on SDS 15% polyacrylamide gels and then transferred to membranes which were immunochemically stained for phosphorylated H1. The amount of protein loaded in each lane was as follows: panel A from left to right: lane 1, 10T½, 1.5 µg; lane 1 (second), 10T½, 2.0 µg; lane 2, Ciras-2, 2.0 µg; lane 3, R-2, 1.5 µg; panel B; lane 1, 10T½, 2 µg; lane 2, Ciras-2, 2 µg. Panels A and B show membranes stained with India ink, and panels C and D show the corresponding immunochemically stained membranes. pb is phosphorylated H1b.

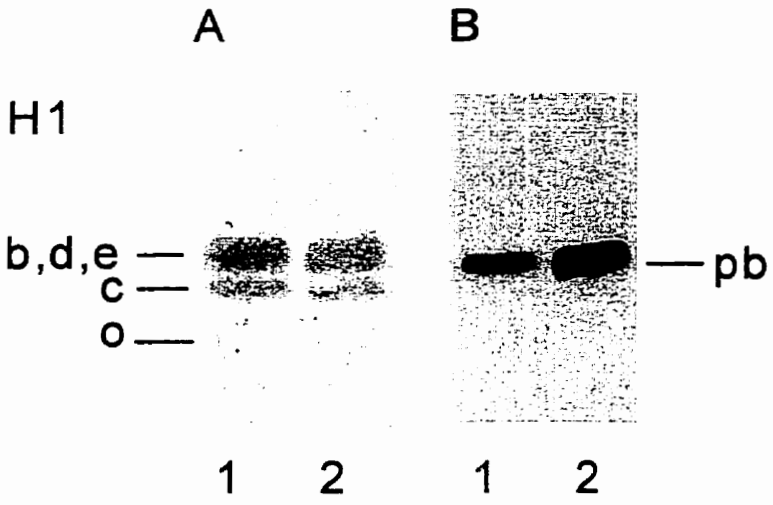

Figure 29. **Immunoblot analysis of phosphorylated H1 isoforms of *ras*-transformed mouse fibroblasts treated with colcemid.** H1 histones (2 µg) were isolated from Ciras-2 cells that were not treated (lane 1) or treated (lane 2) with colcemid. Panel A shows the india ink stained membrane, and panel B shows the corresponding immunochemically stained membrane. pb is phosphorylated H1b.

activation of cyclin-dependent protein kinases (CDKs), some of which phosphorylate H1 (Jansen-Durr et al., 1993; Hunter and Pines, 1994; Filmus et al., 1994; Daksis et al., 1994). Possibly persistent activation of the MAP kinase pathway leads to the increased phosphorylation of H1. To test this idea, we studied the phosphorylation level of H1 in cells transformed with oncogenes encoding the kinases *mos*, *raf*, and *fes* (Egan et al., 1987), which act upon the MAP kinase pathway. Levels of phosphorylated H1 subtypes in an NIH-3T3 cell line transformed with c-*myc*, a target of the MAP kinases, were also analyzed. Table IV shows that the cell cycle distributions of the parental and oncogene-transformed NIH-3T3 mouse fibroblasts were closely matched with the oncogene-transformed cells having more cells in G1. The relative levels of the H1 subtypes H1b, d, e, and c appeared to be similar for the parent and oncogene-transformed cell lines. However, the level of $H1^0$ in the oncogene-transformed cells was lower than in the parental NIH-3T3 fibroblasts (Fig. 30). Densitometric scanning of the Coomassie-blue stained SDS polyacrylamide gel containing the H1 samples showed that the content of $H1^0$ in the oncogene-transformed cells was reduced to approximately 47% of the $H1^0$ levels of parental cells. This observation is consistent with the results obtained by Laitinen *et al.* (1994). In addition to a change in the content of $H1^0$, the oncogene-transformed cells had elevated levels of the c-phosphorylated isoforms of H1b and H1c and pH1b (Fig. 30). The phosphorylated H1b and H1c isoforms were elevated 2-4-fold in the *ras*, *raf*, *fes*, *mos* and *myc*-transformed cells (Table IV). It has been demonstrated that constitutively active MAP kinase kinase

Table IV. Cell cycle distribution and level of phosphorylated H1 of NIH-3T3 mouse fibroblasts and NIH-3T3 cells transformed with *fes*, *mos*, *myc*, *raf*, or constitutively active MAP kinase kinase.

Cell Line	Cell Cycle Phase (% distribution)			Relative Level of Phosphorylated H1 Subtype		
	G1	S	G2/M	c-pH1b	pH1b	c-pH1c
NIH-3T3	35	36	28	1.0	1.0	1.0
FES	43	26	31	2.3	3.5	2.4
MOS	42	41	16	2.6	1.9	2.2
MYC	56	24	21	2.6	3.5	2.4
RAF	47	27	26	2.8	1.7	1.8
NIH-3T3	69	20	12	1.0	1.0	1.0
K97	69	19	13	1.0	0.6	0.8
ΔN3S22D	67	18	15	1.1	3.7	1.0

The H1 histones isolated from the oncogene- or MAP kinase kinase-transformed and parental NIH-3T3 cell lines were resolved on SDS gels, and the level of phosphorylated H1 histones was determined on Coomassie Blue-stained gel patterns or Western blots (shown in Fig. 30 and 31) as described in "Materials and methods".

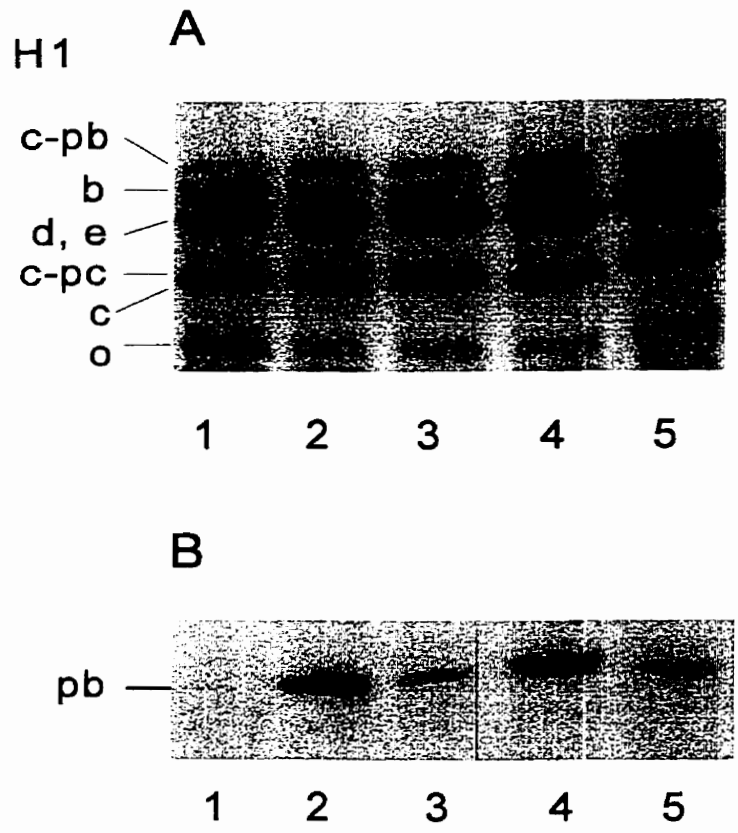

Figure 30. **Phosphorylated H1 isoforms of parental and oncogene-transformed NIH-3T3 mouse fibroblasts.** H1 (2 µg) isolated from NIH-3T3 cells (lane 1) or NIH-3T3 cells transformed with v-*fes* (lane 2), v-*mos* (lane 3), c-*myc* (lane 4), or A-*raf* (lane 5). H1 was resolved on SDS 15% polyacrylamide gels, transferred to membranes which were stained with India ink (panel A) and then immunochemically stained with anti-phosphorylated H1 antibody (panel B). pb is phosphorylated H1b. c-pb and c-pc are the c-phosphorylated isoforms of H1b and H1c, respectively.

transforms NIH-3T3 mouse fibroblasts (Mansour et al., 1994). Fig. 31 shows the content of H1 subtypes and their phosphorylated isoforms in the parental NIH-3T3, K97M (cells transfected with catalytically inactive MAP kinase kinase) and ΔN3S222D (cells transfected with constitutively active MAP kinase kinase). SDS gels indicated that the ΔN3S222D cells had slightly higher amounts of c-pH1b than the parental or K97M cell lines. Differences in the levels of the H1 subtypes including $H1^0$ were not observed. In Western blot analysis of the level of pH1b in the H1 preparations, the content of this phosphorylated H1 isoform was found to be highest in the H1 from ΔN3S222D cells (Fig. 31 and Table IV).

Immunolocalization of pH1b in *ras*-transformed and parental 10T½ cells

Lu *et al.* (1994) demonstrated that anti-phosphorylated H1 antibodies did not stain the nuclei of unsynchronized HeLa cells equivalently (Lu et al., 1994). HeLa cells in the G1 phase of the cell cycle were weakly stained and exhibited a punctate pattern of staining. Cells in the S phase had a uniform, more intense staining but less than the staining observed for G2/M phase cells. Thus, the staining intensity of the nuclei in the various phases of the cell cycle agreed with the biochemical data on changes in H1 phosphorylation during the mammalian cell cycle. We used anti-pH1b to analyze the nuclear localization of pH1b in 10T½ and Ciras-2 cells. Cells growing on coverslips were fixed, and the pH1b isoform was localized by indirect immunofluorescence using the anti-phosphorylated H1 antibody. Fig. 32 shows the immunochemical staining of

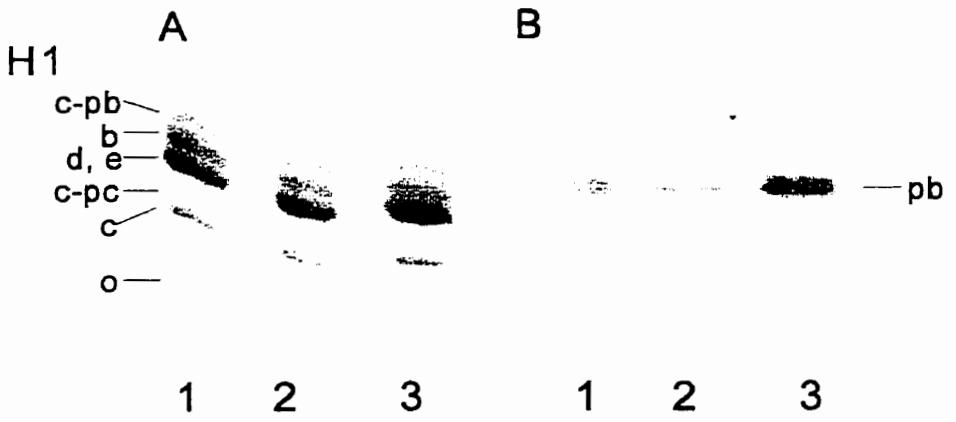

Figure 31. **Phosphorylated H1 of NIH-3T3 cells transformed with constitutively active MAP kinase kinase.** H1 isolated from NIH-3T3 cells (lane 1), K97M (NIH-3T3 cells transfected with inactive MAP kinase kinase) (lane 2), ΔN3S222D (NIH-3T3 cells transfected and transformed with constitutively active MAP kinase kinase) (lane 3). H1 (2 μg) was resolved on SDS 15% polyacrylamide gels, transferred to membranes which were stained with India ink (panel A) and then immunochemically stained with anti-phosphorylated H1 antibody (panel B). pb is phosphorylated H1b. c-pb and c-pc are the c-phosphorylated isoforms of H1b and H1c, respectively.

pre-immune

anti-H1

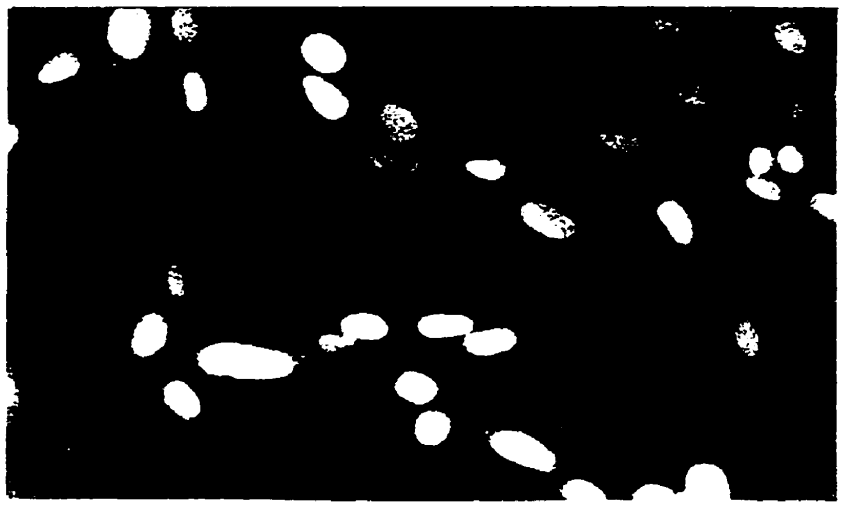

Figure 32. **Localization of phosphorylated histone H1b**. RP-4 cells were grown on coverslips and incubated with either preimmune or anti-phosphorylated H1 antibody. Cells were then incubated with goat anti-rabbit antibody conjugated to FITC. The immunochemically stained cells were photographed at 40X magnification under a fluorescent microscope.

RP-4 cells with preimmune and anti-pH1b. The antibody has a specific intense nuclear staining in comparison to the pre-immune. The majority of the interphase 10T½ and *ras*-transformed (Ciras-2) cells that stained with anti-pH1b had a weak nuclear fluorescence and punctate fluorescent dots dispersed throughout the nucleoplasm (Fig. 33 and 34). The staining of the Ciras-2 nuclei was more diffuse than the 10T½ nuclei. This was probably due to cell and nuclei shape. The 10T½ cells were flat and their nuclei large, while the Ciras-2 cells were round and their nuclei appeared smaller. The number of speckles observed for *ras*-transformed and parental cells appeared to be equivalent. Occasionally, we observed cells that were in M phase (see Fig. 33 B). As might be expected, the mitotic chromosomes stained intensely for phosphorylated H1. The punctate/speckled pattern of nuclear staining observed with this antibody (also see Lu *et al.*, 1994) is reminiscent of the finding that nuclear sites of splicing factors, small nuclear RNAs and RNA synthesis were colocalized (Huang and Spector, 1991; Hassan et al., 1994; Jackson et al., 1993). To ascertain whether the pH1b was colocalizing with the sites of splicing factors and "transcript domains", the monoclonal antibody B1C8 was also used in indirect immunolocalization studies. The B1C8 monoclonal antibody recognizes a 180-kDa human nuclear matrix protein and co-immunoprecipitates exon-containing RNA from in vitro splicing reactions (Wan et al., .1994; Blencowe et al., 1994). B1C8 has recently been shown to associate with splicing complexes and function as a coactivator of pre-mRNA splicing. Also, the B1C8 antibody has been renamed SRm160 (SR-related matrix protein of 160 KDa), but will be referred to

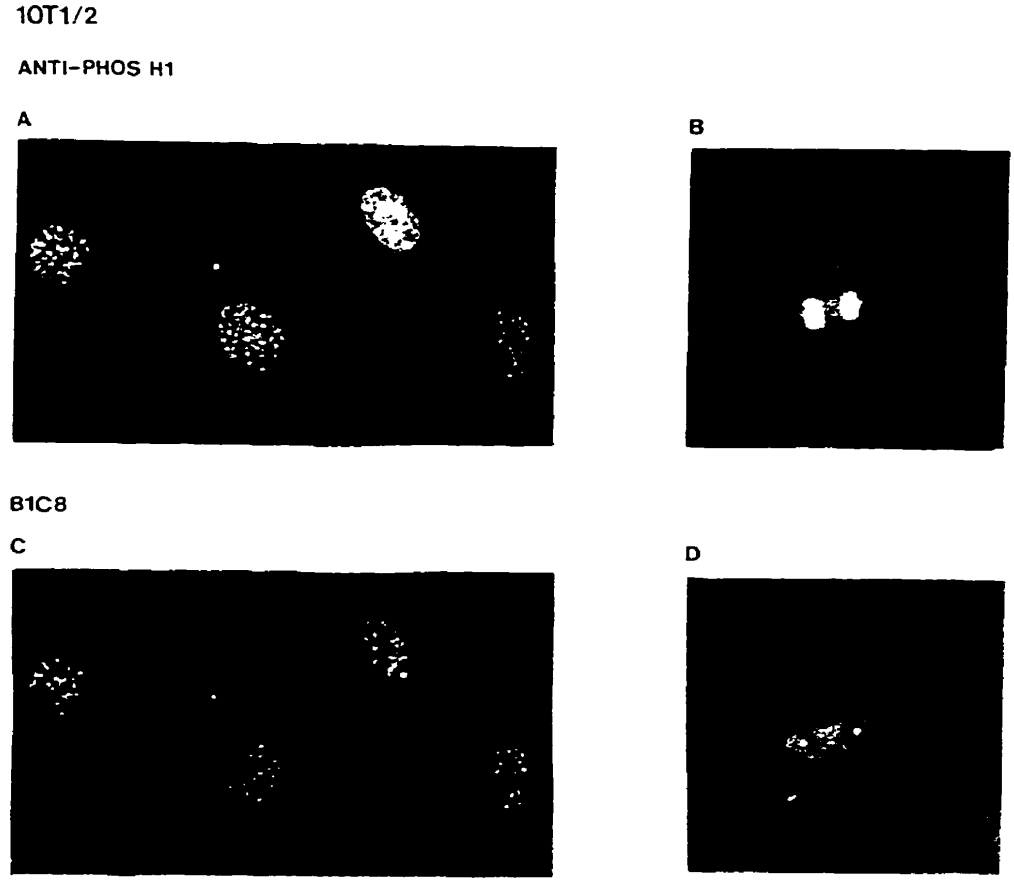

Figure 33. **Phosphorylated H1b colocalizes with the BIC8 nuclear matrix antigen in 10T½ mouse fibroblast nuclei.** Cells were fixed on coverslips and double stained by indirect immunofluorescence with an anti-phosphorylated H1 antibody and B1C8 monoclonal antibody and then goat anti-rabbit antibody conjugated to FITC (green, panels A and B) and goat anti-mouse antibody conjugated to Texas red (red, panels C and D). The immunochemically stained 10T½ cells were photographed at 60X magnification. Panels B and D show a cell in M phase of the cell cycle.

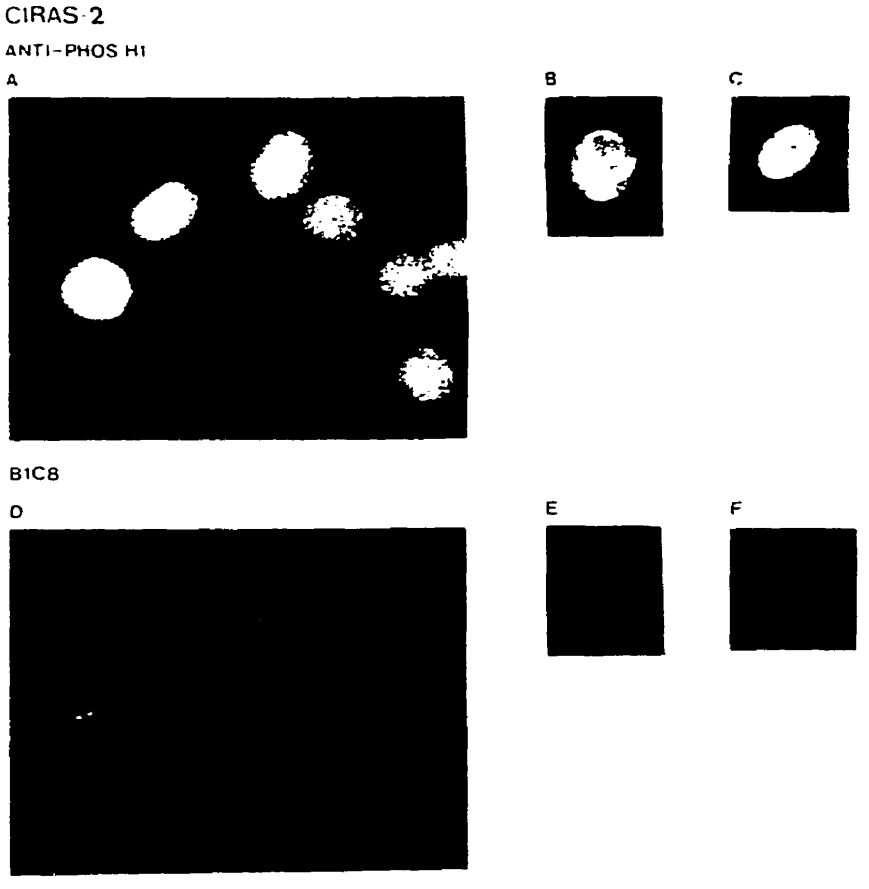

Figure 34. **Phosphorylated H1b colocalizes with the B1C8 nuclear matrix antigen in Ciras-2 mouse fibroblast nuclei.** Ciras-2 cells were fixed on the surface of a coverslip and stained by indirect immunofluorescence with anti-phosphorylated H1 antibody and B1C8 monoclonal antibody and then goat anti-rabbit antibody conjugated to FITC (green, panels A, B and C) and goat-anti mouse antibody conjugated to Texas red (red, panels, D, E and F). The immunochemically stained Ciras-2 cells were photographed at 60X magnification.

as B1C8 throughout this thesis (Blencowe et al., 1998). Western blot experiments with the B1C8 monoclonal antibody and total protein isolated from 10T½ mouse fibroblasts showed that the monoclonal antibody detected a 180-kDa mouse protein (Fig. 35). The relative nuclear positioning of pH1b and the B1C8 antigens was done. Figures 33 and 34 show that the majority of the speckles in the nuclei of 10T½ and Ciras-2 cells observed with the anti-phosphorylated H1 antibody were detected with the B1C8 monoclonal antibody. Of the 40 to 50 speckles illuminated by the antibodies, approximately 80% overlapped. Thus, pH1b appeared to be localized to sites of RNA processing and gene transcription in the majority of the interphase 10T½ and *ras*-transformed cells (Fig. 33 and 34). However, for cells in mitosis the B1C8 staining did not colocalize with the staining for pH1b, where intense staining of B1C8 was found at the spindle poles (see Fig. 33D). This pattern of redistribution of the B1C8 antigen during mitosis in mouse fibroblasts is similar to that observed in human CaSki cells (Wan et al., 1994).

Fibroblasts transformed by combinations of *ras*, *myc* and mutant p53 exhibit increased phosphorylation of histone H1 that is independent of metastatic potential.

We previously reported that cell lines transformed with several oncogenes utilizing the MAP kinase pathway had both a decondensed nucleosomal structure and highly phosphorylated H1 subtypes (Chadee et al., 1995). In this study we compared the level of histone phosphorylation in cells transformed with

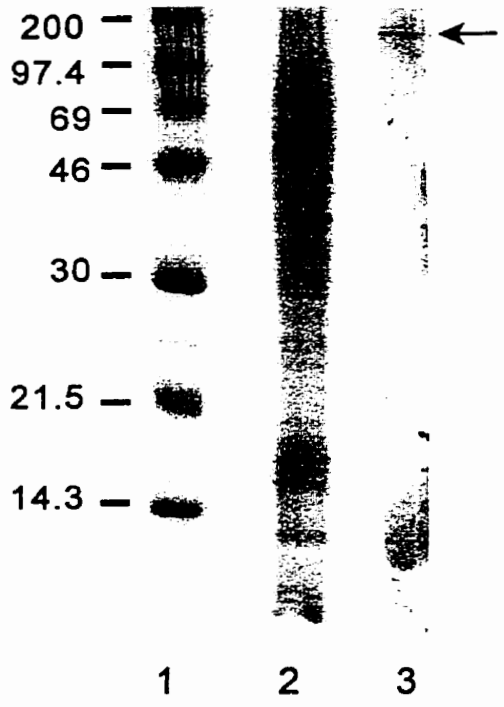

Figure 35. **Detection of B1C8 protein in 10T½ whole cell extracts.** 50 µg of protein from 10T½ whole cell extracts was separated on an SDS 15% polyacrylamide gel. The proteins were transferred to nitrocellulose membrane and immunochemically stained with B1C8 antibody. A Coomassie blue stained gel of molecular weight markers (lane 1) and protein from cell extract (lane 2) is shown. The immunochemically stained membrane is shown in lane 3 and the arrow indicates the single band detected by the antibody.

combinations of *ras*, *myc*, and mutant p53 which differ in malignant potential (experiments were done in collaboration with Dr. W. Taylor). H1 subtypes isolated from murine fibroblasts transformed with combinations of *ras*, *myc*, and mutant p53 were electrophoretically separated in SDS polyacrylamide gels. The H1 subtypes H1°, H1c, H1e, and phosphorylated forms c-pH1b, c-pH1c and pH1b were resolved in this gel system (Fig. 36). All *ras*-transformed cell lines had higher levels of c-pH1b and c-pH1c compared to 10T½ cells (Fig. 36, Table V). The transformed fibroblasts had 1.6- to 2.7-fold higher levels of c-pH1b and 1.3- to 2.3- fold higher levels of c-pH1c (Table V). The increase in these two phosphorylated species was found in all *ras*-transformed cell lines, and the presence of either *myc* or mutant p53 did not significantly alter the relative levels of these phosphorylated H1 subtypes.

Relative level of pH1b in oncogene-transformed cells

H1 isolated from cells transfected with *ras*, *myc* and mutant p53 were separated on SDS polyacrylamide gels immunochemically stained with anti-pH1b. The immunoblot shown in Fig. 37 demonstrates that the parental 10T½ cell line had a low level of phosphorylated H1b. However, cells transformed by combinations of *ras*, *myc*, and mutant p53 contained 3.7- to 5.9-fold higher levels of this modified H1 subtype (Table V).

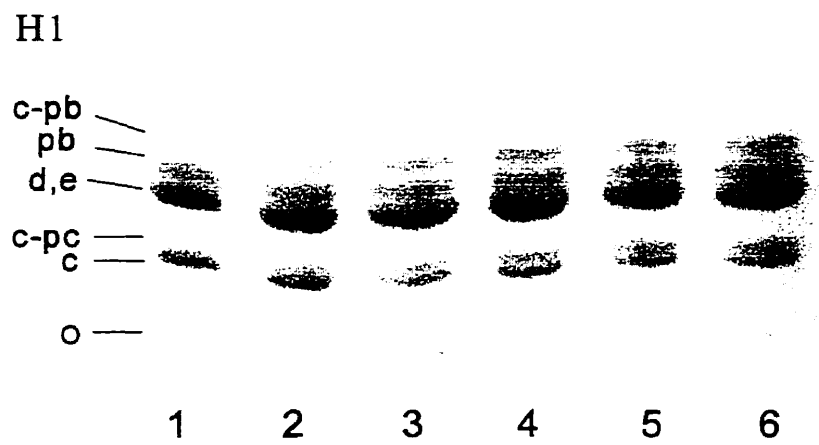

Figure 36. **Electrophoretic analysis of H1 from fibroblasts transfected with *ras*, *myc* and mutant p53**. H1 was extracted and separated by SDS polyacrylamide gel electrophoresis. Two µg of histone were loaded per lane and the gel was stained with Coomassie Blue. Lanes are: (1) 10T½, (2) R-2, (3) RM-5, (4) RP-4, (5) RP-6, (6) RMP-6. Panel A shows the india ink stained membrane, and panel B shows the corresponding immunochemically stained membrane. pb is phosphorylated H1b.

Table V. Cell cycle distribution and level of phosphorylated H1 of 10T½ cells transformed with combinations of *ras*, *myc*, and mutant p53.

Cell Line	Cell Cycle Phase (% distribution)			Relative Level of Phosphorylated H1 Subtype		
	G1	S	G2/M	c-pH1b	pH1b	c-pH1c
10T½	55	26	19	1.0	1.0	1.0
R-2	61	26	13	1.6	3.7	1.3
RM-5	54	25	21	2.2	4.8	1.6
RP-4	49	31	19	2.6	2.9	1.7
RP-6	50	31	24	2.6	6.7	1.8
RMP-6	45	31	24	2.7	5.9	2.3

The H1 histones isolated from the oncogene- transformed parental 10T½ cell lines were resolved on SDS gels, and the level of phosphorylated H1 histones on Coomassie Blue-stained gel patterns or Western blots (shown in Fig. 36 and 37) was determined as described in "Materials and methods".

Figure 37. **Phosphorylated H1 of mouse fibroblasts transfected with combinations of *ras*, *myc* and mutant p53.** H1 was extracted and separated by SDS polyacrylamide gel electrophoresis. Two µg of histone were loaded per lane and the proteins were transferred to polyvinyl difluoride membranes. The membranes were stained with india ink (panel A) and immunoblotting with the anti-pH1b antibody was performed (panel B). Lanes are: (1) 10T½, (2) R-2, (3) RM-5, (4) RP-4, (5) RP-6, (6) RMP-6. pb is phosphorylated H1b and c-pb and c-pc are the c-phosphorylated isoforms of H1b and H1c, respectively.

Cell cycle analysis

The level of H1 phosphorylation varies considerably during the cell cycle (Hohmann, 1983). As previously mentioned, H1 has a low number of phosphorylated sites in G1 phase with approximately 1 phosphorylated amino acid per molecule. The phosphorylation level rises to approximately 6 residues per molecule for some H1 subtypes when cells enter M phase. A different cell cycle distribution for the transformed cell lines compared to that of the control cells might account for the changes in the levels of phosphorylated H1. Table V shows that there were no significant differences in the cell cycle distributions of the transformed cells in comparison to the 10T½ cells. Furthermore, some of the transformed cells (R-2 and RP-6) had fewer G2/M cells than did the 10T½ cells, making it unlikely that the observed increase in the H1 phosphorylation was secondary to altered cell cycle distributions.

Correlation of H1 phosphorylation with cellular transformation but not induction of the malignant phenotype

It has previously been shown that *ras*, *myc* and mutant p53 cooperate in the induction of the metastatic phenotype in 10T½ cells (Taylor et al., 1994). We were interested in determining if increased phosphorylation of H1 may be involved in regulating the metastatic phenotype. We observed no correlation with any of the three phosphorylated histone subtypes with metastatic potential (Table V). Instead, all transfectants exhibited an increase in pH1b. For example, the highly metastatic RMP-6 cell line formed an average of 85.1 lung nodules when

injected intravenously, whereas RP-6 cells did not metastasize in this assay, yet both cell lines had similar levels of all three phosphorylated H1 histone subtypes. Therefore, increased levels of c-pH1b, pH1b and c-pH1c correlated well with cellular transformation but not with induction of the metastatic phenotype.

Discussion

Ras- and c-*myc*-transformed mouse fibroblasts (NIH-3T3 and 10T½) have a less condensed chromatin structure than the parental cells (Chadee et al., 1995; Laitinen et al., 1990; Laitinen et al., 1994). Since H1 stabilizes higher order chromatin structure, it was reasonable to suggest that changes in H1 would be a factor in chromatin decondensation. Alterations in H1 subtypes have been observed in transformed cells (Tan et al., 1982; Davie and Delcuve, 1991). A reduction in the content of $H1^0$ in *ras*-transformed NIH-3T3 mouse fibroblasts may contribute to the decondensation of the chromatin in the *ras*-, *raf*-, *fes*-, *mos*, and *myc*- transformed cells. However, the lower level of histone $H1^0$ in oncogene-transformed mouse fibroblasts was not a general observation. *Ras*-transformed 10T½ mouse fibroblasts and constitutively active MAP kinase kinase-transformed NIH-3T3 cells had a content of H1 subtypes (including $H1^0$) that was similar to that of parental cells.

The single consistent alteration we observed in the oncogene-transformed 10T½ and NIH-3T3 mouse fibroblasts was an increase in the level of phosphorylated H1 subtypes. The content of pH1b and pH1c that have a reduced mobility on SDS gels was elevated in the oncogene-transformed cells.

in Western blot experiments with an antibody that is highly selective for the phosphorylated form of H1b in these cells, we found that the level of this phosphorylated subtype was increased in all oncogene-transformed cells used in this study.

Studies with native and reconstituted chromatin show that phosphorylated H1 destabilize chromatin structure (Kaplan et al., 1984; Hill et al., 1991). Further, in studies with avian fibroblasts transfected with H5 (an H1 variant); H5 was shown to inhibit proliferation in normal fibroblasts but not in transformed cells, in which H5 was phosphorylated. Aubert *et al.* (1991) proposed that phosphorylated H5 lacked the ability to condense chromatin (Aubert et al., 1991). Also, in a number of other systems H1 phosphorylation is correlated with decondensation of chromatin (Halmer and Gruss, 1996b; Lu. et al., 1995; Sweet et al., 1996; Roth and Allis, 1992). Thus, these and other studies provide support for the idea that an increase in the phosphorylation of H1 leads to destabilization of the chromatin in oncogene-transformed cells.

Mouse fibroblasts transformed with *raf*, *fes*, or *mos* had elevated levels of phosphorylated H1 subtypes. These oncogenes code for serine/threonine or tyrosine kinases and act upon the MAP kinase signal transduction pathway (Hunter and Pines, 1994) and these oncogene-transformed cell lines all have elevated Map kinase activity. In addition, cells transformed with combinations of *ras*, *myc* and mutant p53 also exhibited increased levels of phosphorylated H1. *Ras*, Myc and mutant p53 cooperate in the induction of the metastatic potential in these cells. This increase in the level of pH1b, however, did not correlate with

the metastatic potential of the cells. NIH-3T3 cells transformed with constitutively active MAP kinase kinase also had an increased content of pH1b and, to a lesser extent, c-pH1b. These observations suggest that persistent activation of the MAP kinase pathway has a role in the intensified phosphorylation of H1 in the transformed cells. One of the downstream targets of the MAP kinase pathway is the c-Myc protooncogene product. Phosphorylation of c-Myc increases its ability to transactivate genes (Davis, 1993). Myc and activated *Ras* enhance the expression of cyclins D1, E and A (Jansen-Durr et al., 1993; Daksis et al., 1994; Filmus et al., 1994). Overexpression of cyclin E in cells significantly enhances cyclin E associated H1 kinase activity (Resnitzky et al., 1994). It is possible that activation of the MAP kinase signal transduction pathway leads to the phosphorylation of c-Myc which in turn increases the expression of cyclins E and A and activity of a cyclin E or cyclin A associated H1 kinase. In addition, c-Myc itself also requires the MAP kinase pathway to maintain the transformed phenotype (Amundadottir and Leder, 1998). Our studies reveal that acquisition of high levels of phosphorylated H1 is an early event in neoplastic development in this *in vitro* system. The increased level of phosphorylated H1 may affect the expression of genes involved in growth factor dependence and growth control. The high selectivity of the anti-phosphorylated H1 antibody allowed us to ascertain the cellular location of the phosphorylated isoform of H1b. A punctate pattern of nuclear staining of *ras*-transformed and parental 10T½ cells was observed. Clearly, the results show that the phosphorylated isoform of H1b is nonuniform in the nuclei of parental and *ras*-transformed mouse fibroblasts. In

M-phase cells, the punctate pattern of staining is lost, and an intense staining of the mitotic chromosomes is observed. A similar staining was observed for non-S phase HeLa nuclei (Lu et al., 1994). The speckled pattern observed with the anti-phosphorylated H1 antibody closely matched the pattern found with the B1C8 monoclonal antibody. B1C8 colocalizes with other RNA splicing components (SC35, snRNPs) and recently it has been shown to function as a coactivator of pre-mRNA splicing (Blencowe et al., 1994; Blencowe et al., 1998). Several transcribed genes (e.g., c-*fos*) have been located near sites containing RNA splicing components (Blencowe et al., 1994; Xing et al., 1995). Further, the punctate pattern of splicing factors is sensitive to inhibitors of transcription (Huang et al., 1997). Durfee *et al.* (1994) found that the nuclear matrix protein p84, which is present in human and mouse cells and binds to the N-terminal domain of dephosphorylated Rb, colocalizes with the B1C8 antigen (Durfee et al., 1994). Dephosphorylated Rb binds to the transcription factor E2F, which is involved in the activation of several early response genes, including c-*myc*. Although inactive when bound to dephosphorylated Rb, E2F still has the capacity to bind its target DNA (Nevins, 1992; Weintraub et al., 1992). Thus, the nuclear matrix-bound p84, which is near sites containing splicing factors, through its association with dephosphorylated Rb-E2F complex may attract early response genes to sites of RNA processing. Following the release of E2F from Rb, E2F forms a complex with cyclin E (and later with A), p107, and CDK2 (Hunter and Pines, 1994). It is an attractive hypothesis that the transcription factor E2F

directs the H1 kinase activity of CDK2 to transcriptionally active chromatin regions (Devoto et al., 1992).

Part 2: Histone H1b phosphorylation is dependent upon ongoing transcription and replication.

Introduction

Mouse fibroblast 10T½ cells transformed by *ras*, *fes*, *mos*, *myc*, *raf*, or combinations of *ras*, *myc*, and mutant p53 have an increased level of pH1b in comparison to the parental cells (see sections 1 and 2). We have suggested that the increase in pH1b levels is a result of the persistent activation of the MAP kinase signal transduction pathway leading to an increase in CDK2 / cyclin E associated H1 kinase activity. In agreement with our results it has been demonstrated that fibroblasts lacking the tumor suppressor Rb also exhibit an increased level of phosphorylated H1 and relaxed chromatin structure and that deregulation of CDK2 may be directly involved (Herrara et al., 1996). Indirect immunofluorescence studies using an anti-pH1b antibody revealed a punctate pattern of nuclear staining in parental and oncogene-transformed mouse fibroblasts (see section 1). This pattern colocalized with the pattern observed when cells were stained with B1C8, an antibody raised against a human nuclear matrix protein that colocalizes with SC-35 domains and has recently been shown to function as a coactivator of pre-mRNA splicing (Blencowe et al., 1994; Wan et al., 1994; Blencowe et al., 1998). Studies have shown that there is a high degree of spatial association of specific actively transcribed genes with SC-35 domains whereas the non-transcribed genes do not show preferential association (Clemson and Lawrence, 1996; Xing et al., 1995). We have, therefore,

suggested that pH1b is complexed to transcriptionally active chromatin which is localized near sites of RNA splicing (see section 1)

To investigate the relationship of H1 phosphorylation and transcriptionally active chromatin, we treated parental and *ras*-transformed 10T½ mouse fibroblasts with the transcription inhibitors, actinomycin D and DRB. We monitored the level of pH1b by Western blotting with anti-pH1b.

Results

Effect of inhibition of transcription by actinomycin D on levels of pH1b

Actinomycin D, at 10 µg/ml, strongly inhibits RNA polymerase I and RNA polymerase II transcription by intercalating into DNA (Perry, 1963; Chen et al., 1996). 10T½ and Ciras-2 cells were treated with 10 µg/ml actinomycin D for 30 and 70 min. H1 isolated from these cells was electrophoretically resolved on 15% SDS polyacrylamide gels, transferred to membranes, and immunochemically stained with anti-pH1b antibody. Figure 38 (A and B) shows the position of migration of H1 b, c, d, e, and $H1^{\circ}$ subtypes on an SDS-15% polyacrylamide gel. The relative level of pH1b in treated cells was compared to that of untreated cells and was determined as described in the previous section. Incubation of 10T½ cells with 10 µg/ml actinomycin D resulted in a 90% reduction of the level of pH1b after 30 min and after 70 min the pH1b signal was undetectable. In the Ciras-2 cells there was no decrease in the level of pH1b

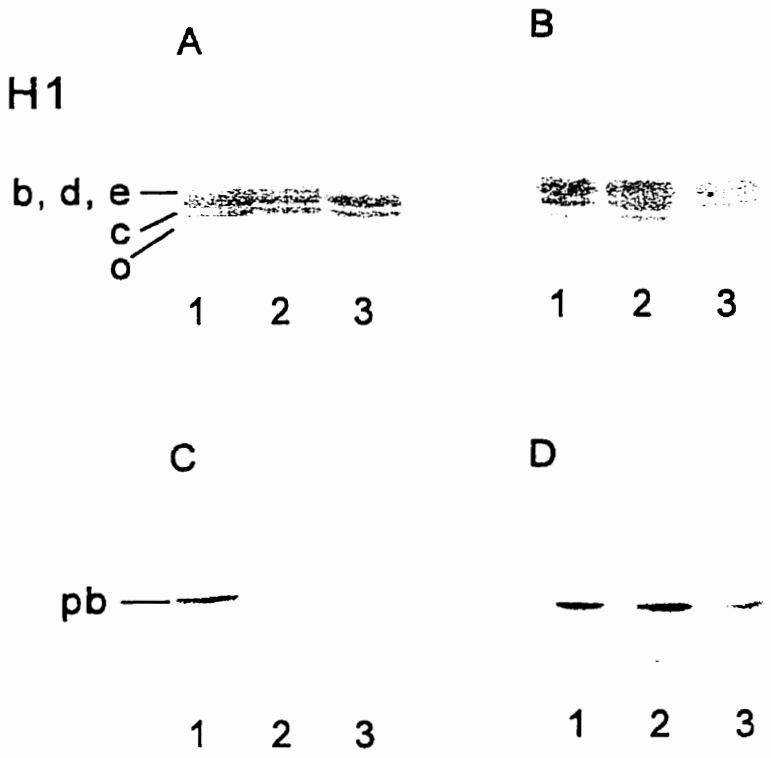

Figure 38. **Effect of inhibition of transcription with actinomycin D on level of H1b phosphorylation.** H1 was extracted from mouse fibroblast 10T½ (panel A) or Ciras-2 (panel B) cells that were untreated (lane 1), incubated with 10 µg/ml actinomycin D for 30 min (lane 2) or 70 min (lane 3). H1 (2 µg) was electrophoretically resolved on an SDS 15% polyacrylamide gels, transferred to membranes which were immunochemically stained with anti-pH1b. Panels A and B show Coomassie Blue stained gels. Panels C and D show the immunochemically stained membranes. pb is the phosphorylated isoform of H1b.

after 30 min; however, after 70 min there was an 82% decrease in the level of pH1b (Fig. 38).

Effect of inhibition of transcription by DRB on levels of pH1b

The adenosine analog DRB selectively inhibits transcription by RNA polymerase II (Codosh et al., 1989). It has been proposed that DRB inhibits transcription at the stage of elongation although the specific mechanism of inhibition remains unclear. DRB has been shown to be a potent inhibitor of the CAK (CDK acivating kinase) associated with the transcription factor TFIIH. It has been suggested that CAK functions in controlling RNA Polymerase II elongation and that DRB inhibits transcription elongation by inhibiting CAK activity (Yankulov et al., 1995). Alternatively, it has also been demonstrated that DRB inhibits casein kinase II, which has been shown to phosphorylate the C-terminal domain of RNA pol II (Zandomeni, 1989; Stevens and Maupin, 1989). As a result, it has been suggested that DRB inhibits transcription by inhibiting phosphorylation of the RNA pol II C-terminal domain by casein kinase II (Zandomeni, 1989; Stevens and Maupin, 1989).

10T½ cells were treated with 150 μM DRB for 70 min and 2 h (Fig. 39). After 70 min, there was an 89% reduction in the level of pH1b. The signal was undetectable after a 2 h treatment. Ciras-2 cells were treated for 2 h and 3 h time periods. Fig. 39 shows that after 2 h there was a 54% reduction in the level of pH1b, and this level remained the same even after a 3 h treatment.

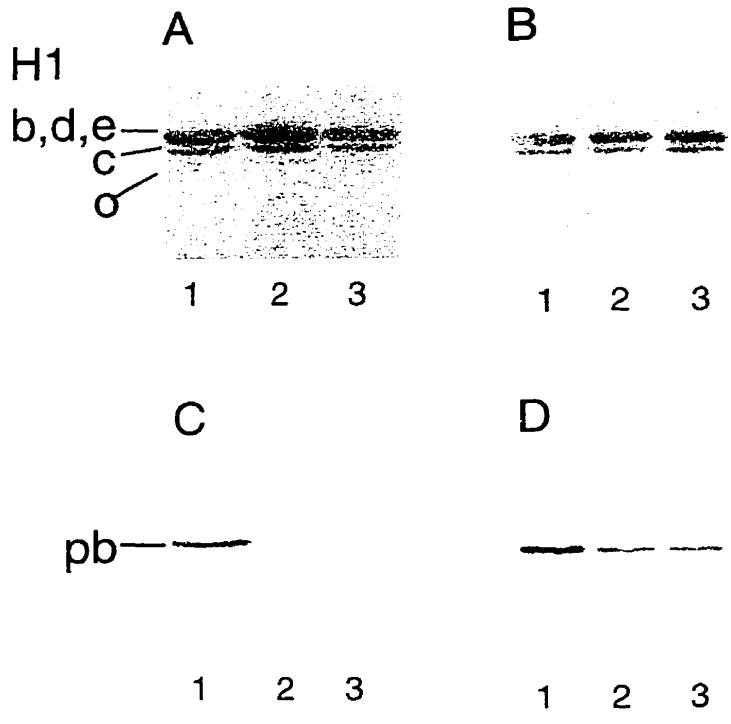

Figure 39. **Effect of inhibition of transcription with DRB on level of H1b phosphorylation.** H1 was extracted from 10T½ cells (panel A) that were untreated (lane 1), or incubated with 150 μM DRB for 70 min (lane 2) or 2 h (lane 3). H1 was extracted from Ciras-2 cells (panel B) that were untreated (lane 1) or treated with 150 μM DRB for 2 h (lane 2), or 3 h (lane 3). H1 (2 μg) was electrophoretically resolved on SDS-15% polyacrylamide gels, transferred to membranes and immunochemically stained with anti-pH1b. Panels A and B show Coomassie Blue stained gels. Panels C and D show the immunochemically stained membranes. pb is the phosphorylated isoform of H1b.

Effect of removal of transcription inhibition by DRB on levels of pH1b

DRB is a reversible inhibitor of RNA polymerase II. We wanted to determine whether the level of pH1b was restored in the DRB treated cells when DRB was removed. We incubated 10T½ cells in the presence of 150 μM DRB for 70 min and then removed the DRB containing medium and replaced it with fresh medium that did not contain DRB. The cells were allowed to recover for 2 h. Fig. 40 shows that after a 2 h period of time, the level of pH1b had been restored.

Effect of inhibition of DNA synthesis on the levels of pH1b

Aphidicolin is a potent inhibitor of DNA polymerase α and inhibits DNA replication (Ikegami et al., 1978) (Arabshahi et al., 1988; Pedrali-Noy and Spadari, 1979). Aphidicolin is a competitive inhibitor of dCTP which is analogous to the mode of inhibition of cellular alpha polymerases. 10T½ and Ciras-2 cells were incubated for 30 and 70 min in the presence of 10 μM aphidicolin. Fig. 41 shows that inhibition of replication by aphidicolin resulted in a dramatic reduction in the level of pH1b after 30 min in both the 10T½ parental and the Ciras-2 transformed cell lines. The level of pH1b was reduced by 94% in 10T½ cells and by 81% in Ciras-2 cells after 30 min.

Effect of inhibition of transcription and replication on the level of pH1b in 10T½ cells

The combination of 150 μM DRB and 10 μM aphidicolin should inhibit both transcription and replication. Fig. 42 shows that incubation of 10T½ cells with a

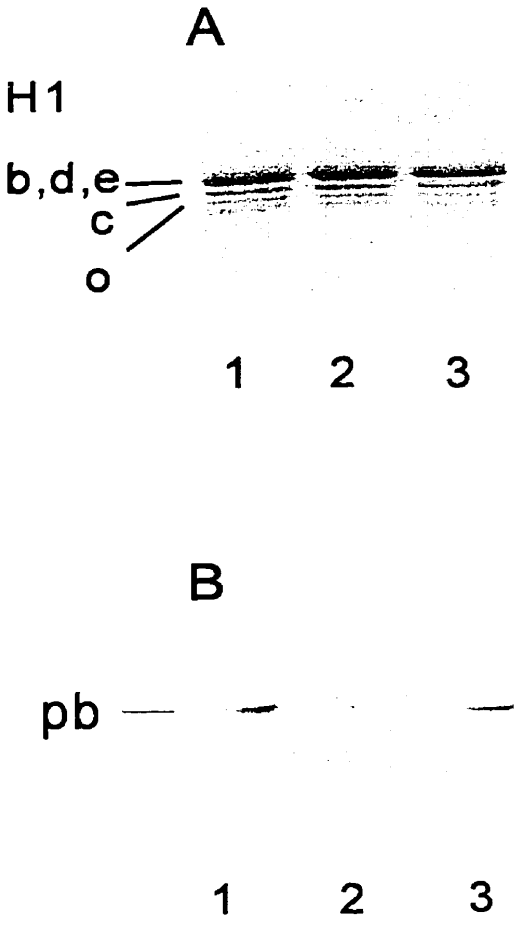

Figure 40. **Effect of removal of DRB treatment on level of H1b phosphorylation.** H1 was extracted from 10T½ cells that were untreated (lane 1), incubated with 150 µM DRB for 70 min (lane 2), or 70 min and a 2 h recovery (lane 3). H1 (2 µg) was electrophoretically resolved on SDS-15% polyacrylamide gels, transferred to membranes and immunochemically stained with anti-pH1b. Panel A shows the Coomassie Blue stained gel. Panel B shows the immunochemically stained membrane. pb is the phosphorylated isoform of H1b.

Figure 41. **Effect of inhibition of replication with aphidicolin on level of H1b phosphorylation**. H1 was extracted from 10T½ (panel A) and CIRAS-2 (panel B) cells that were untreated (lane 1), or incubated with 10 μM aphidicolin for 30 min (lane 2). H1 (2 μg) was electrophoretically resolved on SDS-15% polyacrylamide gels, transferred to membranes and immunochemically stained with anti-pH1b. Panels A and B show Coomassie Blue stained gels. Panels C and D show the immunochemically stained membranes. pb is the phosphorylated isoform of H1b.

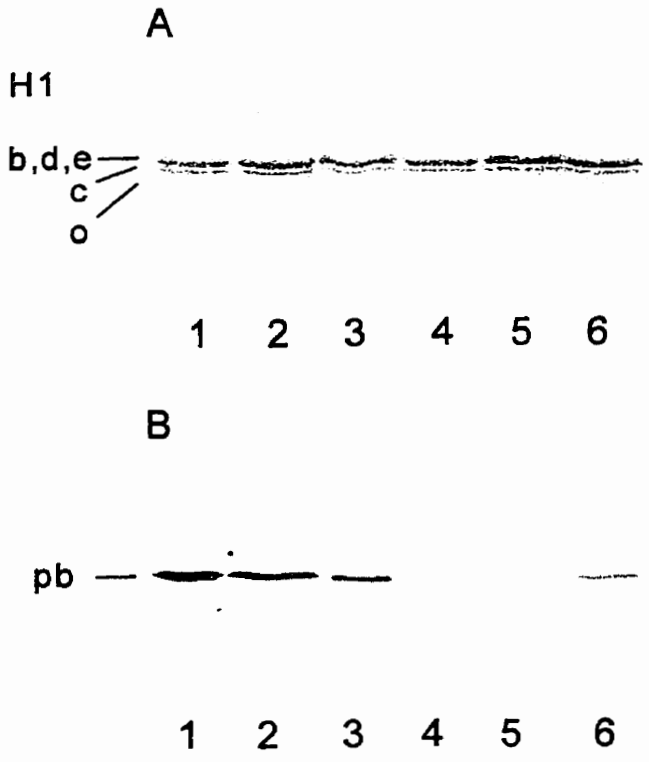

Figure 42. **Effect of inhibition of transcription and replication on the level of H1b phosphorylation in 10T½ cells.** H1 was extracted from 10T½ cells that were untreated (lane 1), incubated with 10 µg/ml actinomycin D for 30 min (lane 2), 150 µM DRB for 30 min (lane 3), 10 µM aphidicolin for 30 min (lane 4), or 10 µg/ml actinomycin D plus 10 µM aphidicolin for 30 min (lane 5), 150 µM DRB plus 10 µM aphidicolin for 30 min (lane 6). H1 (2 µg) was electrophoretically resolved on an SDS-15% polyacrylamide gel, transferred to membranes and immunochemically stained with anti-pH1b. Panel A shows a Coomassie Blue stained gel. Panel B shows the immunochemically stained membrane. pb is the phosphorylated isoform of H1b.

combination of aphidicolin and DRB resulted in a similar reduction in the level of pH1b as when aphidicolin was used alone. Similarily, the combination of actinomycin D and aphidicolin for 30 min resulted in a decrease in the level of pH1b, which was similar to the decrease observed with aphidicolin alone. Fig. 43 shows that incubation of Ciras-2 cells for 70 min with a combination of aphidicolin and actinomycin D or DRB resulted in a similar reduction in the level of pH1b as when aphidicolin was used alone.

Cell cycle analysis

For each of the experiments described above, flow cytometry was performed on the cells to determine if there were any changes in the cell cycle distributions upon treatment with the different transcription and replication inhibitors. As expected, we found that the cell cycle distributions were the same before and after treatment with the different inhibitors (data not shown). We observed a significant decrease in the level of pH1b when cells were treated with actinomycin D, DRB, or aphidicolin. One would expect that the high level of pH1b present in the M phase cells of the population would be unaffected by the transcription and replication inhibitors. Interestingly, for some treatments, the level of pH1b was reduced to less than 10% after 30 min. Thus, we suspect that the pH1b detected by the antibody is probably comprised mostly of G1 and S phase phosphorylation and the contribution of G2/M phase phosphorylation is very low.

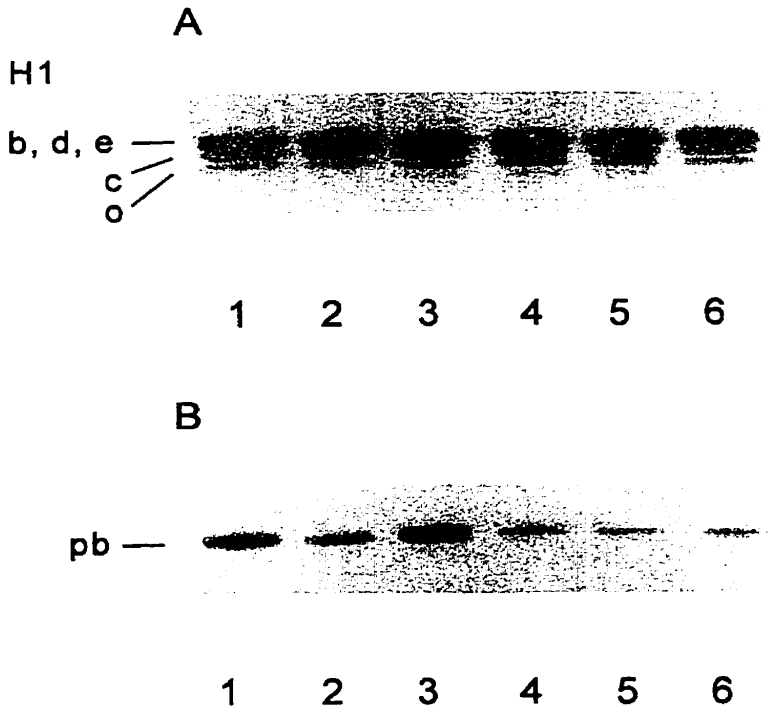

Figure 43. **Effect of inhibition of transcription and replication on the level of H1b phosphorylation in CIRAS-2 cells.** H1 was extracted from Ciras-2 cells that were untreated (lane 1), incubated with 10 µg/ml actinomycin D for 70 min (lane 2), 150 µM DRB for 70 min (lane 3), 10 µM aphidicolin for 70 min (lane 4), 10 µg/ml actinomycin D plus 10 µM aphidicolin for 70 min (lane 5) or 150 µM DRB plus 10 µM aphidicolin for 70 min (lane 6). H1 (2 µg) was electrophoretically resolved on an SDS-15% polyacrylamide gel, transferred to membranes and immunochemically stained with anti-pH1b. Panel A shows a Coomassie Blue stained gel. Panel B shows the immunochemically stained membrane. pb is the phosphorylated isoform of H1b.

Redistribution of pH1b and B1C8 upon inhibition of transcription

We performed immunolocalization studies with anti-pH1b and B1C8 on the cells that were treated with actinomycin D. Previously, a dynamic relocalization of transcritpion and splicing factors had been observed when transcription was inhibited in human CaSki cells and rat 9G cells. In G1 phase cells, transcription and splicing factors localize to 20-50 discrete "speckle" domains or foci. When transcription is inhibited by DRB, actinomycin D, or α-amanitin, there is a redistribution of RNA Pol II and SC35 into 5-15 enlarged speckles (Bregman et al., 1995; Dirks et al., 1997). Since pH1b colocalizes with B1C8, a protein involved in splicing, we wanted to determine if B1C8 and pH1b localization is dynamic and would also relocalize to enlarged speckle domains upon transcription inhibition. We treated 10T½ cells with actinomycin D for 70 minutes and then immunochemically stained the cells with B1C8 and anti-pH1b (Fig. 44). In the untreated 10T½ cells, pH1b and B1C8 were distributed into 20-50 small speckles in the nucleus. After treatment of the cells with actinomycin D for 70 min, we observed a relocalization of both B1C8 and pH1b into fewer and much larger speckles in the nucleus (Fig. 44). This relocalization was similar to the results observed for other proteins such as SC35 and hypophosphorylated RNA pol II (Bregman et al., 1995; Zeng et al., 1997). It has been suggested that these enlarged domains represent storage and/or reassembly sites for splicing factors. Our results demonstrate that B1C8 and pH1b follow a similar pattern of redistribution upon transcription inhibition by actinomycin D.

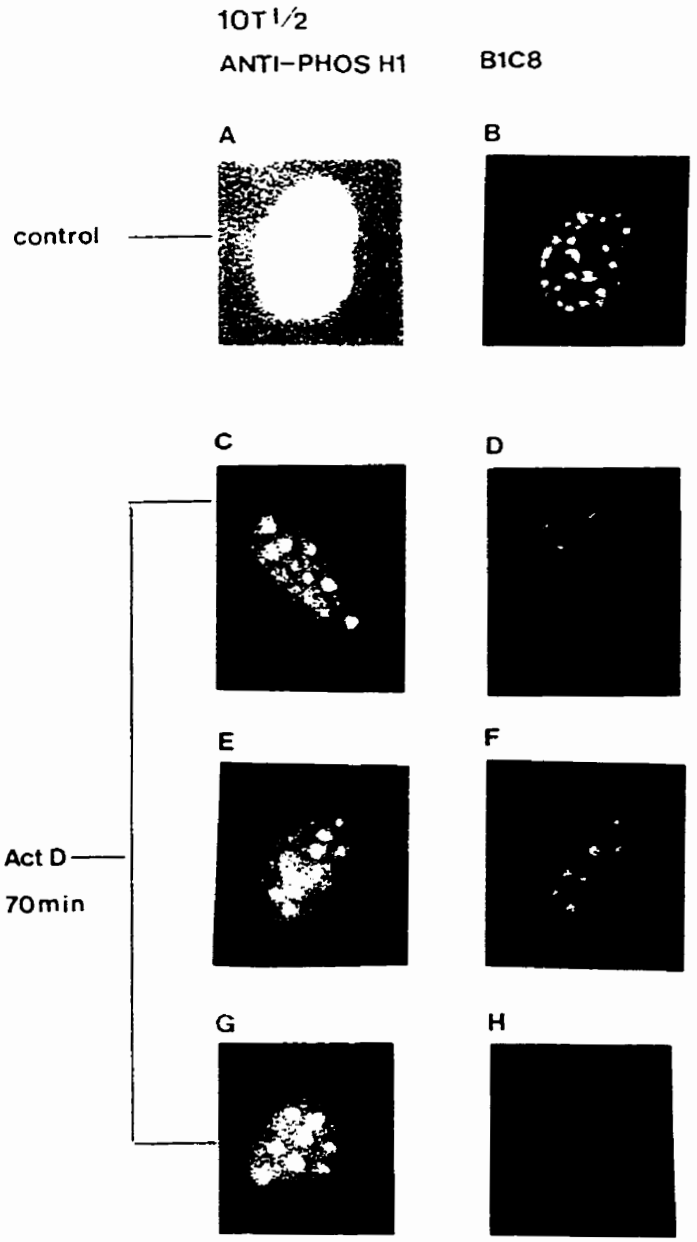

Figure 44. **Redistribution of phosphorylated H1b and BIC8 in 10T½ mouse fibroblast nuclei upon treatment with Actinomycin D.** Cells were untreated (control, panels A and B) or treated with actinomycin D for 70 min (panels C-H). Cells were fixed on coverslips and double stained by indirect immunofluorescence with an anti-phosphorylated H1 antibody and B1C8 monoclonal antibody and then goat anti-rabbit antibody conjugated to FITC (green, panels A, C, E, and G) and goat anti-mouse antibody conjugated to Texas red (red, panels B, D, F, and H). The immunochemically stained cells were photographed at 60X magnification.

Discussion

Transcriptionally active genes are often located near sites of RNA splicing (Kamakaka and Thomas, 1990; Xing et al., 1995). Our observation of pH1b being colocalized with RNA splicing domains, suggested to us that pH1b may be bound to transcriptionally active chromatin. Our data showing that levels of pH1b are dependent upon on-going transcription add further support for this association. The only other histone modification known to be dependent upon on-going transcription is ubiquitination of histone H2B (Davie and Murphy, 1990). In addition to being affected by inhibition of transcription, levels of pH1b are also dependent upon replication. Inhibition of replication with aphidicolin resulted in a marked decline in pH1b. In contrast, ubiquitination of H2B was not affected by inhibition of replication. Thus, to the best of our knowledge, phosphorylation of H1b is the first histone modification found to be dependent upon transcription and replication. Treatment of 10T½ cells with actinomycin D also causes a redistribution of both B1C8 and pH1b to a small number of enlarged speckle domains in the nucleus. This observation is consistent with previous studies that described a similar redistribution of SC-35 and RNA pol II upon inhibition of transcription with actinomycin D, DRB or α-amanitin (Dirks et al., 1997; Zeng et al., 1997; Bregman et al., 1995). These enlarged domains are thought to be storage sites for splicing and transcription factors (O'Keefe et al., 1994). It was also observed that reversal of DRB inhibition results in the relocalization of the splicing factors to the numerous small speckles observed before the inhibition, further emphasizing the dynamic nature of nuclear processes (Bregman et al.,

1995). Our experiments demonstrated that pH1b consistently colocalized with the splicing factor B1C8, both in the presence or absence of transcription inhibition. These results provide evidence that the subnuclear organization of pH1b is dynamic and is closely co-ordinated with the transcriptional process.

Aphidicolin inhibits replication by specifically inhibiting DNA polymerase α. We treated 10T½ and Ciras-2 cells with aphidicolin and observed a decrease in the level of pH1b after 30 min. The effect of the phosphorylation of H1 on chromatin structure and chromatin replication has been investigated. Ajiro *et al.* have studied the phosphorylation sites of human histones H1A and H1B during the HeLa S-3 cell cycle (Ajiro et al., 1981b). They observed two different S-phase phosphorylations, one that precedes and one that follows the onset of replication. This led to the suggestion that the phosphorylation of H1 at a particular site on the C-terminal may produce a chromatin conformation that permits DNA replication (Ajiro et al., 1981b). Further evidence that supports the involvement of H1 phosphorylation in the regulation of chromatin structure during replication comes from studies done with salt-treated SV40 minichromosomes reconstituted with differentially phosphorylated forms of H1. The minichromosomes reconstituted with S-phase histone H1 had a higher replication efficiency than those reconstituted with G0- or M-phase H1 (Halmer and Gruss, 1996a). It was suggested that the chromatin structure induced by the phosphorylation of H1 affects the efficiency of repation.

It has been determined that the accessibility of H1 to the H1 kinase is directly related to its position in the chromatin fibre and that H1 must be

displaced from the chromatin fibre in order for it to be phosphorylated by an H1 kinase (Jermanowski and Cole, 1992). Transcription and replication processes may be the initial disruptive events that lead to the partial displacement of H1b from the chromatin fibre and renders it accessible to the H1 kinase. Further H1b phosphorylation may then be required to maintain an open chromatin conformation for replication and transcription. It has been proposed that phosphorylation of H1 may be involved in inducing chromatin decondensation thereby allowing access to factors for gene expression or replication in addition to chromatin condensation at mitosis (Roth and Allis, 1992). We propose that when transcription or replication processes are inhibited, H1b is no longer exposed to the H1 kinase. Dephosphorylation by protein phosphatases would then reduce the steady state levels of pH1b.

We observed a decrease in the level of pH1b upon inhibition of transcription or replication. The level of pH1b was similar or slightly less when cells were treated with a combination of actinomycin D or DRB with aphidicolin. The phosphorylated isoforms of H1 subtypes isolated from 10T½ and Ciras-2 cells treated with actinomycin D, DRB, aphidicolin, or combinations of these inhibitors were separated on an AUT-15% polyacrylamide gel. There was no observable change in the overall level of phosphorylated H1 isoforms isolated from the various drug treated cells (data not shown). In addition, the levels of the c-phosphorylated subtypes c-pH1b and c-pH1c in these drug treated cells were not greatly affected. Therefore, it appears that inhibition of transcription or replication has the most dramatic effect on the phosphorylation of H1b. In

interphase mouse fibroblasts, the H1b subtype is phosphorylated to the highest extent with a total of 5 phosphorylated forms in comparison to other H1 subtypes which have 1-3 phosphorylated forms (Lennox and Cohen, 1983a). Interestingly, other H1 subtypes (H1a, H1c, H1d, H1e) have a similar number of potential consensus sequence sites for phosphorylation by cdc2 or cAMP-dependent protein kinase but do not aquire the same level of phosphorylation as H1b (Halmer and Gruss, 1996a). One possible explanation for the higher phosphorylation level of H1b is that it may be a result of a preferential location of H1b in chromatin such that it is more accessible to the H1 kinase than other H1 subtypes. Consequently, a disruption of chromatin structure by inhibition of transcription or replication would have the greatest effect on the phosphorylation of H1b.

We treated 10T½ and Ciras-2 mouse fibroblasts with 10 µg/ml actinomycin D which, at this concentration, inhibits both RNA polymerase I and RNA polymerase II. The effect of transcription and replication inhibition on pH1b levels in 10T½ and Ciras-2 cells differs in terms of time to elicit reduced levels of pH1b. Both aphidicolin and actinomycin D or DRB take longer to act in the Ciras-2 cells. The chromatin of *ras*-transformed mouse fibroblasts is less condensed than the chromatin of parental cells (Laitinen et al., 1990). We proposed that oncogene activation of the MAP kinase signal transduction pathway increases the activity of an H1 kinase, resulting in elevated levels of phosphorylated H1 and decondenstion of chromatin (see section 1). This increased kinase activity and less condensed chromatin structure may contribute to the extended times

required to observe a reduced level of pH1b when transcription or replication is inhibited. The extended response time to see a reduction in pH1b levels may also reflect a reduced protein phosphatase activity. Protein phosphatase 1 is thought to be responsible for dephosphorylating H1 (Paulson et al., 1996). Protein phosphatase 1 activity is reduced when it is phosphorylated by cyclin dependent kinases (Dohadwala et al., 1994). Thus, oncogene activation of the MAP kinase signal transduction pathway may result in the activation of CDKs and deactivation of protein phosphatase 1.

In summary, we have demonstrated that the maintenance of levels of pH1b in chromatin is dependent on on-going transcription or replication. This observation suggests that pH1b is associated with transcriptionally active chromatin. Therefore, we propose that H1b phosphorylation may be required to maintain an open chromatin structure thus facilitating subsequent rounds of transcription or replication.

Part 3: Investigation of H1 kinase and phosphatase activities in parental and *ras*-transformed cells.

Introduction

To determine whether the elevated level of pH1b that we observed in *ras*-transformed cells was due to an altered activity of the H1b phosphatase, we analyzed and compared the phosphatase activity in parental and *ras*-transformed cells. Okadaic acid is a polyether fatty acid that has improved the methods for measuring protein phosphatase activities. This is because two of the major phosphatase activities in eukaryotic cells, PP1 and PP2A, have substantially different sensitivities to okadaic acid inhibition. PP2A is completely inhibited at 1 nM okadaic acid; however, the concentration of okadaic acid needed for 50% inhibition of PP1 is 10-15 nM. The H1 phosphatase has been previously studied by Paulson *et al.* (1996). They found that in metaphase arrested HeLa cells, inhibition of H1 phosphatase activity was achieved with okadaic acid and microcystin LR at concentrations which strongly suggest that PP1 and not PP2A is the histone H1 phosphatase (Paulson et al., 1996).

We determined that *ras*-transformed cells have a higher level of phosphorylated H1 than the parental cells. One possible explanation for this elevated level of phosphorylated H1 is that persistent activation of the MAP kinase pathway in these cells may lead to increased activity of an H1 kinase. We suggest that CDK2/cyclin E as a possible candidate H1 kinase. Since the phosphorylation state of a protein is dependent upon a balance between kinase

and phosphatase activities in the cell, an alternative explanation is that there is a decrease in activity of H1 phosphatase in the transformed cells. Dohadwala *et al.* (1994) have demonstrated that PP1 is phosphorylated and inactivated by CDKs. Consequently, an increase in CDK activity could directly result in increased phosphorylation of H1 and/or could result in phosphorylation and inactivation of PP1 which would also generate elevated levels of phosphorylated H1 (Dohadwala et al., 1994).

To determine if the increased levels of phosphorylated H1 is due to increased kinase activity or is a result of decreased phosphatase activity we analyzed the CDK2 H1 kinase and phosphatase activities in the parental and *ras*-transformed cell lines. For the CDK2 kinase assays we compared the kinase activity in 10T½ cells versus Ciras-3 cells. For the analysis of phosphatase activities, we determined which phosphatase(s) was predominantly involved in dephosphorylation of H1b and we compared the phosphatase activities between the two cell lines. Cell extracts prepared from logarithmically growing parental and *ras*-transformed cells were used as a source of enzyme and highly phosphorylated total histone from mitotic 10T½ cells was isolated and used as substrate.

Results

Increased CDK2 activity in *ras*-transformed cells

We compared CDK2 kinase activity from 10T½ and Ciras-3 cells. CDK2 was immunoprecipitated from 10T½ and Ciras-3 cells and incubated with H1

substrate in a kinase assay. We observed that there was a higher level of phosphorylation of H1 by CDK2 immunoprecipitated from Ciras-3 cells in comparison to CDK2 immunoprecipitated from parental cells (Fig. 45). Therefore there is increased CDK2 kinase activity in the *ras*-transformed cells in comparison to the parental cells.

Parental and *ras*-transformed cells have similar phosphatase activities

To compare the phosphatase activities between 10T½ and Ciras-3 cells, H1 histone was incubated in the presence of cell extract from 10T½ or Ciras-3 cells. The reaction was allowed to proceed for 0, 15, 30, 45, and 60 min. We observed that the rate of dephosphorylation of H1b was similar between the two cell lines (Fig. 46).

PP1 is the predominant H1 phosphatase activity present in 10T½ cells

PP1 is inhibited by 100 nM okadaic acid and PP2A is inhibited by 1 nM okadaic acid. Cellular extracts prepared from 10T½ cells were incubated in the presence of 2 nM or 100 nM okadaic acid and 2 µg of highly phosphorylated histone H1. Samples were incubated for 0, 30 and 60 minutes at 37 °C. In the presence of 2 nM okadaic acid dephosphorylation of the substrate proceeded until approximately 10% of the pH1b was remaining after 60 min (Fig. 47). In the presence of 100 nM okadaic acid, dephosphorylation of the substrate was

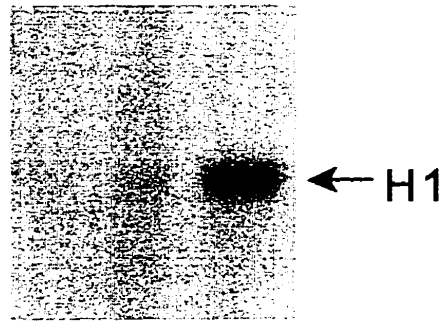

Figure 45. **CDK2 activity in parental and *ras*-transformed mouse fibroblasts.** CDK2 protein was immunoprecipitated from 10T½ (lane 2) and Ciras-3 (lane 3) cell extracts and incubated with histone H1 substrate in a kinase assay. As a control in lane 1, CDK2 antibody was absent for the immunoprecipitation from 10T½ cell extract.

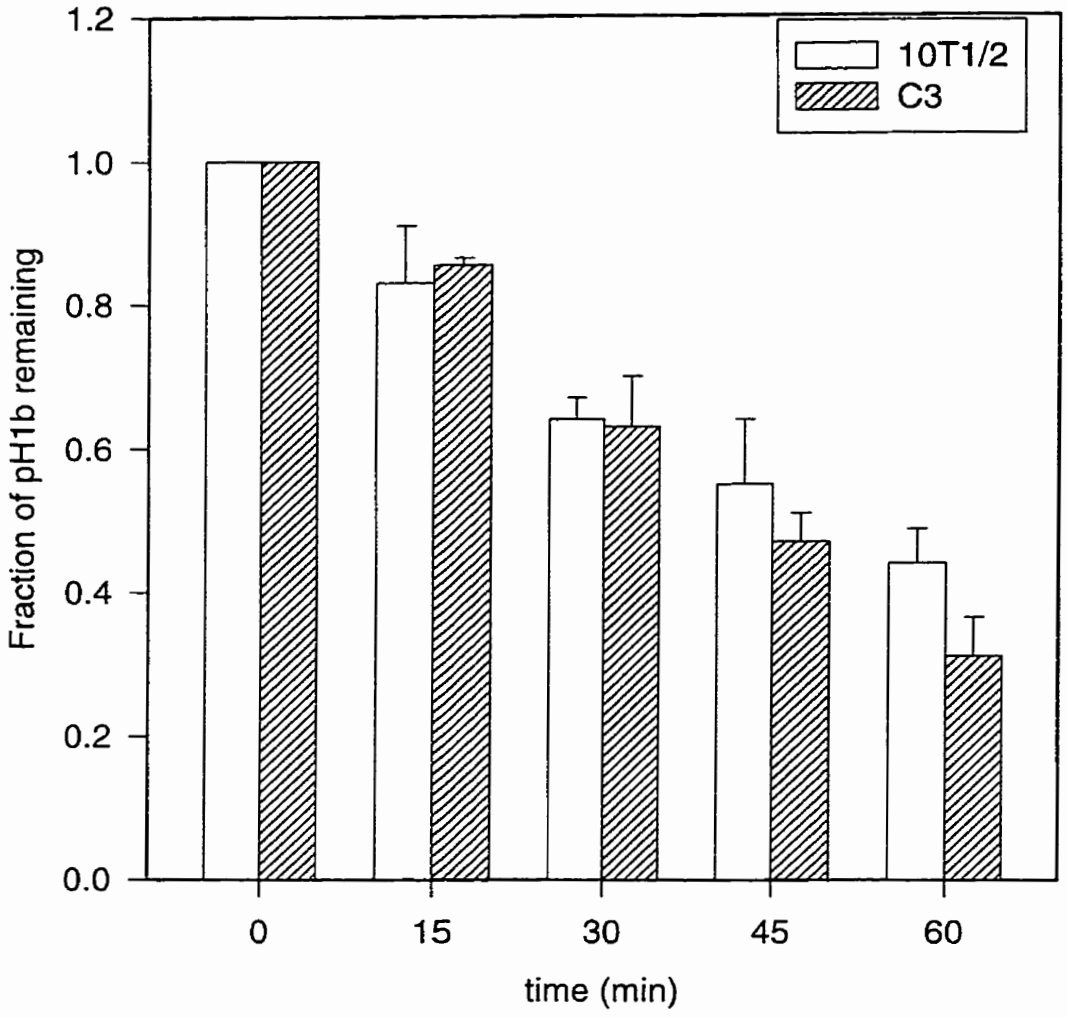

Figure 46. **Comparison of H1b dephosphorylation in lysates from parental and *ras*-transformed cells.** Cell extracts from 10T½ or Ciras-3 were incubated with 5 µg of phosphorylated histone H1 substrate for 0, 15, 30, 45 and 60 minutes at 37°C. The reaction was stopped and the proteins were separated by SDS polyacrylamide gel electrophoresis, transferred to nitrocellulose membranes, and immunochemically stained with anti-pH1b. The percent of pH1b remaining after each time period was determined by denstometric analysis of the Western blots.

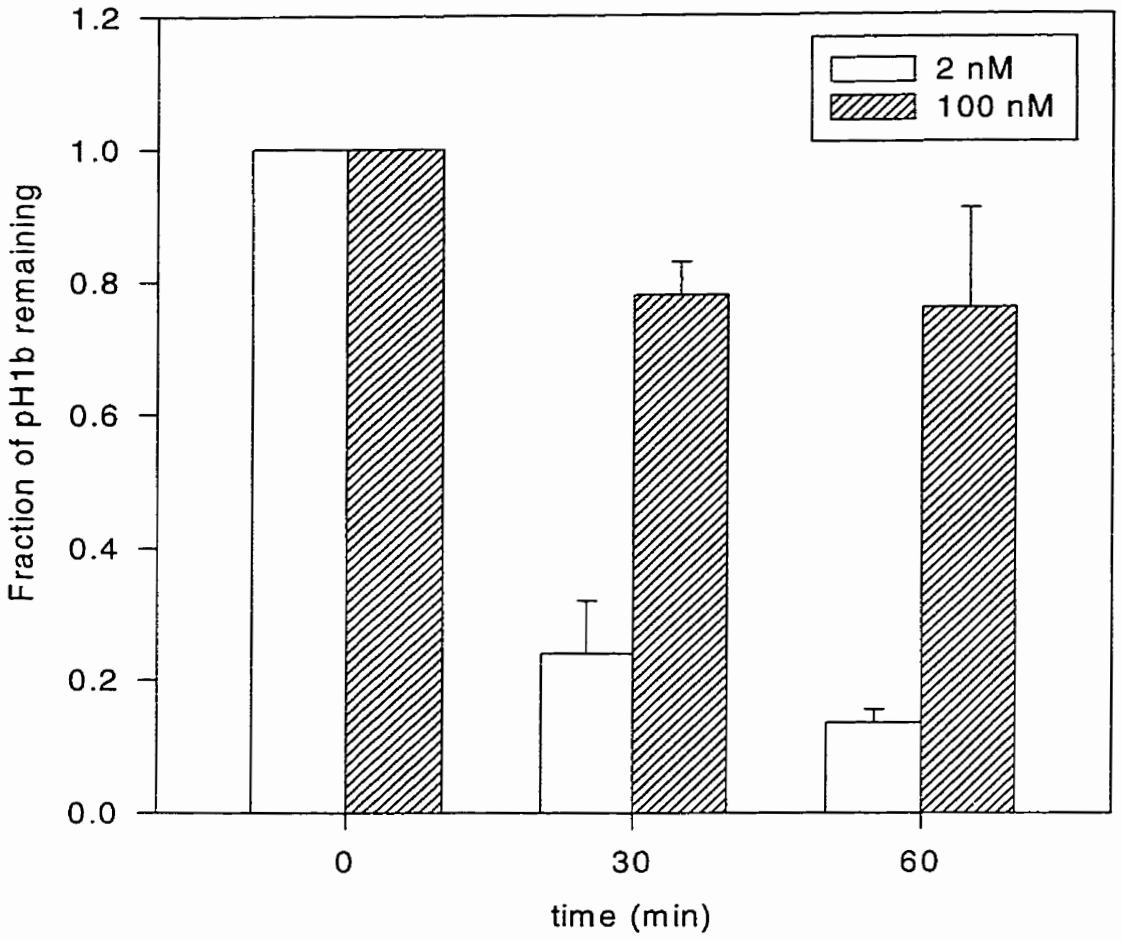

Figure 47. **Inhibition of H1b dephosphorylation by okadaic acid in 10T½ cell extracts**. Cell extracts were incubated in the presence of either 2 nM or 100 nM okadaic acid and 5 µg of total histone as a substrate. The reaction mixture was incubated for 0, 30 or 60 min at 37°C. The reaction was stopped and the proteins were separated separated by SDS polyacrylamide gel electrophoresis, transferred to membranes, and immunochemically stained with anti-pH1b. The percent of pH1b remaining after each time period was determined by densitometric analysis of the Western blots.

inhibited, and 75% of the pH1b was remaining after 60 min (Fig. 47). In agreement with Paulson *et al.* (1996), these results strongly suggest that PP1 is the major phosphatase involved in dephosphorylating pH1b.

Discussion

We previously observed an increased level of pH1b in *ras*-transformed cells in comparison to parental 10T½ cells. This increase in phosphorylation may be due to an increased H1b kinase activity or a decreased H1b phosphatase activity in these cells. A candidate H1b kinase is CDK2 since H1b has many CDK2 consensus sequence sites. CDK2 kinase activity has been found to be altered in transformed cells (Herrara et al., 1996). We compared the CDK2 kinase activity in the *ras*-transformed cells and the parental cells, and we observed a higher level of CDK2 kinase activity toward the H1 substrate in the *ras*-transformed cells in comparison to the parental cells. PP1 and PP2A are the major H1 phosphatase activities in the cell. The H1 phosphatase had been investigated by other research groups, however, there was conflicting results as to whether the phosphatase was PP1 or PP2A (Paulson et al., 1996; Ferrigno et al., 1993). It has been reported that CDK2 phosphorylates and inhibits PP1 (Dohadwala et al., 1994).

To determine if the increased level of pH1b in the *ras*-transformed cells is due to a decreased activity of an H1b phosphatase, we compared the phosphatase activities from the *ras*-transformed and parental 10T½ cells. Our results indicated that the phosphatase activities in these two cell lines were very

similar. Thus, the increased level of pH1b in the *ras*-transformed cells is likely due to an increased H1b kinase activity and not a decreased phosphatase activity. We next identified which phosphatase, PP1 or PP2A, was responsible for the majority of the H1b phosphatase activity in 10T½ cells. We demonstrated that the major H1b phosphatase activity in 10T½ extracts is sensitive to 100 nM okadaic acid and not sensitive to 2 nM okadaic acid. Therefore our results suggest that the H1b phosphatase is PP1, not PP2A. These results are in agreement with the observations of Paulson *et al.* (1996).

Part 4: Increased phosphorylation of Ser-10 of H3 in oncogene transformed and mitogen-induced mouse fibroblasts.

Introduction

Myc and *ras*-transformed and Rb-deficient fibroblasts have a more decondensed chromatin structure than parental cells (Laitinen et al., 1990) (see section 1). A general feature of these oncogene-tranformed and Rb deficient cells is increased H1 phosphorylation. In mouse fibroblasts, phosphorylation of one of the H1 subtypes, H1b, is dependent upon on-going transcription and replication; this is the only histone known to have its modification being dependent upon both of these nuclear processes (see section 2). H1 phosphorylation may relax chromatin by interfering with its action in chromatin folding and intermolecular fiber-fiber interactions (Swank et al., 1997).

In the condensation of chromatin, the N-terminal tail of histone H3 also has a key role (Maru et al., 1995; van Holde and Zlatanova, 1996; Wei et al., 1998). Phosphorylation of H3 at Ser-10 is dramatically elevated during mitosis together with H1 phosphorylation (Shibata and Ajiro, 1993). There is evidence that H1 phosphorylation may facilitate the phosphorylation of H3 (Su et al., 1998), (Shibata and Ajiro, 1993). Phosphorylation of H3 is not limited to mitosis. A rapid induction of H3 phosphorylation occurs when quiescent fibroblasts are stimulated to enter the cell cycle with growth factors or phorbol esters (Mahadevan et al., 1991). This phosphorylation happens concurrently with the transcriptional activation of the immediate early response genes, c-*fos* and c-*jun*

(Mahadevan et al., 1991). Inhibition of transcription does not prevent mitogen-activated H3 phosphorylation (Mahadevan et al., 1991). It was proposed that phosphorylated H3 (pH3) is associated with these immediate early genes and may be a prerequisite to the expression of these genes (Cano et al., 1995). Unlike the extensive mitosis-specific phosphorylation, which occurs on all H3 molecules, this mitogen-stimulated phosphorylation is targeted to a small, hyperacetylation-sensitive nucleosomal fraction (Barratt et al., 1994a). The N-terminal domain of H3 can be phosphorylated on Ser 10 and Ser 28 (Shibata et al., 1990; Taylor, 1982). However, the site of mitogen-induced phosphorylation remains unknown.

To study H3 phosphorylation in growth factor- or phorbol ester-stimulated and oncogene-transformed mouse fibroblasts, we used an antibody that specifically recognizes phosphorylated Ser-10 of H3. We show that mitogenic stimulation, oncogene transformation or induction of oncogenic *ras* expression is accompanied with Ser-10 phosphorylation of H3. We provide the first direct evidence that pH3 is associated with the transcriptionally active c-*fos* and c-*myc* genes in mitogen stimulated fibroblasts.

Results

Induction of H3 phosphorylation in serum-starved 10T½ cells in response to growth factors and phorbol esters

To determine if Ser-10 of H3 is phosphorylated in response to mitogen stimulation, we used an antibody that was generated against Ser-10 pH3;

henceforth called anti-pH3. Serum-starved 10T½ cells were treated with either EGF or TPA for 5 or 30 min, and the level of pH3 was analyzed in immunoblotting experiments. We observed a 7.1-10.3-fold increase in the level of pH3 in the EGF or TPA-treated cells in comparison to the untreated 10T½ cells (Fig. 48). Immunolocalization experiments show very little staining with anti-pH3 in the serum starved cells. When the cells are treated with EGF or TPA, however, there is intense staining of the nuclei again demonstrating that Ser-10 of H3 is phosphorylated in response to EGF or TPA stimulation (Fig. 49). Histone H1 phosphorylation is, however, not inducible by growth factors or phorbol esters (Fig. 50)

Immunolocalization of pH3 in 10T½ cells treated with TPA

In murine cell lines, AT-rich centromeric heterochromatin can be seen as regions of intense DAPI staining. These regions colocalize with the domains of intense H3 phosphorylation observed in a subset of G2/M phase cells, reflecting G2 phosphorylation of centromeric heterochromatin (Hendzel et al., 1997). In TPA-induced 10T½ cells, a second pattern is seen. The pH3 was located in numerous small foci scattered throughout all interphase nuclei (Fig. 51, panel A; performed by Dr. Michael Hendzel). These foci, located outside of condensed regions of chromatin (Fig. 51, panel B), are distributed similarly to highly acetylated euchromatin (Hendzel et al., 1998). This observation is consistent with the idea that pH3 of mitogen stimulated cells is associated with transcribed chromatin.

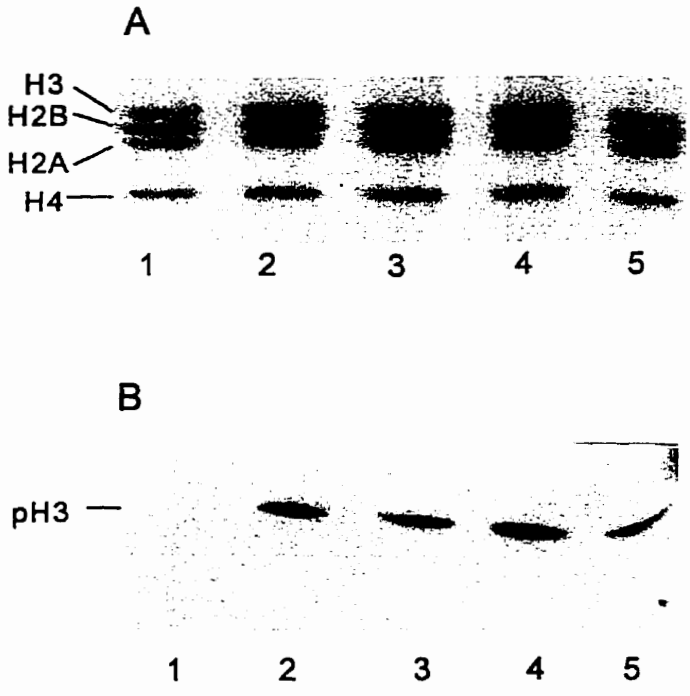

Figure 48. **Effect of EGF and TPA treatment on H3 phosphorylation in quiescent 10T½ mouse fibroblasts.** Total histone was extracted from 10T½ cells that were serum starved and then untreated (lane 1) or treated with 50 ng/ml EGF for 5 min (lane 2), 50 ng/ml EGF for 30 min (lane 3), 100 nM TPA for 5 min (lane 4), or 100 nM TPA for 30 min (lane 5). The total histone sample was electrophoretically resolved on a 12.5% SDS polyacrylamide gel, transferred to membranes and immunochemically stained with anti-pH3. Panel A shows a Coomassie Blue stained gel. Panel B shows the immunochemically stained membrane. pH3 is the phosphorylated isoform of H3.

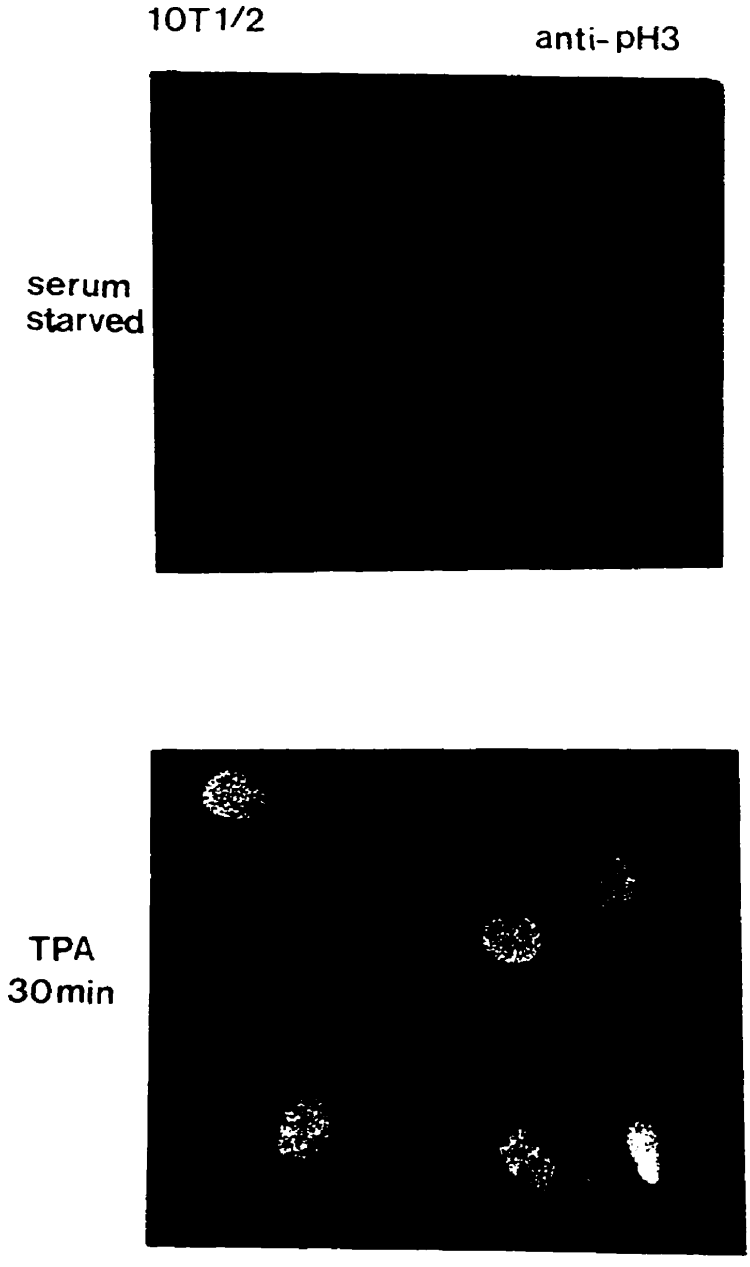

Figure 49. **Immunolocalization of phosphorylated histone H3 in serum starved and TPA-stimulated 10T½ mouse fibroblasts.** Serum starved (panel A) or TPA-stimulated (panel B) 10T½ cells were stained with anti-pH3 antibody and goat anti-rabbit FITC antibody. Cells were photographed at 60 x magnification.

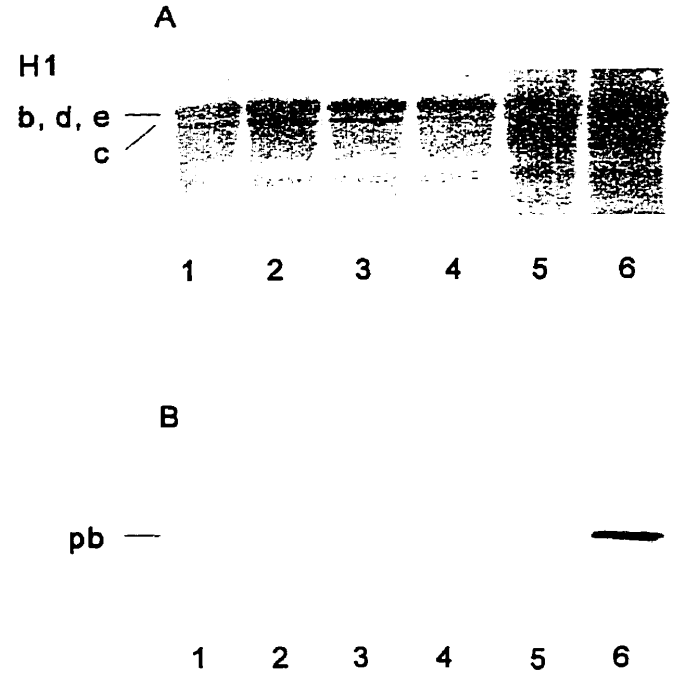

Figure 50. **Effect of EGF and TPA treatment on H1b phosphorylation in quiescent 10T½ mouse fibroblasts**. Total histone was extracted from 10T½ cells that were serum starved and then untreated (lane 1) or treated with 10 µg/ml EGF for 5 min (lane 2), 10 µg/ml EGF for 30 min (lane 3), 100 nM TPA for 5 min (lane 4), or 100 nM TPA for 30 min (lane 5). The total histone sample was electrophoretically resolved on a 12.5% SDS polyacrylamide gel, transferred to membranes and immunochemically stained with anti-pH1b. Panel A shows the india ink stained membrane. Panel B shows the immunochemically stained membrane. Histone H1 from Ciras-3 cells was run in lane 6. Pb is the phosphorylated isoform of H1b.

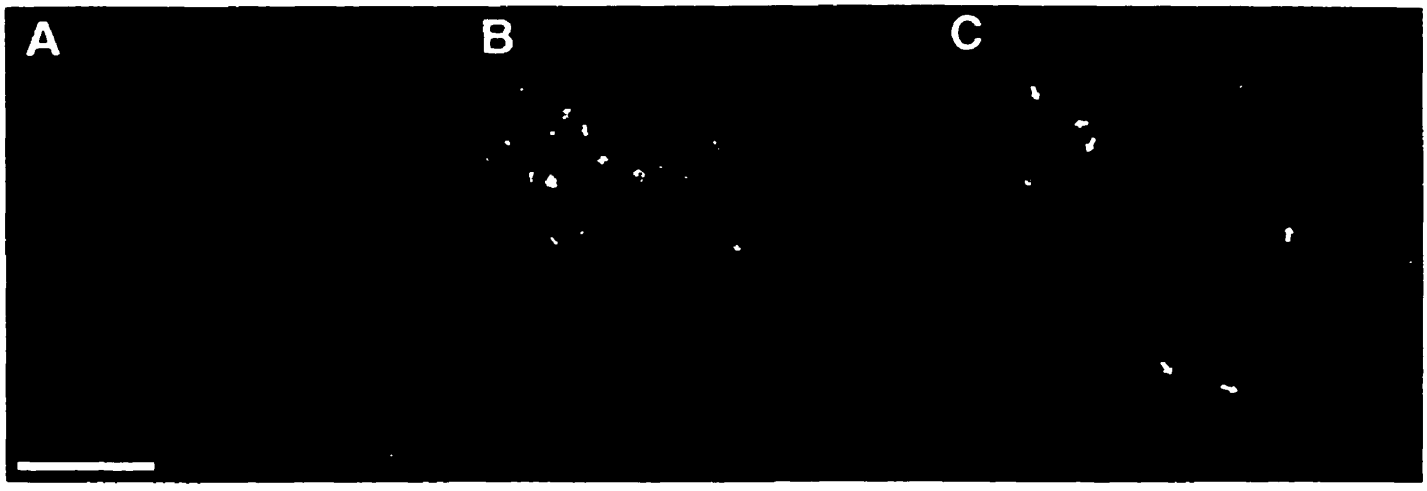

Figure 51. **Relative organization of phosphorylated histone H3 and condensed chromatin in 10T½ mouse fibroblasts.** Cells were co-stained with anti-pH3 antibody and DAPI. Digital optical sections of 0.3 mm were obtained, false coloured red (pH3, panel A) and blue (DAPI, panel C), and a composite image was produced using Adobe Photoshop (panel B). The arrows indicate regions of centromeric heterochromatin. The bar size represents 10 µm.

pH3 is associated with TPA-induced genes

The CHIP (chromatin immunoprecipitation) assay was used to test directly if pH3 was associated with immediate early genes, the expression of which are elevated in mitogen stimulated cells (Chen and Allfrey, 1987; Mahadevan et al., 1991). Fig. 52 shows that pH3 of TPA stimulated cells was associated with c-*fos* and c-*myc* DNA sequences (transcription unit). The c-*fos* DNA probe reproducibly gave a stronger signal than did the c-*myc* DNA probe. Note, however, that the both probes generated a comparable signal when hybridized to the input DNA. In contrast to expressed genes, transcriptionally inactive DNA sequences (immunoglobulin κ matrix associated region DNA and prolactin DNA) did not hybridize to the DNA bound to pH3. As expected the CHIP assay with chromatin from serum starved cells, which had low levels of pH3, failed to show an association of pH3 with any of these DNA sequences. These observations provide direct evidence that pH3 of TPA treated cells is associated with TPA induced c-*myc* and c-*fos* genes.

Ras-transformed fibroblasts have elevated levels of pH3

In immunoblotting experiments, we analyzed the level of pH3 in parental (10T½) and *ras*-transformed (Ciras-3) cells. A 2.4-fold higher level of pH3 was observed in the Ciras-3 cells (Fig. 53, lane 2) in comparison to the parental, 10T½ cells (Fig. 53, lane 1). As massive phosphorylation of H3 occurs during mitosis (Hendzel et al., 1997), it was necessary compare cell cycle distributions of the Ciras-3 and 10T½ cells. Using flow cytometric analysis of the cell

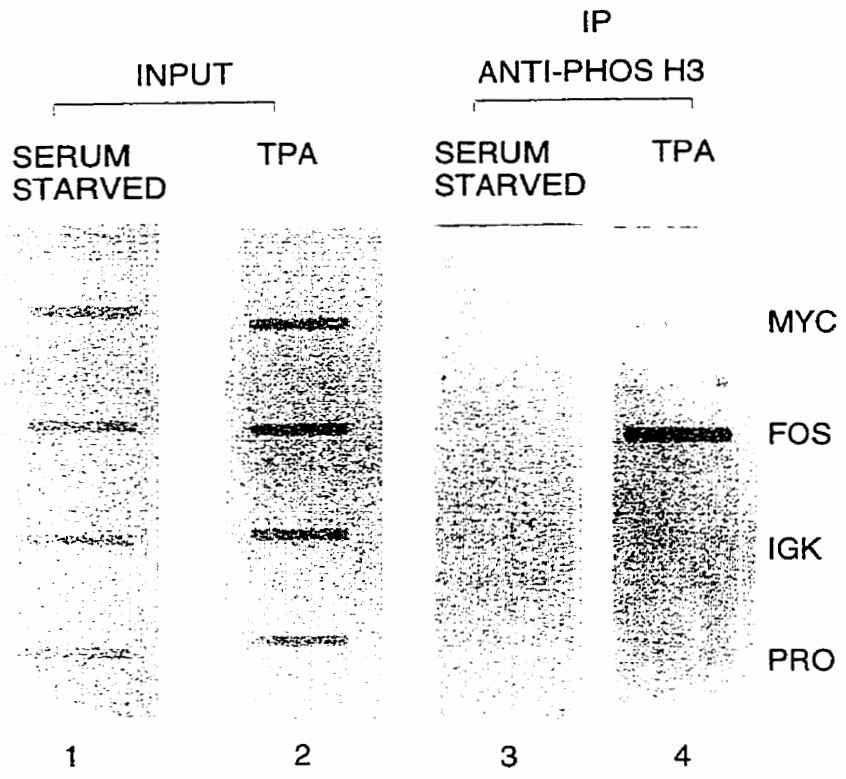

Figure 52. **Association of pH3 with transcriptionally active c-*fos* and c-*myc* genes.** Quiescent 10T½ cells were stimulated with TPA (100 nM) for 30 min (lane 4) or unstimulated (lane 3). DNA fragments associated with pH3 were isolated by immunoprecipitation with anti-pH3, labelled, and hybridized to a slot blot containing 0.5 µg DNA inserts of the c-*myc*, c-*fos*, prolactin and IGK genes. In lanes 1 and 2, the blot was hybridized with DNA isolated and labelled from the total chromatin fraction (input fraction) from the serum starved and TPA treated cells.

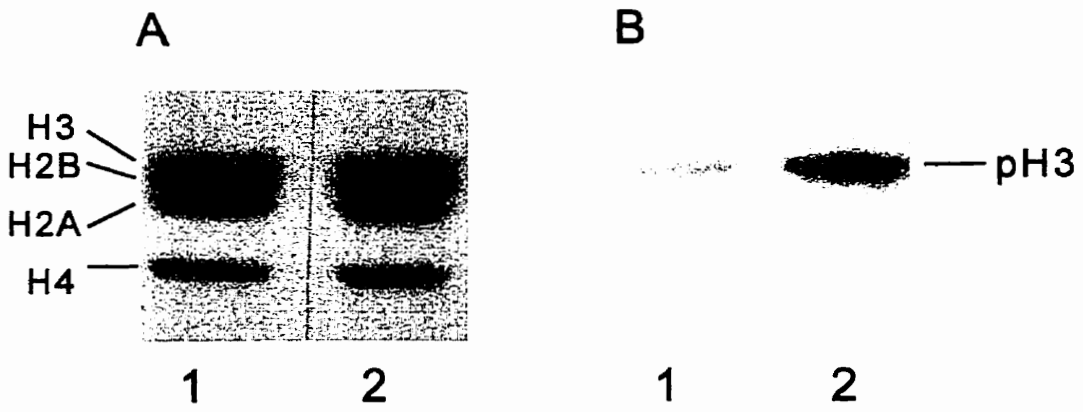

Figure 53. **Phosphorylated H3 of parental and *ras*-transformed mouse fibroblasts.** Total histone was extracted from parental 10T½ cells (lane 1) and Ciras-3 cells (lane 2). The total histone sample (10 μg) was electrophoretically resolved on a 12.5% SDS polyacrylamide gel, transferred to membranes and immunochemically stained with anti-pH3. Panel A shows a Coomassie Blue stained gel. Panel B shows the immunochemically stained membrane. pH3 is the phosphorylated isoform of H3.

populations, we found that the distributions of cells in different cell cycle phases were not significantly different (Table VI). We conclude that the differences in pH3 levels are not due to a higher number of cells in G2/M phase in one cell line.

To provide further evidence that elevated pH3 in Ciras-3 cells was not a mitosis related event, we studied the distribution of pH3 in Ciras-3 cells by indirect immunofluorescence. The distribution of pH3 in Ciras-3 was similar to that of the TPA stimulated 10T½ parental cells (Fig. 54, panel B). Importantly, most pH3 did not colocalize with regions of intense DAPI staining.

These observations suggest that pH3 that is elevated in *ras*-transformed mouse fibroblasts is associated with relaxed chromatin regions.

H3 Phosphorylation in cell lines transformed with oncogenes encoding protein kinases

We studied the phosphoryation level of H3 in cells transformed with oncogenes *fes* and *mos* (Egan et al., 1987), which act upon the MAP kinase pathway (Fanger et al., 1997; Katz and McCormick, 1997). In addition we analyzed NIH-3T3 cells tat were transformed with c- *myc*, which is also a target of MAP kinases (Fanger et al., 1997). The relative level of pH3 in the control NIH-3T3 cells was compared to the pH3 level in the oncogene-transformed cells. There was a 2.1-5.8-fold increase in the level of pH3 in the *fes*-, *mos*-, and *myc*-transformed cells in comparison to the NIH-3T3 parental cells (Fig. 55 and Table VI). Table VI shows that the cell distributions of parental and oncogene-transformed NIH-3T3 fibroblasts were closely matched. These results

Table VI. Relative level of phosphorylated H3 in parental and oncogene-transformed mouse fibroblasts.

Cell Line	Cell Cycle Phase (% distribution)			Relative Level of pH3
	G1	S	G2/M	
10T½	65	14	21	1.0
Ciras-3	62	13	25	2.4
NIH / 3T3	62	12	26	1.0
fes	55	14	31	3.0
mos	62	12	22	2.1
myc	62	12	27	5.8
2H1(control)	55	12	33	1.0
2H1(24h)	51	14	25	6.1

The histones isolated from the oncogene-transformed and parental cell lines were resolved on SDS gels and the relative level of phosphorylated H3 on Western blots (shown in Figs. 53, 55, 56) was determined as described in "Materials and Methods."

Figure 54. **Relative organization of phosphorylated histone H3 and condensed chromatin in *ras*-tansformed Ciras-3 mouse fibroblasts.** Cells were co-stained with anti-pH3 antibody and DAPI. Digital optical sections of 0.3 mm were obtained, false coloured red (pH3, panel A) and blue (DAPI, panel C), and a composite image was produced using Adobe Photoshop (panel B). The arrows indicate regions of centromeric heterochromatin. The bar size represents 10 μm.

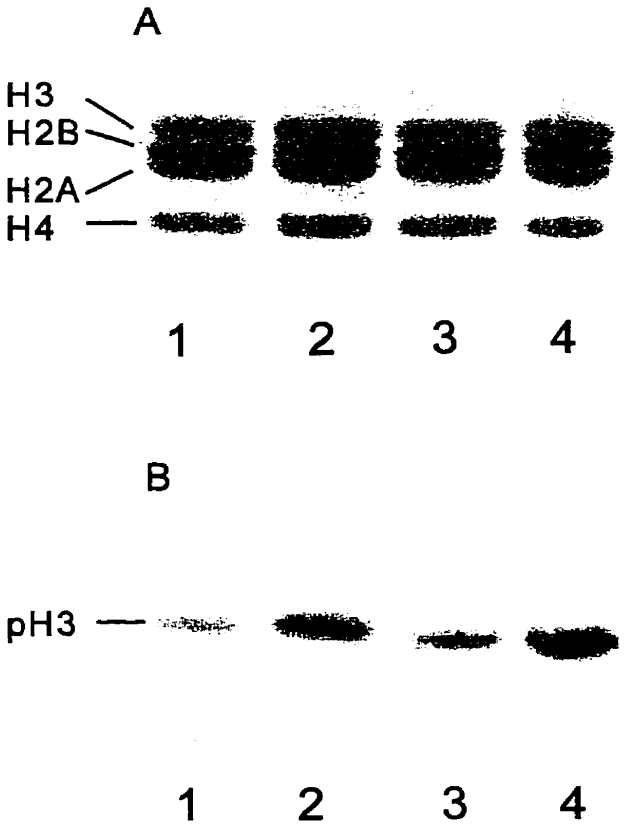

Figure 55. **Phosphorylated H3 of parental and oncogene-transformed mouse fibroblasts**. Total histone was isolated form parental NIH-3T3 (lane 1) and NIH-3T3 cells transformed with v-*fes* (lane 2), *v-mos* (lane 3), *c-myc* (lane 4). The total histone sample (10 μg) was electrophoretically resolved on a 12.5% SDS polyacrylamide gel, transferred to membranes and immunochemically stained with anti-pH3. Panel A shows a Coomassie Blue stained gel. Panel B shows the immunochemically stained membrane. pH3 is the phosphorylated isoform of H3.

show that cells transformed with various oncogenes, which impact upon the MAP kinase pathway, all have increased levels of pH3.

Increase in pH3 and pH1b levels upon induction of *ras* oncogene expression in 2H1 cells

To test if altered levels of pH3 is an early event in cellular transformation, which occurs upon expression of oncogenic *ras,* we used the mouse fibroblast cell line, 2H1, which is transfected with an inducible-*ras* oncogene (Haliotis et al., 1990). In these cells, *ras* oncogene expression is controlled by a metallothionein promoter which can be induced by treating the cells with 100 μM $ZnSO_4$ for 24 h (Haliotis et al., 1990). We observed a 4.8 ± 0.5-fold (n = 3) increase in the level of pH3 in the cells in which the *ras* oncogene had been induced with $ZnSO_4$ in comparison to the control untreated cells (Fig. 56, panel C). We also observed a 6.6 ± 1.9-fold (n = 3) increase in the level of pH1b in the 2H1 cells in which the *ras* oncogene had been induced with $ZnSO_4$ in comparison to the untreated cells (Fig. 56, panel D). This latter observation is consistent with our previous findings that pH1b is elevated in the *ras*-transformed Ciras-3 cells in comparison 10T½ cells and that persistent activation of the MAP kinase pathway in these cells may lead to this effect.

Levels of Ras, H3 and H1b phosphorylation were analyzed by immunoblotting at different times after the induction of the *ras* oncogene. Fig. 57 shows that 1 h after the addition of zinc, Ras levels were increased several-fold, diminishing slightly over 20h. Phosphorylated H3 increased rapidly for 2 h and

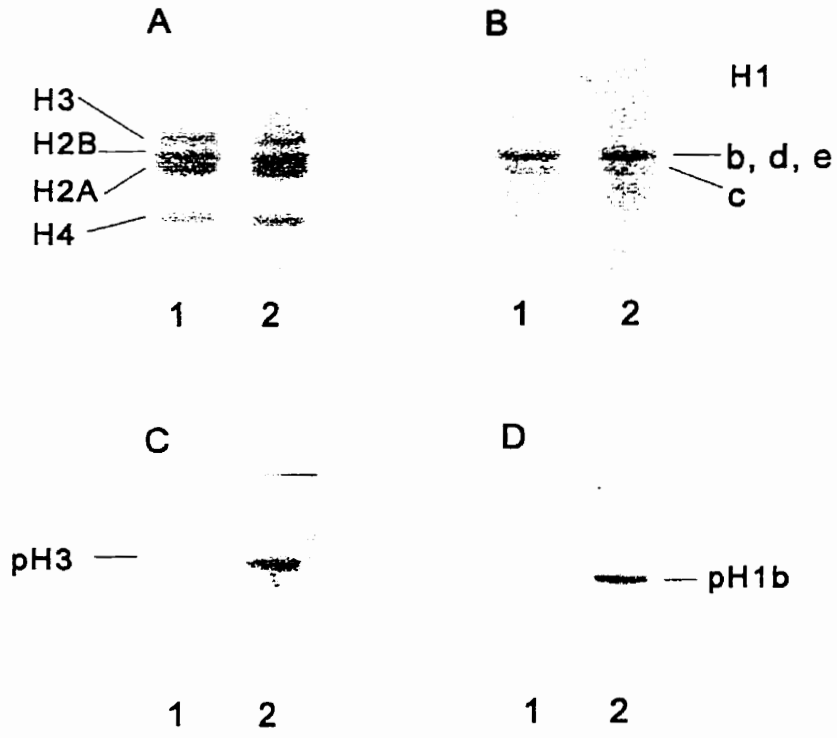

Figure 56. **Effect of induction of the *ras*-oncogene on pH3 and pH1b levels.** Total histone was extracted from 2H1 cells that were untreated (lane 1) or treated with 100 μM $ZnSO_4$ (lane 2) for 24h. The total histone sample (10 μg) was electrophoretically resolved on a 12.5% SDS polyacrylamide gel, transferred to membranes and immunochemically stained with anti-pH3 (panel C) or anti-pH1b (panel D). Panels A and B show Coomassie Blue stained gels. Panel C and D show the immunochemically stained membrane. pH3 is the phosphorylated isoform of H3 and pH1b is the phosphorylated isoform of H1b.

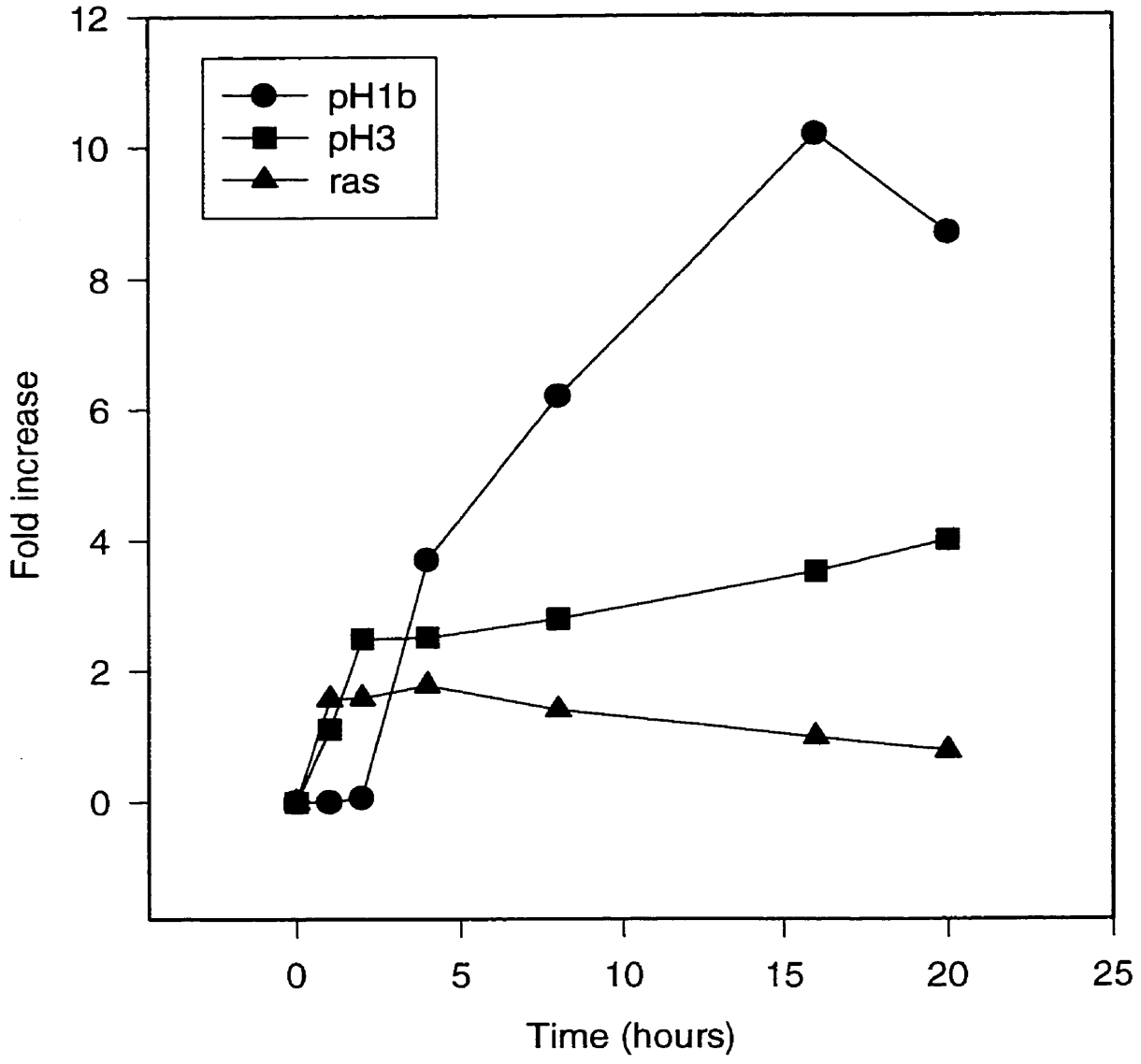

Figure 57. **Effect of induction of ras-oncogene expression on pH1b and pH3 levels**. Total histone was extracted from 2H1 cells that were untreated or treated for 1, 2, 4, 8, 16, or 20 h. The total histone sample was electrophoretically resolved on SDS 12.5% polyacrylamide gels, transferred to membranes, and immunochemically stained with anti-ras, anti-pH1b or anti-pH3 antibodies. The relative level of ras (▲), pH1b (●) and pH3 (■) was determined by densitometric analysis of the Western blots.

then increased at a much slower rate. The levels of pH1b did not increase for 2 h but then steadily increased for 16 h. These observations show the rapidity and sustained phosphorylation of H3 in response to the expression of the oncoprotein Ras.

Discussion

In this study, we show that Ser-10 of H3 is phosphorylated when quiescent murine fibroblasts are stimulated with phorbol esters or growth factors. We demonstrate that the Ser-10 pH3 is located with relaxed chromatin and provide direct evidence that pH3 is associated with the induced c-*fos* and c-*myc* genes. These results provide unequivocal evidence that phosphorylation of H3 on Ser-10 has a role in gene expression and is not limited to chromatin remodelling events occurring at mitosis (Hendzel et al., 1997; Juan et al., 1998).

The elevated expression of c-*fos* and c-*myc* is accompanied with an increased level of unfolded nucleosomes associated with their coding regions (Chen and Allfrey, 1987). The unfolded nucleosomes are associated with dynamically acetylated histones, with the highly acetylated core histones maintaining the unfolded nucleosome structure (Walia et al., 1998). Once transcriptional activity of the gene subsides, the longevity of the unfolded nucleosome is dependent upon the rate that the dynamically acetylated histones are deacetylated. H3 that is phosphorylated in response to phorbol esters or growth factors is dynamically acetylated (Barratt et al., 1994a). Together,

phosphorylation and acetylation may destabilize nucleosomes associated with the coding region, facilitating elongation.

Phosphorylation and acetylation of H3 tails would affect chromatin fiber compaction. Experiments involving reconstitution of chromatin fibres with core histones lacking the N-terminal domain of H3 demonstrate that this domain, in addition to H1, is required for the chromatin fibre to properly three-dimensionally fold (Ausio et al., 1989; van Holde and Zlatanova, 1996). The H3 tail domain is involved in protein-protein interactions with non-histone chromosomal proteins, and phosphorylation/acetylation of H3 may disrupt these interactions leading to a more relaxed chromatin fibre (Trieschmann et al., 1998; Ridsdale et al., 1990).

Our results suggest that following a 30 min stimulation with TPA, there is a differential association of pH3 with the c-*fos* and c-*myc* genes. This difference may reflect the timing of the expression of the two genes upon TPA stimulation or nuclear location and activity of the H3 kinase. Following TPA stimulation, enhanced c-*fos* expression is observed early (15 min) and then subsides to a lower level by 1 h. Increased c-*myc* expression is seen later (30-60 min) (Greenberg and Ziff, 1984; Chen and Allfrey, 1987). However, inhibition of transcription does not arrest dynamic acetylation or phosphorylation of H3. Alternatively, the differential amount of pH3 associated with the two genes may reflect the activity and recruitment of the H3 kinase following TPA stimulation. A third possibility relates to the position of the c-*fos* and c-*myc* DNA inserts within the respective genes. The insert c-*fos* DNA was 2.6 kb and spanned almost the entire length of gene. The c-*myc* DNA insert was 2.1 kb and encompassed a

region of the second and third exons of this much larger gene. If there is differential amounts of phosphorylated H3 associated with the 5' or 3' ends of the gene then there may be a lower signal generated for c-*myc* in comparison to c-*fos*. This is because the c-*myc* insert DNA did not span the entire gene and is therefore not representative of the phosphorylated H3 associated with the entire gene.

Murine fibroblasts transformed with *ras* had elevated levels of Ser-10 pH3. In these oncogene-transformed cells, the pH3 appears to be associated principally with relaxed chromatin regions which is consistent with this modification having a role in destabilizing chromatin packaging (Laitinen et al., 1990). An increased level of pH3 is also observed in cells transformed with *ras*, *fes*, *mos*, and *myc* oncogenes. Several of these oncogenes code for serine/threonine or tyrosine kinases that act upon the MAP kinase signal transduction pathway (Fanger et al., 1997). Myc is a downstream target of the Ras signal transduction pathways (Fanger et al., 1997), and it may indirectly affect these pathways (Amundadottir and Leder, 1998). In addition to the elevated levels of pH3, the levels of phosphorylated H1 histones are increased in these transformed cells. By persistent activation of Ras signalling pathways, the phosphorylated isoforms of H3 and H1 would remain elevated, resulting in the destabilization of chromatin. The exposure of various regions of chromatin to transcription factors and the alterations in interaction of proteins binding to the H3 tails, may be key steps in the process of oncogene-mediated cellular transformation (Trieschmann et al., 1998; Parkhurst, 1998; Palaparti et al., 1997).

To more specifically define the time required for *ras* oncogene expression to affect phosphorylated H3 and H1b levels, we used an inducible-*ras* murine fibroblast cell line. Increased phosphorylation of H3 occurred as soon as Ras oncoprotein expression was activated. In contrast, increased H1b phosphorylation lagged behind. Further, we did not observe an increase in H1b phosphorylation following 30 min after quiescent murine fibroblasts were stimulated with TPA or EGF. This difference in response probably reflects the kinases and processes by which H1b and H3 are phosphorylated. The H3 kinase, which remains to be identified, is rapidly activated by Ras signaling pathways, which are also involved in enhanced phosphorylation of H3 in quiescent cells induced with TPA or EGF (Cano et al., 1995). Phosphorylation of H1b appears to depend on activation of the cyclin E-Cdk2 kinase and transcription (or replication) of the chromatin to which H1b is bound (see sections 1 and 3). Together, these requirements for H1b phosphorylation to go forward could explain why it takes a longer time to observe an increase in H1b phosphorylation compared to that of H3.

Part 5: Investigation of H3 kinase and phosphatase activities in parental and *ras*-transformed cells.

Introduction

As discussed in previous sections, the H3 kinase remains unknown. One particular kinase, pp90^{rsk}, appeared to be a good candidate H3 kinase and we pursued experiments to investigate this possibility. It has previously been demonstrated that pp90^{rsk} can phosphorylate H3 *in vitro* (Chen et al., 1992). In addition, pp90^{rsk} is a downstream target of the MAP kinase pathway and is directly phosphorylated by MAP kinase in response to activating stimuli. There is a strong correlation between the timing of activation of pp90^{rsk} and the induction of H3 phosphorylation in response to these stimuli (Chen and Blenis, 1990; Mahadevan et al., 1991). Both pp90^{rsk} activation and H3 phoshorylation are detected within five minutes after stimulation of serum starved cells with growth factors or phorbol esters (Mahadevan et al., 1991; Chen et al., 1992). Upon stimulation, there is a translocation of pp90^{rsk} to the nucleus where it phosphorylates nuclear proteins such as c-*fos*, and SRF (serum response factor) (Chen et al., 1992). We plannned to compare pp90^{rsk} activity in the parental and oncogene-transformed cells to determine if there was elevated pp90^{rsk} activity in the transformed cells which may be responsible for the increased level of phosphorylated H3 in these cells. We first performed kinase assays to determine if pp90^{rsk} isolated from TPA-stimulated 10T½ cells could phosphorylate H3. In similar experiments as those performed Section 3, we compared the H3

phosphatase activity in the 10T½ and Ciras-3 cells to determine if a decreased H3 phosphatase activity may be responsible for increased levels of phosphorylated H3 in the *ras*-transformed cells. We also investigated which protein phosphatase may be involved in dephosphorylating H3.

Results

pp90^{rsk} phosphorylates histone H2B

pp90^{rsk} was immunoprecipitated from untreated or TPA- stimulated 10T½ cell extracts and kinase assays were performed using total histone as substrate. We observed no phosphorylation of H3 by pp90^{rsk} in either the TPA- treated or untreated cells. Instead we observed that H2B was phosphorylated by pp90^{rsk} in the TPA-stimulated cells (Fig. 58). In a similar kinase assay, cell extracts were prepared from 2H1 cells that were untreated or treated with $ZnSO_4$ for 24 h to stimulated *ras* oncogene expression. pp90^{rsk} was immunoprecipitated from $ZnSO_4$-treated and untreated protein extracts and a kinase assay was performed using total histone as substrate. We observed that there was no phosphorylation of H3 by pp90^{rsk} in the $ZnSO_4$-treated or untreated cells (Fig 58). Instead, histone H2B was phosphorylated by pp90^{rsk} in both the $ZnSO_4$-treated and untreated cells.

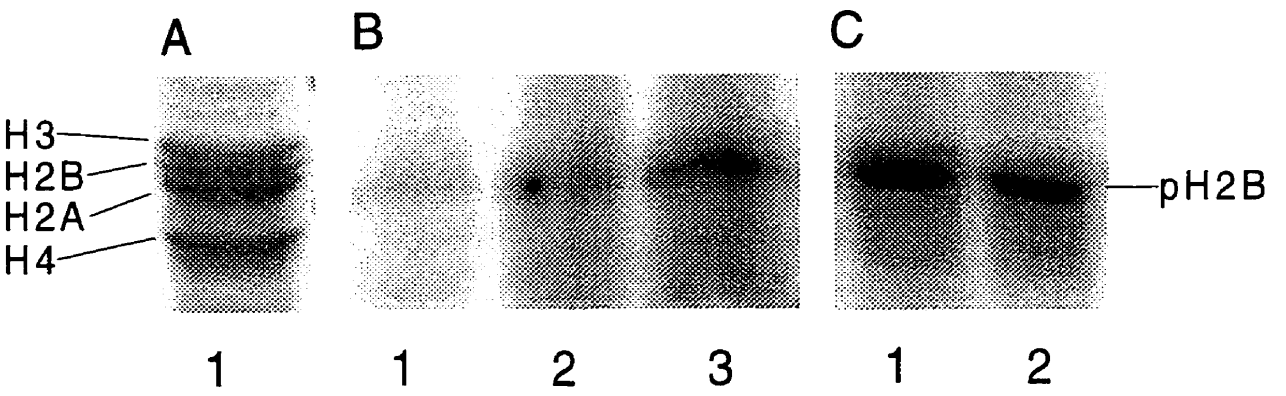

Figure 58. **pp90^{rsk} phosphorylates histone H2B**. pp90^{rsk} was immunoprecipitated from 10T½ cell extracts of 10T½ cells (panel B) that were serum starved (lane 2) or TPA-stimulated (lane 3) or 2H1 (panel C) cells that were untreated (lane 1) or treated with $ZnSO_4$ for 24 h (lane 2). As a control the immunoprecipitation was performed without antibody (panel B, lane 1). Panel A shows the Coomassie blue stained gel of the total histone sample to indicate the position of migration of the core histones. pH2B is phosphorylated H2B.

Parental and *ras*-transformed cells have similar phosphatase activities

To compare the phosphatase activities between 10T½ and Ciras-3 cells, 5 µg of total histone was incubated in the presence of cell extract from 10T½ or Ciras-3 cells. The reaction was allowed to proceed for 0, 15, 30, 45, and 60 min. We observed that the rate of dephosphorylation H3 was similar between the two cell lines (Fig. 59).

PP1 is the predominant H3 phosphatase activity present in 10T½ cells

To monitor pH3 phosphatase activity cellular extracts prepared from 10T½ cells were incubated in the presence of 2 nM or 100 nM okadaic acid and 5 µg of highly phosphorylated total histone. Samples were incubated for 0, 30 and 60 min at 37 °C. In the presence of 2 nM okadaic acid dephosphorylation of the substrate proceeded until approximately 50% of the phosphorylated H3 was remaining (Fig. 60). In the presence of 100 nM okadaic acid dephosphorylation of the substrate was inhibited and 100% of the phosphorylated H3 was remaining after 60 min. These results suggest that the major phosphatase involved in dephosphorylated pH3 is PP1.

Discussion

From our preliminary experiments we were not fully convinced that $pp90^{rsk}$ is a strong candidate H3 kinase. In kinase assays with immunoprecipitated $pp90^{rsk}$ from TPA stimulated cells we observed that there was no phosphorylation

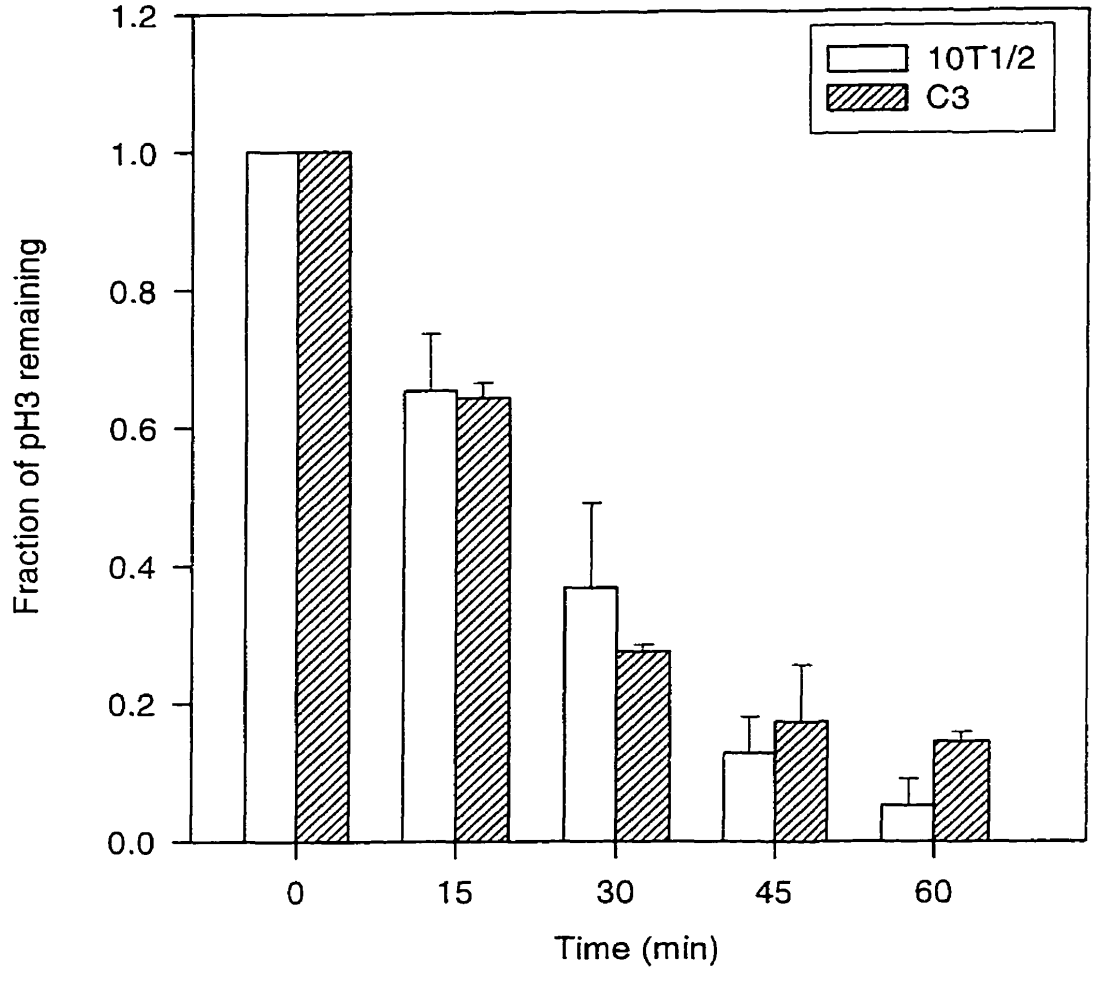

Figure 59. **Comparison of H3 dephosphorylation in extracts from parental and *ras*-transformed cells.** Cell extracts from 10T½ or Ciras-3 were incubated with 5µg of total histone substrate for 0, 15, 30, 45 and 60 minutes at 37 °C. The reaction was stopped and the proteins were separated by SDS polyacrylamide gel electrophoresis, transferred to nitrocellulose membranes and immunochemically stained with anti-pH3. The percent of pH3 remaining after each time period was determined by denstometric analysis of the Western blots.

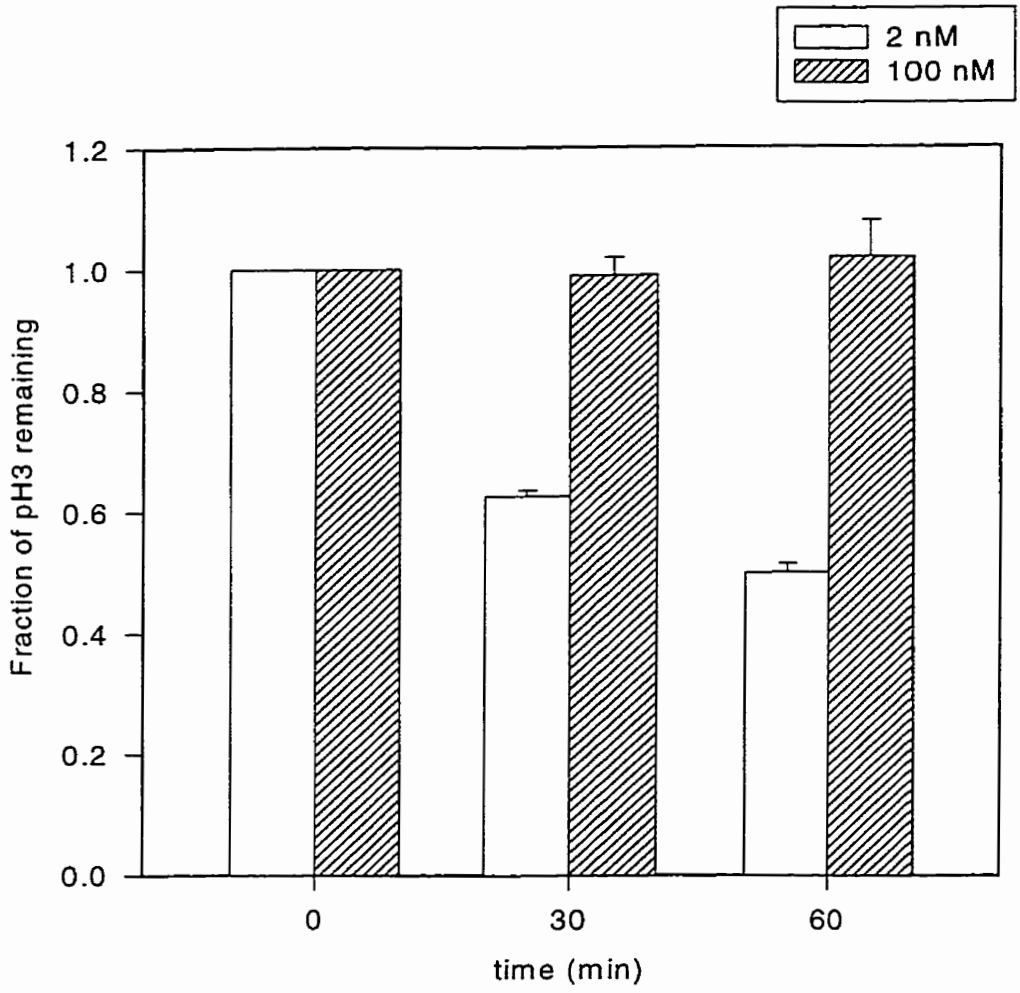

Figure 60. **Inhibition of H3 dephosphorylation by okadaic acid in 10T½ cell extracts**. Cell extracts were incubated in the presence of either 2 nM or 100nM okadaic acid and 5 µg of total histone as substrate. The reaction mixture was incubated for 0, 30 or 60 min at 37 °C. The reaction was stopped and the proteins were separated on an SDS polyacrylamide gel, transferred to membranes, and immunochemically stained with anti-pH3. The percent of pH3 remaining after each time period was determined by densitometric analysis of the Western blots.

of H3. Instead we observed that H2B was phosphorylated. Similarily, we observed that $pp90^{rsk}$ isolated from 2H1 cells treated with $ZnSO_4$ phosphorylated H2B and not H3. Upon further investigation we found that H2B has two sites, Ser 32 and Ser 36 that are contained within the $pp90^{rsk}$ consensus sequence motif "RXXS" (Fisher and Blenis, 1996). The two potential phosphorylation sites of H3, Ser 10 and Ser 28, are contained within the sequence "RXS". In further experiments performed by Cheryl Tylipski, it was determined that H2B was not phosphorylated *in vivo*. The two H2B phosphorylation sites are positioned close to or within the globular domain of the molecule and are probably not accessible to kinases *in vivo*. In our kinase assays, however, the H2B histone may have been partially or fully denatured and, therefore, the phosphorylation sites were available to the kinase. Also, in these assays, H2B may have been preferentially phosphorylated instead of H3 by $pp90^{rsk}$. Further experiments using purified H3 as substrate are needed to resolve these discrepancies. In addition, other kinases such as DLK and MSK1 which also are activated by the MAP kinase pathway also warrant investigation as potential H3 kinases (Kogel et al., 1998; Deak et al., 1998).

To determine if the increased level of pH3 is due to a decreased activity of an H3 phosphatase, we compared the H3 phosphatase activities from the *ras*-transformed and parental 10T½ cells. Our results indicated that the phosphatase activities in these two cell lines were very similar. As a result, the increased level of pH3 in the *ras*-transformed cells is likely due to an increased H3 kinase activity not a decreased H3 phosphatase activity. In experiments using the phosphatase

inhibitor, okadaic acid, we determined that the major H3 phosphatase activity in 10T½ cell extracts is sensitive to 100 nM okadaic acid and not sensitive to 2 nM okadaic acid. Therefore, our results suggest that PP1 not PP2A, is the major H3 phosphatase in 10T½ cells.

CONCLUSIONS

The work presented in this thesis deals with the analysis of phosphorylated histones H1 and H3 in oncogene-transformed cells and the relationship betweeen histone phosphorylation and transcription.

The altered chromatin structure of cancer cells may reflect changes in the cell's histones. The presence of globular and N-terminal domains of H1 and the N-terminal domain of H3 are necessary for proper three-dimensional folding of chromatin (van Holde and Zlatanova, 1996). H1 is modified by a number of post-translational processes such as ubiquitination, phosphorylation, and methylation. H3 is modified by these processes and also by acetylation. Two of these processes, histone acetylation and phosphorylation, have been linked to cellular transformation (Herrara et al., 1996; Brehm et al., 1998; Magnaghi-Jaulin et al., 1998). Core histone tail domains are essential in chromatin folding and oligonucleosome self-association (chromatin fiber-fiber interactions), processes which mediate DNA compaction in the nucleus (Fletcher and Hansen, 1996; Hansen and Ausio, 1992; Tse and Hansen, 1997). Modification of H1 and H3 tail domains by phosphorylation may disrupt fiber-fiber interactions and lead to chromatin decondensation.

Acetylated histones are associated with transcriptionally active DNA sequences and the discovery that the transcriptional coactivator GCN5 has histone acetyltransferase activity revealed, for the first time, how acetyltransferases may be recruited to specific genes (Brownell et al., 1996;

Mizzen et al., 1996). Histone deacetylation was first linked with cancer when histone deacetylase activity was found associated with the tumor suppressor, Rb (Brehm et al., 1998; Magnaghi-Jaulin et al., 1998). Rb represses the activity of E2F-regulated genes by binding to E2F and preventing it from binding and activating its target genes. Histone deacetylation has long been linked to transcriptional repression and the discovery that histone deacetylase associates with the tumor suppressor Rb suggests an additional mechanism by which Rb may inhibit E2F-regulated genes. The histone deacetylase activity associated with Rb may deacetylate histones on the target genes and thereby repress transcription (Brehm et al., 1998; Magnaghi-Jaulin et al., 1998). The repression of the E2F regulated genes is important in preventing cell cycle progression.

Both H1 and H3 can be phosphorylated, and our studies suggest that H1 and H3 phosphorylation is deregulated in oncogene-transformed cells. We observed an elevated level of phosphorylated H1 and H3 in the transformed cells in comparison to normal cells. Furthermore, we observed that expression of the *ras* oncogene results in an increase in the levels of phosphorylated H1 and H3. We proposed that oncogene activation of the MAP kinase pathway leads to increased activity of an H1b and H3 kinase resulting in increased levels of pH1b and pH3 (Fig. 61).

All of the oncogenes we studied impact upon the MAP kinase pathway which eventually leads to the phosphorylation of c-Myc (Fanger et al., 1997; Katz and McCormick, 1997). Overexpression of c-Myc results in elevated levels of cyclins E and A which form active kinase complexes with CDK2. We, therefore,

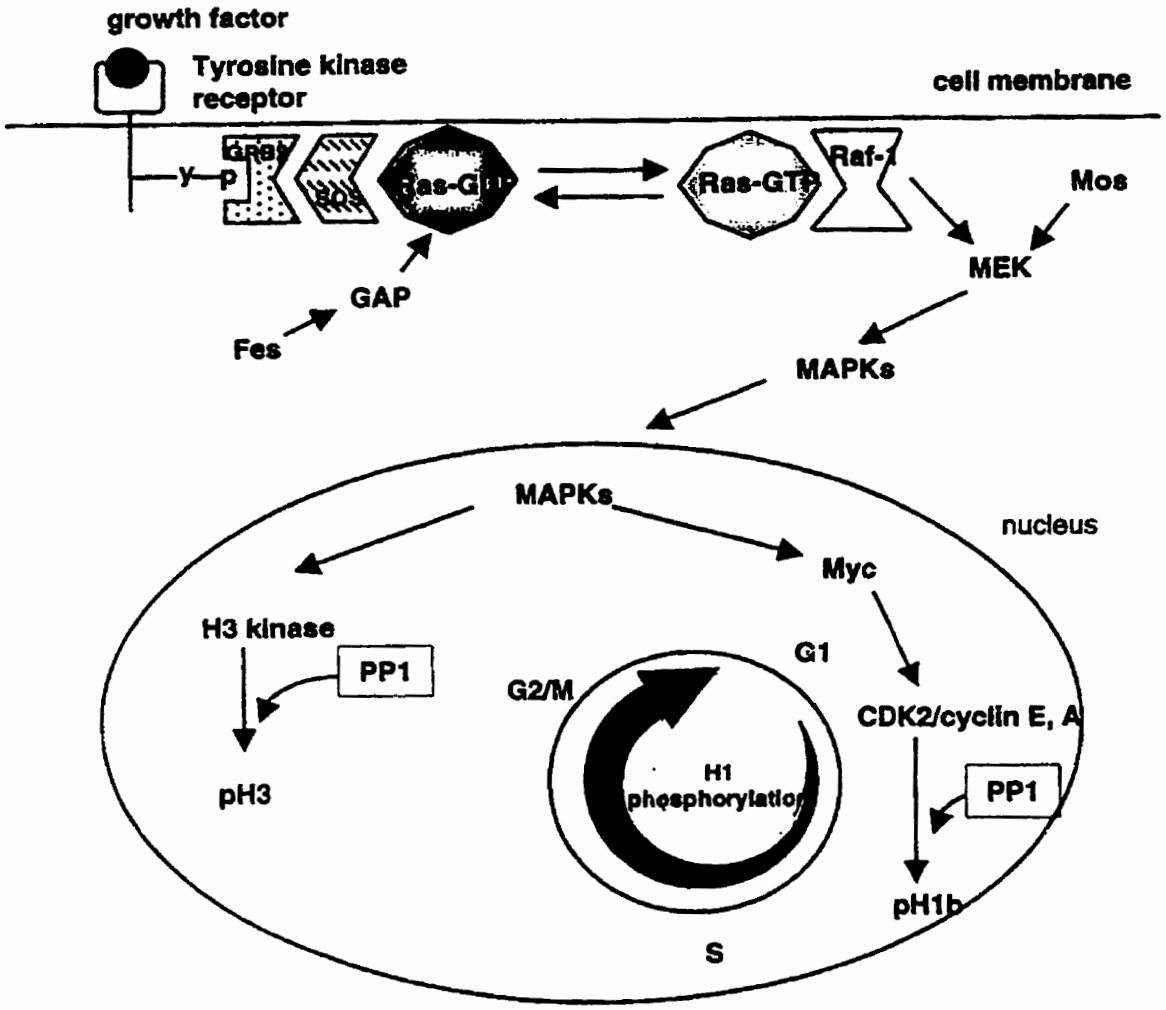

Figure 61. **A model for histone H1b and H3 phosphorylation via the Ras-MAP kinase signal transduction pathway.** See text for details.

believe that CDK2/cyclin E is a strong candidate for the H1b kinase. Indeed, CDK2 activity has been found to be deregulated in transformed cells and altered cyclin E protein levels have been found in cancer cells (Herrara et al., 1996; Keyomarsi et al., 1994). CDK2 kinase activity is regulated by a number of different events; phosphorylation of Thr160 and Tyr15, association with cyclin E or A, and binding to CDK inhibitors. It is possible that increased CDK2 activity in the oncogene-transformed cells is a result of deregulation of CAK, the kinase that phosphorylates and activates CDK2. The protein levels and immunolocalization of CDK7/CAK have been analyzed in a wide range of normal and tumor cells and no substantial differences were observed (Bartkova et al., 1996). A second possibility is the presence of increased levels of cyclin E or cyclin E isoforms in the transformed cells which may contribute to deregulated CDK2 activty. There have been reports on the presence of altered levels of cyclin E in breast cancer cells (Gray-Bablin et al., 1996; Keyomarsi et al., 1994). A third possibility is that the association of CDK2 with CDK inhibitors is disrupted resulting in premature and deregulated expression of CDK2 and altered cell cycle events. Expression of p27 in Rat-1 cells inhibits CDK2 activity and results in growth arrest. However, the induction of growth arrest and the association of $p27^{kip1}$ with CDK2/cyclin E is abrogated by the prior expression of c-Myc (Bartkova et al., 1996; Vlach et al., 1996). Myc expression induced the sequestering of p27 in a form unable to bind CDK2/cyclin E (Bartkova et al., 1996; Vlach et al., 1996). Since increased c-Myc expression is found in many transformed cells, the sequestering of p27 would result in inappropriately active CDK2/cyclin E complexes that can phosphorylate

Rb and promote cell cycle progression. It has also been reported that induction of *ras* oncogene expression leads to the degradation of p27 and increase in CDK2 kinase activity (Weber et al., 1997). Possibly, upon *ras* oncogene expression, these active CDK2/cyclin E complexes could phosphorylate H1 and promote a chromatin conformation amenable to transcription.

We provided evidence that levels of pH1b are dependent upon on-going transcription. The only other histone modification known to be dependent upon on-going transcription is ubiquitination of histone H2B (Davie and Murphy, 1990). In addition to being affected by inhibition of transcription, levels of pH1b are also dependent upon replication. It has been determined that the accessibility of H1 to the H1 kinase is directly related to its position in the chromatin fiber and that H1 must be displaced from the chromatin fiber in order for it to be phosphorylated by an H1 kinase (Jermanowski and Cole, 1992). Transcription and replication processes may be the initial disruptive events that lead to the partial displacement of H1b from the chromatin fiber and renders it accessible to the H1 kinase. We propose that when transcription or replication processes are inhibited, H1b is no longer exposed to the H1 kinase. Dephosphorylation by protein phosphatases would then reduce the steady state levels of pH1b (Fig. 62).

The H3 kinase remains unknown, however, H3 phosphorylation is induced by activation of both the growth factor responsive (ERK1 and 2) and stress responsive (JNK1 and 2) MAP kinase pathways (Barratt et al., 1994b). Possible candidate H3 kinases that are activated in response to these

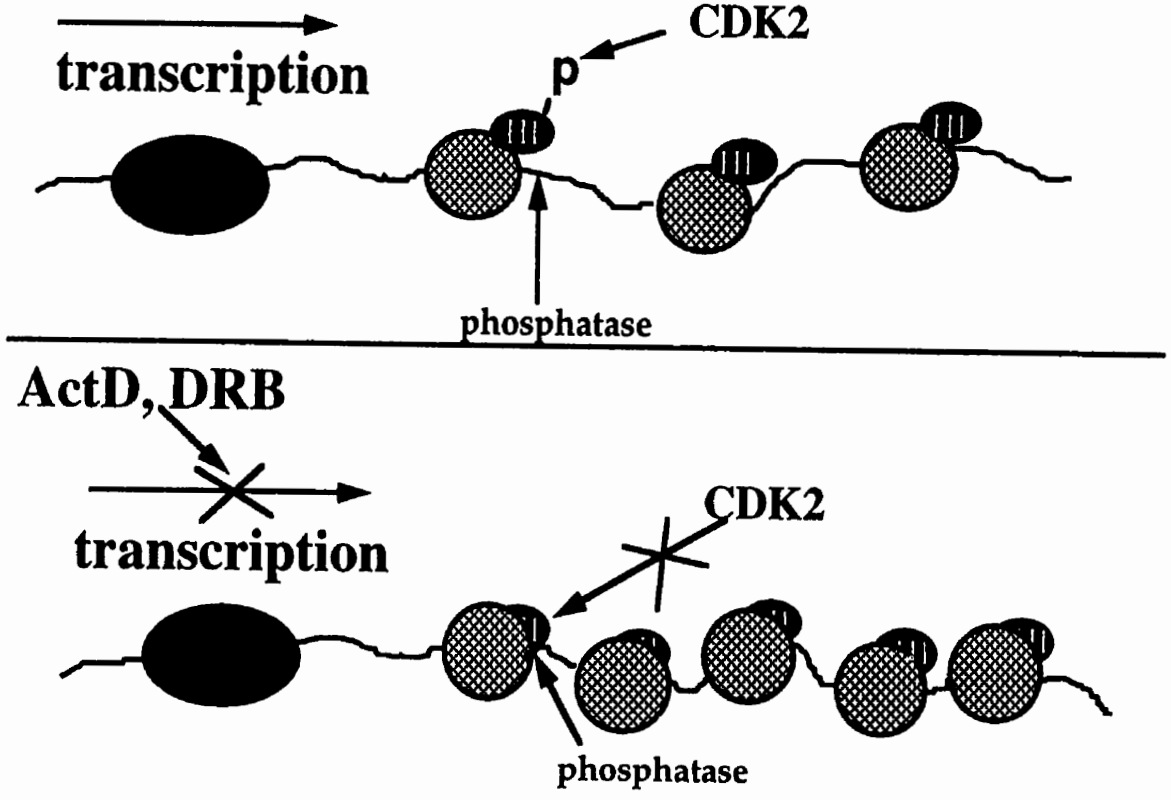

Fig.62. A model illustrating the effect of inhibition of transcription on the phosphorylation of H1b. See text for details.

pathways include DLK and MSK1 (Kogel et al., 1998; Deak et al., 1998). The identification of the H3 kinase awaits future study.

When serum starved cells are treated with growth factors or phorbol esters, the Ras/MAPK pathway is activated and there is an increase in c-*fos* and c-myc expression which can be observed as early as 5 min after treatment. This expression is transient, however, and declines after 2 h. We have demonstrated that phosphorylated H3 from TPA treated cells is associated with c-*fos* and c-*myc* DNA sequences. A recent report indicates that the c-*fos* gene is transcribed in serum-starved cells (Pinaud and Mirkovitch, 1998). It was observed that in the absence of gene activation signals, the c-*fos* gene presents an active chromatin structure and that regulatory proteins constitutively occupy the promoter region. In serum starved cells, engaged RNA polymerases continuously initiate transcription, however, the transcripts are terminated near the promoter (Pinaud and Mirkovitch, 1998). When the cells are stimulated, the full-length transcript is made. The authors proposed that the c-*fos* gene is regulated at the level of transcription elongation and therefore the activation of c-*fos* expression is due to the release of the transcription elongation block (Pinaud and Mirkovitch, 1998). It has been proposed that other genes such as c-*myc* and c-*myb* are also regulated at the level of transcription elongation (Pinaud and Mirkovitch, 1998). Phosphorylation and acetylation of histone H3 may be involved in overcoming the elongation block by promoting the formation of an open chromatin structure that permits elongation. Previous findings indicate that treatment of cells with activators results in a dramatic increase in the DNase I sensitivity of the c-*fos*

gene beginning in the 5' region and eventually spanning the entire coding region (Feng and Villeponteau, 1992). Upon exposure to activating stimuli, the H3 kinase could be activated and recruited to sites of early response genes causing phosphorylation of H3 and localized decondensation. The histone acetyltransferase, CBP, which is part of the RNA Pol II holoenzyme, is present prior to induction and, therefore, H3 may also be engaged in acetylation. Together, H3 acetylation and phosphorylation may work to overcome an inhibitory chromatin structure which may be a key contributing factor to the transcription elongation block (Fig. 63).

A remaining question is what turns off the transcription of these genes? For transcriptional activation of the human interferon-β gene, a multi-protein complex called the enhanceosome is assembled. It consists of the transcriptional activators NF-κB, IRF1, ATF2/c-jun, and the architectural protein HMGI(Y) (Thanos and Maniatis, 1995). The binding of two molecules of HMG I(Y) to four sites within the enhancer alters the structure of the DNA, and allows the binding of interferon-β gene activators that assemble into an extremely stable enhanceosome structure (Thanos and Maniatis, 1995). The recruitment of CBP/p300 by the interferon-β enhanceosome is required for synergistic activation of transcription. Interestingly, the acetylation of HMGI(Y) by CBP actually turns off the interferon-β expression by causing dissasembly and destabilization of the enhanceosome (Munshi et al., 1998). Possibly, similar mechanisms are in place for turning off genes such as c-*fos* and c-*myc*.

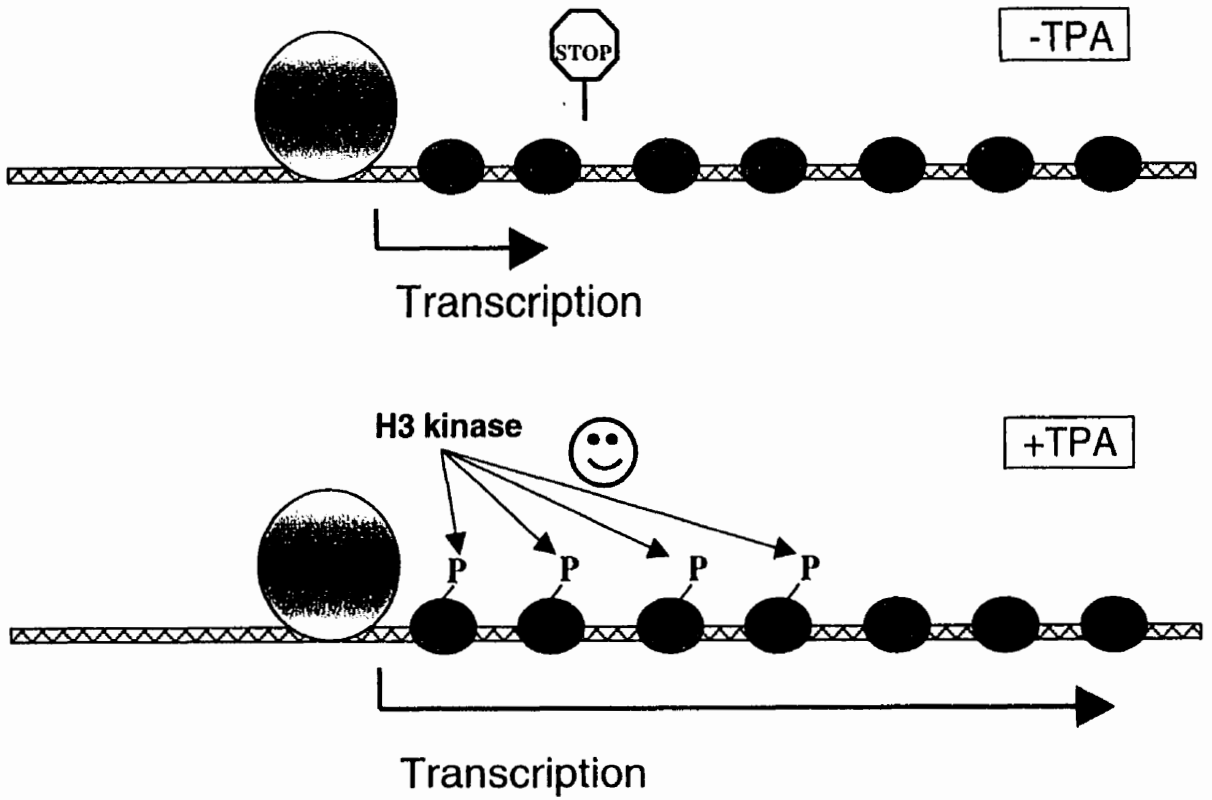

Figure 63. **A model for the function of H3 phosphorylation in induction of immediate early gene expression**. See text for details.

In cancer cells, the constitutive activation of the MAPK results in increased phosphorylation of histones H1 and H3 and relaxation of chromatin structure. A more relaxed chromatin structure may result in aberrant expression of genes, such as immediate early genes, thus facilitating the process of malignant transformation.

REFERENCE LIST

Ajiro, K., Borun, T.W., Shulman, S.D., McFadden, G.M., and Cohen, L.H. (1981a). Comparison of the structures of human histones 1A and 1B and their intramolecular phosphorylation sites during the HeLa S-3 cell cycle. Biochemistry *20*, 1454-1464.

Ajiro, K., Buron, T.W., and Coen, L.H. (1981b). Phosphorylation states of different histone 1 subtypes and their relationship to chromatin functions during the HeLa S-3 cell cycle. Biochemistry *20*, 1445-1454.

Ajiro, K. and Nishimoto, T. (1985). Specific site of histone H3 phosphorylation related to the maintenance of premature cromosome condensation. Evidence for catalytically induced interchange of the subunits. J. Biol. Chem. *260*, 15379-15381.

Allfrey, V. G., Faulkner, R. M., and Mirsky, A. E. (1964) Proc. Natl. Acad. Sci. U.S.A. 51, 786-794.

Amundadottir, L.T. and Leder, P. (1998). Signal transduction pathways activated and required for mammary carcinogenesis in response to specific oncogenes. Oncogene *16*, 737-746.

Arabshahi, L., Brown, N., Khan, N., and Wright, G. (1988). Nucleic Acids Res. *16*, 5107-5113.

Arents, G., Burlingame, R.W., Wang, B.C., Love, W.E., and Moudrianakis, E.N. (1991). The nucleosomal core histone octamer at 3.1 A resolution: a tripartite protein assembly and a left-handed superhelix. Proc. Natl. Acad. Sci. U.S.A. *88*, 10148-10152.

Arion, D., Meijer, L., Brizuela, L., and Beach, D. (1988). Cdc2 is a component of the M phase-specific histone H1 kinase: evidence for identity with MPF. Cell *55*, 371-378.

Ashihara, T. and Baserga, R. (1979). Cell synchronization. Methods Enzymol. *58:248-62*, 248-262.

Aubert, D., Garcia, M., Benchaibi, M., Poncet, D., Chebloune, Y., Verdier, G., Nigon, V., Samarut, J., and Mura, C. (1991). Inhibition of proliferation of primary avian fibroblasts through expression of histone H5 depends on the degree of phosphorylation of the protein. J. Cell Biol. *113*, 497-506.

Ausio, J., Dong, F., and Van Holde, K.E. (1989). Use of selectively trypsinized nucleosome core particles to analyze the role of the histone "tails" in the stabilization of the nucleosome. J. Mol. Biol. *206*, 451-463.

Avruch, J., Zhang, X., and Kyriakis, J.M. (1994). Raf meets Ras: Completing the framework of a signal transduction pathway. Trends Biochem. Sci. *19*, 279-283.

Aznavoorian, S., Murphy, A.N., Stetler-Stevenson, W.G., and Liotta, L.A. (1993). Molecular aspects of tumor cell invasion and metastasis. Cancer *71*, 1368-1383.

Bannister, A.J. and Kouzarides, T. (1996). The CBP co-activator is a histone acetyltransferase. Nature *384*, 641-643.

Barratt, M.J., Hazzalin, C.A., Cano, E., and Mahadevan, L.C. (1994a). Mitogen-stimulated phosphorylation of histone H3 is targeted to a small hyperacetylation-sensitive fraction. Proc. Natl. Acad. Sci. USA *91*, 4781-4785.

Barratt, M.J., Hazzalin, C.A., Zhelev, N., and Mahadevan, L.C. (1994b). A mitogen- and anisomycin-stimulated kinase phosphorylates HMG-14 in its basic amino-terminal domain in vivo and on isolated mononucleosomes. EMBO J. *13,19*, 4524-4535.

Bartkova, J., Zemanova, M., and Bartek, J. (1996). Expression of CDK7/CAK in normal and tumor cells of diverse histogenesis, cell-cycle position and differentiation. Int. J. Cancer *66*, 732-737.

Bates, S., Bonetta, L., MacAllan, D., Parry, D., Holder, A., Dickson, C., and Peters, G. (1994). CDK6 (PLSTIRE) and CDK4 (PSK-J3) are a distinct subset of the cyclin- dependent kinases that associate with cyclin D1. Oncogene *9*, 71-79.

Belyavsky, A.V., Bavykin, S.G., Goguadze, E.G., and Mirzabekov, A.D. (1980). Primary organization of nucleosomes containing all five histones and DNA 175 and 165 base-pairs long. J. Mol. Biol. *139*, 519-536.

Bernard, O., Cory, S., Gerondakis, S., Webb, E., and Adams, J.M. (1983). Sequence of the murine and human cellular *myc* oncogenes and two modes of *myc* transcription resulting from chromosome translocation in B lymphoid tumours. EMBO J. *2*, 2375-2383.

Blackwood, E.M. and Eisenman, R.N. (1991). Max: a helix-loop-helix zipper protein that forms a sequence-specific DNA-binding complex with Myc. Science *251*, 1211-1217.

Blair, D.G., Oskarsson, M., Wood, T.G., McClements, W.L., Fischinger, P.J., and Vande, W.G. (1981). Activation of the transforming potential of a normal cell sequence: a molecular model for oncogenesis. Science *212*, 941-943.

Blencowe, B.J., Issner, R., Nickerson, J.A., and Sharp, P.A. (1998). A coactivator of pre-mRNA splicing. Genes Dev. *12*, 996-1009.

Blencowe, W.J., Nickerson, J.A., Issner, R., Penman, S., and Sharp, P.A. (1994) Association of nuclear matrix antigens with exon containing splicing complexes. J. Cell. Biol. *127*, 593-607.

Blumer, K.J. and Johnson, G.L. (1994). Diversity in function and regulation of MAP kinase pathways. Trends. Biochem. Sci. *19*, 236-240.

Boffa, L.C., Walker, J., Chen, T.A., Sterner, R., Mariani, M.R., and Allfrey, V.G. (1990). Factors affecting nucleosome structure in transcriptionally active chromatin. Histone acetylation, nascent RNA and inhibitors of RNA synthesis. Eur. J. Biochem. *194*, 811-823.

Bregman, D.B., Du, L., van der Zee, S., and Warren, S.L. (1995). Transcription-dependent redistribution of the large subunit of RNA polymerase II to discrete nuclear domains. J. Cell Biol. *129*, 287-298.

Brehm, A., Miska, E.A., McCance, D.J., Reid, J.L., Bannister, A.J., and Kouzarides, T. (1998). Retinoblastoma protein recruits histone deacetylase to repress transcription. Nature *391*, 597-601.

Brownell, J.E., Zhou, J., Ranalli, T., and Kobayashi, R. (1996). Tetrahymena histone acetyltransferase A: a homolog to yeast Gcn5p linking histone acetylation to gene activation. Cell *84*, 843-851.

Canaani, E., Robbins, K.C., and Aaronson, S.A. (1979). The transforming gene of Moloney murine sarcoma virus. Nature *282*, 378-383.

Cano, E., Hazzalin, C.A., Kardalinou, E., Buckle, R.S., and Mahadevan, L.C. (1995). Neither ERK nor JNK/SAPK MAP kinase subtypes are essential for histone H3/HMG-14 phosphorylation or c-*fos* and c-*jun* induction. J. Cell Sci. *108*, 3599-3609.

Carter, K.C., Bowman, D., Carrington, W., Fogarty, K., McNeil, J.A., Fay, F.S., and Lawrence, J.B. (1993). A three-dimensional view of precursor messenger RNA metabolism within the mammalian nucleus [see comments]. Science *259*, 1330-1335.

Chadee, D.N., Taylor, W.R., Hurta, R.A., Allis, C.D., Wright, J.A., and Davie, J.R. (1995). Increased phosphorylation of histone H1 in mouse fibroblasts transformed with oncogenes or constitutively active mitogen- activated protein kinase kinase. J. Biol. Chem. *270*, 20098-20105.

Chen, H., Liu, X., and Patel, D.J. (1996). DNA bending and unwinding associated with actinomycin D antibiotics bound to partially overlapping sites on DNA. J. Mol. Biol. *258*, 457-479.

Chen, R. and Blenis, J. (1990) Identification of Xenopus S6 protein kinase homologs ($pp90^{rsk}$) in somatic cells: phosphorylation and activation during initiation of cell proliferation. Mol. Cell. Biol. 10(6), 3204-3215.

Chen, R., Samecki, C., and Blenis, J. (1992). Nuclear localization and regulation of ERK- and RSK-encoded protein kinases. Mol. Cell. Biol. *12,3*, 915-927.

Chen, R.H., Juo, P.C., Curran, T., and Blenis, J. (1996). Phosphorylation of c-Fos at the C-terminus enhances its transforming activity. Oncogene *12*, 1493-1502.

Chen, T.A. and Allfrey, V.G. (1987). Rapid and reversible changes in nucleosome structure accompany the activation, repression, and superinduction of murine fibroblast protooncogenes c-*fos* and c-*myc*. Proc. Natl. Acad. Sci. U.S.A. *84*, 5252-5256.

Chiu, R., Boyle, W.J., Meek, J., Smeal, T., Hunter, T., and Karin, M. (1988). The c-Fos protein interacts with c-Jun/AP-1 to stimulate transcription of AP-1 responsive genes. Cell *54*, 541-552.

Cho, H., Orphanides, G., Sun, X., Yang, X.J., Ogryzko, V., Lees, E., Nakatani, Y., and Reinberg, D. (1998). A human RNA polymerase II complex containing factors that modify chromatin structure. Mol. Cell. Biol. *18*, 5355-5363.

Ciechanover, A., Finley, D., and Varshavsky, A. (1984). The ubiquitin-mediated proteolytic pathway and mechanisms of energy- dependent intracellular protein degradation. J. Cell. Biochem. *24*, 27-53.

Clark, D.J. and Felsenfeld, G. (1991). Formation of nucleosomes on positively supercoiled DNA. EMBO J. *10*, 387-395.

Clemson, C.M. and Lawrence, J.B. (1996). Multifunctional compartments in the nucleus: insights from DNA and RNA localization. J. Cell. Biochem. *62*, 181

Cockerill, P.N. and Garrard, W.T. (1986). Chromosomal loop anchorage of the kappa immunoglobulin gene occurs next to the enhancer in a region containing topoisomerase II sites. Cell *44*, 273-282.

Codosh, L.A., Fire, A., Samuels, M., and Sharp, P.A. (1989). 5,6-dichloro-1-β-D-ribofuranosylbenzimidazole inhibits transcription elongation by RNA Pol II *in vitro*. J. Biol. Chem. *264*, 2250-2257.

Coffin, J.M., Varmus, H.E., Bishop, J.M., Essex, M., Hardy, W.D.J., Martin, G.S., Rosenberg, N.E., Scolnick, E.M., Weinberg, R.A., and Vogt, P.K. (1981). Proposal for naming host cell-derived inserts in retrovirus genomes. J. Virol. *40*, 953-957.

Cole, R.D. (1987). Microheterogeneity in H1 histones and its consequences. Int. J. Peptide Protein Res. *30*, 433-449.

Colledge, W.H., Carlton, M.B., Udy, G.B., and Evans, M.J. (1994). Disruption of c-mos causes parthenogenetic development of unfertilized mouse eggs [see comments]. Nature *370*, 65-68.

Colosi, P., Talamantes, F., and Linzer, D.I. (1987). Molecular cloning and expression of mouse placental lactogen I complementary deoxyribonucleic acid. Mol. Endocrinol. *1*, 767-776.

Cooper, G.M. (1995). Oncogenes (London, England: Jones and Bartlett Publishers International).

Cowley, S., Paterson, H., Kemp, P., and Marshall, C.J. (1994). Activation of MAP kinase kinase is necessary and sufficient for PC12 differentiation and for transformation of NIH 3T3 cells. Cell *77*, 841-852.

Cox, A.D., Hisaka, M.M., Buss, J.E., and Der, C.J. (1992). Specific isoprenoid modification is required for function of normal, but not oncogenic, Ras protein. Mol. Cell. Biol. *12*, 2606-2615.

Crissman, H.A., Gadbois, D.M., Tobey, R.A., and Bradbury, E.M. (1991). Transformed mammalian cells are deficient in kinase-mediated control of progression through through G1 phase of the cell cycle. Proc. Natl. Acad. Sci. *88*, 7580-7584.

Daksis, J.I., Lu, R.Y., Facchini, L.M., Marhin, W.W., and Penn, L.J.Z. (1994). Myc induces cyclin D1 expression in the absence of de novo protein synthesis and links mitogen-stimulated signal transduction to the cell cycle. Oncogene *9*, 3635-3645.

Dalla-Favera, R., Bregni, M., Erikson, J., Patterson, D., Gallo, R.C., and Croce, C.M. (1982). Human c-*myc* oncogene is located on the region of chromosome 8 that is translocated in Burkitt lymphoma cells. Proc. Natl. Acad. Sci. U.S.A. *79*, 7824-7827.

Davie, J.R. (1995). The nuclear matrix and the regulation of chromatin organization and function. Int. Rev. Cytol. *162A:* 191-250.

Davie, J.R. (1997). Nuclear matrix, dynamic histone acetylation and transcriptionally active chromatin. Mol. Biol. Rep. *24*, 197-207.

Davie, J.R. and Candido, E.P. (1978). Acetylated histone H4 is preferentially associated with template-active chromatin. Proc. Natl. Acad. Sci. U.S.A. *75*, 3574-3577.

Davie, J.R. and Delcuve, G.P. (1991). Characterization and chromatin distribution of the H1 histones and high-mobility-group non-histone chromosomal proteins of trout liver and hepatocellular carcinoma. Biochem. J. *280*, 491-497.

Davie, J.R. and Murphy, L.C. (1990). Level of ubiquitinated histone H2B in chromatin is coupled to ongoing transcription. Biochemistry *29*, 4752-4757.

Davis, R.J. (1995). Transcriptional regulation by MAP kinases. Mol. Reprod. Dev. *42*, 459-467.

Deak, M., Clifton, A.D., Lucocq, L.M., and Alessi, D.R. (1998). Mitogen- and stress-activated protein kinase-1 (MSK1) is directly activated by MAPK and SAPK2/p38, and may mediate activation of CREB. EMBO J. *17*, 4426-4441.

Delcuve, G.P. and Davie, J.R. (1989). Chromatin structure of erythroid-specific genes of immature and mature chicken erythrocytes. Biochem. J. *263*, 179-186.

Delcuve, G.P. and Davie, J.R. (1992). Western blotting and immunochemical detection of histones electrophoretically resolved on acid-urea-triton- and sodium dodecyl sulfate-polyacrylamide gels. Anal. Biochem. *200*, 339-341.

Denhardt, D.T. (1996). Signal-transducing protein phosphorylation cascades mediated by Ras/Rho proteins in the mammalian cell: the potential for multiplex signalling. Biochem. J. *318*, 729-747.

Devoto, S.H., Mudryj, M., Pines, J., Hunter, T., and Nevins, J.R. (1992). A cyclin A-protein kinase complex possesses sequence-specific DNA binding activity: p33cdk2 is a component of the E2F-cyclin A complex. Cell *68*, 167-176.

Dirks, R.W., de Pauw, E.S., and Raap, A.K. (1997). Splicing factors associate with nuclear HCMV-IE transcripts after transcriptional activation of the gene, but dissociate upon transcription inhibition: evidence for a dynamic organization of splicing factors. J. Cell Sci. *110*, 515-522.

Dohadwala, M., da, C., Hall, F.L., Williams, R.T., Carbonaro-Hall, D.A., Naim, A.C., Greengard, P., and Berndt, N. (1994). Phosphorylation and inactivation of protein phosphatase 1 by cyclin- dependent kinases. Proc. Natl. Acad. Sci. U.S.A. *91*, 6408-6412.

Duesberg, P.H., Bister, K., and Vogt, P.K. (1977). The RNA of avian acute leukemia virus MC29. Proc. Natl. Acad. Sci. U.S.A. *74* , 4320-4324.

Durfee, T., Mancini, M.A., Jones, D., Elledge, S.J., and Lee, W.-H. (1994). The amino-terminal region of the retinoblastoma gene product binds a novel nuclear matrix protein that co-localizes to centers for RNA processing. J. Cell Biol. *127*, 609-622.

Ebinu, J.O., Bottorff, D.A., Chan, E.Y., Stang, S.L., Dunn, R.J., and Stone, J.C. (1998). RasGRP, a Ras guanyl nucleotide- releasing protein with calcium- and diacylglycerol-binding motifs. Science *280*, 1082-1086.

Edmondson, D.G., Smith, M.M., and Roth, S.Y. (1996). Repression domain of the yeast global repressor Tup1 interacts directly with histones H3 and H4. Genes Dev. *10*, 1247-1259.

Egan, S.E., Giddings, B.W., Brooks, M.W., Buday, L., Sizeland, A.M., and Weinberg, R.A. (1993). Association of Sos Ras exchange protein with Grb2 is implicated in tyrosine kinase signal transduction and transformation. Nature *363*, 45-51.

Egan, S.E., McClarity, G.A., Jarolim, L., Wright, J.A., Spiro, I., Hager, G., and Greenberg, A.H. (1987). Expression of H-ras correlates with metastatic potential: evidence for direct regulation of the metastatic phenotype in 10T½ and NIH 3T3 cells. Mol. Cell. Biol. *7:2*, 830-837.

Egan, S.E. and Weinberg, R.A. (1993). The pathway to signal achievement. Nature *365*, 781-783.

Egan, S.E., Wright, J.A., Jarolim, L., Yanagihara, K., Bassin, R.H., and Greenberg, A.H. (1987). Transformation by oncogenes encoding protein kinases induces the metastatic phenotype. Science *238*, 202-205.

el-Deiry, W.S., Harper, J.W., O'Connor, P.M., Velculescu, V.E., Canman, C.E., Jackman, J., Pietenpol, J.A., Burrell, M., Hill, D.E., and Wang, Y. (1994). WAF1/CIP1 is induced in p53-mediated G1 arrest and apoptosis. Cancer Res. *54*, 1169-1174.

El-Shemerly, M.Y., Besser, D., Nagasawa, M., and Nagamine, Y. (1997). 12-O-Tetradecanoylphorbol-13-acetate activates the Ras/extracellular signal-regulated kinase (ERK) signaling pathway upstream of SOS involving serine phosphorylation of Shc in NIH3T3 cells. J. Biol. Chem. *272*, 30599-30602.

Fanger, G.R., Gerwins, P., Widmann, C., Jarpe, M.B., and Johnson, G.L. (1997). MEKKs, GCKs, MLKs, PAKs, TAKs, and tpls: upstream regulators of the c- Jun amino-terminal kinases? Curr. Opin. Genet. Dev. *7*, 67-74.

Feldman, R.A., Gabrilove, J.L., Tam, J.P., Moore, M.A., and Hanafusa, H. (1985). Specific expression of the human cellular Fps/Fes-encoded

protein NCP92 in normal and leukemic myeloid cells. Proc. Natl. Acad. Sci. U.S.A. *82*, 2379-2383.

Feller, S.M., Ren, R., Hanafusa, H., and Baltimore, D. (1994). SH2 and SH3 domains as molecular adhesives: the interactions of Crk and Abl. Trends. Biochem. Sci. *19*, 453-458.

Feng, J. and Villeponteau, B. (1992). High-resolution analysis of c-*fos* chromatin accessibility using a novel DNase I-PCR assay. Biochim. Biophys. Acta *1130*, 253-258.

Ferrigno, P., Langan, T.A., and Cohen, P. (1993). Protein phosphatase 2A is the major enzyme in vertebrate cell extracts that dephosphorylates several physiological substrates for cyclin-dependent protein kinases. Mol. Biol. Cell. *4*, 669-677.

Filmus, J., Robles, A.I., Shi, W., Wong, M.J., Colombo, L.L., and Conti, C.J. (1994). Induction of cyclin D1 expression by activated Ras. Oncogene *9*, 3627-3633.

Fisher, T.L. and Blenis, J. (1996). Evidence for two catalytically active kinase domains in $pp90^{rsk}$. Mol. Cell Biol. *16*, 1212-1219.

Fletcher, T.M. and Hansen, J.C. (1996). The nucleosomal array: structure/function relationships. Crit. Rev. Eukaryot. Gene Expr. *6*, 149-188.

Franco, R. and Rosenfeld, M.G. (1990). Hormonally inducible phosphorylation of a nuclear pool of ribosomal protein S6. J. Biol. Chem. *265*, 4321-4325.

Frawley, B.P.J., Tien, X.Y., Hartmann, S.C., Wali, R.K., Niedziela, S.M., Davidson, N.O., Sitrin, M.D., Brasitus, T.A., and Bissonnette, M. (1994). TPA causes divergent responses of Ca(2+)-dependent and Ca(2+)-independent isoforms of PKC in the nuclei of Caco-2 cells. Biochim. Biophys. Acta *1222*, 301-305.

Fusauchi, Y. and Iwai, K. (1984). Tetrahymena histone H2A. Acetylation in the N-terminal sequence and phosphorylation in the C-terminal sequence. J. Biochem. (Tokyo.) *95*, 147-154.

Garcia-Ramirez, M., Rocchini, C., and Ausio, J. (1995). Modulation of chromatin folding by histone acetylation. J. Biol. Chem. *270*, 17923-17928.

Getzenberg, R.H., Pienta, K.J., Ward, W.S., and Coffey, D.S. (1991). Nuclear structure and the three-dimensional organization of DNA. J. Cell Biochem. *47*, 289-299.

Giancotti, B., Pani, B., D'Adrea, P., Berlingieri, M.T., Di Fiore, P.P., Fusco, A., Vecchio, G., Philip, R., Crane-Robinson, C., Nicolas, R.H., Wright, C.A., and Goodwin, G.H. (1987). Elevated levels of a specific class of nuclear phosphoproteins in cells transformed with v-*ras* and v-*mos* oncogenes and by cotransfection with c-*myc* and polyoma middle T genes. EMBO J. *6:7*, 1981-1987.

Glass, D.B. and Krebs, E.G. (1982). Phosphorylation by guanosine 3':5'-monophosphate-dependent protein kinase of synthetic peptide analogs of a site phosphorylated in histone H2B. J. Biol. Chem. *257*, 1196-1200.

Goldknopf, I.L., Sudhakar, S., Rosenbaum, F., and Busch, H. (1980a). Timing of ubiquitin synthesis and conjugation into protein A24 during the HeLa cell cycle. Biochem. Biophys. Res. Commun. *95*, 1253-1260.

Goldknopf, I.L., Wilson, G., Ballal, N.R., and Busch, H. (1980b). Chromatin conjugate protein A24 is cleaved and ubiquitin is lost during chicken erythropoiesis. J. Biol. Chem. *255*, 10555-10558.

Gray-Bablin, J., Zalvide, J., Fox, M.P., Knickerbocker, C.J., DeCaprio, J.A., and Keyomarsi, K. (1996). Cyclin E, a redundant cyclin in breast cancer. Proc. Natl. Acad. Sci.U.S.A. *93*, 15215-15220.

Greenberg, M.E. and Ziff, E.B. (1984). Stimulation of 3T3 cells induces transcription of the c-*fos* proto- oncogene. Nature *311*, 433-438.

Gu, Y., Turck, C.W., and Morgan, D.O. (1993). Inhibition of CDK2 activity *in vivo* by an associated 20K regulatory subunit. Nature *366*, 707-710.

Halazonetis, T.D., Georgopoulos, K., Greenberg, M.E., and Leder, P. (1988). c-Jun dimerizes with itself and with c-Fos, forming complexes of different DNA binding affinities. Cell *55*, 917-924.

Haliotis, T., Trimble, W., Chow, S., Bull, S., Mills, G., Girard, P., Kuo, J.F., and Hozumi, N. (1990). Expression of ras oncogene leads to down-regulation of protein kinase C. .Int. J. Cancer *45*, 1177-1183.

Halmer, L. and Gruss, C. (1995). Influence of histone H1 on the *in vitro* replication of DNA and chromatin. Nucleic Acids Res. *23*, 773-778.

Halmer, L. and Gruss, C. (1996b). Effects of cell cycle dependent histone H1 phosphorylation on chromatin structure and chromatin replication. Nucleic Acids Res. *24*, 1420-1427.

Hancock, J.F., Magee, A.I., Childs, J.E., and Marshall, C.J. (1989). All Ras proteins are polyisoprenylated but only some are palmitoylated. Cell *57*, 1167-1177.

Hannon, G.J. and Beach, D. (1994). p15INK4B is a potential effector of TGF-beta-induced cell cycle arrest [see comments]. Nature *371*, 257-261.

Hansen, J.C. and Ausio, J. (1992). Chromatin dynamics and the modulation of genetic activity. Trends. Biochem. Sci. *17*, 187-191.

Harper, J.W. and Elledge, S.J. (1996). Cdk inhibitors in development and cancer. Curr. Opin. Genet. Dev. *6*, 56-64.

Hartwell, L. (1992). Defects in a cell cycle checkpoint may be responsible for the genomic instability of cancer cells. Cell *71*, 543-546.

Hashimoto, E., Takeda, M., Nishizuka, Y., Hamana, K., and Iwai, K. (1976). Studies on the sites in histones phosphorylated by adenosine 3':5'-monophosphate-dependent and guanosine 3':5'-monophosphate-dependent protein kinases. J. Biol. Chem. *251*, 6287-6293.

Hashimoto, N., Watanabe, N., Furuta, Y., Tamemoto, H., Sagata, N., Yokoyama, M., Okazaki, K., Nagayoshi, M., Takeda, N., and Ikawa, Y. (1994). Parthenogenetic activation of oocytes in *c-mos*-deficient mice [see comments] [published erratum appears in Nature 1994 Aug 4;370(6488):391]. Nature *370*, 68-71.

Hassan, A.B., Errington, R.J., White, N.S., Jackson, D.A., and Cook, P.R. (1994). Replication and transcription sites are colocalized in human cells. J. Cell Sci. *107*, 425-434.

Hebbes, T.R., Thorne, A.W., Clayton, A.L., and Crane-Robinson, C. (1992). Histone acetylation and globin gene switching. Nucleic Acids Res. *20*, 1017-1022.

Hebbes, T.R., Thorne, A.W., and Crane Robinson, C. (1988). A direct link between core histone acetylation and transcriptionally active chromatin. EMBO J. *7*, 1395-1402.

Hendzel, M.J. and Bazett-Jones, D.P. (1995). RNA polymerase II transcription and the functional organization of the mammalian cell nucleus. Chromosoma *103*, 509-516.

Hendzel, M.J. and Davie, J.R. (1991a). Dynamically acetylated histones of chicken erythrocytes are selectively methylated. Biochem. J. *273*, 753-758.

Hendzel, M.J., Delcuve, G.P., and Davie, J.R. (1991b). Histone deacetylase is a component of the internal nuclear matrix. J. Biol. Chem. *266*, 21936-21942.

Hendzel, M.J., Kruhlak, M.J., and Bazett-Jones, D.P. (1998). Organization of Highly Acetylated Chromatin around Sites of Heterogeneous Nuclear RNA Accumulation. Mol. Biol. Cell *9*, 2491-2507.

Hendzel, M.J., Wei, Y., Mancini, M.A., Van Hooser, A., Ranalli, T., Brinkely, B.R., Bazett-Jones, D.P., and Allis, C.D. (1997). Mitosis-specific phosphorylation of histone H3 initiates primarily within pericentromeric heterochromatin durning G2 and spreads in an ordered fashion coincident with chromosome condensation. Chromosoma *106*, 348-360.

Herrara, R.E., Chen, F., and Weinberg, R.A. (1996). Increased histone H1 phosphorylation and relaxed chromatin structure in Rb-deficient fibroblasts. Proc. Natl. Acad. Sci. USA *93*, 11510-11515.

Hill, C.S., Rimmer, J.M., Green, B.N., Finch, J.T., and Thomas, J.O. (1991). Histone-DNA interactions and their modulations by phosphorylation of Ser-Pro-X-Lys-Arg- motifs. EMBO J., 1939-1948.

Hinds, P.W. and Weinberg, R.A. (1994). Tumor suppressor genes. Curr. Opin. Genet. Dev. *4*, 135-141.

Hohmann, P. (1983). Phosphorylation of H1 Histones. Mol. Cell. Biochem. *57*, 81-92.

Holth, L.T., Chadee, D.N., Spencer, V.A., Samuel, S.K., Safneck, J.R., and Davie, J.R. (1998). Chromatin, nuclear matrix and the cytoskeleton: role of cell structure in neoplastic transformation (Review). Int. J. Oncol. *13*, 827-837.

Howe, L., Ranalli, T.A., Allis, C.D., and Ausio, J. (1998). Transcriptionally active Xenopus laevis somatic 5 S ribosomal RNA genes are packaged with hyperacetylated histone H4, whereas transcriptionally silent oocyte genes are not. J. Biol. Chem. *273*, 20693-20696.

Huang, L., Zhang, W., and Roth, S.Y. (1997). Amino termini of histones H3 and H4 are required for a1-alpha2 repression in yeast. Mol. Cell. Biol. *17*, 6555-6562.

Huang, S. and Spector, D.L. (1991). Nascent pre-mRNA transcripts are associated with nuclear regions enriched in splicing factors. Genes & Dev. *5*, 2288-2302.

Huebner, R.J. and Todaro, G.J. (1969). Oncogenes of RNA tumor viruses as determinants of cancer. Proc. Natl. Acad. Sci. U.S.A. *64*, 1087-1094.

Hunter, T. and Pines, J. (1994). Cyclins and cancer II: cyclin D and CDK inhibitors come of age. Cell *79*, 573-582.

Ikegami, S., Taguchi, T., Ohashi, M., Oguro, M., Nagano, H., and Mano, Y. (1978). Aphidicolin prevents mitotic cell division by interfering with the activity of DNA polymerase-alpha. Nature *275*, 458-460.

Ip, Y.T., Jackson, V., Meier, J., and Chalkley, R. (1988). The separation of transcriptionally engaged genes. J. Biol. Chem. *263*, 14044-14052.

Jackson, D.A., Hassan, A.B., Errington, R.J., and Cook, P.R. (1993). Visualization of focal site of transcription within human nuclei. EMBO J. *12:3*, 1059-1065.

Jansen-Durr, P., Meichle, A., Steiner, P., Pagano, M., Finke, K., Botz, J., Wessbecher, J., Dreatta, G., and Eilers, M. (1993). Differential modulation of cyclin gene expression by Myc. Proc. Natl. Acad. Sci. *90*, 3685-3689.

Jansen, H.W., Lurz, R., Bister, K., Bonner, T.I., Mark, G.E., and Rapp, U.R. (1984). Homologous cell-derived oncogenes in avian carcinoma virus MH2 and murine sarcoma virus 3611. Nature *307*, 281-284.

Jermanowski, A. and Cole, R.D. (1992). Partial displacement of histone H1 from chromatin is required before it can be phosphorylated by mitotic H1 kinase in vitro. J. Biol. Chem. *267,12*, 8514-8520.

Juan, G., Traganos, F., James, W.M., Ray, J.M., Roberge, M., Sauve, D.M., Anderson, H., and Darzynkiewicz, Z. (1998). Histone H3 phosphorylation and expression of cyclins A and B1 measured in individual cells during their progression through G2 and mitosis. Cytometry *32*, 71-77.

Kamakaka, R.T. and Thomas, J.O. (1990). Chromatin structure of transcriptionally competent and repressed genes. EMBO J. *9*, 3997-4006.

Kamb, A., Gruis, N.A., Weaver-Feldhaus, J., Liu, Q., Harshman, K., Tavtigian, S.V., Stockert, E., Day, R.S., Johnson, B.E., and Skolnick, M.H. (1994). A cell cycle regulator potentially involved in genesis of many tumor types [see comments]. Science *264*, 436-440.

Kaplan, L.J., Bauer, R., Morrison, E., Langan, T.A., and Fasman, G.D. (1984). The structure of chromatin reconstituted with phosphorylated H1. J. Biol. Chem. *259*, 8777-8785.

Kardalinou, E., Zhelev, N., Hazzalin, C.A., and Mahadevan, L.C. (1994). Anisomycin and rapamycin define an area upstream of p70/85S6k containing a bifurcation to histone H3-HMG-like protein phosphorylation and c-fos-c-jun induction. Mol. Cell Biol. *14*, 1066-1074.

Kato, G.J. and Dang, C.V. (1992). Function of the c-Myc oncoprotein. Faseb *6*, 3065-3072.

Katz, M.E. and McCormick, F. (1997). Signal transduction from multiple Ras effectors. Curr. Opin. Genet. Dev. *7*, 75-79.

Kelly, K., Cochran, B.H., Stiles, C.D., and Leder, P. (1983). Cell-specific regulation of the c-*myc* gene by lymphocyte mitogens and platelet-derived growth factor. Cell *35*, 603-610.

Keyomarsi, K., O'Leary, N., Molnar, G., Lees, E., Fingert, H.J., and Pardee, A.B. (1994). Cyclin E, a potential prognostic marker for breast cancer. Cancer Res. *54*, 380-385.

Keyomarsi, K. and Pardee, A.B. (1993). Redundant cyclin overexpression and gene amplification in breast cancer cells. Proc. Natl. Acad. Sci. U.S.A. *90*, 1112-1116.

King, R.W., Jackson, P.K., and Kirschner, M.W. (1994). Mitosis in transition. Cell *79*, 563-571.

Kogel, D., Plottner, O., Landsberg, G., Christian, S., and Scheidtmann, K.H. (1998). Cloning and characterization of Dlk, a novel serine/threonine kinase that is tightly associated with chromatin and phosphorylates core histones. Oncogene *17*, 2645-2654.

Kolch, W., Heidecker, G., Kochs, G., Hummel, R., Vahidi, H., Mischak, H., Finkenzeller, G., Marme, D., and Rapp, U.R. (1993). Protein kinase C alpha activates RAF-1 by direct phosphorylation. Nature *364*, 249-252.

Komatsu, S., Murata-Hori, M., Totsukawa, G., Murai, N., Fujimoto, H., Mabuchi, I., and Hosoya, H. (1997). Identification of p34cdc2 kinase from sea urchin Hemicentrotus pulcherrimus and its involvement in the phosphorylation of myosin II regulatory light chain in the metaphase extract. Gene *198*, 359-365.

Kyriakis, J.M., App, H., Zhang, X., Banerjee, P., Brautigan, D.L., Rapp, U.R., and Avruch, J. (1992). Raf-1 activates MAP kinase-kinase. Nature *358*, 417-421.

Kyriakis, J.M. and Avruch, J. (1996a). Protein kinase cascades activated by stress and inflammatory cytokines. BioEssays *18* , 567-577.

Kyriakis, J.M. and Avruch, J. (1996b). Sounding the alarm: protein kinase cascades activated by stress and inflammation. J. Biol. Chem. *271*, 24313-24316.

Kyriakis, J.M., Banerjee, P., Nikolakaki, E., Dai, T., Rubie, E.A., Ahmad, M.F., Avruch, J., and Woodgett, J.R. (1994). The stress-activated protein kinase subfamily of c-Jun kinases. Nature *369*, 156-160.

Kyriakis, J.M., Woodgett, J.R., and Avruch, J. (1995). The stress-activated protein kinases. A novel ERK subfamily responsive to cellular stress and inflammatory cytokines. Ann. N.Y. Acad. Sci. *766:303-19*, 303-319.

Lachman, H.M. and Skoultchi, A.I. (1984). Expression of c-myc changes during differentiation of mouse erythroleukaemia cells. Nature *310*, 592-594.

Laemmli, U.K. (1970). Cleavage of structural proteins during the assembly of the head of bacteriophage T4. Nature *227*, 680-685.

Laitinen, J., Sistonen, L., Alitalo, K., and Holtta, E. (1990). c-Ha-*ras* (val 12) oncogene-transformed NIH-3T3 fibroblasts display more decondensed nucleosomal organization than normal fibroblasts. J. Cell Biol. *111*, 9-17.

Laitinen, J., Sistonen, L., Alitalo, K., and Holtta, E. (1994). Cell transformation by c-Ha-ras (val12) oncogene is accompanied by a decrease in Histone H10 and an increase in nucleosomal repeat length. J. Cell Biochem. *57*, 1-11.

Land, H., Parada, L.F., and Weinberg, R.A. (1983). Tumorigenic conversion of primary embryo fibroblasts requires at least two cooperating oncogenes. Nature *304*, 596-602.

Landschulz, W.H., Johnson, P.F., and McKnight, S.L. (1988). The leucine zipper: a hypothetical structure common to a new class of DNA binding proteins. Science *240*, 1759-1764.

Lange-Carter, C.A. and Johnson, G.L. (1994). Ras-dependent growth factor regulation of MEK kinase in PC12 Cells. Science *265*, 1458-1461.

Larsen, A. and Weintraub, H. (1982). An altered DNA conformation detected by S1 nuclease occurs at specific regions in active chick globin chromatin. Cell *29*, 609-622.

Leach, F.S., Elledge, S.J., Sherr, C.J., Willson, J.K., Markowitz, S., Kinzler, K.W., and Vogelstein, B. (1993). Amplification of cyclin genes in colorectal carcinomas. Cancer Res. *53*, 1986-1989.

Lee, H.L. and Archer, T.K. (1998). Prolonged glucocorticoid exposure dephosphorylates histone H1 and inactivates the MMTV promoter. EMBO J *17*, 1454-1466.

Lee, W.M., Schwab, M., Westaway, D., and Varmus, H.E. (1985). Augmented expression of normal c-*myc* is sufficient for cotransformation of rat embryo cells with a mutant *ras* gene. Mol. Cell Biol. *5*, 3345-3356.

Leevers, S.J., Paterson, H.F., and Marshall, C.J. (1994). Requirement for Ras in Raf activation is overcome by targeting Raf to the plasma membrane. Nature *369*, 411-414.

Lennox, R.W. and Cohen, L.H. (1983a). J. Biol. Chem *258*, 262-268.

Lennox, R.W. and Cohen, L.H. (1983b). The histone H1 complements of dividing and nondividing cells of the mouse. J. Biol. Chem. *258*, 262-268.

Lennox, R.W. and Cohen, L.H. (1988). The production of tissue-specific histone complements during development. Biochem. Cell Biol. *66*, 636-649.

Lennox, R.W., Oshima, R.G., and Cohen, L.H. (1982). The H1 histones and their interphase phosphorylated states in differentiated and undifferentiated cell lines derived from murine teratocarcinomas. J. Biol. Chem. *257:9*, 5183-5189.

LeRoy, G., Orphanides, G., Lane, W.S., and Reinberg, D. (1998). Requirement of RSF and FACT for transcription of chromatin templates *in vitro*. Science *282*, 1900-1904.

Leuba, S.H., Bustamante, C., Zlatanova, J., and van Holde, K. (1998). Contributions of linker histones and histone H3 to chromatin structure: scanning force microscopy studies on trypsinized fibers. Biophys. J. *74*, 2823-2829.

Li, J. and Smithgall, T.E. (1998). Fibroblast transformation by Fps/Fes tyrosine kinases requires Ras, Rac, and Cdc42 and induces extracellular signal-regulated and c-Jun N- terminal kinase activation. J. Biol. Chem. *273*, 13828-13834.

Lu, M.J., Dadd, C.A., Mizzen, C.A., Perry, C.A., McLachlan, D.R., Annunziato, A.T., and Allis, C.D. (1994). Generation and characterization of novel antibodies highly selective for phosphorylated linker histone H1 in Tetrahymena and HeLa cells. Chromosoma *103*, 111-121.

Lu, X. and Lane, D.P. (1993). Differential induction of transcriptionally active p53 following UV or ionizing radiation: defects in chromosome instability syndromes? Cell *75*, 765-778.

Lu., M.J., Mpoke, S.S., Dadd, C.A., and Allis, C.D. (1995). Phosphorylated and dephosphorylated linker histone H1 reside in distinct chromatin domains in Tetrahymena acronuclei. Mol. Biol. Cell *6*, 1077-1087.

Luger, K., Mader, A.W., Richmond, R.K., Sargent, D.F., and Richmond, T.J. (1997). Crystal structure of the nucleosome core particle at 2.8 A resolution [see comments]. Nature *389*, 251-260.

Luo, R.X., Postigo, A.A., and Dean, D.C. (1998). Rb interacts with histone deacetylase to repress transcription. Cell *92*, 463-473.

Luscher, B. and Eisenman, R.N. (1990). New light on Myc and Myb. Part I. Myc. Genes Dev. *4*, 2025-2035.

MacDonald, I., Levy, J., and Pawson, T. (1985). Expression of the mammalian c-Fes protein in hematopoietic cells and identification of a distinct Fes-related protein. Mol. Cell. Biol. *5*, 2543-2551.

Madhani, H.D. and Fink, G.R. (1998). The riddle of MAP kinase signaling specificity. Trends. Genet. *14*, 151-155.

Magnaghi-Jaulin, L., Groisman, R., Naguibneva, I., Robin, P., Lorain, S., Le Villain, J.P., Troalen, F., Trouche, D., and Harel-Belan, A. (1998). Retinoblastoma protein represses transcription by recruiting a histone deacetylase. Nature *391*, 601-604.

Mahadevan, L.C., Willis, A.C., and Barratt, M.J. (1991). Rapid histone H3 phosphorylation in response to growth factors, phorbol esters, okadaic acid, and protein synthesis inhibitors. Cell *65*, 775-783.

Mansour, S.J., Matten, W.T., Hermann, A.S., Candia, J.M., Rong, S., Fukasawa, K., Vande Woude, G.F., and Ahn, N.G. (1994). Transformation of mammalian cells by constitutively activated MAP Kinase Kinase. Science *265*, 966-970.

Marion, C., Roux, B., and Coulet, P.R. (1983a). Role of histones H1 and H3 in the maintenance of chromatin in a compact conformation. Study with an immobilized enzyme. FEBS Lett. *157*, 317-321.

Marion, C., Roux, B., Pallotta, L., and Coulet, P.R. (1983b). Study of chromatin organization with trypsin immobilized on collagen membranes. Biochem. Biophys. Res. Commun. *114*, 1169-1175.

Maru, Y., Peters, K.L., Afar, D.E., Shibuya, M., Witte, O.N., and Smithgall, T.E. (1995). Tyrosine phosphorylation of BCR by FPS/FES protein-tyrosine kinases induces association of BCR with GRB-2/SOS. Mol. Cell Biol. *15*, 835-842.

Matsushime, H., Ewen, M.E., Strom, D.K., Kato, J.Y., Hanks, S.K., Roussel, M.F., and Sherr, C.J. (1992). Identification and properties of an atypical catalytic subunit (p34PSK- J3/cdk4) for mammalian D type G1 cyclins. Cell *71*, 323-334.

Maxwell, S.A. and Arlinghaus, R.B. (1985). Serine kinase activity associated with Maloney murine sarcoma virus-124- encoded p37mos. Virology *143*, 321-333.

Mello, M.L.S. and Chambers, A.F. (1994). Image analysis of feulgen-stained transformed NIH 3T3 cells differing in p21 expression and metastatic ability. Anal. Quan. Cyt. & Hist. *16:2*, 113-123.

Meyerson, M. and Harlow, E. (1994). Identification of G1 kinase activity for Cdk6, a novel cyclin D partner. Mol. Cell Biol. *14*, 2077-2086.

Miller, A.D., Curran, T., and Verma, I.M. (1984). c-Fos protein can induce cellular transformation: a novel mechanism of activation of a cellular oncogene. Cell *36*, 51-60.

Mizzen, C.A., Yang, X.J., Kokubo, T., Brownell, J.E., Bannister, A.J., Owen-Hughes, T., Workman, J., Wang, L., Berger, S.L., Kouzarides, T., Nakatani, Y., and Allis, C.D. (1996). The $TAF_{II}250$ subunit of TFIID has histone acetyltransferase activity. Cell *87*, 1261-1270.

Morgan, D.O. (1995). Principles of CDK regulation. Nature (London) *374*, 131-134.

Mougneau, E., Lemieux, L., Rassoulzadegan, M., and Cuzin, F. (1984). Biological activities of v-*myc* and rearranged c-*myc* oncogenes in rat fibroblast cells in culture. Proc. Natl. Acad. Sci. U.S.A. *81*, 5758-5762.

Munshi, N., Merika, M., Yie, J., Senger, K., Chen, G., and Thanos, D. (1998). Acetylation of HMG I(Y) by CBP turns off IFN beta expression by disrupting the enhanceosome. Mol. Cell *2*, 457-467.

Nacheva, G.A., Guschin, D.Y., Preobrazhenskaya, O.V., Karpov, V.L., Ebralidse, K.K., and Mirzabekov, A.D. (1989). Change in the pattern of histone binding to DNA upon transcriptional activation. Cell *58*, 27-36.

Nebreda, A.R. and Hunt, T. (1993). The *c-mos* proto-oncogene protein kinase turns on and maintains the activity of MAP kinase, but not MPF, in cell-free extracts of Xenopus oocytes and eggs. EMBO J. *12*, 1979-1986.

Nevins, J.R. (1992). Transcriptional regulation. A closer look at E2F [news]. Nature *358*, 375-376.

Nobori, T., Miura, K., Wu, D.J., Lois, A., Takabayashi, K., and Carson, D.A. (1994). Deletions of the cyclin-dependent kinase-4 inhibitor gene in multiple human cancers. Nature *368*, 753-756.

Nurse, P. (1994). Ordering S phase and M phase in the cell cycle [comment]. Cell *79*, 547-550.

O'Keefe, R.T., Mayeda, A., Sadowski, C.L., Krainer, A.R., and Spector, D.L. (1994). Disruption of pre-mRNA splicing *in vivo* results in reorganization of splicing factors. J.Cell Biol. *124*, 249-260.

Ogryzko, V.V., Schiltz, R.L., Russanova, V., Howard, B.H., and Nakatani, Y. (1996). The transcriptional coactivators p300 and CBP are histone acetyltransferases. Cell *87*, 953-959.

Ord, M.G. and Stocken, L.A. (1966). Metabolic properties of histones from rat liver and thymus gland. Biochem. J. *98*, 888-897.

Palaparti, A., Baratz, A., and Stifani, S. (1997). The Groucho/transducin-like enhancer of split transcriptional repressors interact with the genetically defined amino-terminal silencing domain of histone H3. J. Biol. Chem. *272*, 26604-26610.

Papst, P.J., Sugiyama, H., Nagasawa, M., Lucas, J.J., Maller, J.L., and Terada, N. (1998). Cdc2-cyclin B phosphorylates p70 S6 kinase on Ser411 at mitosis. J. Biol. Chem. *273*, 15077-15084.

Parkhurst, S.M. (1998). Groucho: making its Marx as a transcriptional co-repressor. Trends. Genet. *14*, 130-132.

Parseghian, M.H., Henschen, A.H., Krieglstein, K.G., and Hamkalo, B.A. (1994). A proposal for a coherent mammalian histone H1 nomenclature correlated with amino acid sequences. Protein Sci. *3*, 575-587.

Paulson, J.R., Patzlaff, J.S., and Vallis, A.J. (1996). Evidence that the endogenous histone H1 phosphatase in HeLa mitotic chromosomes is protein phosphatase 1, not protein phosphatase 2A. J. Cell. Sci. *109*, 1437-1447.

Paulson, J.R. and Taylor, S.S. (1982). Phosphorylation of histones 1 and 3 and nonhistone high mobility group 14 by an endogenous kinase in HeLa metaphase chromosomes. J. Biol. Chem. *257*, 6064-6072.

Pear, W.S., Wahlstrom, G., Nelson, S.F., Axelson, H., Szeles, A., Wiener, F., Bazin, H., Klein, G., and Sumegi, J. (1988). 6;7 chromosomal translocation in spontaneously arising rat immunocytomas: evidence for c-*myc* breakpoint clustering and correlation between isotypic expression and the c-*myc* target. Mol. Cell Biol. *8*, 441-451.

Pedrali-Noy, G. and Spadari, S. (1979). Effect of aphidicolin on viral and human DNA polymerases. Biochem. Biophys. Res. Commun. *88*, 1194-1202.

Perez-Estevez, A., Diaz-Jullien, C., Covelo, G., Salgueiro, M.T., and Friere, M. (1997). A 180-kDa protein kinase seems to be responsible for the phosphorylation of prothymosin alpha observed in proliferating cells. J. Biol. Chem. *272*, 10506-10513.

Perry, R.P. (1963). Exp. Cell Res. *29*, 400-406.

Pinaud, S. and Mirkovitch, J. (1998). Regulation of *c-fos* expression by RNA polymerase elongation competence. J. Mol. Biol. *280*, 785-798.

Posada, J. and Cooper, J.A. (1992). Requirements for phosphorylation of MAP kinase during meiosis in Xenopus oocytes. Science *255*, 212-215.

Rattner, J.B., Hendzel, M.J., Furbee, C.S., Muller, M.T., and Bazett-Jones, D.P. (1996). Topoisomerase IIa is associated with the mammalian centromere in a cell-cycle and species specific manner and is required for proper centromere/kinetochore structure. J. Cell. Biol. *134*, 1097-1107.

Ravichandran, K.S., Lorenz, U., Shoelson, S.E., and Burakoff, S.J. (1995). Interaction of Shc with Grb2 regulates association of Grb2 with mSOS. Mol.Cell Biol. *15*, 593-600.

Reeves, R. and Nissen, M.S. (1995). Cell cycle regulation and functions of HMG-I(Y). Prog. Cell Cycle Res. *1*, 339-349.

Reneker, J. and Brotherton, T.W. (1991). Postsynthetic methylation of core histones in K562 cells is associated with bulk acetylation but not with transcriptional activity. Biochemistry *30*, 8402-8407.

Resing, K.A., Mansour, S.J., Hermann, A.S., Johnson, R.S., Candia, J.M., Fukasawa, K., Vande, W.G., and Ahn, N.G. (1995). Determination of v-Mos-catalyzed phosphorylation sites and autophosphorylation sites on MAP kinase kinase by ESI/MS. Biochemistry *34*, 2610-2620.

Resnitzky, D., Gossen, M., Bujard, H., and Reed, S.I. (1994). Acceleration of the G1/S phase transition by expression of cyclins D1 and E with an inducible system. Mol. Cell. Biol. *14,3*, 1669-1679.

Ridsdale, J.A., Hendzel, M.J., Delcuve, G.P., and Davie, J.R. (1990). Histone acetylation alters the capacity of the H1 histones to condense transcriptionally active/competent chromatin. J. Biol. Chem. *265,9*, 5150-5156.

Roth, S.Y. and Allis, C.D. (1992). Chromatin condensation: does histones H1 dephosphorylation play a role? Trends Biochem. Sci. 93-98.

Roth, S.Y., Collini, M.P., Draetta, G., Beach, D., and Allis, C.D. (1991). A cdc2-like kinase phosphorylates histone H1 in the amitotic macronucleus of Tetrahymena. EMBO J. *10:8*, 2069-2075.

Said, T.K. and Medina, D. (1995). Cell cyclins and cyclin-dependent kinase activities in mouse mammary tumor development. Carcinogenesis *16*, 823-830.

Sambrook, J., Fritsh, E.F., and Maniatis, T. (1989). Molecular cloning: a laboratory manual (Cold Spring Harbor Laboratory Press; Cold Spring Harbor, New York).

Samuel, S.K., Minish, T.M., and Davie, J.R. (1997). Altered nuclear matrix protein profiles in oncogene-transformed mouse fibroblasts exhibiting high metastatic potential. Cancer Res. *57*, 147-151.

Samuel, S.K., Spencer, V.A., Bajno, L., Sun, J.M., Holth, L.T., Oesterreich, S., and Davie, J.R. (1998). *In situ* cross-linking by cisplatin of nuclear matrix-bound transcription factors to nuclear DNA of human breast cancer cells. Cancer Res. *58*, 3004-3008.

Sanghera, J.S., Peter, M., Nigg, E.A., and Pelech, S.L. (1992). Immunological characterization of avian MAP kinases: evidence for nuclear localization. .Mol. Biol. Cell *3*, 775-787.

Schafer, W.R. and Rine, J. (1992). Protein prenylation: genes, enzymes, targets, and functions. Annu. Rev. Genet. *26:209-37*, 209-237.

Schonthal, A., Herrlich, P., Rahmsdorf, H.J., and Ponta, H. (1988). Requirement for fos gene expression in the transcriptional activation of collagenase by other oncogenes and phorbol esters. Cell *54*, 325-334.

Schonwasser, D.C., Marais, R.M., Marshall, C.J., and Parker, P.J. (1998). Activation of the mitogen-activated protein kinase/extracellular signal-regulated kinase pathway by conventional, novel, and atypical protein kinase C isotypes. Mol. Cell. Biol. *18*, 790-798.

Sheiness, D. and Bishop, J.M. (1979). DNA and RNA from uninfected vertebrate cells contain nucleotide sequences related to the putative transforming gene of avian myelocytomatosis virus. J. Virol. *31*, 514-521.

Shen, X. and Gorovsky, M.A. (1996). Linker histone H1 regulates specific gene expression but not global transcription in vivo. Cell *86*, 475-483.

Shibata, K. and Ajiro, K. (1993). Cell cycle-dependent suppressive effect of histone H1 on mitosis-specific H3 phosphorylation. J. Biol. Chem. *268,25*, 18431-18434.

Shibata, K., Inagaki, M., and Ajiro, K. (1990). Mitosis-specific histone H3 phosphorylation in vitro in nucleosome structures. Eur. J. Biochem. *192*, 87-93.

Shih, C. and Weinberg, R.A. (1982). Isolation of a transforming sequence from a human bladder carcinoma cell line. Cell *29*, 161-169.

Smith, M.R., DeGudicibus, S.J., and Stacey, D.W. (1986). Requirement for c-Ras proteins during viral oncogene transformation. Nature *320*, 540-543.

Smithgall, T.E., Yu, G., and Glazer, R.I. (1988). Identification of the differentiation-associated p93 tyrosine protein kinase of HL-60 leukemia cells as the product of the human c-fes locus and its expression in myelomonocytic cells. J. Biol. Chem. *263*, 15050-15055.

Spector, D.L. (1993). Macromolecular domains within the cell nucleus. Annu. Rev. Cell Biol. *9:265-315*, 265-315.

Spector, D.L., Fu, X.D., and Maniatis, T. (1991). Associations between distinct pre-mRNA splicing components and the cell nucleus. EMBO J. *10*, 3467-3481.

Spencer, V.A., Coutts, A.S., Samuel, S.K., Murphy, L.C., and Davie, J.R. (1998). Estrogen regulates the association of intermediate filament proteins with nuclear DNA in human breast cancer cells. J. Biol. Chem. *273*, 29093-29097.

Stevens, A. and Maupin, M.K. (1989). 5,6-Dichloro-1-beta-D-ribofuranosylbenzimidazole inhibits a HeLa protein kinase that phosphorylates an RNA polymerase II-derived peptide. Biochem. Biophys. Res. Commun. *159*, 508-515.

Struhl, K. (1996). Chromatin structure and RNA polymerase II connection: implications for transcription. Cell *84*, 179-182.

Studisky, V.M., Clark, D.J., and Felsenfeld, G. (1994). A histone octamer can step around a transcribing polymerase without leaving the template. Cell *76*, 371-382.

Su, T.T., Sprenger, F., DiGregorio, P.J., Campbell, S.D., and O'Farrell, P.H. (1998). Exit from mitosis in Drosophila syncytial embryos requires proteolysis and cyclin degradation, and is associated with localized dephosphorylation. Genes Dev *12*, 1495-1503.

Sung, M.T. and Dixon, G.H. (1970). Modification of histones during spermiogenesis in trout: a molecular mechanism for altering histone binding to DNA. Proc. Natl. Acad. Sci. U.S.A. *67*, 1616-1623.

Swank, R.A., Th'ng, J.P., Guo, X.W., Valdez, J., Bradbury, E.M., and Gurley, L.R. (1997). Four distinct cyclin-dependent kinases phosphorylate histone H1 at all of its growth-related phosphorylation sites. Biochemistry *36*, 13761-13768.

Sweet, M.T., Jones, K., and Allis, C.D. (1996). Phosphorylation of linker histone is associated with transcriptional activation in a normally silent nucleus. J. Cell Biol. *135*, 1219-1228.

Talasz, H., Helliger, W., Puschendorf, B., and Lindner, H. (1993). G1- and S-phase synthesis of histone H1 subtypes from mouse NIH fibroblasts and rat C6 glioma cells. Biochemistry *32*, 1188-1193.

Talasz, H., Helliger, W., Puschendorf, B., and Lindner, H. (1996). *In vivo* phosphorylation of histone H1 variants during the cell cycle. Biochemistry *35*, 1761-1767.

Tam, S.W., Theodoras, A.M., Shay, J.W., Draetta, G.F., and Pagano, M. (1994). Differential expression and regulation of Cyclin D1 protein in normal and tumor human cells: association with Cdk4 is required for Cyclin D1 function in G1 progression. Oncogene *9*, 2663-2674.

Tamanoi, F. (1993). Inhibitors of Ras farnesyltransferases. Trends. Biochem. Sci. *18*, 349-353.

Tan, K.B., Borun, T.W., Charpentier, R., Cristofalo, V.J., and Croce, C.M. (1982). Normal and neoplastic human cells have different histone H1 compositions. J. Biol. Chem. *257*, 5337-5338.

Taub, R., Kirsch, I., Morton, C., Lenoir, G., Swan, D., Tronick, S., Aaronson, S., and Leder, P. (1982). Translocation of the c-*myc* gene into the immunoglobulin heavy chain locus in human Burkitt lymphoma and murine plasmacytoma cells. Proc. Natl. Acad. Sci. U.S.A. *79*, 7837-7841.

Taylor, S.S. (1982). The in vitro phosphorylation of chromatin by the catalytic subunit of cAMP-dependent protein kinase. J. Biol. Chem. *257*, 6056-6063.

Taylor, W.R., Egan, S.E., Mowat, M., Greenberg, A.H., and Wright, J.A. (1994). Evidence for synergistic interactions between *ras*, *myc*, and a mutant form of p53 in cellular transformation and tumor dissemination. Oncogene *7*, 1383-1390.

Thanos, D. and Maniatis, T. (1995). Virus induction of human IFN beta gene expression requires the assembly of an enhanceosome. Cell *83*, 1091-1100.

Thomas, G., Lange, H.W., and Hempel, K. (1975). Kinetics of histone methylation in vivo and its relation to the cell cycle in Ehrlich ascites tumor cells. Eur. J. Biochem. *51*, 609-615.

Tjian, R. and Maniatis, T. (1994). Transcriptional activation: a complex puzzle with few easy pieces. Cell *77*, 5-8.

Trieschmann, L., Martin, B., and Bustin, M. (1998). The chromatin unfolding domain of chromosomal protein HMG-14 targets the N-terminal tail of histone H3 in nucleosomes [published erratum appears in Proc Natl Acad Sci U S A 1998 Jul 21;95(15):9059]. Proc. Natl. Acad. Sci. U.S.A. *95*, 5468-5473.

Tse, C. and Hansen, J.C. (1997). Hybrid trypsinized nucleosomal arrays: identification of multiple functional roles of the H2A/H2B and H3/H4 N-termini in chromatin fiber compaction. Biochemistry *36*, 11381-11388.

van Holde, K. and Zlatanova, J. (1996). What determines the folding of the chromatin fiber? Proc. Natl. Acad. Sci. USA *93*, 10548-10555.

Van Holde, K.E. (1988). Chromatin (New York: Springer-Verlag).

Van Holde, K.E., Lohr, D.E., and Robert, C. (1992). What happens to nucleosomes during transcription? J. Biol. Chem. *267*, 2837-2840.

Vlach, J., Hennecke, S., Alevizopoulos, K., Conti, D., and Amati, B. (1996). Growth arrest by the cyclin-dependent kinase inhibitor p27Kip1 is abrogated by c-Myc. EMBO J. *15*, 6595-6604.

Waga, S., Hannon, G.J., Beach, D., and Stillman, B. (1994). The p21 inhibitor of cyclin-dependent kinases controls DNA replication by interaction with PCNA [see comments]. Nature *369*, 574-578.

Walia, H., Chen, H.Y., Sun, J.M., Holth, L.T., and Davie, J.R. (1998). Histone acetylation is required to maintain the unfolded nucleosome structure associated with transcribing DNA. J. Biol. Chem. *273*, 14516-14522.

Wan, K.M., Nickerson, J.A., Krockmalnic, G., and Penman, S. (1994). The B1C8 protein is in the dense assemblies of the nuclear matrix and relocates to the spindle and pericentriolar filaments at mitosis. Proc. Natl. Acad. Sci. *91*, 594-598.

Wang, H.G., Rapp, U.R., and Reed, J.C. (1996). Bcl-2 targets the protein kinase Raf-1 to mitochondria [see comments]. Cell *87*, 629-638.

Wang, H.G. and Reed, J.C. (1998). Bc1-2, Raf-1 and mitochondrial regulation of apoptosis. Biofactors *8*, 13-16.

Waring, P., Khan, T., and Sjaarda, A. (1997). Apoptosis induced by gliotoxin is preceeded by phosphorylation of histone H3 and enhanced sensitivity of chromatin to nuclease digestion. J. Biol. Chem. *272*, 17929-17936.

Watts, C.K., Brady, A., Sarcevic, B., deFazio, A., Musgrove, E.A., and Sutherland, R.L. (1995). Antiestrogen inhibition of cell cycle progression in breast cancer cells in associated with inhibition of cyclin-dependent kinase

activity and decreased retinoblastoma protein phosphorylation. Mol. Endocrinol. *9*, 1804-1813.

Weber, J.D., Hu, W., Jefcoat, S.C.J., Raben, D.M., and Baldassare, J.J. (1997). Ras-stimulated extracellular signal-related kinase 1 and RhoA activities coordinate platelet-derived growth factor-induced G1 progression through the independent regulation of cyclin D1 and p27. J. Biol. Chem. *272*, 32966-32971.

Wei, Y., Mizzen, C.A., Cook, R.G., Gorovsky, M.A., and Allis, C.D. (1998). Phosphorylation of histone H3 at serine 10 is correlated with chromosome condensation during mitosis and meiosis in Tetrahymena. Proc. Natl. Acad. Sci. *95*, 7480-7484.

Weintraub, H. and Groudine, M. (1976). Chromosomal subunits in active genes have an altered conformation. Science *193*, 848-856.

Weintraub, S.J., Prater, C.A., and Dean, D.C. (1992). Retinoblastoma protein switches the E2F site from positive to negative element. Nature *358*, 259-261.

Widmer, R.M., Lucchini, R., Lezzi, M., Meyer, B., Sogo, J.M., Edstrom, J.E., and Koller, T. (1984). Chromatin structure of a hyperactive secretory protein gene (in Balbiani ring 2) of Chironomus. EMBO J. *3*, 1635-1641.

Wilson, C.J., Chao, D.M., Imbalzano, A.N., Schnitzler, G.R., Kingston, R.E., and Young, R.A. (1996). RNA polymerase II holoenzyme contains SWI/SNF regulators involved in chromatin remodeling. Cell *84*, 235-244.

Won, K.A., Xiong, Y., Beach, D., and Gilman, M.Z. (1992). Growth-regulated expression of D-type cyclin genes in human diploid fibroblasts. Proc. Natl. Acad. Sci. U.S.A. *89*, 9910-9914.

Wu, R.S., Kohn, K.W., and Bonner, W.M. (1981). Metabolism of ubiquitinated histones. J. Biol. Chem. *256*, 5916-5920.

Xing, Y., Johnson, C.V., Dobner, P.R., and Lawrence, J.B. (1993). Higher level organization of individual gene transcription and RNA splicing [see comments]. Science *259*, 1326-1330.

Xing, Y., Johnson, C.V., Moen, P.T.J., McNeil, J.A., and Lawrence, J. (1995). Nonrandom gene organization: structural arrangements of specific pre-mRNA transcription and splicing with SC-35 domains. J. Cell Biol. *131*, 1635-1647.

Xiong, Y., Hannon, G.J., Zhang, H., Casso, D., Kobayashi, R., and Beach, D. (1993). p21 is a universal inhibitor of cyclin kinases [see comments]. Nature *366*, 701-704.

Yankulov, K., Yamashita, K., Roy, R., Egly, J.M., and Bentley, D.L. (1995). The transcriptional elongation inhibitor 5,6-dichloro-1-beta-D-ribofuranosylbenzimidazole inhibits transcription factor IIH-associated protein kinase. J. Biol. Chem. *270*, 23922-23925.

Yasuda, H., Matsumoto, Y., Marunouchi, T., and Yamada, M. (1981). A mouse temperature-sensitive mutant defective in H1 histone phosphorylation is defective in deoxyribonucleic acid synthesis and chromosome condensation. Biochemistry *20,15*, 4414-4419.

Yew, N., Strobel, M., and Vande, W.G. (1993). Mos and the cell cycle: the molecular basis of the transformed phenotype. Curr. Opin. Genet. Dev. *3*, 19-25.

Zandomeni, R.O. (1989). Kinetics of inhibition by 5,6-dichloro-1-beta-D-ribofuranosylbenzimidazole on calf thymus casein kinase II. Biochem. J. *262*, 469-473.

Zeng, C., Kim, E., Warren, S.L., and Berget, S.M. (1997). Dynamic relocation of transcription and splicing factors dependent upon transcriptional activity. EMBO J. *16*, 1401-1412.

Zervos, A.S., Gyuris, J., and Brent, R. (1993). Mxi1, a protein that specifically interacts with Max to bind Myc-Max recognition sites [published erratum appears in Cell 1994 Oct 21;79(2):following 388]. Cell *72*, 223-232.

Zhang, X., Settleman, J., Kyriakis, J.M., Takeuchi-Suzuki, E., Elledge, S.J., Marshall, M.S., Bruder, J.T., Rapp, U.R., and Avruch, J. (1993). Normal and oncogenic p21ras proteins bind to the amino-terminal regulatory domain of c-Raf-1. Nature *364*, 308-313.

Zhao, Y., Bjorbaek, C., and Moller, D. E. Regulation and interaction of $pp90^{rsk}$ isoforms with mitogen-activated protein kinases. J.Biol.Chem. 271(47), 29773-29779. 1996.

Zhou, Y.B., Gerchman, S.E., Ramakrishnan, V., Travers, A., and Muyldermans, S. (1998). Position and orientation of the globular domain of linker histone H5 on the nucleosome. Nature *395*, 402-405.